



ALMA MATER STUDIORUM
UNIVERSITÀ DI BOLOGNA



POLITÉCNICA

**Alma Mater Studiorum – Università di Bologna
in cotutela con Univesidad Politécnica de Madrid**

**DOTTORATO DI RICERCA IN
INGEGNERIA CIVILE, CHIMICA, AMBIENTALE E DEI
MATERIALI**

Ciclo XXXV

Settore Concorsuale: 08/B3 Tecnica delle Costruzioni

Settore Scientifico Disciplinare: ICAR09

**Seismic vulnerability of buildings
and non-structural elements:
insights from the 2011 Lorca earthquake**

Presentata da: M.Sc. Arch. Laura Araceli Navas Sánchez

Coordinatore Dottorato

Prof. Alessandro Tugnoli

Supervisore

Prof. Arch. Jaime Cervera

Prof. Ing. Marco Savoia

Co-Supervisore

PhD. Ing. Francesca Ferretti

Esame finale anno 2023

UNIVERSIDAD POLITÉCNICA DE MADRID

Departamento de Estructuras de Estructuras y Física de la Edificación

Escuela Técnica Superior de Arquitectura de Madrid

PhD in Estructuras de la Edificación

&

ALMA MATER STUDIORUM – UNIVERSITY OF BOLOGNA

Department of Civil, Chemical, Environmental and Materials Engineering

PhD in Civil, Chemical, Environmental and Materials Engineering

**Seismic vulnerability of buildings and non-structural
elements: insights from the 2011 Lorca earthquake**

Laura Araceli Navas Sánchez

Arch. Msc. in Building Structures

ADVISORS

Jaime Cervera Bravo

Prof. Architect

Marco Savoia

Prof. Civil Engineer

CO-ADVISOR

Francesca Ferretti

PhD. Civil Engineer

Abstract

This PhD dissertation presents a profound study of the vulnerability of buildings and non-structural elements stemmed from the investigation of the Lorca 2011 earthquake. This moderate magnitude seism, M_w 5.2, constitutes one of the most significant earthquakes in Spain in recent decades, as it left nine fatalities due to falling debris from reinforced concrete buildings, 394 injured and material damage valued at 800 million euros.

Within this framework, the most relevant international and national initiatives and projects concerning the vulnerability assessment of buildings within the context of seismic risk studies have been presented. Besides, the exposure of the city has been analysed and the knowledge about the different typologies expanded. Said studies have revealed two lines of research for this work. Firstly, the existence of a gap in the literature, the lack of a rational method to determine the adequacy of a specific fragility curve for the particular seismic risk study of a region. Secondly, the relevance of advancing in a field still under development, that related to the seismic performance of non-structural elements such as masonry parapets and infill walls.

As a consequence, on the one hand, a method to assess and select fragility curves for seismic risk studies from the catalogue of those available in the literature has been elaborated and calibrated by means of a case study. Said methodology is based on a multidimensional index and provides a ranking that classifies the curves assessed in terms of technical suitability, suitability for the local system and building class similarity with the typology object of study. The results of its application to the case of Lorca indicate the adequacy of the fragility curves selected in previous studies is limited. With this outcome in mind, fragility curves for the typologies of unreinforced masonry buildings present in Lorca have been elaborated using actual buildings of the region as samples and more updated methods. Moreover, a simplified method for accounting for the unpredictable directionality of the seism in the creation of fragility curves has been contributed.

On the other hand, the characterisation of the seismic capacity and demand of the non-structural elements that caused most of the human losses has been studied: unreinforced masonry parapets and exterior infill walls pertaining to four to six-storey infilled frame RC structure buildings. Concerning the capacity, an analytical approach derived from theoretical considerations to characterise the complete out-of-plane seismic response curve of unreinforced masonry cantilever walls has been provided; as well as a simplified and more practical trilinear version of it. Concerning the demand, a number of methods for characterising the Floor Response Spectra of the reinforced concrete buildings present in the area have been tested by means of case studies. The results of the analyses conducted have led to the recommendation of the implementation of the methodologies already included in the Italian regulation, NTC18, in the upcoming Spanish regulation, NCSR22.

Finally, some future lines of research related to ways of combining the advances in exposure and vulnerability when performing seismic risk studies are presented.

Resumen

Esta Tesis presenta un estudio profundo de la vulnerabilidad de los edificios y elementos no estructurales derivado de la investigación del terremoto de Lorca de 2011. Este seísmo de magnitud moderada, M_w 5,2, constituye uno de los sismos más significativos en España en las últimas décadas, ya que dejó nueve víctimas mortales por caída de escombros de edificios de hormigón armado, 394 heridos y daños materiales valorados en 800 millones de euros.

En este marco, se han presentado las iniciativas y proyectos internacionales y nacionales más relevantes en materia de evaluación de la vulnerabilidad de las edificaciones en el contexto de los estudios de riesgo sísmico. Además, se ha analizado la exposición de la ciudad y se ha ampliado el conocimiento sobre las diferentes tipologías. Dichos estudios han revelado dos líneas de investigación para este trabajo. En primer lugar, la existencia de un vacío en la literatura, la falta de un método racional para determinar la adecuación de una curva de fragilidad específica para el estudio de riesgo sísmico particular de una región. En segundo lugar, la relevancia del avance en un campo aún en desarrollo, el relacionado con el comportamiento sísmico de elementos no estructurales como parapetos y cerramiento de fábrica.

En consecuencia, por un lado, se ha elaborado un método para evaluar y seleccionar curvas de fragilidad para estudios de riesgo sísmico del catálogo de los disponibles en la literatura, el cual ha sido calibrado mediante un estudio de caso. Dicha metodología se basa en un índice multidimensional y proporciona un ranking que clasifica las curvas evaluadas en términos de adecuación técnica, adecuación al sistema local y similitud de clase del edificio con la tipología objeto de estudio. Los resultados de su aplicación al caso de Lorca indican que la adecuación de las curvas de fragilidad seleccionadas en estudios previos es limitada. Teniendo en cuenta este resultado, se han elaborado curvas de fragilidad para las tipologías de edificación de fábrica de mampostería no armada presentes en Lorca, utilizando como muestra edificios reales de la región y métodos más actualizados. Además, se ha aportado un método simplificado para dar cuenta de la direccionalidad impredecible del sismo en la creación de curvas de fragilidad.

Por otro lado, se ha estudiado la caracterización de la capacidad y demanda sísmica de los elementos no estructurales que causaron la mayor parte de las pérdidas humanas: parapetos de mampostería no reforzada y rellenos exteriores pertenecientes a edificios de estructura de hormigón armado de entre cuatro y seis plantas. En cuanto a la capacidad, se ha proporcionado un enfoque analítico derivado de consideraciones teóricas para caracterizar la curva de respuesta sísmica completa fuera del plano de muros en voladizo de mampostería no reforzada; así como una versión trilineal simplificada y más práctica de la misma. En cuanto a la demanda, se han probado varios métodos para caracterizar los espectros de respuesta del suelo de los edificios de hormigón armado presentes en la zona mediante estudios de casos. Los resultados de los análisis realizados han llevado a recomendar la implementación de las metodologías ya recogidas en la normativa italiana, NTC18, en la próxima normativa española, NCSR22.

Finalmente, se exponen algunas futuras líneas de investigación relacionadas con formas de combinar los avances en exposición y vulnerabilidad al realizar estudios de riesgo sísmico.

Acknowledgements

First and foremost, I am extremely grateful to my esteemed supervisors, Prof. Cervera, Prof. Savoia and Prof. Ferretti for their invaluable advice and guidance during this PhD. Their immense knowledge and experience have been crucial. Each one has offered me a different vision, which has given rise to a PhD dissertation that I consider half Spanish and half Italian.

To Prof. Jaime Cervera for motivating me to do this PhD dissertation and for his commitment and support throughout all of it. His impressive mastery in the field of building structures and personal example have taught me more than any student could wish for.

To Prof. Marco Savoia for his always-right recommendations, for opening the doors of his workplace and research group at the DICAM in such a cosy way and for providing me with materials and opportunities that without any doubt have improved this work.

To Prof. Francesca Ferretti for her excellent ideas, continuous guidance, time and patience.

Additionally, I have to mention all the people, institutions and research groups for which I am really thankful.

To the research group in Seismic Engineering at the Universidad Politécnica de Madrid (GIIS-Topography) and her coordinator, Prof. Belén Benito, for their contributions to the elaboration of this research, for becoming much more than colleagues and for helping me to find my vocation.

To the Department of Civil, Chemical, Environmental and Materials Engineering (DICAM) at the University of Bologna for offering me their help, advice and a friendly environment to work in.

To the Reale Collegio di Spagna in Bologna, for allowing me to live this extraordinary experience there and giving me the opportunity of studying seismic engineering in Italy and developing this research in co-tutorship. As well as to my colleagues for making the stay in Bologna so pleasant and fruitful in all senses.

To my colleagues from the Departamento de Estructuras y Física de la Edificación (DEFE) of the Escuela Técnica Superior de Arquitectura de Madrid, UPM, for facilitating me to carry out this research in the best conditions.

To all the good people that I have had the opportunity to know thanks to this dissertation and during it, especially to those that have become partners and friends.

To my best friends for all the moments shared.

To my family for their never-ending love, especially my mother, who is at the heart of it all, and my godson Leo, the joy of it all.

To my resilience and eagerness to learn.

To the Heart of the world, Jesus, for always being at my right hand.

*A Dios,
a mi familia por apoyarme,
a mis amigos por alegrarme,
a mis maestros por enseñarme.*

Contents

Introduction	1
0.1 Motivation	1
0.1.1 Framework of the PhD dissertation	1
0.1.2 The case of Lorca	2
0.2 Objectives and scope of the study	3
0.3 Structure of the PhD dissertation	4
References	6
1 State of the art	8
1.1 Seismic risk	8
1.2 Seismic vulnerability of buildings	11
1.2.1 Probability and costs: fragility	11
1.2.2 Methodologies for assessing seismic vulnerability of buildings	15
1.3 Seismic vulnerability of non-structural elements	19
1.3.1 Seismic capacity of non-structural elements	19
1.3.2 Seismic demand of non-structural elements: filtering effects of the building	21
1.4 The case of Lorca	22
1.4.1 The city of Lorca and seismicity	23
References	32
2 Exposure of Lorca: maps and analyses	37
2.1 Exposure	37
2.1.1 State of the art	37
2.1.2 Exposure maps	40
2.2 Masonry and reinforced concrete typologies	49
2.2.1 Reports	49
2.2.2 Masonry typologies	49
2.2.3 Reinforced Concrete structure typologies	56
2.3 Conclusions	63
References	64
3 A methodology to assess and select fragility curves for seismic risk studies	66
3.1 State of the art	66
3.2 Select.FC: a methodology to assess and select fragility curves	67
3.2.1 Variable selection and evaluated dimension	68
3.2.2 Practicality of the methodology	75
3.2.3 Classification of fragility curves	75
3.3 Application to the case of Costa Rica	76
3.3.1 The Costa Rica case study	76
3.3.2 Results and discussion	77
3.4 Application to the case of Lorca	89
3.5 Conclusions and future lines of research	91
References	94

4	Vulnerability of Lorca masonry buildings: fragility curves	98
4.1	Methodology	98
4.2	A simplified method: RE.SIS.TO®	101
4.2.1	Phase 1) Geometric Survey	102
4.2.2	Phase 2) Shear resistance	103
4.2.3	Phase 3) Comparison between acceleration and demand	104
4.3	Buildings' features and seismic vulnerabilities	105
4.3.1	Buildings' features	105
4.4	Characterization of the seismic vulnerability by means of the RE.SIS.TO® method	105
4.4.1	Capacity estimate	106
4.4.2	Variability depending the seismic directionality	114
4.4.3	Demand estimate	117
4.4.4	Vulnerability and comparison Demand—Capacity	126
4.4.5	RE.SIS.TO classification	126
4.4.6	Possible interventions	127
4.5	Fragility curves of the masonry typologies of the municipality of Lorca	127
4.5.1	Methodology to develop the fragility curves	128
4.5.2	Results	133
4.6	Conclusions and future line of development of seismic risk studies	143
	References	144
5	Capacity of non-structural elements of RC buildings. A model for the characterisation of the out-of-plane behaviour of URM walls	147
5.1	State of the art	147
5.2	Methodology	150
5.2.1	Analytical approach	151
5.2.2	Calculation of the fundamental periods and energies	162
5.3	Results and discussion	167
5.3.1	Comparison with different experimental studies reported in the literature	167
5.3.2	Comparison with other proposals	170
5.4	Conclusions	171
	References	172
6	Demand of non-structural elements of RC buildings. Filtering effects	175
6.1	4 to 6-storey RC residential buildings: case studies	176
6.1.1	Case studies	176
6.2	Bare structure models	178
6.2.1	Results in terms of Floor Response Spectra and discussion	179
6.2.2	Conclusions for the bare structure model	182
6.3	Model updating considering non-structural elements	182
6.3.1	Dynamic properties and numerical model of the case study	182
6.3.2	Floor Response Spectra	189
6.3.3	Results in terms of Floor Response Spectra	191
6.3.4	Conclusions and recommendations	195
	References	195
7	Conclusions and future lines of research	198
	Appendices	202
A	RESISTO: example of application	203
A.0.1	Description	203
A.0.2	Application of the RE.SI.STO method	205
A.0.3	Vulnerability and comparison Demand—Capacity	211
A.0.4	RE.SIS.TO classification	211

B Buildings A and B	212
B.1 Building A	212
B.1.1 Report	212
B.2 Building B	218
B.2.1 Report	218

List of Figures

1.1	Relationships between human fatalities and material damage and human fatalities and earthquake magnitude. Figures taken from [23]	12
1.2	Conceptual scheme of the performance-based seismic design method. Left: the intersection of the capacity and demand curves defines the performance point (red circle). Right: the intersection between the performance point (represented by the vertical red line) with the fragility curves provide the estimate of damage to buildings. Taken from [90].	15
1.3	Correlation between vulnerability classes and structural types. Source: EMS-98 [34]	18
1.4	Localization of the city of Lorca	23
1.5	1: Buildings of Lorca depending on the year of construction	24
1.6	1: Buildings of Lorca depending on the year of construction	25
1.7	Photograph of a neighborhood of Lorca.	27
1.8	Damage probabilities for existing construction typologies in Lorca, evaluated for the same seismic input. Figures taken from the RISMUR II project [51]. Top: results from the application of the fragility curves proposed by Lagomarsino and Giovinazzi (2006) Bottom: results from the application of the fragility curves proposed within the RISK-UE project.	30
2.1	Typologies Murcia	39
2.2	Map of historical evolution in relation to the appearance of the different Spanish seismic codes	42
2.3	Map of masonry typologies	43
2.4	Map of masonry typologies classified by height	44
2.5	Map of RC typologies	45
2.6	Map of RC typologies classified by height	46
2.7	Map of the state of damage of buildings	47
2.8	Total RC buildings vs reports by year	48
2.9	Type M11-pre. Traditional materials of construction in Lorca: rock walls.	51
2.10	Wood flooring systems: typologies M11-pre and M31-pre	52
2.11	Typology M11-pre. Typical damage: disconnection between walls.	53
2.12	Type M31-pre and M34-pre: typical load-bearing walls in Lorca.	54
2.13	Type M34. Typical flooring systems in Lorca: RC joists.	55
2.14	Statistical analyses of four to six-storey RC residential buildings on the basis of 65 experts' reports.	58
2.15	Damages to unreinforced masonry infill walls located on vertical communication cores	59
2.16	Damages to non-structural elements located in the common areas of the ground floor	59
2.17	Damages to interior and exterior claddings panels	60
2.18	Damages to exterior infill walls (interior and exterior façades)	60
2.19	Damages to interior infill walls	61
2.20	Damages to unreinforced masonry roof parapets	61
2.21	Damages to unreinforced masonry roof chimneys	62
3.1	Conceptualization, dimensions, and variables of the index proposed to evaluate FCs. Maximum scores in brackets.	69

3.2	Dimensions, variables, and categories of the index to evaluate FCs and their corresponding weights. Moreover, an example of the evaluation of three FCs in the case of two-storey reinforced confined masonry buildings of Costa Rica. Note: SDOF: Single Degree of Freedom, IDR: inter-story drift ratio, PGA: Peak Ground Acceleration, PGD: Peak Ground Displacement, EMS-98: European Macroseismic Scale, SB: Specific building, BPR: Building prototype. The 3 sources of uncertainty of FC parameters are: (i) uncertainty in the seismic demand, (ii) uncertainty in the capacity of the building, (iii) uncertainty in the definition of damage thresholds ([52, 7]) Classification: Class A: (85, 100], Class B: (65, 85], Class C: (55, 65], Class D: (47, 55], Class E: (40, 47] and Class F: (0, 40] points.	74
3.3	Conceptualization and example of applicability of the different dimensions defined for the methodology.	75
3.4	Fragility curves classification.	76
3.5	Example of application: Costa Rica. Note: TH (ThresHold) class refers to the threshold for each specified class.	83
3.6	Comparison of the scores of the different sub-dimensions and dimensions for the FC evaluated.	84
3.7	Correlation matrix between the sub-dimensions of the technical suitability dimension for FC of Costa Rica.	84
3.8	Fragility curves evaluated in the study: MRC+CBH/LWAL/HEX:2, 2-storey reinforced confined masonry building. Note: DS: Damage State. DS1-4: Slight - Moderate - Severe damage - Collapse. (X): Class of the curve, also differentiated by colours. Attributes: SS - Structural System, NF - Number of floors and DUC - ductility. Acronyms for the attributes regarding Building Class Similarity dimension: SS - Structural System, NF -Number of floors and DUC - ductility. When the acronym of a specific attribute or several of them (connected by the "+" symbol) appear into the legend is because said attribute can be considered equal for both typologies, the typology for which the FC was elaborated and the studied typology. Otherwise, its absence (symbolized by"—") means that said attribute is not equal for both typologies.	85
3.9	Fragility curves evaluated in the study: MRC+CBH/LWAL/HEX:1, 1-storey reinforced confined masonry building. See Figure 3.8 for label descriptions.	89
3.10	Example of fragility curves evaluated in the study: RC/LDUAL/HBET:11+/IRRE/FC, more than eleven-storey reinforced concrete with dual system. See Figure 3.8 for label descriptions. (X)*PROPOSAL (dotted line curve): FC proposed by the authors, result of a consolidation of the FCs in the best class with the conflation method.	90
3.11	Example of fragility curves evaluated in the study: RC/LWAL/HBET:5,1/IRRE/FC, One to five-storey reinforced concrete with wall system. See Figure 3.8 for label descriptions.	91
3.12	Example of fragility curves evaluated in the study: RC/LDUAL/HBET:5,1/IRRE/FC, one to five-storey reinforced concrete with dual system. See Figure 3.8 for label descriptions. (X)*PROPOSAL (dotted line curve): FC proposed by the authors, result of a consolidation of the FCs in the best class with the conflation method.	93
4.1	Studied masonry typologies	99
4.2	Studied masonry typologies (zoom)	100
4.3	logoRESISTO	104
4.4	Different plan configurations. (GNDT II Level Form)	111
4.5	Different elevation configurations. (GNDT II Level Form)	111
4.6	Different plan configurations. (GNDT II Level Form)	112
4.7	Resistance of all the buildings under study	115
4.8	Relationship between a number of parameters studied and the PGA_c of all the buildings under study	116
4.9	Vulnerability of all the buildings under study	117
4.10	Relationship between the maximum and the minimum Sa_c of all the buildings under study	118
4.11	Vs30 map of Lorca city following criteria from the EC8 and NERRP site class codes (Holzer et al. 2005; NEHRP 2001; EN 1998). (Credits: Figure 11, [16])	122
4.12	Seismic hazard maps for Lorca, Spain	124
4.13	Buildings classification according to the RESISTO method.	126
4.14	Buildings classification according to the RESISTO method.	127

4.15	Type of vulnerability for each of the studied parameters (see Table 4.1). Parameters: 1. Type and organization of the resistant system; 2. Quality of the resistant system; 4. Location of the building and foundations; 5. Horizontal structural elements; 6. Plan configuration; 7. Elevation configuration; 8. Maximum distance between walls; 9. Roof system; 10. Non-structural elements; 11. State of conservation.	128
4.16	Conceptual schema of the proposal basis.	133
4.17	M11: Calibration of the response surfaces parameters for the different cases considered	135
4.18	M31: Calibration of the response surfaces parameters for the different cases considered	136
4.19	M34: Calibration of the response surfaces parameters for the different cases considered	137
4.20	M11: Calibration of the FC for the different cases	138
4.21	M31: Calibration of the FC for the different cases	139
4.22	M31: Calibration of the FC for the different cases	140
4.23	Fragility curves in Sa_c for the different cases: (i) Minimum capacity, (ii) Maximum capacity and (iii) case considering the seismic directionality. (See Fig. 4.24 for a better interpretation of results).	141
4.24	Fragility curves typology by typology in Sa_c for the different cases: (i) Minimum capacity, (ii) Maximum capacity and (iii) case considering the seismic directionality. Top: typology M11; center: typology M31; bottom: typology M34	142
4.25	Fragility curves in Sa_c for the (iii) case: considering the seismic directionality according to the proposed methodology.	144
5.1	Figura de Lorca, con permiso	148
5.2	Boundaries and loading conditions	151
5.3	Eccentricities and limit stresses	152
5.4	Deflection and deformed shape of the wall relative to the elastic deflection	156
5.5	Capacity curve of walls	157
5.6	Trilinear curve parameter setting	160
5.7	Laws of $\beta(\lambda, t/(\sigma_c/\rho), E/\sigma_c, \sigma_t/\sigma_c)$	161
5.8	Expressions for the key points of the trilinear curves	162
5.9	Free vibration modes of the elastic cantilever	164
5.10	Function for the period of oscillation of the rigid block	166
5.11	Mass coefficient, rigid body	167
5.12	Comparison between experimental and analytical results	169
5.13	Quotient between the period estimated according to the NZSEE regulation [29] (T_a , eq. 5.95) and the analytical approach and formulae herein proposed (T_b , eq. 5.96).	172
6.1	Schema of the seismic wave transformations from the earthquake origin to the NSC Node of Control. - Actual transformations [0 \rightarrow 2 \rightarrow 3 \rightarrow 4]: (0) Epicentre \rightarrow (2) Building base \rightarrow (3) NSC base \rightarrow (4) NSC node of control. - Analytically simulated transformations [1 \rightarrow 2 \rightarrow 3]: (1) LOR Station (actual registers) \rightarrow (2) Building base [[4]] \rightarrow (3) NSC base (input used for state of damage analysis)	176
6.2	Map of RC buildings' typologies and heights, with the location of the fatalities in the 2011 Lorca earthquake	177
6.3	Bare structure models of Building A and Building B	179
6.4	a) and b) Comparison between linear and non-Linear FRS in two points of Building A for two different directions of motion c) and d) Comparison of FRS of three different Ground Floor Stiffness Ratios ($R_{GF, stiff}$): 1, 0.8 and 0.4. Range of periods: Rigid NSC, elastic period for rigid NSE such as URM Spanish parapets according to OMA analysis (see also Fig. 5.12); T1 PW and IMW, values of T1 for Spanish parapets and infill walls according to [16]'s trilinear simplification; T2 PW and IMW, values of T1 for Spanish parapets and infill walls according to [16]'s trilinear simplification. See the said publication for greater detail.	180
6.5	Comparison between non-linear and [19] FRS: a) and b) in two points of Building A for two different directions of motion; and c) in column 1 of building B. B.A.= Building A; B.B.= Building B; Col.= Column.	181
6.6	Photograph of the Tromino (MoHo s.r.l.) portable 3D velocity sensor during the measurements in Lorca	183
6.7	Results in terms of SSRR vs frequencies according to the SSRR technique for Building A. See Fig. 6.10 for the location of points P1, P2, P3 and P4.	184
6.8	Conceptual schema of the SSI technique.	185
6.9	Building A	186

6.10	(Left) 3D model of the case study: a RC residential building of Lorca (diagonal struts in red; stairs and wall of the elevator in blue). (Centre) First mode of vibration. (Right) Location of the Tromino Device during the Ambient Vibration Tests carried out (Number of Floor in Roman Numbers).	187
6.11	Comparison of the mode shapes of the firsts three modes of Building A. Obtaining from: top) modal analysis of the bare structure numerical model; centre) modal analysis of the bare structure numerical model; and bottom) comparison of the SSRR resulting from the operational modal analysis.	188
6.12	SSRR vs frequency obtained for the 4th floor according to the SSRR technique for Building A. See Fig. 6.10 for the location of points P1, P2, P3 and P4.	189
6.13	FRS floor by floor for two different columns of the building with out-of-plane acceleration in orthogonal directions (See Figure 6.3 for the locations of Columns 1 and 2 on Building A and Figure 6.10 for the infilled framed model used for the analysis). LTHA with synthetic the accelerograms elaborated for SP11 (the nearest point to Building A), SP2 (the nearest point to Building B) and LOR (the accelerograms recorded at the LOR station). The three colours represent three different orientations for the seismic inputs: Orange= in the same direction as the Lorca actual earthquake; Green= the North direction of the input (main one) is applied in the longitudinal direction of the building; and Blue= the North direction of the input (main one) is applied in the transversal direction of the building.	192
6.14	Spectra in X (longitudinal) and Y (transversal) direction for the point A of the case study building (4th floor).	193
6.15	Results in terms of frequencies according to the SSRR technique for a parapet located in the fifth floor of Building A.	194
6.16	Spectra in X (longitudinal) and Y (transversal) direction for the 4th floor, points A and B of Building A considering three different models and analyses: (i) bare structure model and LTHA; (ii) bare structure model and NLTHA; and (iii) infilled frame model and LTHA. Gray points indicates possible intermediate states that depends on the frequency content of the seismic wave.	194
A.1	Geometry of the building selected to illustrate the RESISTO method	204
A.2	Representation in plan view of the areas of load-bearing masonry walls of the building under study: x-direction in red and y-direction in turquoise	206
A.3	Photographs of the building under study	208
A.4	Photographs of the building under study	209
A.5	Photographs of the building under study	210
A.6	Photographs of the building under study	211
B.1	Photographs of Building A: general	214
B.2	Building A: structural design	215
B.3	Photographs of Building B: structural elements damage	216
B.4	Photographs of Building A: non-structural elements damage	217
B.5	Photographs of Building B: general	221
B.6	Building B: structural design (damaged columns enumerated)	222
B.7	Photographs of Building B: structural elements damage	223
B.8	Photographs of Building B: non-structural elements damage	224

List of Tables

1.1	Structural typologies present in the municipality of Lorca. Table included in the report of the RISMUR II project. [51]. Nomenclatures were established according to RISK-UE [76]	29
2.1	Transfer matrix proposed by Patrick Murphy for the assignation of typologies	40
2.2	CARTIS form for the types identified in Lorca	50
3.1	Attributes considered and their corresponding scores for the adjustment coefficient related to building class similarities. Note: Height ranges: low, 1 to 3 stories; mid, 4 to 7 stories; and high, 8 or more stories (based on [21]. *When the typology studied and that of the FC present one, two, or three, or more of any of the attributes listed, it receives a score of 0.70, 0.85, or 1, respectively, in this dimension.	73
3.2	Principal studies and projects on seismic vulnerability in Costa Rica. [Table 1/3]	78
3.3	Principal studies and projects on seismic vulnerability in Costa Rica [Table 2/3].	79
3.4	Principal studies and projects on seismic vulnerability in Costa Rica. [Table 3/3]	80
3.5	Scores and final class for FCs assessed for some building typologies in Costa Rica following the methodology proposed. CC BV: Capacity Curve Block of Variables(BV), FC BV: Fragility Curve BV, SQ BV: Source Quality BV, TS: Technical Suitability dimension, LS:local System dimension, BCS: Building Class Similarity. References: [28, 34, 21, 19, 32, 13, 37, 62, 15, 4, 30].	86
3.6	Scores and final class for FCs assessed for some building typologies in Costa Rica following the methodology proposed. CC BV: Capacity Curve Block of Variables(BV), FC BV: Fragility Curve BV, SQ BV: Source Quality BV, TS: Technical Suitability dimension, LS:local System dimension, BCS: Building Class Similarity. References: [28, 34, 21, 19, 32, 13, 37, 62, 15, 4, 30].	87
3.7	Scores and final class for FCs assessed for some building typologies in Costa Rica following the methodology proposed. CC BV: Capacity Curve Block of Variables(BV), FC BV: Fragility Curve BV, SQ BV: Source Quality BV, TS: Technical Suitability dimension, LS:local System dimension, BCS: Building Class Similarity. References: [28, 34, 21, 19, 32, 13, 37, 62, 15, 4, 30].	88
3.8	Scores and final class for FCs assessed for some building typologies in Costa Rica following the methodology proposed. CC BV: Capacity Curve Block of Variables(BV), FC BV: Fragility Curve BV, SQ BV: Source Quality BV, TS: Technical Suitability dimension, LS:local System dimension, BCS: Building Class Similarity. References: [33], [25] and Chapter 4 of this PhD dissertation. fl. s.= flooring system	92
4.1	Parameters, vulnerability classes, scores and weights of the GNDT seismic vulnerability sheets II level for masonry buildings	103
4.2	Values of loads per unit area of each floor [kN/m^2]. FS = flooring system. W= wood, Cñ =“Cañizo” (straw and canes joint with plaster), RC= Reinforced Concrete.	107
4.3	Values of $S_{(a,c)}[g]$ and $PGA_c[g]$ for all the buildings under study. X*: buildings with one floor. [M34]: type M34 with steel pillars	114
4.4	values of $\alpha_{PM}, \alpha_{AD}, \alpha_{DT}$ and α_{DUC} for the buildings under study	114
4.5	Values of $S_{(a,c)}[g]$ and $PGA_c[g]$ for all the buildings under study in the most favorable direction. X*: buildings with one floor. [M34]: type M34 with steel pillars	118
4.6	Coefficient C_U according to each class of use	119
4.7	Coefficient V_N according to the type of construction	120
4.8	Summary of main parameters	120
4.9	Probability of exceeding the limit for S_a during the reference period according to the limit state under study	120

4.10	<i>PGA_d</i> : Demand of Peak Ground Acceleration according to the different regulations and the seismic hazard maps applicable to Lorca.	126
4.11	Summary of parameters for the building taken as an example	126
4.12	Main features of the buildings studied in relation to the development of FCs. Parameters denoted with the word <i>unique</i> make reference to the Directionality Case (iii). - τ_0 in kN/m^2 ; - $A_r/A_{t,min}$ or max or <i>unique</i> without units. $A_{r,min}$ and $A_{r,max}$ are the resistant area of the walls in either direction of the two main orthogonal considered, specifically, the one corresponding to the story with the minimum resistant capacity in terms of $S_{a,c}$. A_t is the floor area corresponding to the floor with the resistant area considered for $A_{r,min}$ and $A_{r,max}$. $A_{r,unique}$ is the A_r calculated according to the proposal to consider the seismic directionality (Eq. 4.31), and A_t the floor area for which has been calculated; - $S_{a,min}$ or max or <i>unique</i> in g . * In some cases, the worst floor is not the same when considering the x and y directions. For that reason, in these cases, it may occur that $A_{r,min}$ is greater than $A_{r,max}$, or, $A_r/A_{t,min}$ is greater than $A_r/A_{t,max}$ or $A_r/A_{t,unique}$. This is for example the <i>m3</i> building case. In these situations, $A_{r,max}$ has not been considered the area of greater value because, for coherence, it must correspond with the value that relates to the maximum resistant capacity in terms of $S_{a,c}$	132
4.13	Summary of coefficients of the response surfaces.	134
4.14	Summary of parameters. Buildings data: median and standard deviation of the parameters used as inputs of the Monte Carlo procedure, A_r/A_t and τ_0 . FC for both directions: values of the median and standard deviation of the FC resulting from the application of the procedure for each typology in both directions (FC represented in Figs. 4.23 and 4.24).	143
4.15	Summary of parameters. Unique FC for both directions: values of the median and standard deviation of the FC resulting from the application of the procedure for each typology according to the proposal (FC represented in Figs. 4.23, 4.24 and 4.25). Conflation applied to Model B Equation for the Cases of M31 and M34.	143
5.1	Most significant experimental studies regarding flexible cantilever URM walls subjected to OOP loading and their contributions to the field. CM= Cantilever Mechanism, SDOF= Single Degree of Freedom.	149
5.2	Force-displacement ($F-d$) idealisations proposals available to date, including fundamentals and main characteristics. CM= Cantilever Mechanism, SSW = Simply Supported Walls, MBM= Multi-Block Mechanisms.	150
5.3	values for the fundamental variables of masonries	156
5.4	Masonry quality values for setting graphs	160
5.5	Coefficients for the first free oscillation modes of the elastic cantilever ($\eta_i = 2\pi\gamma_i^2$). $T_{0,i} = \eta_1 \sqrt{\frac{mh^3}{EI}}$	164
5.6	Dynamic parameters of walls: alternatives.	166
5.7	Brief description of the samples and their corresponding experiments: 1. The experiment, 2. The results documented in terms of relationships between displacements and frequencies or forces, 3. Dimensions and materials, 4. Estimate of the undocumented properties.	168
5.8	values for the fundamental variables of masonries	170
5.9	values for the fundamental variables of masonries	170
6.1	Main frequencies of vibration of Buildings A. Values ordered for an easy comprehension of similar results.	185
A.1	Areas in square meters [m^2] of load-bearing walls in the building under study and interstorey height [m]. $A_{x,i}$: walls area in x direction. $A_{y,i}$: walls area in y direction. $A_{t,i}$: total surface area of the floor. h: interstorey height. Gf: ground floor.	205
A.2	Values for the mechanical properties: minimum-(medium)-maximum according to the NTC08 regulation.	206
A.3	Values of loads per unit area of each floor [kN/m^2]. FS = flooring system. W= wood. Cñ =“Cañizo” (straw and canes joint with plaster).	206
A.4	values of resistant cuts, stress cuts and the relationships between them, considering $\tau_0 = 15kN/m^2$ and $w = 19kN/m^3$	207
A.5	Values of the parameter (1) to (11) for the building under study	209
A.6	Values of the reductive coefficient $C_{r,id}$ for the building under study	210
A.7	Summary of parameters for the building taken as an example	211

Introduction

0.1 Motivation

Earthquakes are unavoidable natural phenomena that can cause great human and economic losses if the population is not properly prepared. Six earthquakes appear among the ten catastrophes with the highest rate of mortality, with the number of fatalities in developing countries being particularly dramatic. Moreover, two earthquakes have provoked the most expensive disasters stemming from a natural phenomenon. Therefore, insisting on the reduction of the vulnerability of constructions and on the improvement of the seismic regulations constitutes an ethical imperative and a very cost-worthy investment.

In recent decades, several earthquakes have highlighted the vital importance of knowing the hazard and the seismic risk that affects a population, in order to introduce mitigation measures such as the preparation of emergency plans for rapid and effective post-event actions aimed at reducing the effects after the earthquake. However, the main objective is always prevention. And this concept points directly to more profound research in the field of seismic design and performance, given the decisive influence exerted by the behaviour of buildings on the final results of human and economic losses. The improvement of the seismic-resistant design of the infrastructures and buildings is equivalent to a drastic reduction of the probability of an occurrence of a disaster, as exemplified by the following cases.

On the one hand, an earthquake of moderate magnitude can cause a disaster when a city with a low level of seismic hazard has very vulnerable buildings due to the absence of seismic-resistant design standards. The 2010 Haiti earthquake, of moderate magnitude, $7 M_w$, caused about 300,000 fatalities and the destruction of almost a quarter of the homes in Port-au-Prince. The cost of rebuilding houses, schools, streets and other infrastructure was valued at around 14 billion dollars.

On the other hand, earthquakes of higher magnitudes can cause much lower human and economic losses in countries with very good seismic codes for buildings and infrastructures. This is the case of the $7.6 M_w$ Guanacaste earthquake in Costa Rica, which occurred only two years after the 2010 Haiti earthquake. In this case, although the shock was quite strong, only two people died and the damage was not too severe. Specifically, only 56 schools in the country had to be demolished and rebuilt, and the costs for public infrastructure and housing were valued at 44 million dollars [2]. In relation to such a particular country, the author of this dissertation has been able to verify first-hand that, its low level of seismic vulnerability is the fruit of continuous development in seismic regulations. This benefit is also extended to humble dwellings located in disadvantaged neighbourhoods as construction workers with fewer resources reproduce in their own houses the construction techniques seen when constructing buildings designed by a structural engineer.

In addition, experience has demonstrated that the vulnerability of buildings and infrastructures makes a crucial difference regarding the seismic impact on society in terms of human losses versus economic costs. The highest numbers of human losses are mainly located in the less developed regions of the world, while the economic ones are located mostly in the developed world. This fact can be partially observed in the lists of the ten worst events of the 20th century and of the 21st century (so far) from the perspective of each type of damage (see Chapter 1, [5]).

0.1.1 Framework of the PhD dissertation

This PhD dissertation is being developed within the framework of the Kuk-Ahpán project of the Spanish State Research Plan. Its full title is Kuk-Ahpán: Integrated Regional Study of the Structure and 4D Evolution of the Lithosphere in Central America. Implications in the Calculation of the Seismic Hazard And Risk. Said project

involves the participation of researchers from all Central American countries (Honduras, Nicaragua, Costa Rica, El Salvador, Guatemala, Panama and Mexico) and several European institutions (from Spain and Norway). That establishes scientific-technical cooperation to conduct research in two application scenarios: Central America and Southeast Spain.

The project is proposed with two large application scenarios:

1. Central America and the Caribbean, a region that, due to the high speed of convergence between the Cocos, North America and Caribbean plates, presents high seismicity, which constitutes a natural laboratory for experimentation;
2. Southeast of Spain (SE), a region with a rate of deformation lower than that of the previous scenario, which implies a smaller volume of records available, entailing the need to apply models and techniques experienced in areas such as the previous one.

In summary, the general idea of the project is to involve a high number of experts from different disciplines from all over the world in order to develop a multidisciplinary work that can produce feedback among locations and researchers.

Furthermore, this dissertation is the product of a co-tutorship agreement between the Universidad Politécnica de Madrid (UPM) and the University of Bologna (UniBo). This collaboration has permitted the author of this research to learn from Italian experts and incorporate Italian methodologies into the study of Lorca and Central America. Good examples of this learning are the application of a methodology developed at the UniBo, RESISTO®, for characterising the vulnerability of Lorca building or the assessment of the accuracy of the Italian code (NTC-18, [12]) for the characterization of the seismic demand of non-structural elements pertaining to Spanish buildings.

0.1.2 The case of Lorca

The general objective of this work is to research into the vulnerability of structural and non-structural elements on the basis of the earthquake of magnitude M_w 5.2 occurred in Lorca, Region of Murcia, on May 11, 2011.

The selection of the 2011 Lorca earthquake as the object of the investigation is based on two facts. The first one is that, despite being moderate, said seismic event left nine fatalities, 394 injured, a great number of buildings damaged and material damage valued at 800 million euros, being one of the most significant earthquakes in Spain in recent years. This seismic event was especially catastrophic due to the combination of moderate magnitude with little depth and a short epicentral distance to the population. The second one is that several research projects have been developed focused on these topics constituting a very appropriate starting point for further research on vulnerability:

- The seismic risk in general. The PhD dissertation of Ligia Elena Quirós-Hernández (2017), [16], and the RISMUR I (2008) and RISMUR II (2014) projects, [8] and [9].
- The exposure and vulnerability from an urban point of view. The PhD dissertation of Sandra Martínez-Cuevas (2014) [11].
- Particular aspects of the vulnerability of Lorca buildings. For example, the works of [7], [1] and [3].

Nonetheless, some vulnerability aspects were not within the scope of these works or sufficiently covered, such as the development of specific fragility curves for the buildings of Lorca or the proposal of more advanced techniques or alternative methodologies to characterise the seismic capacity and demand of non-structural elements. Moreover, said seismic risk studies reveal the lack of a methodology to assess the adequacy of fragility curves available in the literature for its application to a specific typology within the framework of a seismic risk study. These issues are within the scope of this research.

Underestimating the hazard and not taking measures to reduce seismic vulnerability is the reason why some moderate-magnitude earthquakes turn into disasters.

0.2 Objectives and scope of the study

This PhD dissertation has been developed with the purpose of providing knowledge on some aspects of the seismic vulnerability of structural and non-structural elements of buildings. Its objectives have been established from insights made after the study of the 2011 Lorca earthquake and its consequences. Several lines of research have been identified. In the following the objectives corresponding to the areas of investigation identified are presented.

(1) To elaborate an updated state of the art regarding the vulnerability of the structural and non-structural elements applicable to the Lorca buildings within the context of seismic risk studies .

This state-of-the-art must include the contributions to the vulnerability field of previous seismic risk studies and methodologies within which the city of Lorca can be included.

(2) To analyse and summarise the information available about the vulnerability of the main typologies of Lorca buildings and its completion by means of the analysis of a database of the buildings reports elaborated by architects and engineers .

Starting from the information contributed by previous exposure studies developed after the 2011 Lorca earthquake, further research on the most vulnerable aspects of the typologies identified can be performed on the basis of a database of experts' reports collected in the aftermath of the earthquake. This research will be focused on the identification of the most dangerous structural and non-structural elements and on their characterization.

(3) To propose a methodology to assess and select fragility curves for seismic risk studies consisting of a multidimensional index based on the most influential variables with respect to the seismic performance of buildings. This index can facilitate the creation of a rational ranking of the fragility curves applicable to the typology under study in terms of adequacy .

Seismic risk studies must deal with different types of uncertainties whose assessment methods are still under development, such as the complexity of selecting fragility curves from the catalogue of those available in the literature. The appropriate use of fragility curves allows a better approximation of the level of performance of a structural system in the face of seismic hazards. The calibration of the index with a case study and its application to the Lorca case study are also sub-objectives.

(4) To elaborate specific fragility curves for the typologies of the Lorca buildings .

The application of recent methodologies so as to develop fragility curves specifically for the building typologies of the city of Lorca. These typologies can be found all over Spain according to different authors.

(5) To develop a profound study about the capacity and demand concerning the non-structural elements of Lorca .

The nine fatalities incurred during the 2011 Lorca earthquake were due to falling debris from non-structural elements. A better comprehension of their behaviour is crucial for reducing their seismic vulnerability and the hazard they entail.

The scope of the dissertation is the development of methodologies that can be applied in Spain and Central America.

0.3 Structure of the PhD dissertation

The work developed for this doctoral dissertation is structured into seven chapters, which are described below.

Chapter 1: State of the art

In this Chapter, the state-of-the-art concerning different aspects of the vulnerability assessment of buildings and non-structural elements is introduced. Firstly, the framework of seismic risk and the concept of vulnerability in relation to it are presented. After that, the vulnerability of structural elements, mainly buildings, including definitions and the international initiatives for assessing it on a large scale are briefly discussed. Next, the topic of the vulnerability of non-structural elements is presented and recent prominent research works are introduced. In addition, the city of Lorca, the May 2011 earthquake, and the seismic risk studies developed in the said city are described. Finally, some aspects of buildings and non-structural elements' vulnerability concerning this city and its typologies of buildings are introduced and possible lines of research are revealed.

Chapter 2. Exposure of Lorca: maps and analyses

In this Chapter, the seismic exposure of Lorca is statistically and graphically studied and a number of exposure maps are elaborated. Moreover, the typologies of buildings identified are thoroughly characterised by means of the analysis of a database of more than 300 reports documented by experts just after the 2011 Lorca earthquake. Additionally, the most hazardous non-structural elements pertaining to common residential unreinforced concrete frame buildings are studied.

This research reveals the importance of characterizing adequately the capacity and demand of non-structural elements pertaining to infill framed reinforced concrete structure buildings. Particularly, reinforced masonry façades, infills and parapets. Moreover, it emphasizes the existence of some construction techniques that considerably increase the structural vulnerability of masonry buildings.

Chapter 3. A methodology for assessing and selecting fragility curves for seismic risk studies

This Chapter contributes a methodology for assessing and selecting fragility curves for seismic risk studies from a catalogue of existing proposals available in the literature. Moreover, the proposed methodology permits the recognition of the reliability level of the fragility curves obtained depending on which class the curve was classified into based on its score. Therefore, it allows the establishment of a manner of determining the adequacy and uncertainty related to the selected fragility curves, which is a subject that researchers should consider in seismic vulnerability and risk studies.

This research reveals the gap in the literature of adequate fragility curves to characterise the vulnerability of Lorca buildings, particularly those with a masonry structure.

This research has been accepted and is pending for publication in an International Journal:

- [Navas-Sánchez L.](#), Jiménez-Martínez M., González-Rodrigo B., Hernández-Rubio O., Dávila-Migoya LD., Orta-Rial B., Hidalgo-Leiva D. (2023). **A methodology to assess and select seismic fragility curves: Application to the case of Costa Rica.** *Earthquake Spectra*, 0(0). [10]

Chapter 4. Vulnerability of Lorca masonry buildings: fragility curves

This Chapter involves the calculation of the fragility curves for the residential masonry typologies of Lorca, by means of the application of the RE.SIS.TO method to estimate their seismic vulnerability. Moreover, the application of the Monte Carlo method to expand the results permits the prediction of a wider number of samples' responses in order to construct a more robust fragility curve.

The studied typologies are load-bearing masonry walls composed of rubble stone and/or fieldstone, load-bearing unreinforced masonry walls with wooden flooring systems and load-bearing unreinforced masonry walls with reinforced concrete flooring systems. The residential unreinforced masonry buildings studied in order to characterise their fragility curves have been taken from the database of reports by experts in the aftermath of the 2011 Lorca earthquake.

Chapter 5. Capacity of non-structural elements of RC buildings. A model for the characterisation of the out-of-plane behaviour of URM walls

This Chapter proposes an analytical approach derived from theoretical considerations to characterise the complete out-of-plane seismic response curve of unreinforced masonry cantilever walls. Masonry parapets and historical façades fall within this scope since in the past it was not customary to firmly connect walls to the horizontal structural elements in the past.

This research also provides a straightforward way of elaborating a simplified trilinear version of these curves by means of a series of non-dimensional mathematical expressions. Additionally, the characterisation of the oscillating periods and the kinetic energies of the walls are thoroughly discussed. Finally, the capability of the approach in terms of capturing linear and non-linear behaviour of masonry walls under horizontal loads is demonstrated via comparison with several tests reported in the literature.

This research has been published in an International Journal:

- [Navas-Sánchez L.](#), & Cervera Bravo J. (2022). **A theory-based simplified trilinear model for characterisation of the out-of-plane behaviour of URM walls.** *Engineering Structures*, 259, 114058. [14]

Chapter 6: Demand of non-structural elements of RC buildings. Filtering effects

This Chapter presents a study of the seismic wave transmission from the building base to the non-structural element base of four to six-storey RC Spanish residential buildings with a structure comprising reinforced concrete frames and interior and exterior unreinforced masonry infill walls and parapet walls by means of a case study. The bare structure as well as the infilled framed structure model cases are studied.

The research is particularly focused on the building properties that influence non-structural elements' damage and collapse by means of the Floor Response Spectra type of characterization of the seismic demand. Moreover, the accuracy of the Eurocode formulae (EN-1998) [6] for characterizing the Floor Response Spectra is addressed, and the possibility of implementing the proposals already included in the Italian code (NTC-18) [12] in the upcoming Spanish regulation (NCSR-22) [18] studied through the analysis of the response of a case study; namely, a building located in Lorca pertaining to the described structural type.

The results of this research have been published in two documents:

- [Navas-Sánchez L.](#), Cervera Bravo J., Benito MB., Gaspar-Escribano JM., Martínez-Cuevas S. (2021). **Damages in non-structural elements of RC residential buildings caused by the 2011 Lorca earthquake.** In 17th World Conference on Earthquake Engineering. *Sendai: 17WCEE*. [15].
- [Navas-Sánchez L.](#), Ferretti F., Savoia M., Gamboa-Canté C., Cervera Bravo J. (2023). **NSE seismic demand characterization: the case of a Spanish RC residential building.** *Procedia Structural Integrity*, vol. 44, pp. 418-425. [13].

Chapter 7. Conclusions and future lines of research

This Chapter contains a summary of the work carried out, together with the conclusions derived from the results of all the chapters, recommendations and future lines of research.

Appendices

Complementary and detailed information on methods or samples applied in this dissertation that may be useful for future studies is included.

Other results concerning the research

The author of this dissertation is also co-author of four of the eight chapters that composed the following book about seismic engineering:

- Conde-Conde J., Benito MB., Bernabeu Larena A., de la Cal Manteca M., Cervera Bravo J., Gómez-Mateo J., Muñoz Millán MA., Navas-Sánchez L., & de la Torre, J. F. (2021). **Estructuras sismorresistentes: Fundamentos de proyecto**. UPM Press. [5].

Moreover, she has presented contributions in the following conferences in several countries:

- 17WCEE, World Conference of Seismic Engineering. *Sendai, Japan: 2021*
- XIX ANIDIS, Associazione Nazionale Italiana di Ingegneria Sismica) Conference of Seismic Engineering in Italy. *Turin, Italy: XIX ANIDIS - SSA annual meeting 2023, Seismological Society of America Annual Conference 2023. San Juan, Puerto Rico: 2023*
- XXIV ISPRS Congress, International Society for Photogrammetry and Remote Sensing. *Nice, France: 2021*
- XIV Congreso Geológico de América Central y VII Congreso Geológico Nacional. *San José, Costa Rica: 2022*
- DinEst 2018, 1st Spanish Conference on Structural Dynamics. *Madrid, Spain: 2022*
- 10ª Asamblea Hispano Portuguesa de Geodesia y Geofísica. *Toledo, Spain: 2023*
- CIGEO'17, Primer Congreso en Ingeniería Geomática. *Valencia, Spain: 2017*

- Romero-Jaren, R., Arranz, JJ., Navas-Sánchez L., Erduran, E., Martínez-Cuevas, S., Benito, B. (2021). **Automatic segmentation of point clouds in the architecture environment**. *International Archives of Photogrammetry, Remote Sensing and Spatial Information Sciences*, vol. XLIII-B2-2021. [17].

In addition, she is a co-author of a journal paper regarding the ductility of structures, a relevant concept for the field of seismic engineering.

- Cervera Bravo J. & Navas-Sánchez L. (2021). **Prestress behaviour and ductility requirements in structures: solutions from a unified algebraic approach**. *Royal Society Open Science*, 8(12), 210459. [4]

Finally, with respect to the methodology presented in Chapter 3 to select seismic fragility curves, *Select.FC*, it is worth mentioning that an application with an open database of fragility curves for specialists of seismic risk is being developed thanks to a competitive aid awarded by a Spanish bank (Eurocaja Rural) specifically for this.

References

- [1] R Álvarez-Cabal, E Díaz-Pavón, and R Rodríguez-Escribano. “El terremoto de Lorca: Efectos en los edificios”. In: *Madrid, Consorcio de Compensación de Seguros, Ministerio de Economía y Competitividad* (2013).
- [2] Rafael Barquero and Wilfredo Rojas. “The Guanacaste (Costa Rica) Earthquake of September 5th, 2012 (Mw 7, 6)”. In: *EERI Report available online. Last visit 10/05/2023*. (2012). URL: <https://www.eeri.org/wp-content/uploads/THE-GUANACASTE-COSTA-RICA-EARTHQUAKE-OF-SEPTEMBER-5th-2012-Mw-76.pdf>.
- [3] Luis Cabañas Rodríguez et al. “Informe del sismo de Lorca del 11 de mayo de 2011. Last visit 10/05/2023”. In: *Instituto Geográfico Nacional (España)* (2011). URL: <http://hdl.handle.net/10261/62381>.
- [4] Jaime Cervera Bravo and Laura Navas-Sánchez. “Prestress behaviour and ductility requirements in structures: solutions from a unified algebraic approach”. In: *Royal Society Open Science* 8.12 (2021), p. 210459. DOI: [10.1098/rsos.210459](https://doi.org/10.1098/rsos.210459).
- [5] Jorge Conde-Conde et al. *Estructuras sismorresistentes: Fundamentos de proyecto*. UPM Press, 2021. ISBN: 8418661100.
- [6] EN-1998. “Eurocode 8: Design of structures for earthquake resistance - Part 1 : General rules, seismic actions and rules for buildings”. In: *European Committee for Standardization, Brussels*. (2003).
- [7] Lutz Hermanns et al. “Performance of buildings with masonry infill walls during the 2011 Lorca earthquake”. In: *Bulletin of Earthquake Engineering* 12.5 (2014), pp. 1977–1997.
- [8] RISMUR I. *Estudio de Riesgo Sísmico en la provincia de Murcia (Proyecto RISMUR)*. *Broadway Malyan, Grupo de Tectónica Activa y Paleosismicidad (Universidad Complutense de Madrid, UCM), Grupo de Ingeniería Sísmica (Universidad Politécnica de Madrid, UPM)*. 2008.
- [9] RISMUR II. *Servicio de Actualización del Análisis de Riesgo Sísmico (RISMUR) en la Región de Murcia. ETSI Topografía, Geodesia y Cartografía (Universidad Politécnica de Madrid, UPM), Grupo de Ingeniería Sísmica (UPM)*. 2014.

- [10] Navas-Sánchez L et al. “A methodology to assess and select seismic fragility curves: Application to the case of Costa Rica”. In: *Earthquake Spectra* 0(0) (2023). DOI: [10.1177/87552930231171177](https://doi.org/10.1177/87552930231171177).
- [11] Sandra Martínez Cuevas. “Evaluación de la vulnerabilidad sísmica urbana basada en tipologías constructivas y disposición urbana de la edificación. Aplicación en la ciudad de Lorca, región de Murcia”. PhD thesis. Universidad Politécnica de Madrid, 2014. URL: oa.upm.es/30447/.
- [12] NTC18. “Aggiornamento delle Norme tecniche per le costruzioni, 20 febbraio”. In: *Decreto Ministeriale del Ministero delle Infrastrutture e dei Trasporti* 42 (2018).
- [13] L Navas-Sánchez et al. “NSE seismic demand characterization: the case of a Spanish RC residential building”. In: *Procedia Structural Integrity* 44 (2023), pp. 418–425. DOI: [10.1016/j.prostr.2023.01.055](https://doi.org/10.1016/j.prostr.2023.01.055).
- [14] Laura Navas-Sánchez and Jaime Cervera Bravo. “A theory-based simplified trilinear model for characterisation of the out-of-plane behaviour of URM walls”. In: *Engineering Structures* 259 (2022), p. 114058. DOI: [10.1016/j.engstruct.2022.114058](https://doi.org/10.1016/j.engstruct.2022.114058).
- [15] L. Navas-Sánchez et al. “Damages in non-structural elements of RC. residential buildings caused by the 2011 Lorca earthquake”. In: ed. by 17WCEE 17th World Conference on Earthquake Engineering. Vol. 10a-0048. 2021.
- [16] Ligia Elena Quirós Hernández. “Modelizaciones y análisis de sensibilidad en la evaluación integral del riesgo sísmico a escala urbana: aplicación a la ciudad de Lorca”. PhD thesis. Universidad Politécnica de Madrid, 2017. URL: oa.upm.es/48042/1/LIGIA_ELENA QUIROS_HERNANDEZ.pdf.
- [17] R. Romero-Jaren et al. “Automatic segmentation of point clouds in the architecture environment”. In: *Automatic segmentation of point clouds in the architecture environment XLIII-B2-2021* (2021). DOI: [10.5194/isprs-archives-XLIII-B2-2021-215-2021](https://doi.org/10.5194/isprs-archives-XLIII-B2-2021-215-2021).
- [18] NCSE-02. Comisión permanente de normas sismorresistentes. “España. Norma de construcción sismorresistente: Parte general y edificación”. In: *RD 997/2002, Spain* (2002). URL: www.boe.es/eli/es/rd/2002/09/27/997.

Chapter 1

State of the art

1.1 Seismic risk

An earthquake is the shaking of the surface of the Earth resulting from a sudden release of energy in the Earth's lithosphere that creates seismic waves. It is an unpredictable and unexpected natural phenomenon that can result in a huge number of fatalities, injuries, refugees and economic losses if the region is not properly prepared. The study of the seismic risk in a particular area requires a multidisciplinary approach from a number of study fields, ranging from seismology, geology, geodesy, physics, topography, mathematics, structural engineering, architecture, economy, to psychology, humanities and social science and all the institutions involved.

According to the United Nations Disaster Relief Organization (UNDRO), risk is defined as the expected physical damage and the connected losses that are computed from the convolution of the probability of occurrence of hazardous events and the vulnerability of the exposed elements to a certain hazard. For its part, seismic risk entails a set of events (earthquakes likely to happen), the associated consequences (damage and loss in the broadest sense), and the associated probabilities of occurrence (or exceed) over a defined time period [72].

For a deterministic analysis, seismic hazard refers to the shaking effects at a certain site caused by a earthquake scenario. While the term exposure represents the availability and inventory of buildings, infrastructure facilities and people in the respective study area subjected to a certain seismic event. Structural vulnerability stands for the susceptibility of each individual element to suffer damage given the level of tremor [96]. The correlation between damage to buildings and deaths is clearly identified in risk studies [20].

Furthermore, according to [23], the seismic risk (R) can be measured by the convolution of the integral or the combined product of a number of variables (Eq. 1.1):

- (H) hazard, which is defined as the probability of exceeding a certain value of the intensity of the ground movement produced by earthquakes;
- (E) exposure, that is, the amount of possible assets located in said area;
- (V) vulnerability, defined as the tendency of a building to undergo structural or non-structural damage in case of a seismic event of a specific intensity;
- (C) costs, human or cost of recovery from that degree of damage in the case of material damages.

$$R = H \times E \times V \times C \quad (1.1)$$

Seismic risk studies are carried out all over the world with the objective of preventing or mitigating the damages produced by earthquakes so as to reduce the consequences for the human beings of a determinate area. The inputs needed to estimate these damages are earthquake source, ground motion prediction equations, local geology at the site which is responsible for site amplification, building inventory and associated structural vulnerability, and the corresponding epistemic uncertainties related to that information. The knowledge of the data available and the parameters on which it is possible to intervene is crucial. In the following, a further description of the variables and the possibility of intervention on them is presented.

Hazard The Hazard (H) or seismic threat is the field of study of seismologists. The commonly accepted definition of hazard was given by UNDRO (1980) [99], according to which the hazard is represented by means of a probability

function of the parameter indicative of the intensity of the movement, x , at a location s , according to Eq. 1.2:

$$H = P[x(s) \geq x_0; t] \quad (1.2)$$

where P represents the probability of exceeding a threshold value x_0 of the parameter chosen for a time t .

Since the parameters inherent to the movement are the displacement, the velocity and acceleration, the hazard to countries is often estimated based on the maximum values of these parameters, usually called PGD (Peak Ground Displacement), PGV (Peak Ground Velocity) and PGA (Peak Ground Acceleration). However, its expression is also common in terms of macroseismic intensity, related to the destructiveness of the earthquake.

The hazard of countries located in areas seismically active is represented in seismic hazard maps. These seismic hazard maps illustrate the probability of occurrence of seismic movements together with their intensity. Its importance is based on the fact that they allow experts to design structures capable of resisting seismic action and represent a very useful information for planning the city from an urban point of view. Currently seismic hazard studies are focused on proposing seismic hazard maps for seismic risk studies and for seismic regulations.

The hazard depends on the geophysical and geological conditions and geotechnical characteristics of the site and, as a consequence, the possibility to intervene on it is very limited or non-existent.

Exposure The exposure (E) is the study of the exhibition of buildings and infrastructure susceptible to seismic damage by the earthquake. The database of exposed buildings should contain information as detailed as possible regarding the different structures, that is to say, all the features that may influence their vulnerability. The most relevant characteristics of the buildings exhibited that should be known to assess the damage, where possible, include:

- Height and/or number of stories
- Built area (m^2)
- Main structure of the building (reinforced concrete, masonry, steel ...)
- Type of flooring system
- Type of roof
- Wall material
- Type of façade
- Construction date
- Standard or design code
- Current status and maintenance
- Repairs or reinforcements
- Geometry irregularities
- Use

However, in practice, the possibility of knowing all this data depends on the area for which the seismic risk study is being developed. Unfortunately, in a wide number of cases it is found that the countries on which the consequences of the seismic events can be more destructive, the lesser is the information available. This is the case of Haiti or Honduras. Whereas, in countries such as Spain or Costa Rica, where the vulnerability is markedly inferior, the data available is higher. For that reason, some research projects combine these two situations to obtain mutual feedback.

Nonetheless, the minimum parameters for assigning vulnerability based on the methodologies of analysis of seismic risk are:

- Construction materials for the structure and enclosures
- The year of construction (as it is related to the regulations in force at that moment)
- The number of floors
- The quality of the construction techniques in relation to the ductility of the building

In this respect, the evolution of the seismic resistance standards of a country provides useful information regarding the study of the buildings vulnerability, as the appearance of new seismic codes, which usually mark the beginning of the development of less vulnerable constructions. For this reason, some methodologies developed for the calculation of the seismic risk on an urban scale existing in the literature differentiate buildings into classes according to their level of earthquake resistant design:

- buildings without seismic resistant design;
- *pre-code*, with low level of seismic resistant design;
- *low-code*, with moderate level of seismic resistant design;
- *high-code*, with high level of seismic resistant design.

Moreover, some useful tools like forms can be found in the literature for a more in depth characterization of the built environment of municipalities. A primary example of these methodologies is the CARTIS form ([53], [104],[68]), which is mainly focused on buildings made of ordinary reinforced concrete and masonry buildings with residential use. The 1st level CARTIS survey form collects the parameters of an area characterized by homogeneity among building types. The variation of the parameters within the same area studied may lead to the definition of several typological-structural groups of buildings, which can be characterized by different vulnerability [84]. The CARTIS tool is based on face-to-face interviews between an expert in earthquake engineering (usually with an academic background) and another technician, the interviewed, selected from among local engineers or architects. Usually (and preferably) the interviewer is a senior employee of the cities public works department as the knowledge of local experts is critical to the success of the methodology [12].

Furthermore, in order to give a correct geographical location for the different variables described, it is necessary to design and develop a Geographic Information System (GIS). A GIS is an organized integration of tools, data geographic and human resources, designed to store, edit and analyse information geographically referenced, in order to solve complex planning and management problems. Therefore, this system facilitates the analysis and representation of information of the database in the same reference system.

In developed countries, there are several governmental and regional agencies that have data on the building stock of a city. In the case of Spain, the National Statistics Institute (INE) and the Cadastre. The INE carries out campaigns on the characteristics of buildings with abundant information, useful for conducting a vulnerability study.

Exposure maps permit to establish a relationship between the different intensities of hazard and the catalogue of buildings and structures exposed. Moreover, they can serve as the basis for reducing risk through land use regulations. For example, limiting the constructions close to faults, or on liquefiable land; or with more sophisticated procedures, such as establishing standards of heights that distance the buildings' natural frequencies of vibration from those predominant for each specific soil or area, when the seismic risk is the principal one in a region. It is an area where architects and urban planners can contribute some type of risk limiting effect.

Vulnerability. The Vulnerability variable (V) is one of the elements in which intervention best fits, precisely from the realization of constructions and installations capable of successfully withstanding the actions derived from the foreseeable earthquake. It is the field of action of the seismic engineering, and the main scope of this PhD dissertation, therefore, it will be more profoundly studied throughout the document. The different vulnerability of buildings in different countries explains the difference in human damage compared to earthquakes of magnitudes similar.

Human and economic costs. The term Cost (C) is associated with the damage or loss caused to people or societies or with the monetary value of the goods themselves. The methods to quantify human and economic losses on the basis of the buildings' state of damage and the number of people per construction are being improved based on the data collected after recent earthquakes. In general, this constitutes a variable in which the potential intervention is scarce and mainly of a preventive nature. An example of possible interventions that can reduce risk is by planning alternatives to limit indirect costs due to loss of opportunity derived from damage to production facilities.

Other variables. Other variables that highly influence the damages and losses caused by a seismic event are being incorporated in current seismic risk studies. Some prime examples of these variables are the resilience of an area or population, or the appropriate legislation in reference to the people displaced due to the uninhabitability

of their homes or the closure of their jobs.

In summary, although the hazard is unavoidable, the risk can be reduced by limiting the vulnerability through the improvement and application of seismic regulations. Moreover, adequate planning of the emergency services work can mitigate the physical and psychological impact on the victims. The natural phenomenon is not avoidable, but the disaster is, and that is precisely the objective of seismic risk studies.

1.2 Seismic vulnerability of buildings

The concept of global vulnerability [102] considers vulnerability not only in regard to its physical dimension, but also including other aspects such as the impact on other factors, for example economic, social, environmental, etc.

The seismic vulnerability of a building is expressed by a set of parameters capable of predicting the type of structural damage, the failure mode and the resistant capacity of the structure under probable earthquake conditions. This is assigned through the analysis of the construction typologies at the site based on existing vulnerability assessment methodologies for the seismic risk evaluation. For the estimation of damages there are different methodologies, based on the use of fragility curves, damage probability matrices, relationships between vulnerability indexes and damage indexes, spectrums of capacity and demand, etc. In all of them, the objective is to estimate the percentage of each degree of damage to each typology of structures resulting from a predefined seismic event.

Therefore, seismic vulnerability is a structure's inherent predisposition to suffer damage in the occurrence of an earthquake [9]. That is, it is directly associated with factors such as the geometrical and structural characteristics of the construction: material, height of the building, earthquake-resistance construction design, urban position, etc.

The vulnerability of the buildings and infrastructures establishes a crucial difference concerning the seismic impact on a society in terms of human losses and economic costs. The greater human losses are located predominantly in the less developed regions of the world, while the greater economic ones are located mostly in the developed world. According to [23], Chapter 1, this fact can be partially observed in the lists of the ten worst events of the 20th century and so far in those of the 21st century from the perspective of each type of damage. Figure 1.1 illustrates the fact that although there is a clear correlation between the levels of damage and the magnitude of seismic events (Figure 1.1b), there is no correlation between material damage and human fatalities, as seen in the almost zero slope of the graphs shown in Figure 1.1a, that relates both types of damage. The slope would decrease further on that graph if the recent events of this first part of the 21st century were included in the calculus, since they were illustrated but not considered for the slopes. See [100] for more detail about the worst seismic events in terms of human and economic losses.

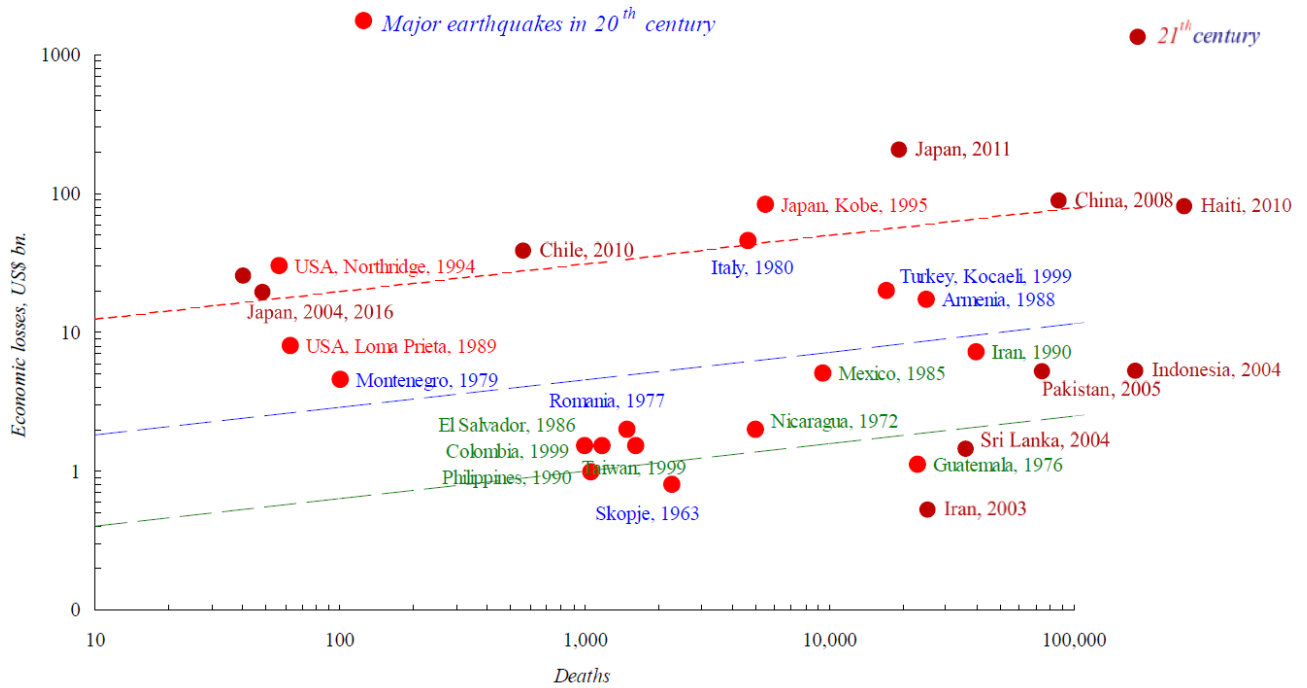
1.2.1 Probability and costs: fragility

In order to probabilistically estimate the risk, it is necessary to establish a relationship between hazard and damages and/or costs that accounts for the vulnerability of each specific element. The most extended statistical tool to characterise these relationships are fragility curves and vulnerability functions.

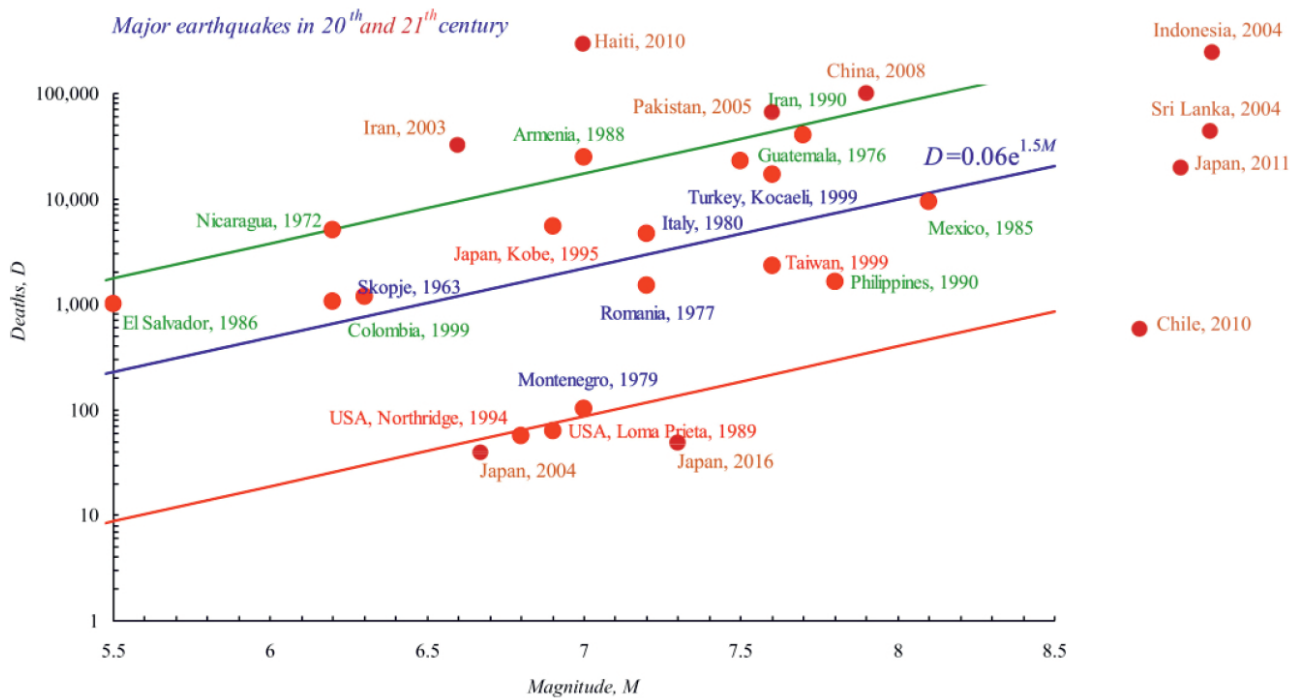
Accurate seismic fragility curves can be considered as a very useful decision-making tool for both pre- and post-earthquake situations. Moreover, these graphical representation of the function of cumulative distribution of the probability of reaching or exceeding a limit damage state or cost may help develop future local code provisions.

Specifically, fragility curves define the relationship between the probability of exceeding a particular damage state (or performance) of an infrastructure component, and the intensity of the applied hazard. Whereas vulnerability curves define the relationship between expected losses (such as economic losses) and this same intensity. Consequently, fragility functions and vulnerability functions are closely related and can usually be converted using an economic model or a similar tool.

The choice of curves that adequately represent the particular behavior of the buildings that make up the building stock of the region is fundamental to minimise the error of seismic risk studies. However, when trying to select a fragility curve from the literature, two different difficulties can be faced. On the one hand, the researcher can find a severe lack of fragility curves openly available for the specific region under study. While, on the other hand,



(a) Relationship between human fatalities and material damage. Tendencies just for the XX century.



(b) Relationships between earthquake magnitude and human fatalities for the seismic events of the XX and XXI centuries. Elaborated by Jaime Cervera Bravo based on Vacareanu et al. (2004)[100] and EM-DAT data [33]

Figure 1.1: Relationships between human fatalities and material damage and human fatalities and earthquake magnitude. Figures taken from [23]

the existence of a significant number of fragility curves available for a particular region, and a lack of a robust methodology to select the most adequate from such a catalogue can be faced. This latter case is giving rise to regions with seismic risk studies where the characterization of the vulnerability of the same construction typology is very dissimilar, for example Costa Rica (see Section 3.3). Needless to say that this gives rise to contradictory results between studies.

Nonetheless, a certain degree of uncertainty in the selection of curves that represent the behavior of buildings will always exist. This unavoidable uncertainty is due to the fact that although the fragility curves were made on the basis of models of buildings or database of past earthquakes with similar structural characteristics, design and materials of construction, the particular capacity and fragility also depend on the geometry and construction techniques, and these features can vary from one building to another within the same structural typology.

Fragility curves

Fragility curves were initially introduced and developed for conducting seismic risk assessments at nuclear power plants ([58], [57]). Currently, a great number of publications concerning fragility curves are still in the area of seismic risk assessment (e.g., [83]). Nonetheless, recently, different researchers are elaborating fragility curves for insured assets such as housing stock for the insurance industry, for other hazards, including wind, flooding and hurricanes (e.g., [63], [32]) or for the assessment of other elements such as the resilience of electricity networks (e.g., [29]).

The general equation to develop fragility or conditional probability is expressed by [80] as:

$$\text{Fragility} = P[\text{LS} \mid \text{IM} = y] \quad (1.3)$$

where,

LS is the limit state or damage state (DS),

IM is the intensity measure (ground motion), and

Y is the realized condition of ground motion IM.

Various equations were derived from different research studies. However, all the equations are based on said general equation (Eq. 1.3), see [83] for further detail.

A particular well-known version of this equation is:

$$P(x) = \Phi \left(\frac{\ln x - \lambda}{\varsigma} \right) \quad (1.4)$$

where,

$\Phi[\cdot]$ is the standardized normal distribution,

λ is the mean of $\ln x$, and

ς is the standard deviation of $\ln x$.

Most researchers such as Yamaguchi and Yamazaki (2000) [103] and Ibrahim and El-Shami (2011) [52] used Eq. 1.4 in their studies, which constitutes the simplest particular version. Yamaguchi and Yamazaki (2000) [103] tested Eq. 1.4 for different types of structures and found it to be suitable for use in all structural types.

Another prominent version of Eq. 1.3 is that proposed by Barbat (2014) [8] for moment resisting concrete frames (Eq. 1.5).

$$P[i/\text{sd}] = \phi \left[\frac{1}{\beta_{\text{ds}_i}} \text{Ln} \left(\frac{\text{sd}}{\text{sd}_{\text{ds}_i}} \right) \right] \quad (1.5)$$

where,

sd is the spectral displacement,

sd_{ds_i} is the mean value of lognormal distribution which corresponds to damage state threshold, and

β_{ds_i} is the standard deviation of natural logarithm of spectral displacement of ds.

As mentioned before, the fragility curves are closely related to the capacity of the topology studied.

Characterization of the capacity

The capacity curve is a graph of the lateral load resistance of the building expressed as a characteristic lateral displacement function. Normally the capacity curve is constructed by comparing the shear force at the base of the building against the displacement at the roof [40]. The characterisation of the capacity curves can be done by experimental, analytical or hybrid methods. To obtain this curve, a lateral load analysis is carried out on a sample or on the analytical model of the bare structure or infilled structure considering the nonlinear properties of the force-deformation curve due to the inelastic response of the material (non-linear analysis). As loads are applied, the formation of plastic hinges is detected in the elements and the consequent loss of stiffness. This manner of characterising the capacity are also applicable to non-structural elements.

To characterise the capacity curves based on analytical methods, it is necessary to elaborate a numerical model and carry out some kind of non-linear analysis on it. Said analyses can be categorized into two main groups, namely, Non-Linear Static Analysis (NLSA) and Non-Linear Dynamic Analysis (NLDA). In general, capacity models are developed to represent the response of the first mode of vibration of the building assuming that this is the predominant mode and that it primarily controls the damage genesis and progress.

Non-Linear Dynamic Analysis (NLDA) The NLDA or the Non-Linear Time History Analysis (NLTHA) method considers geometrical non-linearity and material inelasticity in predicting the displacement behavior and collapse load. In addition, this method requires a ground motion. A suitable set of ground motions is needed to ensure the accuracy of the fragility curves [83].

Nonlinear static analysis (NLSA) This analysis, also known as pushover analysis (POA), is one of the methods used to analytically assess the seismic capacity of a building or typology of buildings. Polese et al. (2013) [88] initially evaluated the appropriateness of pushover analysis in damage analysis, from which they developed the fragility curve. They conducted the analysis of intact structures and damaged buildings, resulting in a capacity curve. Moreover, Kumar et al. (2014) [60] mentioned that capacity curves can represent mean or mean plus/minus one/two/three times the standard deviation of capacity curves.

These capacity curves can result in fragility curves by means of the application of simplified formulae like those proposed in international methodologies for seismic risk projects, such as the RISK-UE [76] project, which is described later, or by means of the application of the performance based seismic design methodology, among other methods.

The Performance-Based Seismic Design (PBSD) is a seismic design methodology that ascertains the likely state of damage of an existing element during an earthquake, that is, it relates the performance level to a hazard level.

According to Manafpour and Moghaddam (2014) [67], the Performance-Based Seismic Design can be used for several purposes in relation to seismic design:

- (i) obtain better performance results for new buildings,
- (ii) determine performance in accordance with code provisions with the subsequent development of the required adjustment,
- (iii) enhance current provisions to obtain good designs, and
- (iv) provide an efficient retrofit design procedure.

There is a growing consensus among designers to follow this approach as a replacement of the existing force-based design procedures as it allows the expert to determine the appropriate levels of ground motion and Performance Objectives for the building and the nonstructural components.

Moreover, the Performance Based Seismic Design provides a quantitative measurement for structural damage based on the percentage of maximum interstorey drift —the dependent variable of the capacity curve— by considering specific earthquake level —the independent variable of the capacity curve—. Therefore, it can relate the capacity and the fragility, particularly if the measure of the intensity of the earthquake is the Peak Ground Acceleration (PGA) (Figure 1.2). See [92] for more detail about the procedure.

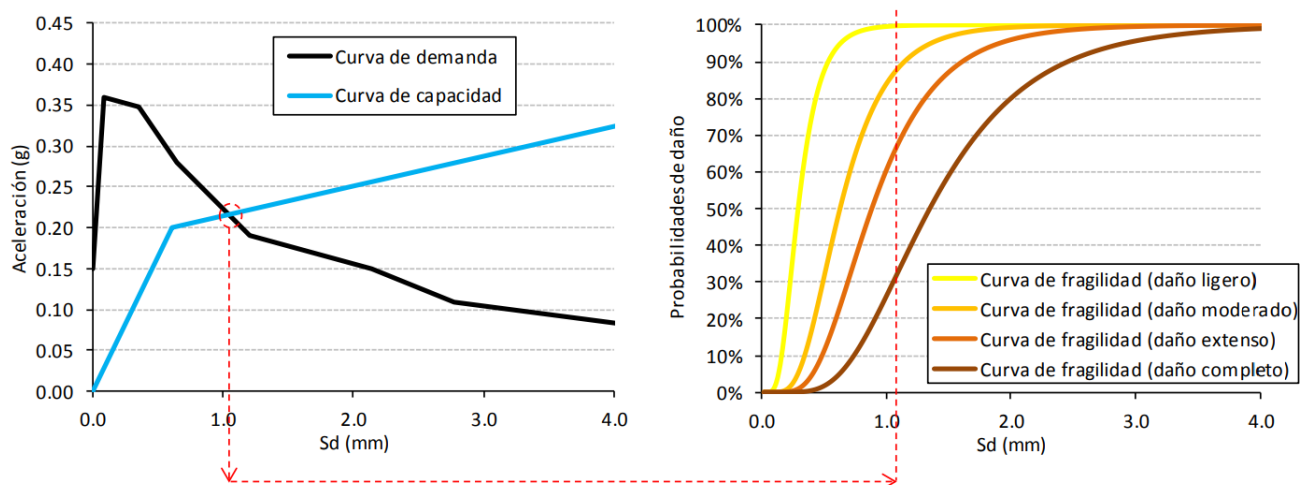


Figure 1.2: Conceptual scheme of the performance-based seismic design method. Left: the intersection of the capacity and demand curves defines the performance point (red circle). Right: the intersection between the performance point (represented by the vertical red line) with the fragility curves provide the estimate of damage to buildings. Taken from [90].

1.2.2 Methodologies for assessing seismic vulnerability of buildings

A wide variety of methodologies and techniques have been proposed by several authors for the estimate of the different construction typologies' vulnerability. The selection of a certain methodology is closely related to the scale of the analysis, the information available and the characteristics of the elements to be studied. This has led some researchers to the elaboration of different proposals of classifications in an effort to systematize existing methodologies. In the following, some of these classifications are briefly exposed.

One of the best-known classifications is that of Corsanero and Petrini (1990) [25], who group the vulnerability assessment techniques based on the type of result they produce in direct, indirect, conventional and hybrid techniques.

- Direct techniques, which make it possible to directly predict the damage caused by an earthquake; and
- Indirect techniques, which determine a vulnerability index and relate damage to seismic intensity;
- Conventional techniques, which introduce a vulnerability index independent of damage prediction; and
- Hybrid Techniques; that combine elements of the above methods with expert judgment.

Dolce et al. (1994), [28], proposes a classification based on the previous one, considering three types of methods: statistical, mechanical and expert judgment methods.

- Statistical methods, based on a statistical analysis of the buildings;
- Mechanical methods, in which the parameters that govern the dynamic behavior of the studied structures; and
- Methods based on expert judgments, which evaluate qualitatively and quantitatively the factors that govern the seismic response of buildings.

Other proposal of Kappos ([28]) distinguishes three types of methods according to the source of information: empirical, analytical and experimental methods.

- Empirical methods, based on the experience and data collected after a particular earthquake;
- Analytical methods, which evaluate the estimated resistance of structures to ground movement based on mechanical models and mechanical characteristics of the structures; and
- Experimental methods, which use "in situ" tests to determine the dynamic properties, soil-structure interaction, incidence of elements not structural etc.

Mena et al. (1998) [75] suggests that the result of a seismic vulnerability study is related to the description of the damage and the seismic movement, and that the relationship of these can be formulated discretely, by means of matrices, or continuously, by means of curves and eigenfunctions that reflect the construction aspects of the study region. Based on this, the author classifies the vulnerability according to the manner of obtaining of these functions, in:

- Calculated vulnerability, when the curves are obtained analytically by simulating the response of structures of the same typology; and
- Observed vulnerability, when obtained empirically through damage observation in buildings in areas affected by earthquakes.

Later, Nazri (2018) [83], based on a literature review, propose the classification of methods to develop fragility curves into four, namely: expert-based or judgmental, empirical, analytical, and hybrid. The advantages and disadvantages of each method to develop fragility curves according to Billah and Alam (2014) [80] are these:

- Expert based: this constitutes a simple method in which all factors may be included. However, it is very subjective, totally dependent on the panel expertise and not so accurate.
- Empirical: this method shows the actual vulnerability, representing a realistic picture. Nonetheless, it presents the disadvantages of a lack of data and inconsistency in damage observations.
- Analytical: this is the least biased method and considers all types of uncertainties. Nevertheless, it is costly in terms of computation.
- Hybrid: this method has the advantage of considering post-earthquake data and of potentially reducing the computational effort. Despite this, it presents significant drawbacks: requires multiple data in order to combine experimental and analytical methods and may present high inconsistency in the demand model.

Two methodologies that combine analytical and empirical methods and that are widely used for their applicability to other countries are the HAZUS-MH, [47], and the RISK-UE, [76] and [79], methodologies. In particular, both were used in the RISMUR I and II projects ([49] and [51]) for the study of the seismic risk of the Murcia region. Nonetheless, there are in existence other well-known international initiatives and projects. In the following, a number of relevant ones are briefly described.

International Projects

All international projects and initiatives carry out an exhaustive study on the structural and construction behavior of buildings to assess their vulnerability as an isolated element. Moreover, some international initiatives such as the Italian vulnerability index, the EMS-98 and the Risk-UE projects, herein described, warn of the importance of the urban parameters [70].

ATC: matrix functions The Californian Applied Technology Council (ATC) is a non-profit society whose objective is to advise and assist professionals in the fields of civil engineering and architecture. This society, commissioned by the Federal Agency for Emergency Management (FEMA), prepared two reports referenced as ATC-13 (1985) [1] and ATC-25 (1991) [2] for seismic risk analysis.

The ATC-13 report, titled *Earthquake Damage evaluation data for California*, is part of a project to evaluate seismic damage caused by earthquakes in California. The report includes a total of 78 matrices with the probability of damage corresponding to different types of facilities and services (Facility Classes), 40 of which correspond to buildings and the remaining 38 to other structures or infrastructures.

The ATC-25 report, titled *Seismic Vulnerability and impact of disruption of lifelines in the conterminous United States*, analyzes the damage and impact of the interruption of vital lines because of earthquakes. Moreover, this second report updates and generalizes the matrices and functions that allow an estimation of damage to vital structures and infrastructures. Said generalization renders the matrices and functions developed in the ATC-13 solely for California applicable to any zone of the United States. It makes recommendations for its application and proposes penalties to accomplish the said purpose. For this reason, the application of this methodology to a different area outside the United States requires a careful and expert analysis that allows its adaptation, adequately quantifying the corresponding penalties. Nonetheless, this methodology constitutes an extremely useful reference tool that makes it possible to evaluate, quickly and efficiently, the expected damage in almost all infrastructures.

Italy: a Vulnerability Index This Italian method was the first proposal incorporating an index to assess the vulnerability of buildings. It stems from 1982, when a group of Italian researchers developed a methodology called *Vulnerability Index Methodology*. Said methodology was based on a database of damage to buildings caused by earthquakes since the 1976 Friuli earthquake and its relationship to the intensity of the seismic events. In these studies, said experts began to use damage inspection forms, which were later improved on the occasion of the Irpinia earthquake of 1980, and which are the basis of those used today.

As a consequence of having been applied in different cities in Italy with good results, it was officially adopted by the government agency for civil protection (Gruppo Nazionale per la Difesa dei Terremoti, GNDT), which has updated the different forms and created manuals, [97]. This constitutes an empirical methodology that is widely applied in studies at the urban level.

The method proposes to complete a reference form in which the most influential eleven parameters for the vulnerability are established by in-situ expert inspection. Later, the determination of the quality of the seismic design of the buildings is performed via a coefficient called Vulnerability Index, which ponders such parameters.

This proposal has given rise to different methods for estimating the seismic vulnerability of reinforced concrete and masonry buildings such as that of Lourenço and Roque (2006) [65], applied in [66], or that included in Mazzotti et al., (2013) [71], called RESISTO, applied in Chapter 4 to develop fragility curves for Lorca.

EMS-98: classes of vulnerability The European Macroseismic Scale (EMS-98) [34] intensity scale is an update of the Medvedev–Sponheuer–Karnik scale (MSK-64) [74]. In reference to buildings, the inclusion of a greater number of construction typologies is perhaps the most innovative contribution of this new version.

The EMS-98 intensity scale, like the MSK scale that preceded it, belongs to a family of intensity scales whose origin was the popular ten-degree scale elaborated by Rossi and Forel; which was revised by Mercalli, later expanded to twelve degrees by Cancani, and posteriorly defined in a very complete formula by Sieberg as the Mercalli - Cancani Sieberg scale (MCS). This is the scale that serves as a starting point not only for the scale MSK/EMS-98 but also for numerous versions of the "Modified Mercalli" scale.

Most of these twelve degree scales are approximately equivalent in their present values, and they only differ in the degree of sophistication used for their formulation. The word *vulnerability* is used throughout the European Macroseismic Scale to express the differences in the way in which buildings respond to vibrations caused by earthquakes. If two groups of buildings are subjected to exactly the same vibration caused by an earthquake and one group responds better than the other, it can be said that the less damaged buildings have a lower seismic vulnerability than the most damaged buildings, or that the buildings less damaged were more earthquake resistant than the others and vice versa. Moreover, this scale reflects the fact that dissimilar typologies can show similar damage for the same seismic intensity.

In the EMS there are six classes of decreasing vulnerability, from A to F, being A the most vulnerable and F the least one. This vulnerability depends on the structural material and construction techniques. See Figure 1.3.

EMS-98 also lists other factors that affect the vulnerability of a structure along with the type of construction: quality and manufacture, state of preservation, regularity, ductility, location, reinforcement and seismic resistant design. EMS-98 does not quantify these factors as the ATC, the Italian Index method or the Risk-UE project do, it only indicates that based on the knowledge of the experts, the accumulation of strengths or weaknesses can vary the initial vulnerability classification already shown.

HAZUS: capacity and fragility curves The HAZUS-MH (2003) methodology [47], was developed in the United States in 1999 to assess the seismic vulnerability of cities using the capacity spectrum method (a performance based seismic design method). Currently, it constitutes one of the most well-known and employed methodologies for the analysis of seismic vulnerability. This uses the displacements and spectral accelerations as a measurement of the seismic action, instead of the seismic intensity used in ATC-13 [1].

For the analysis of seismic vulnerability, the HAZUS-MH (2003) methodology is based on the methods proposed in ATC-38 [3] and the analytical methods developed in FEMA-440 (also known as ATC-55) [35]. A classification of 36 types of buildings according to their structure, and the damage of these 36 structural models is estimated

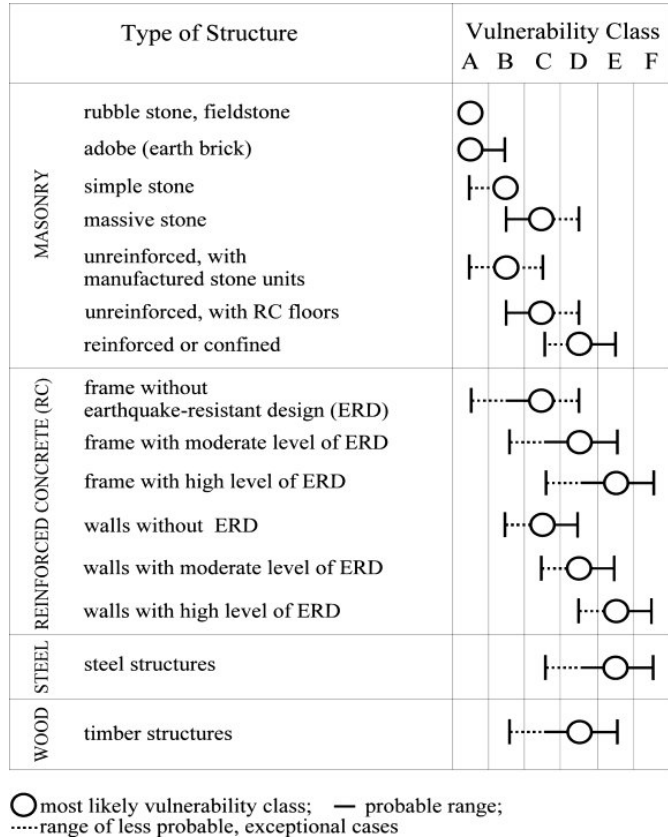


Figure 1.3: Correlation between vulnerability classes and structural types. Source: EMS-98 [34]

from expert opinion. For each model, the four states of structural damage are described: slight, moderate, severe and collapse. Non-structural damage is analyzed separately. For each type of construction and design level, parameters are given that allow the definition of the capacity of the structure, the maximum interstorey drifts and the displacements spectral values at the thresholds of the different damage states considered.

The powerful technique provided by HAZUS-MH for earthquake loss estimation is so closely connected to environments in the United States and its seismic code that it is not easy to apply to other countries [78].

RISK-UE: a vulnerability index and capacity and fragility curves The main objective of the Risk-UE project, [76] and [79], was to propose advanced methods of seismic risk analysis that allow incorporating the characteristics of the buildings, cultural heritage and typical European urban societies. The European countries participants in the Risk-UE project were Bulgaria, Greece, France, Italy, Former Republic Yugoslav, Republic of Macedonia, Romania and Spain.

The modular organization of the project comprised seven work modules or workpackages (WP). The WP4, titled *Vulnerability Study of Current Buildings*, assesses the vulnerability of a building using two methodologies. The first methodology is based on the Vulnerability Index method and the second on the performance based seismic design method (capacity and demand spectra) and curves of fragility.

The Vulnerability Index methodology, also called Level I Risk-UE, classifies the building stock of the city in vulnerability classes, to later carry out an analysis of the vulnerability of each individual building. Whereas the capacity spectrum method, also called Level II Risk-UE, requires the obtainance of the specific capacity and fragility curves for the buildings analyzed. The capacity is approximated in a bilinear curve and expressed by means of two points called yield point and capacity ultimate point.

1.3 Seismic vulnerability of non-structural elements

The category of non-structural elements includes all those components not part of the primary structure, namely:

- 1) architectural components, i.e. façades, partitions, ceilings;
- 2) building utility services, i.e. mechanical and electrical building equipment;
- 3) building contents.

Said elements are generally not considered part of the main load-bearing system of a building or industrial facility due to the fact that they are mainly designed for architectural purposes, for example, thermal, acoustic or fire, and that they can be replaced without the need of consulting a structural engineer or architect. Nonetheless, despite not being included in the seismic design process, non-structural systems may be subjected to large seismic demands depending on their own characteristics, and they can determine the structural behaviour of the building, as in the cases of short column or soft storey effects.

The importance of the research into the seismic performance of these elements stems from their influence on the structural behaviour along with the fact that some recent medium and high-magnitude events have shown that a considerable percentage of deaths are caused by falling debris from non-structural elements, even when buildings continue to be habitable. The 2010/2011 Canterbury seismic sequence is a prime example of this fact: 70 % of fatalities (35 people) were caused by falling pieces of these elements [22, 54]).

Moreover, their response can significantly affect the building functionality after earthquakes, even for low-intensity events. The poor performance of non-structural elements can result in substantial economic losses and business interruption.

The research into preventing the human and economic costs caused by non-structural elements involves the characterization of their seismic demand as well as their capacity and fragility. In this respect, [11] presents a general overview of the seismic vulnerability of alternative systems, either based on traditional construction practice or on innovative solutions; along with a collection of main literature references regarding the study of the seismic behaviour and damage states for facades, partitions and ceilings, since many different systems are available worldwide.

Nonetheless, a significant part of the investigations carried out on this topic is specially focused on the characterization of non-structural unreinforced masonry elements, such as freestanding parapets or infill walls. This is due to these elements having demonstrated to be particularly hazardous and widespread in areas where there is a tradition of using masonry in residential buildings. For example, in relation to human losses, the nine fatalities occurred during the 2011 Lorca earthquake were due to falling debris of unreinforced masonry non-structural elements [46], mainly parapets due to out-of-plane failure. Moreover, in relation to economic losses, the masonry infill and the partition walls were the most affected non-structural elements during the 2016 Central Italy earthquake [85]. It is worth mentioning that, according to this same work, in general, the extent of the observed non-structural damage was mainly related to the lack of proper anchorage of the various elements to the structure.

1.3.1 Seismic capacity of non-structural elements

In the last few decades, several approaches are being investigated in order to idealise the seismic capacity of non-structural elements, from simple analytical idealisations to complex numerical simulations.

The behaviour and damage to the non-structural elements are usually classified on the basis of their cause: by in-plane loading, by out-of-plane loading or by a combination of both types of lateral loadings [46].

In this respect, it is worth mentioning that the degradation and collapse of some elements such as parapets is solely due to out-of-plane loading. Whereas infilled walls, such as interior and exterior unreinforced masonry walls, are subjected to the combination of both types of seismic loading: in-plane seismic loading (as the interaction between infills and structural frames can cause the infills to be subjected to inter-storey drift) and out-of-plane seismic loading (as an effect of its inertial mass) [7, 6, 17, 89].

Additionally, damage to reinforced concrete frame structures initially occurs in non-structural elements since they usually exhibit a more rigid and brittle behaviour than structural ones. In order to characterise specifically the infill walls' capacity against seismic loading, it is usual to study separately the in-plane and out-of-plane behaviours

(e.g., [27], [38], [43], among others) due to the lack of information and methodologies for combining both effects. Nevertheless, it should be noted that buildings are subjected to movements in all seismic directions at the same time. This means that in an actual building subjected to an earthquake, infill wall collapse has two stages: an initial stage where the in-plane loads degrade and crack the infill, and a second stage where out-of-plane seismic loading causes the overturning of the wall in the out-of-plane direction [64].

Despite this, there are cases in which this separate study is quite realistic, when the magnitude of the in-plane and out-plane loads are markedly dissimilar. In this respect, it is common that the lowest floors are subjected to the maximum in-plane requirements and the highest floors are subject to the maximum out-of-plane accelerations. Therefore, when attending to the biaxial capacity curve proposed by Al-Chaar (2002) [4], it seems reasonable to study both effects separately. Said curve establishes a relationship between the capacity of a wall against in-plane, out-of-plane and a combination of both types of loading for unreinforced masonry infill walls. This relationship establishes that the in-plane capacity begins to reduce when the out-of-plane load exceeded 20% of the capacity, reaching a 20–25% reduction when the relationship between the out-of-plane force applied represents 50% of the maximum out-of-plane force, and vice versa. This assumption would be particularly valid when the building is oriented parallelly or perpendicularly to the main direction of the motion.

In-plane response

The vulnerability of masonry elements subjected to in-plane actions has been investigated in several experimental and numerical studies (see [19]) obtaining that it depends on the possible failure mechanisms, which are influenced by a number of parameters: (a) mechanical properties of masonry; (b) constraint conditions; (c) vertical compression levels; (d) slenderness of the wall; and (e) masonry texture.

The mechanical properties directly influence both the maximum capacity and ductility of masonry walls, while their constraint conditions and slenderness drive their failure modes toward shear or flexural mechanisms. In the case of low compression levels, a sliding shear failure is generally favored in regular masonry walls, while flexural and diagonal shear failures may occur for medium–high levels of compression. Moreover, masonry texture can affect the type of shear failure (diagonal or sliding shear) [18].

A prominent example of fragility curves for in-plane seismic loading is contributed by [16]. These curves can be directly used within the FEMA P-58-1 [36] and FEMA P-58-2 [37] framework for the seismic performance assessment of reinforced concrete frame buildings with masonry infills. They were elaborated considering a large number of specimens by means of the combination of results of several studies (55 specimens). Several of the samples used similar materials and construction techniques to Spain (e.g., 7 specimens from Italy [21, 14], 3 from Greece [56] and 5 from Croatia [93].).

Out-of-plane response

With respect to the out-of plane capacity, it should be noted that the response of cantilevers such as parapets and simply-supported walls is essentially different because of its strong dependency on boundary conditions. For instance, thick simply-supported walls with vertical loads or concrete frames on their top can develop a beneficial arching action in this direction, that cantilevers cannot.

Nonetheless, it has been proven by several studies, most of them based on the formulation of the rocking motion of a rigid block proposed by Housner (1963)[48] that the behaviour of both elements also presents significant similarities. This similitude is mainly related to the comparison between their actual load-displacement capacity curve and the same curve derived from a simpler modelling by means of rigid blocks under rotation.

In line with this, it is worth mentioning the research of Doherty et al. (2002) [27] and Kafle et al. (2011) [55]. The former proposed a model of uncracked unreinforced masonry walls (parapets and infills as elastoplastic blocks) with a final stage of collapse as a rigid block. The latter, effectively demonstrated that the risk of overturning is significantly correlated with the peak displacement demand (PDD) of ground shaking. Therefore, based on this methodology, infills and parapets behaviour can be assimilated to deformable blocks and modelled as a single degree of freedom system (SDOF). Moreover, it can be established that its capacity curve, commonly simplified as

a trilinear curve, is dependent on the weight, slenderness and state of degradation of mortar joints ([27, 62, 44, 45]).

In relation to fragility curves, [16] contributes a proposal for the prediction of infill masonry walls' collapse whose term of comparison is the Peak Floor Acceleration (PFA). Said curve does not differentiate between load bearing and non-load bearing walls, is developed for infills without openings, and is considered to be equal for infills with openings.

For further detail about the State of the Art of the research into out-of-plane behaviour of unreinforced masonry non-structural elements see Section 5.1.

1.3.2 Seismic demand of non-structural elements: filtering effects of the building

The characterization of the seismic demand concerning acceleration and demand sensitive non-structural elements can be considered a topic still under development. Acceleration, velocity and displacement demands vary along the height of a structure, being filtered and amplified according to the dynamic characteristics of the main system. The wide number of parameters involved in its characterization — geometry and non-linearity of the building, the influence of masonry infills... — renders it a complex task. Nonetheless, a great number of researchers have been prompted to advance the state of knowledge. Most of them have focused their attention on infilled frame reinforced concrete structure buildings as they are among the most hazardous ones.

The most accurate and robust analytical method to characterise the seismic demand of non-structural elements is the Non-Linear Time History Analysis (NLTHA), which can be carried out by different software devoted to structural engineering. However, it is a very time-consuming task as the engineer has to elaborate a detailed 3D numerical model of the infilled frame building and involves significant computational resources.

For that reason, in a great number of regulations, the most common approach to obtaining the filtered acceleration demand on the acceleration sensitive non-structural element base consists of the application of a Floor Response Spectra simplified method (for example, EN-1998 [30]). However, recent seismic codes, such as the Italian NTC2018 [82], are also introducing more complex methods in order to provide a better estimation of the floor seismic demand magnitude. Nevertheless, at the present moment all the existing approaches have limitations: they are either simple but unreliable, especially for structural typologies with differences from those for which they were developed, or trustworthy but require relatively advanced analysis capabilities and complex processing.

In the case of the Time History Analysis (THA) method, some advantages can be mentioned in comparison with the simplified procedures. These kinds of analyses contemplate the consideration of the duration of the ground motion in addition to its intensity and frequency content. Factors that Raghunandan and Liel (2013) [91] recommends to be considered in structural design and assessment of seismic risk as a result of their research on the collapse of reinforced concrete structures. Moreover, the computational THA method generates different responses or outputs (Floor Response Spectra (FRS), accelerograms, energies, forces, etc.) at each node of the modelled structural elements from the ground acceleration time history. Therefore, this procedure allows engineers to apply the output generated at the specific node of control that corresponds to the non-structural element base.

In the following, some outstanding works on the topic of non-structural elements seismic demand characterization in terms of acceleration are listed.

In their works, Miranda and Taghavi (2005) [77] and Taghavi and Miranda (2005) [95] present an approximate procedure to estimate floor acceleration demands in multistorey buildings with the use of only a small number of parameters. According to the authors, the method assumes that the structure responds elastically, hence it is aimed at computing floor acceleration demands for estimating the seismic performance of acceleration-sensitive nonstructural elements and building contents at performance levels in which the structure is expected to remain elastic or practically elastic (as would be the case of a great number of reinforced concrete buildings that suffered the 2011 Lorca earthquake). The approximate method takes into account the contribution of the first three modes of vibration of the building. The accuracy of the method is evaluated by comparing the results of the approximate method for Peak Floor Acceleration (PFA) estimation of generic buildings using a continuous linear-elastic shear–flexural beam model to those computed using response history analyses of complete structural models and to those recorded in instrumented structures during recent earthquakes.

Later, Medina et al. (2006), [73], analyses statistically the peak acceleration demands for acceleration-sensitive non-structural components supported on elastic and inelastic regular moment-resisting frame structures with different heights (3, 6, 9 and 18 stories) subjected to a set of 40 ground motions. Said study contributes an evaluation and quantification of the dependence of peak component accelerations on several factors, namely, the location of the non-structural component in the structure, the damping ratio of the component, and the properties of the supporting structure such as its modal periods, height, stiffness distribution and strength.

For their part, Calvi and Sullivan (2014) [15], extended the methodology developed and tested by Sullivan et al. (2013) [94] for the simplified construction of floor spectra, at various levels of elastic damping, from single-degree-of-freedom structures to multi-degree-of-freedom (MDOF) supporting systems responding in the elastic range.

The new method first scales floor acceleration components obtained from modal analyses by empirical dynamic amplification factors that are set as a function of the period of the supporting structure and the period and elastic damping of the supported component. The acceleration demands for each mode are then combined using the square root of the sum of the squares (SRSS) approach to give the predicted floor spectra on upper levels. The procedure was tested numerically by comparing predictions with floor spectra obtained from time-history analyses of reinforced concrete wall structures of 2 to 20-storeys in height using a set of 47 recorded ground motions. While the procedure is currently limited to prediction of floor spectra in the elastic range, this procedure could still be particularly useful for engineers interested in controlling damage at the serviceability limit state for which elastic response of the supporting structure would typically be expected. Nevertheless, future research should further develop the approach to permit the prediction of floor spectra in multi-degree of freedom (MDOF) systems that respond in the inelastic range.

Moreover, Petrone et al. (2015) [87] conducted a parametric study in order to evaluate the seismic demand on light acceleration-sensitive nonstructural components caused by frequent earthquakes. Based on this research, a novel formulation was proposed for an easy implementation in future building codes based on the actual Eurocode provisions [30]. Said formulation provides a good estimation of the floor spectral accelerations and of the envelope of the floor spectral peaks owing to the higher modes. Nonetheless, the authors underline that the results and conclusions of the formulae proposed are related and limited to a set of frame reinforced concrete structures designed according to EN1998. Furthermore, they state that a larger set of structures, characterized by different materials and structural typologies, should be considered in a future study in order to validate the formulation.

More recently, in Perrone et al. (2020) [86], the effect of masonry infills on absolute acceleration and relative displacement floor response spectra for reinforced concrete buildings subjected to frequent (serviceability level) earthquakes is investigated through a probabilistic framework. A database of one hundred masonry infilled reinforced concrete frames, representative of the European context, was generated and each building analyzed through nonlinear time history analyses. From the results of these analyses, the acceleration and displacement response spectra at different floor levels of both bare and infilled frame archetypes were then computed.

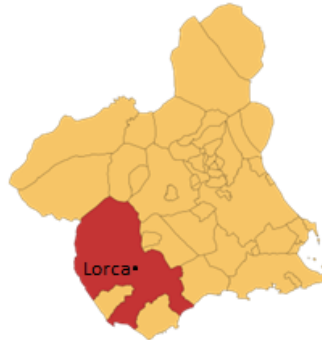
In addition to these formulations for the characterization of the seismic demand by means of the Floor Response Spectra, in the case of Europe, it is worth mentioning the contributions of the Italian NTC18 [82] seismic code which provides from simplified to complex proposals. Among them, the general formulation, the simplified formulation and the simplified formulation for Moment Resisting Frame buildings can be found (see Section 6.3.2 for more detail).

1.4 The case of Lorca

In May 2011, the earth around Lorca, a town in the Spanish province of Murcia, was shaken twice. Although the quake was of moderate magnitude, the proximity of its epicentre and its superficial depth caused a brief but enormously violent surface tremor. The horizontal acceleration recorded, 0.38 g, was unprecedented in Spain. As a direct result of the quakes, many architectural elements, including roof parapets, façade panels and store front enclosures, fell from buildings and onto the street. The nine fatalities and the vast majority of the injuries were due to the impact of falling debris.



(a) Map of Spain highlighting the Autonomous Community of the Region of Murcia in red.



(b) Map of Murcia highlighting the district Lorca in red, and the city of Lorca

Figure 1.4: Localization of the city of Lorca

1.4.1 The city of Lorca and seismicity

Lorca is a city in the Autonomous Community of the Region of Murcia in south-eastern Spain comprising of around three km^2 , whose building typologies are not very different from the majority Spanish cities of around 100,000 inhabitants. Figure 1.4 shows the localization of Murcia within the Spanish map, and of the city of Lorca within the Murcia map. Moreover, Figure 1.5 illustrates its historical evolution in terms of urban development and buildings constructions and Figure 1.6 the quantity of buildings versus the number of floors until 2013 according to the Cadastral information (see Chapter 2 for more detail about the map and the treatment of the Cadastral information).

On the afternoon of May 11, 2011, two earthquakes occurred in the mediations of the Urban center of Lorca. The first of them, at 5:05 p.m. (local time), reached a magnitude of 4.5 degrees and was felt throughout the Murcia region and in some towns in the provinces surrounding. Some non-structural elements fell in the urban area. The second earthquake was felt at 6:47 p.m. It reached a M_w 5.2 magnitude and could be felt in towns as far away as Madrid. According to the official report elaborated by the Spanish Geographic National Institute or Instituto Geográfico Nacional (IGN) together with the Universidad Complutense de Madrid (UCM), Universidad Politécnica de Madrid (UPM), the Instituto Geológico y Minero de España and the Asociación Española de Ingeniería Sísmica, [13], the two earthquakes had their epicenter at very close points, located a few kilometers from the city of Lorca, and at a similar depth of around 2 kilometers. The second earthquake, despite its moderate magnitude, has generated the greatest accelerations registered in our country 0.38g.

This earthquake produced 9 fatalities and more than 300 injuries, in addition to causing the evacuation of more

512940.94

614940.94

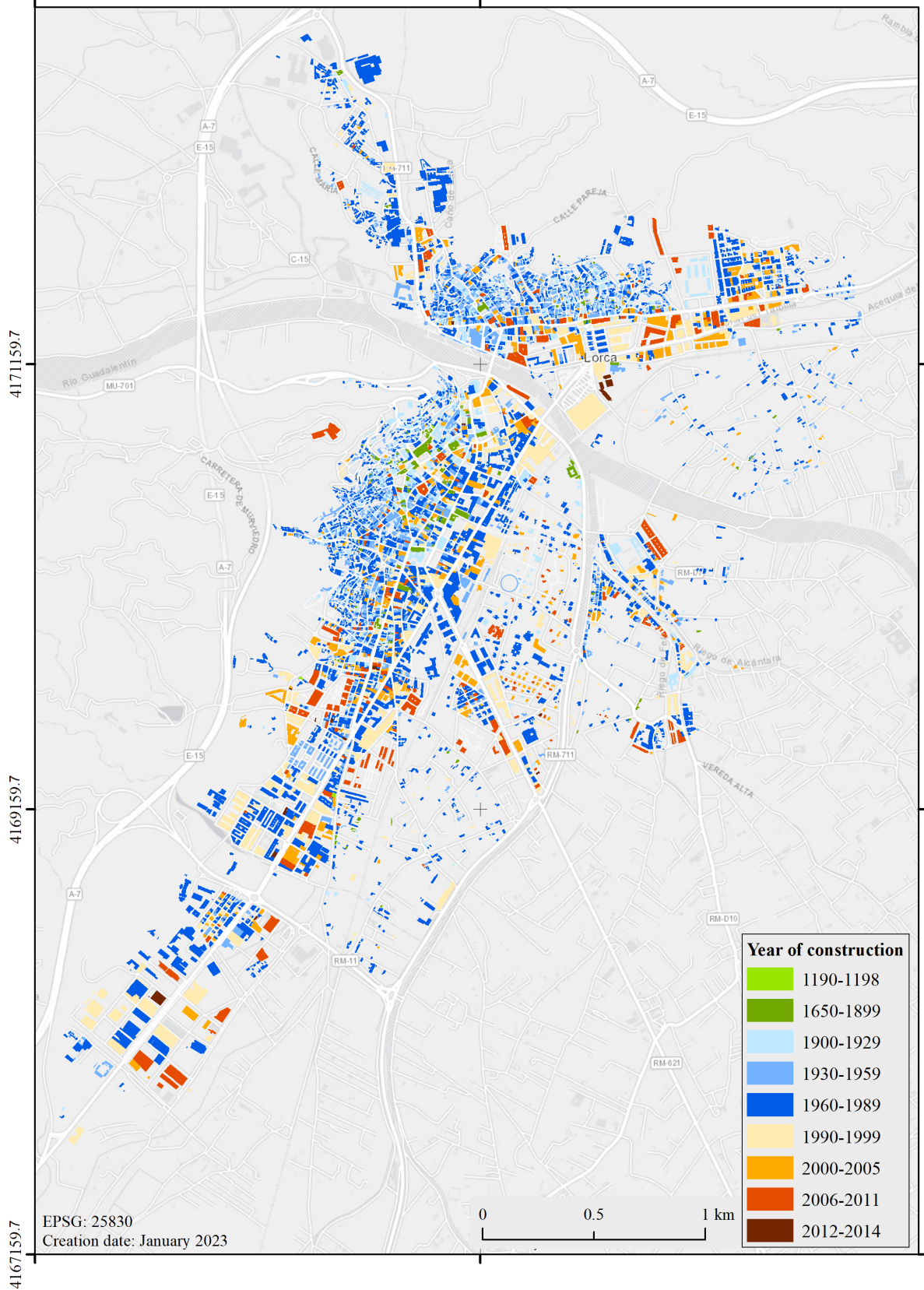


Figure 1.5: Historical evolution of Lorca

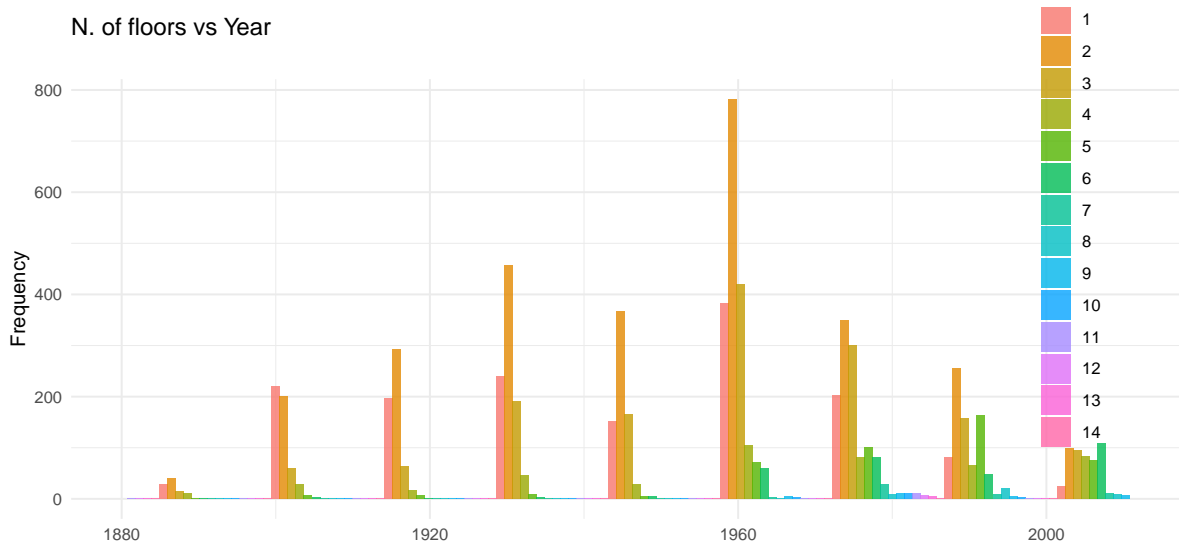


Figure 1.6: Historical evolution of the Lorca buildings: number of floors vs year of construction

than 10,000 people (4,000 were relocated in a camp authorized by the administration), the transfer of patients from the Hospital, etc. Moreover, the earthquake caused a large amount of damage to facades and roof parapets (which, when falling, produced the greatest personal damage). Only one residential building collapsed but partial collapses occurred in masonry buildings and in some historical buildings [5].

Martínez-Cuevas et al. (2017) [69] studied this city in great detail after the 2011 earthquake and identified the urban features of the constructions of the three most damaged neighborhoods in order to calibrate the urban modifiers of the seismic vulnerability of this city. Said author highlights the following aspects of the urban configuration and geotechnical structure of Lorca:

- The city is developed on a continuous slope as a result of its location on a hillside, which has conditioned the structural configuration of many of its buildings.
- The same situation on the hillside justifies a complex geotechnical structure. While the higher neighborhoods, at the foot of a well-known heritage building, the Castle of Lorca, are generally based on rock or hard ground, the most recent ones are located on sedimentary soils formed by transport of erosion materials.
- The development of the city itself has softened the original profile, filling in valleys and softening the most abrupt profiles.

Seismicity in the area

The Iberian Peninsula (or Iberian subplate) is located in a convergence zone between the plates of Africa and Eurasia. This convergence, with rates of movement between 2 and 5 mm/year and with directions NW - SE to WNW - ESE conditions the general seismotectonics of the area. The tectonic displacement between both continents is responsible for the seismic activity of the Mediterranean countries and therefore of the great earthquakes that occur in areas such as Algeria, Greece or Turkey. The most western part of the conjunction between these plates is the fracture called Azores-Gibraltar-Tunisia, which is the one that affects Spain. The IGN seismic catalogue comprises earthquakes from 1370 A.D. to present [31], including that occurred in Lorca in 2011.

From the seismotectonic point of view, the Region of Murcia presents great interest in terms of obtaining useful data for calculating seismic hazard. The Betic Cordillera constitutes the most seismically active sector of the Iberian Peninsula, at least in terms of rate of exercise. The southeastern part of the mountain range has suffered major earthquakes in the last 500 years, some of them with high intensities.

Among all of them, these stands out: the Torrevieja 1829 earthquake of intensity X, the Jacarilla 1919 earthquakes, those of intensity VIII occurred along the Alhama de Murcia fault and along the Valle del Segura and the Cehegín 1948 earthquake. Most of these earthquakes caused numerous losses of human life and the partial

destruction of some populations. The last four earthquakes occurred in the province of Murcia also presented important effects in Mula (1999), Bullas (2002), La Paca (2005) and Lorca (2011). In a period of 12 years, four events have taken place that, together have caused the greatest damage reported by earthquakes in Spain in recent decades.

Lorca is located practically on the trace of one of the central branches of the Alhama de Murcia, a fault line that is located in the northwest limit of the Guadalentín basin and extends more than 80 km of longitude, practically crossing the province. It is a wide area in which earthquakes of magnitude similar to that of May 2011 are relatively frequent. Those of Mula (1999), Bullas (2002) and La Paca (2005) reached magnitudes between 4.8 and 5.0, that is to say, not much lower than that of Lorca. The proximity to the population is the factor that justifies the severe damages provoked by the May 2011 earthquake and the other similar magnitude tremors, whose damages were not significant.

Hazard maps

In Spain, the first seismic hazard map appeared in the first seismic regulation of 1962.

The latest one was commissioned by the Ministry of Development of the Government of Spain and developed in 2013, resulting in a book *Update of seismic hazard maps of Spain 2012* [98]. The coordination and execution of the said work was carried out by the IGN and the Universidad Politécnica de Madrid, through the Seismic Engineering Research Group (GIIS) of the Superior Technical School of Engineers in Topography, Geodesy and Cartography (ETSII, UPM). This publication is of great importance for the field of seismic engineering in Spain, since it improves the seismic hazard map of Spain adopted in the current seismic standard NCSE-02, [105] (in force since 2002).

In the results obtained, the authors indicate that the new map is not directly comparable with the one adopted in the NCSE-02 norm. The map of the norm defines the hazard of the territory, for a period of return of 500 years, from the seismic acceleration value a_b , and the contribution coefficient K . Whereas the new hazard map of Spain is a collection of maps for different parameters of Peak Ground Accelerations (PGA) and Spectral accelerations ($S_a(T_i)$) calculated for various exceedance probabilities or return periods (T_R). The hazard map obtained in this study for PGA ($T_R = 475$) corresponds to the maximum horizontal acceleration of a rock soil. This parameter could be used as reference acceleration, in the type of soil (type I), with respect to which the seismic action of the other types of soils can be defined.

The results of both hazard maps mentioned are illustrated and compared in Chapter 4 of this dissertation.

Exposure of Lorca

In order to estimate the damage to the building stock that makes up an urban nucleus in the face of a seismic event, an assignation of a fragility curve or a classification of the vulnerability of the buildings that compose it in classes is required. As mentioned before, this classification requires, in first place, the determination of the construction typologies, taking into account their main features, and identifying in them those that influence most their seismic behavior according to the scientific literature.

In this respect, the knowledge of the seismic codes in force at the moment in which the typology under study was built permits the researchers to develop fragility curves based on more realistic numerical models (with respect to elements that influence the ductility of the buildings such as reinforcements, joints or construction details).

In the case of Spain, the dates of the mandatory seismic resistance standards constitute a useful tool to classify the buildings present in the region from 1962, when the first code appeared. In Chapter 2, the successive seismic codes are detailed.

According to [39, 81], two large types can be distinguished among the conventional residential buildings found in the urban centers of Spain:

- **Traditional buildings.** These buildings are based on construction practices of empirical tradition, endorsed by good results for centuries. Traditionally, the structure of residential buildings has been made by means of a system of load-bearing walls that serve as support for other elements of the building (flooring systems and the structure of the roofs) and transmit their weight to the foundation, which usually consists of strip footings. The walls were built with different materials (mud wall, stones, bricks, ashlar stone, etc.). These

buildings are based on concepts of good construction practices and form the largest part of the traditional construction carried out before the 40s or 50s.

- **Technological buildings.** For these buildings, the forces on the structure are calculated by different technological procedures, and specific solutions developed for each structural member according to said results. These buildings are habitually constituted by a system of columns and beams, which are usually made of reinforced concrete or steel. The implementation of the technological stage occurs over several decades, but it is useful to relate it to the publication of the first Spanish seismic regulation, which came into force in the year 1962.

Figure 1.7 illustrates a prime example of a Lorca neighborhood in which all typologies are found.



Figure 1.7: Photograph of a neighborhood of Lorca.

The assignment of the vulnerability —vulnerability indexes, vulnerability classes or fragility curves— depends on the methodology employed. In the following, the seismic risk studies carried out on the region of Murcia, the methodologies followed and some of their conclusions regarding exposure and vulnerability are presented. Additionally, see Chapter 2 for further details about the aforementioned typologies.

National Initiatives carried out in the Autonomous Community of Murcia

Currently, there is a framework law in force in Spain, the *Basic Guideline for Civil Protection Against Seismic Risk* [26], which obligates the autonomous communities and cities of Spain to make risk estimates and, where appropriate, to formalize seismic emergency plans.

The two most important seismic risk studies carried out in the Region of Murcia have been RISMUR and SISMIMUR. For the elaboration of the SISMIMUR, the elaboration of the RISMUR project was crucial. In fact, RISMUR was the baseline study to define the SISMIMUR plan, which was commissioned and financed by the National Geographic Institute together with the General Directorate of Civil Protection of the Region of Murcia.

RISMUR The scope of the RISMUR I and II projects is the seismic risk of the entire geographical area of the Autonomous Community of the Region of Murcia.

- *Seismic Risk of the Autonomous Community of the Region of Murcia* (RISMUR I, 2008), [49] and [10]; and

- *Service of Updating of the RISMUR Seismic Risk of the Autonomous Community of the Region of Murcia* (RISMUR II, 2014) [51].

Both of them constitute a fundamental part of the *Emergency Plan for Seismic Risk of the Autonomous Community of the Region of Murcia*.

RISMUR I The RISMUR I project was developed by a multidisciplinary team, bringing together specialists from all the fields involved in calculating seismic risk, namely, seismology, geotechnics, geology, architecture, seismic

engineering and economic, among others.

It was coordinated in several phases in order to cover all the aspects that a risk study requires, from the characterization of the seismic action to the estimation of losses due to the movement expected with a return period of 475 years at any point in the Region of Murcia. The final risk estimate is established in terms of level of damage to each of the typologies of buildings included in the different classes of vulnerability, also estimating the total damages and the number of uninhabitable dwellings, for each population entity of the Region of Murcia.

The final document is divided into these five volumes:

- Volume 1: *Assessment of seismic hazard*, by the Higher Technical School of Topographic, Geodesic and Cartographic Engineering of Universidad Politécnica Madrid
- Volume 2: *Geotechnical characterization*, by the Universidad Complutense de Madrid
- Volume 3: *Seismic vulnerability*, by Patrick Murphy, an architect specialised in seismic vulnerability
- Volume 4: *Transfer of Coulomb forces*, by the Universidad Complutense de Madrid
- Volume 5: *Seismic risk assessment*, by the Higher Technical School of Topographic, Geodesic and Cartographic Engineering of Universidad Politécnica Madrid

This project draws the most relevant conclusions on the *Evaluation of the seismic hazard, Geotechnics and analysis of the local seismic effect of the soil, Vulnerability of the buildings, Accumulation of forces* and the *Evaluation of seismic risk* sections. Its results served as the base of the SISMIMUR Emergency Planning.

In, Volume 3, *Seismic vulnerability*, the complete building stock of the region of Murcia is assessed in terms of vulnerability, ranging from old traditional building to current buildings. The building stock of the Region of Murcia is classified according to the vulnerability classes of the EMS-98 and the resultant damages are estimated based on it. The classification of the Vulnerability is based on the buildings' typologies, the year of construction and the construction quality.

In the final results of this project, the city of Lorca was considered to be the population with the highest expected damage of the region of Murcia and with a higher order of priority established for the definition of particular hazard scenarios and risk.

RISMUR II The RISMUR II project constitutes an update of the first project.

In this updated project (RISMUR II), a new seismic risk study of the Region is carried out incorporating new methodologies in the estimation of hazard and seismic risk, as well as more recent data in the calculation variables from the information generated as a result of the Lorca earthquake of 2011.

According to said document, [51], the most significant contributions of this new study are classified into two blocks of actions. Herein, those most relevant are listed and those related to vulnerability are highlighted.

1. Update of the starting data:

- The catalogue of seismic records was updated up to October 2013, allowing the incorporation of the last destructive earthquake that occurred in the region, the 2011 Lorca earthquake, into the hazard calculation.
- The zones catalogue was updated with the new zoning developed for Spain in recent years, especially the zoning used in the New Seismic Hazard Map of Spain [50] that is expected to be used to review the future standard national seismic resistance, the currently under development NCSR-22 [24].
- The catalogue of active faults in the region has been updated with the new QAFI database [41].
- The catalogue of strong motion models (GMPE, Ground Motion Prediction Equation) has been revised and updated.
- *The database with the building stock of the Murcia region has been updated up to September 2013, incorporating new data related to the structure of the buildings that has allowed to incorporate new seismic vulnerability classifications in buildings and households.*

2. Application of new calculation methodologies:

- The definition of the seismic sources for the estimation of the hazard has been carried out including a hybrid model of faults and zones.
- The estimation of the structural damage was carried out by means of different methodologies, employing empirical*

and analytical methods and combining their results by means of a logical tree. The former being based on the vulnerability model described in the EMS-98 scale, as an empirical method (used in RISMUR I). The latter being applied by assigning capacity and fragility curves to the vulnerability classes identified in the region and modeling the hazard through curves of demand (or response spectra) that cover the different spectral ordinates of interest for structures.

-Seismic risk was characterized not only in terms of structural damage to buildings and uninhabitable buildings, but also estimated human and economic losses.

The existing buildings in the studied locality were classified into four groups of construction typologies: three types of masonry and one of reinforced concrete. These, in turn, were subdivided according to their height and design code, giving a total of thirteen typologies of construction that are described in Table 1.1. Moreover, these typologies will be further detailed in Section 2.2.

Typology	Brief description of the struct. system	N. of storeys
M11L	load bearing masonry walls composed of	1-2
M11M	rubble stone and/or fieldstone	3-5
M31L	load bearing unreinforced masonry walls	1-2
M31M	with wooden slabs	3-5
M34L	load bearing unreinforced masonry walls	1-2
M34M	with reinforced concrete slabs	3-5
M34M		≥ 6
RC31L-pre	reinforced concrete frame structures	1-3
RC31M-pre	without seismic-resistant design	4-7
RC31H-pre		≥ 8
RC31L-low	reinforced concrete frame structures	1-3
RC31M-low	with low level of seismic-resistant design	4-7
RC31H-low		≥ 8

Table 1.1: Structural typologies present in the municipality of Lorca. Table included in the report of the RISMUR II project. [51]. Nomenclatures were established according to RISK-UE [76]

According to said project report, there is a significant degree of uncertainty in the selection of fragility curves that represent the behavior of buildings. This is due to the fact that they are elaborated on the basis of models of buildings with structural characteristics, design and construction materials that can be considered similar. However, their real behaviour also depends on the geometry and construction techniques, which vary from one building to another or from one region to another within the same structural typology.

The fragility curves finally selected in the RISMUR II study for the application of the RISK-UE methodology were taken from Lagomarsino and Giovinazzi (2006) [61] in the case of masonry buildings, and from HAZUS-MH [47] in the case of reinforced concrete buildings. It is worth mentioning that Lagomarsino and Giovinazzi were members of the RISK-UE Project working group who, in 2006, presented a study in which calibrated and standardized the RISK-EU curves for European countries.

Not all the fragility curves were selected from those proposed by the RISK-UE project despite applying this methodology. This is because certain inconsistencies within results were found for masonry as well as for reinforced concrete buildings when applying the RISK-UE methodology to calculate the damage for the same seismic input in a checking simulation. In the following, these inconsistencies are detailed.

On the one hand, in Figure 1.8, it can be seen that for the RISK-UE curves, the M11 typology presents much greater damage than the M31 typology, which presents a result without any type of damage. Moreover, the reinforced concrete typologies presented greater probabilities of damage than most of the masonry buildings when subjected to the same seismic input, which a priori seemed incongruous to the researchers.

Later, said experts analyse the possible origin of these unreliable results for the RISK-UE methodology: the fact that the capacity and fragility curves were developed by different institutions participant in the project.

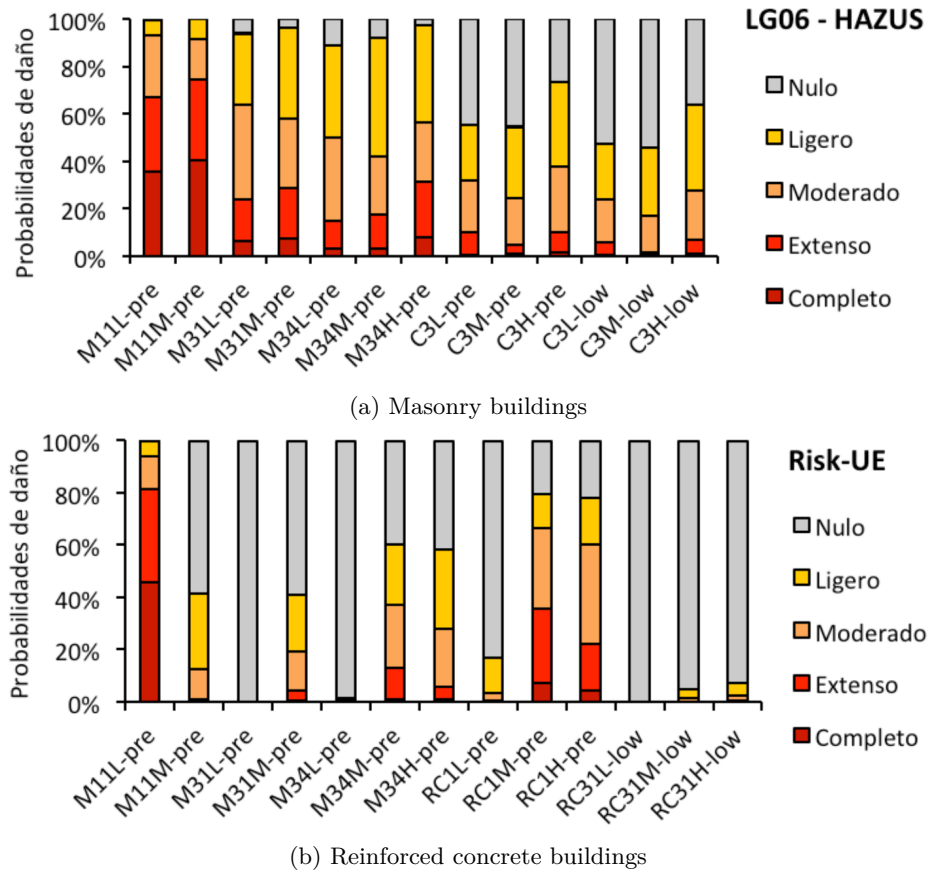


Figure 1.8: Damage probabilities for existing construction typologies in Lorca, evaluated for the same seismic input. Figures taken from the RISMUR II project [51]. Top: results from the application of the fragility curves proposed by Lagomarsino and Giovinazzi (2006) Bottom: results from the application of the fragility curves proposed within the RISK-UE project.

On the other hand, these were the arguments for selecting curves from Lagomarsino and Giovinazzi (2006) and HAZUS-MH:

- The Lagomarsino and Giovinazzi (2006) curves for masonry buildings provide homogeneity against the curves provided by RISK-UE. Furthermore, they were developed for European buildings.
- The HAZUS curves for reinforced concrete buildings, since reinforced concrete buildings are not so different in the US and Europe. Furthermore, the work of Lagomarsino and Giovinazzi (2006) does not cover infilled frame reinforced concrete structure buildings.

In Chapter 3 of this dissertation, a new methodology for assessing the adequacy of fragility curves for a particular region is presented. Therein, the aforementioned curves applied in RISMUR II are evaluated.

SISMIMUR The SISMIMUR is a Special Plan for Civil Protection Against Seismic Risk in the Region of Murcia. The previous elaboration of the RISMUR project was essential for the elaboration of this Plan. The object of the SISMIMUR plan is to know the existing hazard in the Region of Murcia against seismic risk; estimate the vulnerability of buildings whose destruction may cause victims, interrupt an essential service or increase damages due to associated catastrophic effects; as well as to establish the organization and procedures of action of the resources and services in order to deal with the seismic emergency. Or, as part of the organization of the State Plan, provide the necessary collaboration and resources for when such situations occur in any other part of the national territory.

Chapter 5.2 of the same document provides an estimate of the seismic vulnerability of buildings, with the same methodology and results as the RISMUR project.

MERISUR The MERISUR Project [42], *Methodology for an Effective RiSk assessment of URban areas*, aimed at developing an effective methodology for urban seismic risk assessment that provided solutions to some deficiencies detected after recent damaging events worldwide, including risk mitigation actions based on benefit/cost ratios. It was developed by the same research group from the Universidad Politécnica de Madrid that elaborated the RISMUR projects.

Firstly, in relation to hazard, the models used for risk estimation were developed and improved. A procedure to determine the seismogenic fault that controls seismic hazard for a given probability level was established.

Secondly, in relation to exposure and vulnerability, a more complete description of seismic vulnerability was accomplished, including urban modifiers to incorporate the effects of urban parameters on vulnerability classes. Moreover, attention was paid to the damage caused by falling debris from non-structural elements of buildings.

Furthermore, two campaigns for data collection were carried out in four selected districts of Lorca. A specific rapid visual survey was fulfilled for each building containing its characteristics (structural and non-structural elements) and other data regarding urban features, such as height differences with adjacent buildings, position within the building block, plan irregularities, etc. These data are used to check the reliability of the cadastral database and to estimate the distribution of seismic vulnerability using empirical methods (Vulnerability Index approach and EMS98 vulnerability classifications). The project was completed with a set of geomatic tools, such as a geographic information system and a web map server, for disseminating all the information and results of the project (see [101]).

The information about the seismic exposure of Lorca buildings developed within the framework of this project is used in Chapter 2 for the elaboration of the maps presented.

KUK-AHPÁN The Kuk-Ahpán research study [59] is a project of the Spanish State Research Plan in which this PhD dissertation is framed. Its full title is *Kuk-Ahpán: Integrated Regional Study Of The Structure And 4d Evolution Of The Lithosphere In Central America. Implications In The Calculation Of The Seismic Hazard And Risk*. It is a coordinated project that consists of two subprojects: KUK-AHPAN 1-Geophysics, and KUK-AHPAN 2- Seismic hazard and risk. The project involves the participation of researchers from all Central American countries (Honduras, Nicaragua, Costa Rica, El Salvador, Guatemala, Panama and Mexico) and several European institutions (from Spain and Norway). That framework establishes a scientific-technical cooperation to conduct research in two application scenarios: Central America and Southeast Spain.

The ultimate goal of the Subproject 2, within which vulnerability is included, is to advance in the evaluation of seismic hazard, integrating the most recent results regarding knowledge of active tectonics, rheology, paleoseismicity studies, modeling of crustal deformations with GPS and interferometry radar and Coulomb static stress transfer, as well as seismic risk assessment integrating modern geospatial technologies and methodologies for characterising the buildings vulnerability. The project is proposed for two large application scenarios:

1. Central America and the Caribbean, a region that, due to the high speed of convergence between the Cocos, North America and Caribbean plates, presents high seismicity, which constitutes a natural laboratory for experimentation; and
2. Southeast of Spain (SE), a region with a rate of deformation lower than that of the previous scenario, which implies a smaller volume of records available, entailing the need to apply models and techniques tested in areas such as the previous one.

The objectives regarding Subproject 2 are the following:

- Development of field campaigns to extract exposure data and vulnerability in sampling to be carried out in Murcia and in the populations of the Autonomous Community where subsequently, risk studies will be carried out.
- Preparation of a map of exposed elements and cataloging of the construction typologies in Murcia.
- Application of different geospatial technologies to characterize the exposure and vulnerability in Murcia. Development, in addition, of field campaigns with on-site inspections and comparison with the results of the applied technologies. Extract conclusions about the suitability of the different technologies.*
- Application of the integral methodology for calculating seismic risk to the city of Murcia.

Lines of research identified and investigated in this PhD dissertation

Within this context, a series of lines of research have been identified concerning vulnerability, which are covered within this dissertation.

Firstly, the study of the RISMURII seismic risk project and the state of the art have revealed the existence of a gap in the literature, the lack of a rational method to determine the adequacy of a specific fragility curve for the particular seismic risk study of a region. For this reason, in Chapter 3, this line of investigation is covered and the elaborated methodology applied to the case of Lorca. As a consequence of the results obtained, in Chapter 4, new fragility curves for the different unreinforced masonry building typologies typical of Lorca are created

Secondly, the relevance of advancing in a field still under underdevelopment, that related to the seismic performance of non-structural elements such as masonry parapets and infills has been manifested. In Chapters 5 and 6, the contributions concerning these complex topics are presented.

References

- [1] ATC-13 and Applied Technology Council. “Earthquake damage evaluation data for California”. In: Redwood City, California, 492pp. Funded by FEMA. 1985.
- [2] ATC-25 and Applied Technology Council. “Seismic Vulnerability and impact of disruption of lifelines in the conterminous United States”. In: Redwood City, California, 492pp. Funded by FEMA. 1991.
- [3] *ATC-38 Postearthquake Building Performance Assessment Form*. URL: <https://www.atcouncil.org/pdfs/atc38assmtfrm.pdf>.
- [4] Ghassan Al-Chaar. *Evaluating strength and stiffness of unreinforced masonry infill structures*. Tech. rep. ENGINEER RESEARCH and DEVELOPMENT CENTER CHAMPAIGN IL CONSTRUCTION ..., 2002.
- [5] R Álvarez-Cabal, E Díaz-Pavón, and R Rodríguez-Escribano. “El terremoto de Lorca: Efectos en los edificios”. In: *Madrid, Consorcio de Compensación de Seguros, Ministerio de Economía y Competitividad* (2013).
- [6] Filip Anić et al. “A review of experimental and analytical studies on the out-of-plane behaviour of masonry infilled frames”. In: *Bulletin of Earthquake Engineering* 18 (2020), pp. 2191–2246. DOI: [10.1007/s10518-019-00771-5](https://doi.org/10.1007/s10518-019-00771-5). URL: <https://doi.org/10.1007/s10518-019-00771-5>.
- [7] PG Asteris et al. “Numerical modelling of out-of-plane response of infilled frames: State of the art and future challenges for the equivalent strut macromodels”. In: *Engineering Structures* 132 (2017), pp. 110–122.
- [8] Horia Alejandro Barbat Barbat et al. “Probabilistic assessment of the seismic damage in reinforced concrete buildings”. In: *Proceedings of the 10th International Symposium Computational Civil Engineering: Iasi, Romania-May 25th, 2012*. Societatea Academica. 2012, pp. 43–61.
- [9] Álex Horia Barbat. *El riesgo sísmico en el diseño de edificios*. Calidad siderúrgica, 1998.
- [10] B Benito et al. “The RISMUR project: seismic risk assessment of the Murcia province (SE Spain)”. In: *Boll. Geofis. Teor. Applic* 49 (2008), pp. 3–15.
- [11] Simona Bianchi, Jonathan Ciurlanti, and Stefano Pampanin. “Seismic vulnerability of non-structural components: from traditional solutions to innovative lowdamage systems”. In: *Proceedings SECED 2019 Conference*. 2019.
- [12] Giuseppe Brando et al. “A CARTIS-based method for the rapid seismic vulnerability assessment of minor Italian historical centres”. In: *International Journal of Disaster Risk Reduction* 63 (2021), p. 102478.
- [13] Luis Cabañas Rodríguez et al. “Informe del sismo de Lorca del 11 de mayo de 2011. Last vist 10/05/2023”. In: *Instituto Geográfico Nacional (España)* (2011). URL: <http://hdl.handle.net/10261/62381>.
- [14] G.M. Calvi, D. Bolognini, and A. Penna. “Seismic performance of masonry-infilled R.C. frames: benefits of slight reinforcements”. In: *Sismica 2004, Congreso Nacional de Sismología e Engenharia Sísmica*, (2004).
- [15] Paolo M Calvi and Timothy J Sullivan. “Estimating floor spectra in multiple degree of freedom systems”. In: *Earthquakes and Structures* 7.1 (2014), pp. 17–38.
- [16] Donatello Cardone and Giuseppe Perrone. “Developing fragility curves and loss functions for masonry infill walls”. In: *Earthquakes and Structures* 9.1 (2015), pp. 257–279.
- [17] Liborio Cavaleri, Maria Zizzo, and Panagiotis G Asteris. “Residual out-of-plane capacity of infills damaged by in-plane cyclic loads”. In: *Engineering Structures* 209 (2020), p. 109957.

- [18] Thomas Celano et al. “In-Plane Behaviour of Masonry Walls: Numerical Analysis and Design Formulations”. In: *Materials* 14.19 (2021), p. 5780.
- [19] Thomas Celano et al. “Literature review of the in-plane behavior of masonry walls: Theoretical vs. experimental results”. In: *Materials* 14.11 (2021), p. 3063.
- [20] Andrew Coburn and Robin Spence. *Earthquake protection*. John Wiley & Sons, 2003.
- [21] Felice Colangelo. “Experimental evaluation of member-by-member models and damage indices for infilled frames”. In: *Journal of earthquake engineering* 7.01 (2003), pp. 25–50.
- [22] Canterbury Earthquakes Royal Commission. *Final Report. Volume 4: Earthquake-Prone Buildings*. Tech. rep. New Zealand., 2012.
- [23] Jorge Conde-Conde et al. *Estructuras sismorresistentes: Fundamentos de proyecto*. UPM Press, 2021. ISBN: 8418661100.
- [24] NCSR-22. Norma de Construcción Sismorresistente (upcoming). “Consulta pública previa sobre el borrador de Real Decreto por el que se aprueba la Norma de Construcción Sismorresistente NCSR-2022. Last visit 10/05/2023”. In: (). URL: www.mitma.gob.es/el-ministerio/buscador-participacion-publica/audiencia-e-informacion-publica-sobre-el-proyecto-de-real-decreto-por-el-que-se-aprueba-la-norma-de-construccion-sismorresistente-ncsr-22.
- [25] A Corsanego and V Petrini. “Seismic vulnerability of buildings”. In: *Proceedings of the SEISMED 3* (1990).
- [26] Directriz Básica de Protección Civil ante el Riesgo Sísmico. “(Basic Guideline for Civil Protection Against Seismic Risk). Secretaría de Estado de Interior”. In: *BOE-05/05/1995* (1995).
- [27] K.T. Doherty et al. “Displacement-based seismic analysis for out-of-plane bending of unreinforced masonry wall”. In: *Earthquake Engineering and Structural Dynamics* 31 (2002), pp. 833–850.
- [28] M Dolce et al. “Report of the EAEE Working Group 3: Vulnerability and risk analysis”. In: *Proceedings of the 10th European conference on earthquake engineering*. Vol. 4. 1994, pp. 3049–3077.
- [29] Sarah Dunn et al. “Fragility curves for assessing the resilience of electricity networks constructed from an extensive fault database”. In: *Natural Hazards Review* 19.1 (2018).
- [30] EN-1998. “Eurocode 8: Design of structures for earthquake resistance - Part 1 : General rules, seismic actions and rules for buildings”. In: *European Committee for Standardization, Brussels*. (2003).
- [31] *Earthquake catalogue*. DOI: <https://doi.org/10.7419/162.03.2022>. URL: <https://www.ign.es/web/sis-catalogo-terremotos>.
- [32] Bruce R Ellingwood et al. “Fragility assessment of light-frame wood construction subjected to wind and earthquake hazards”. In: *Journal of Structural Engineering* 130.12 (2004), pp. 1921–1930.
- [33] *Emergency Events Database (EM-DAT)*. URL: <https://www.emdat.be>.
- [34] European Seismological Commission. “European Macroseismic Scale 1998”. In: *Cahiers du Centre Européen de Géodynamique et de Séismologie*. Ed. by G. Grünthal. Vol. 15. Luxembourg: Conseil de l’Europe, 1998. ISBN: 2-87977-008-4.
- [35] FEMA-440. “USA Improvement of nonlinear static seismic analysis procedures. Redwood City, California,” in: *Applied Technology Council (ATC-55 Project)* (2005).
- [36] FEMA P-58-1. “Next-generation Seismic Performance Assessment of Buildings. Red wood City, California, USA.” In: *Applied Technology Council (ATC Project)* 1 (2012).
- [37] FEMA P-58-2. “Next-generation Seismic Performance Assessment of Buildings. Red wood City, California, USA.” In: *Applied Technology Council (ATC Project)* 2 (2012).
- [38] Tiago Miguel Ferreira et al. “Experimental characterization of the out-of-plane performance of regular stone masonry walls, including test setups and axial load influence”. In: *Bulletin of Earthquake Engineering* 13.9 (2015), pp. 2667–2692.
- [39] Carlos Flores. *Arquitectura popular española*. Vol. 4. Aguilar, 1973.
- [40] Sigmund A Freeman. “The capacity spectrum method as a tool for seismic design”. In: *Proceedings of the 11th European conference on earthquake engineering*. Citeseer. 1998, pp. 6–11.
- [41] J García-Mayordomo et al. “Modelo de zonas sismogénicas para el cálculo de la peligrosidad sísmica en España”. In: *Proceedings of the VII Asamblea Hispano Portuguesa de Geodesia y Geofísica* (2012), pp. 23–28.

- [42] Jorge M Gaspar-Escribano et al. “Methodology for an effective risk assessment of urban areas: progress and first results of the MERISUR project”. In: *Proceedings, 16 th World Conference on Earthquake Engineering, 16WCEE 2017* (2017). URL: <https://oa.upm.es/49862/>.
- [43] Marta Giaretton, Dmytro Dizhur, and Jason M Ingham. “Dynamic testing of as-built clay brick unreinforced masonry parapets”. In: *Engineering Structures* 127 (2016), pp. 676–685.
- [44] Michael C Griffith et al. “Evaluation of out-of-plane stability of unreinforced masonry walls subjected to seismic excitation”. In: *Journal of Earthquake Engineering* 7.spec01 (2003), pp. 141–169.
- [45] Michael Craig Griffith et al. “Experimental investigation of unreinforced brick masonry walls in flexure”. In: *Journal of Structural Engineering* 130.3 (2004), pp. 423–432.
- [46] Lutz Hermanns et al. “Performance of buildings with masonry infill walls during the 2011 Lorca earthquake”. In: *Bulletin of Earthquake Engineering* 12.5 (2014), pp. 1977–1997.
- [47] WILLIAM Holmes. “HAZUS-MH: Multi-hazard loss estimation methodology: Technical manual”. In: *Washington, DC: Federal Emergency Management Agency* (1999).
- [48] George W Housner. “The behavior of inverted pendulum structures during earthquakes”. In: *Bulletin of the seismological society of America* 53.2 (1963), pp. 403–417.
- [49] RISMUR I. *Estudio de Riesgo Sísmico en la provincia de Murcia (Proyecto RISMUR)*. Broadway Malyan, Grupo de Tectónica Activa y Paleosismicidad (Universidad Complutense de Madrid, UCM), Grupo de Ingeniería Sísmica (Universidad Politécnica de Madrid, UPM). 2008.
- [50] IGN, 2015. Developed by IGN and UPM. Last visit 08/02/2022. URL: <https://www.ign.es/web/mapas-sismicidad>.
- [51] RISMUR II. *Servicio de Actualización del Análisis de Riesgo Sísmico (RISMUR) en la Región de Murcia. ETSI Topografía, Geodesia y Cartografía (Universidad Politécnica de Madrid, UPM) , Grupo de Ingeniería Sísmica (UPM)*. 2014.
- [52] Yasser E Ibrahim and Mostafa M El-Shami. “Seismic fragility curves for mid-rise reinforced concrete frames in Kingdom of Saudi Arabia”. In: *The IES Journal Part A: Civil & Structural Engineering* 4.4 (2011), pp. 213–223.
- [53] Scheda CARTIS 2014. Presidenza del Consiglio dei Ministri Dipartimento della Protezione Civile of Italy. “Scheda di 1 Livello per la CARatterizzazione TIpologica-Strutturale dei comparti urbani costituiti da edifice ordinari”. In: *Available online*. (2014). URL: geoportale.comune.cavadetirreni.sa.it/file/38732/download?token=x4arE236.
- [54] David Johnston et al. “The 2010/2011 Canterbury earthquakes: context and cause of injury”. In: *Natural Hazards* 73.2 (2014), pp. 627–637.
- [55] Bidur Kafle et al. “Displacement controlled rocking behaviour of rigid objects”. In: *Earthquake engineering and structural dynamics* 40.15 (2011), pp. 1653–1669.
- [56] DJ Kakaletsis and CG Karayannis. “Influence of masonry strength and openings on infilled R/C frames under cycling loading”. In: *Journal of Earthquake Engineering* 12.2 (2008), pp. 197–221.
- [57] Stan Kaplan, Harold F Perla, and Dennis C Bley. “A methodology for seismic risk analysis of nuclear power plants”. In: *Risk Analysis* 3.3 (1983), pp. 169–180.
- [58] Robert P Kennedy et al. “Probabilistic seismic safety study of an existing nuclear power plant”. In: *Nuclear Engineering and Design* 59.2 (1980), pp. 315–338.
- [59] *Kuk-Ahpán: Integrated Regional Study Of The Structure And 4d Evolution Of The Lithosphere In Central America. Implications In The Calculation Of The Seismic Hazard And Risk*. URL: <https://blogs.upm.es/projectokukahpan/>.
- [60] CR Kumar, KB Narayan, and D Venkat Reddy. “Probabilistic seismic risk evaluation of rc buildings”. In: *Int. J. of Research in Engineering and Technology* 3 (2014), pp. 484–495.
- [61] Sergio Lagomarsino and Sonia Giovinazzi. “Macroseismic and mechanical models for the vulnerability and damage assessment of current buildings”. In: *Bulletin of Earthquake Engineering* 4.4 (2006), pp. 415–443.
- [62] Nelson Tung-Kiu Lam et al. “Time–history analysis of URM walls in out-of-plane flexure”. In: *Engineering structures* 25.6 (2003), pp. 743–754.
- [63] Isaac Felipe Lima-Castillo, Roberto Gómez-Martínez, and Adrián Pozos-Estrada. “Methodology to develop fragility curves of glass façades under wind-induced pressure”. In: *International Journal of Civil Engineering* 17.3 (2019), pp. 347–359.

- [64] Francesco Longo et al. “Application of an in-plane/out-of-plane interaction model for URM infill walls to dynamic seismic analysis of RC frame buildings”. In: *Bulletin of Earthquake Engineering* 16.12 (2018), pp. 6163–6190.
- [65] P.B. Lourenço and J.A. Roque. “Simplified indexes for the seismic vulnerability of ancient masonry buildings”. In: *Construction and Building Materials* 20.4 (May 2006), pp. 200–208. DOI: [10.1016/j.conbuildmat.2005.08.027](https://doi.org/10.1016/j.conbuildmat.2005.08.027).
- [66] P.B. Lourenço et al. “Simplified indexes for the seismic assessment of masonry buildings: International database and validation”. In: *Engineering Failure Analysis* 34 (Dec. 2013), pp. 585–605. DOI: <https://doi.org/10.1016/j.engfailanal.2013.02.014>.
- [67] Ali Reza Manafpour and Parisa Kamrani Moghaddam. “Probabilistic approach to performance-based seismic design of RC frames”. In: *Vulnerability, uncertainty, and risk: Quantification, mitigation, and management* (2014), pp. 1736–1745.
- [68] Manuale Scheda CARTIS 2014, Progetto Reluis 2014-2016, Dipartimento della Protezione Civile, Italy. “Manuale per la compilazione della Scheda di 1 Livello per la CARatterizzazione TIpologico-Strutturale dei comparti urbani costituiti da edificio ordinari”. In: (2016). URL: <https://geoportale.comune.cavadetirreni.sa.it/file/38732/download?token=x4arE236>.
- [69] S Martínez-Cuevas et al. “Urban modifiers of seismic vulnerability aimed at Urban Zoning Regulations”. In: *Bulletin of Earthquake Engineering* 15.11 (2017), pp. 4719–4750.
- [70] Sandra Martínez Cuevas. “Evaluación de la vulnerabilidad sísmica urbana basada en tipologías constructivas y disposición urbana de la edificación. Aplicación en la ciudad de Lorca, región de Murcia”. PhD thesis. Universidad Politécnica de Madrid, 2014. URL: oa.upm.es/30447/.
- [71] Claudio Mazzotti et al. “Una metodologia speditiva per la valutazione di vulnerabilità sismica di edifici in muratura e calcestruzzo armato [A simplified method for seismic vulnerability assessment of masonry and reinforced concrete buildings]”. In: *Progettazione Sismica* 4.2 (2013), pp. 95–112. DOI: [10.7414/PS.4.2.95-112](https://doi.org/10.7414/PS.4.2.95-112).
- [72] Robin K McGuire. *Seismic hazard and risk analysis*. Earthquake Engineering Research Institute, 2004.
- [73] Ricardo A Medina, Ragunath Sankaranarayanan, and Kevin M Kingston. “Floor response spectra for light components mounted on regular moment-resisting frame structures”. In: *Engineering structures* 28.14 (2006), pp. 1927–1940.
- [74] S Medvedev, W Sponheuer, and V (MSK-64) Karník. “Neue seismische Skala Intensity scale of earthquakes, 7. Tagung der Europäischen Seismologischen Kommission vom 24.9. bis 30.9. 1962”. In: *Jena, Veröff. Institut für Bodendynamik und Erdbebenforschung in Jena* 77 (1964), pp. 69–76.
- [75] Ulises Mena, Álex H Barbat, and Fabrizio Yépez Moya. “Evaluación probabilista del riesgo sísmico en zonas urbanas”. In: *Revista internacional de métodos numéricos para cálculo y diseño en ingeniería* (1998), pp. 247–268.
- [76] Zoran V Milutinovic and Goran S Trendafiloski. “RISK-UE: An advanced approach to earthquake risk scenarios with applications to different European towns”. In: *European Project Risk-UE* (2003).
- [77] Eduardo Miranda and Shahram Taghavi. “Approximate floor acceleration demands in multistory buildings. I: Formulation”. In: *Journal of structural engineering* 131.2 (2005), pp. 203–211.
- [78] S Molina, DH Lang, and CD Lindholm. *SELENA v3. 5 User and Technical Manual, NORSAR*. In: Lin Shibin et al. (2010). “Performance-based ...”. 2008.
- [79] P Mouroux et al. “The European RISK-UE project: an advanced approach to earthquake risk scenarios”. In: *Proc. of the 13th World Conference on Earthquake Engineering*. 2004.
- [80] AHM Muntasir Billah and M Shahria Alam. “Seismic fragility assessment of highway bridges: a state-of-the-art review”. In: *Structure and infrastructure engineering* 11.6 (2015), pp. 804–832.
- [81] Patrick Murphy. *Informe final proyecto RISNA. Evaluación del Riesgo Sísmico en Navarra*. 2008.
- [82] NTC18. “Aggiornamento delle Norme tecniche per le costruzioni, 20 febbraio”. In: *Decreto Ministeriale del Ministero delle Infrastrutture e dei Trasporti* 42 (2018).
- [83] Fadzli Mohamed Nazri and F Fragility Curves. *Seismic fragility assessment for buildings due to earthquake excitation*. Springer, 2018.
- [84] Francesca Pasqual et al. “Seismic vulnerability assessment of RC buildings at compartment scale: the use of CARTIS form”. In: *Procedia Structural Integrity* 44 (2023), pp. 203–210.

- [85] D Perrone et al. “Seismic performance of non-structural elements during the 2016 Central Italy earthquake”. In: *Bulletin of Earthquake Engineering* 17.10 (2019), pp. 5655–5677.
- [86] Daniele Perrone et al. “Probabilistic estimation of floor response spectra in masonry infilled reinforced concrete building portfolio”. In: *Engineering Structures* 202 (2020), p. 109842.
- [87] Crescenzo Petrone, Gennaro Magliulo, and Gaetano Manfredi. “Seismic demand on light acceleration-sensitive nonstructural components in European reinforced concrete buildings”. In: *Earthquake engineering & Structural dynamics* 44.8 (2015), pp. 1203–1217.
- [88] Maria Polese et al. “Damage-dependent vulnerability curves for existing buildings”. In: *Earthquake engineering & structural dynamics* 42.6 (2013), pp. 853–870.
- [89] Bharat Pradhan et al. “Prediction Equations for Out-of-Plane Capacity of Unreinforced Masonry Infill Walls Based on a Macroelement Model Parametric Analysis”. In: *Journal of Engineering Mechanics* 147.11 (2021), p. 04021096.
- [90] Ligia Elena Quirós Hernández. “Modelizaciones y análisis de sensibilidad en la evaluación integral del riesgo sísmico a escala urbana: aplicación a la ciudad de Lorca”. PhD thesis. Universidad Politécnica de Madrid, 2017. URL: oa.upm.es/48042/1/LIGIA_ELENA_QUIROS_HERNANDEZ.pdf.
- [91] Meera Raghunandan and Abbie B Liel. “Effect of ground motion duration on earthquake-induced structural collapse”. In: *Structural Safety* 41 (2013), pp. 119–133.
- [92] Lin Shibin et al. “Performance-based methodology for assessing seismic vulnerability and capacity of buildings”. In: *Earthquake engineering and engineering vibration* 9.2 (2010), pp. 157–165.
- [93] Vladimir Sigmund and Davorin Penava. “Experimental study of masonry infilled R/C frames with opening”. In: *Proceedings of the 15WCEE, Lisbon, Portugal* (2012).
- [94] Timothy J Sullivan, Paolo M Calvi, and Roberto Nascimbene. “Towards improved floor spectra estimates for seismic design”. In: *Earthquakes and Structures* 4.1 (2013), pp. 109–132.
- [95] Shahram Taghavi and Eduardo Miranda. “Approximate floor acceleration demands in multistory buildings. II: Applications”. In: *Journal of Structural Engineering* 131.2 (2005), pp. 212–220.
- [96] Yadir Torres et al. “A first approach to earthquake damage estimation in Haiti: advices to minimize the seismic risk”. In: *Bulletin of Earthquake Engineering* 14.1 (2016), pp. 39–58.
- [97] Regione Toscana. “Manuale per la compilazione della scheda GNDT/CNR di II livello versione modificata della Regione Toscana, Direzione Generale delle Politiche Territoriali ad Ambientali, Settore: Servizio Sismico Regionale”. In: *Progettazione Sismica* 2 (2003).
- [98] IGNUPM Grupo de Trabajo. “Actualización de Mapas de Peligrosidad Sísmica de España, 2012”. In: *Editorial Centro Nacional de Información Geográfica, Madrid* (2013).
- [99] Natural Disasters UNDR0. “Vulnerability analysis”. In: *Report of Experts Group Meeting, Geneva*. 1980.
- [100] R. Vacareanu et al. *WP7 report seismic risk scenarios handbook. RISKUE project of the EC: an advanced approach to earthquake risk scenarios with applications to different European towns*. 2004.
- [101] *Web Map Server elaborated within the MERISUR Project: Methodology for an Effective RISK assessment of URban areas. Last visit 10/05/2023*. URL: <http://merisur.topografia.upm.es/index.html>.
- [102] Gustavo Wilches-Chaux. *Herramientas Para la Crisis Desastres, Ecologismo y Formacion Profesional*. Servicio Nacional de Aprendizaje, SENA, 1989.
- [103] Naoya Yamaguchi and Fumio Yamazaki. “Fragility curves for buildings in Japan based on damage surveys after the 1995 Kobe earthquake”. In: *Proceedings of the 12th world conference on earthquake engineering, Auckland, New Zealand*. 2000, p. 2451.
- [104] G Zuccaro et al. “La scheda CARTIS per la caratterizzazione tipologico-strutturale dei comparti urbani costituiti da edifici ordinari. Valutazione dell’esposizione in analisi di rischio sismico”. In: *Proceedings of the GNGTS* (2015).
- [105] NCSE-02. Comisión permanente de normas sismorresistentes. “España. Norma de construcción sismorresistente: Parte general y edificación”. In: *RD 997/2002, Spain* (2002). URL: www.boe.es/eli/es/rd/2002/09/27/997.

Chapter 2

Exposure of Lorca: maps and analyses

Evaluating buildings' seismic vulnerability on a large scale requires an exposure model. For that reason, building exposure and vulnerability models for seismic risk assessment have been the focus of a huge number of research all over the world in recent years. Said exposure models quantify the building stock in terms of structural characteristics, spatial location, and occupancy.

The most significant parameters of the buildings regarding exposure are their structural characteristics, which must be uniformly covered by structural typologies. Moreover, structural typologies that take into account the regional specificities of design and construction provide more accurate and reliable exposure models [20].

Although exposure models being key for mitigating seismic risk and drawing emergency plans, collection of the data that are needed as input for such models is usually not part of established data collection processes [5]. Determining the structural characteristics along with the spatial location of a stock of buildings is not a simple task in developing countries, but neither is it in developed ones. These latter, present the advantage of having a database of cadastral information and census-based information. Nonetheless, these data banks are often outdated or incomplete regarding exposure [10]. For example in Spain, they do not provide information about the structural materials or typologies. For this reason, an habitual manner of assigning this feature is based on the knowledge the researcher does have despite being limited. Usually, the year of construction, height and the knowledge of the seismic codes applicable through history together with expert criteria are the elements involved in said assignment.

Throughout this document, some relevant (regarding vulnerability) Lorca exposure maps are presented on the basis of the typologies identified and assigned in previous research.

Additionally, once the presence of the different typologies are being statistically analysed and illustrated graphically, a database concerning more than 300 reports of Lorca buildings is studied in order to account the regional specificities of design and construction of each typology. Said reports were documented by experts just after the 2011 Lorca earthquake and includes Visual Reports and Reparation Projects (plans, details, budgets...). Such analysis addresses a detailed characterisation of the most common features of the structural as well as the non-structural elements of the typologies present in Lorca.

2.1 Exposure

Herein, the state of the art of the exposure of Lorca is illustrated by means of several exposure maps in order to allow the reader a better comprehension of the typologies present in Lorca. Moreover, some results of said distribution of typologies are statistically analysed and some conclusions drawn.

2.1.1 State of the art

The state of the art regarding the exposure of Lorca is briefly summarised in Section 1.4.1 and thoroughly illustrated in this Section. Moreover, some references to International Projects are included, see Section 1.2.2 for more detail.

National seismic codes

The elaboration of the exposure maps have taken into account the criteria detailed in Chapter 1, more specifically in Section 1.1, and the successive national regulations applicable to structural and non-structural elements.

In the following, the seismic regulations in force during the periods of construction of the Spanish buildings analysed and its main improvements are detailed:

- **PGS-1** [7] (1968-1973);
- **PDS-1** [6] (1974-1994), which includes a hazard map, some calculation methods and some mandatory and recommended construction rules;
- **NCSE-94** [26] (1995-2001), a standard that represented a great advance by including a probabilistic seismic hazard map, expressed in terms of basic seismic acceleration;
- **NCSE-02** [25], (2002-currently). In force when the Lorca earthquake occurred. This regulation incorporates a novelty in the cases of high-intensity earthquakes: if they cause damages to buildings, an inspection and an evaluation of the severity of the damages must be carried out. Reports derived from compliance with this law constitute the data used for this study. Moreover, it establishes design rules and rigorous constructive prescriptions and details, especially for the design of the structure of unreinforced masonry buildings and reinforced concrete buildings. Lastly, it provides some criteria to prevent non-structural elements such as chimneys, infill and parapet masonry walls from detaching, in order to reduce the number of casualties.
- **NCSR-22** [4]. This constitutes an upcoming regulation, currently in draft version.

Typologies identified in Lorca

In the RISMUR I and II projects, the most common typologies for Murcia were identified: M11, M31, M34 and RC31. Said typologies are herein detailed along with some consideration based on the seismic codes implemented, a transfer matrix developed for Lorca and some research into the aforementioned experts' reports.

The mentioned transfer matrix was developed by the architect and expert in vulnerability Patrick Murphy for the typologies that were identified in Lorca with local experts. The assignation of the typologies was carried out on the basis of the number of floors and the year of construction. It reflects some key considerations for the masonry and reinforced concrete (RC) typologies (see Table 2.1).

The nomenclatures and description of the typologies are provided in the following manner:

Nomenclature according to RISK-UE: description according to RISK-UE [18][correspondence with Lagormarsino and Giovinazzi (2006) [15]; correspondence with HAZUS [11]].

For further information, see Table 3.7, [21].

Masonry buildings :

- **M11-pre:** load bearing masonry walls composed of rubble stone and/or fieldstone, pre-code Seismic Resistant Design (SRD) [M1;-].
- **M31-pre:** load bearing unreinforced masonry walls with wooden slabs, pre-code SRD [M5;URM].
- **M34-pre:** load bearing unreinforced masonry walls with RC slabs, pre-code SRD [M6;URM].

Considerations:

- In 1940, M11-pre disappears
- In 1960, M31-pre disappears
- In 1994, when the NCSE-94 regulation came into force, all the masonry typologies disappear except from one to two-storeys M34-pre typology.

RC buildings

- **RC31-pre and RC31-low:** Reinforced concrete framed structures (beams and columns) with unreinforced masonry infill walls, pre-code and low code SRD [-;C3].

Considerations:

- There are no RC31-pre before 1940
- There are no RC31-low before 1994 (when the NCSE-94 regulation came into force)
- In 1994, all the pre-code RC buildings disappear.

Whereas the considerations for RC buildings were based on the inclusion of the Spanish successive regulations already mentioned; those considerations made with respect to masonry buildings will be compared with the results of the analyses of the reports. Some of the masonry buildings presented are made without a technician so that the appearance of the different codes cannot be considered a criteria to establish a limit.

As can be seen in Fig. 2.1, taken from the report of the RISMUR II project [13], these same typologies constitute the most habitual ones for all the different municipalities of Murcia. Furthermore, as [2] states, in general terms, the construction observed in Lorca does not present any difference with respect to what, according to their (and ours) experience, can be expected in any other Spanish city. Neither the materials used nor the construction systems or execution procedures differ from those observed in other cities, which cannot be considered positive because the seismicity of the area should impose obvious differences. The widespread of these typologies all over the country can be considered a fact that highlights the importance and applicability of developing fragility curves that adequately represent their vulnerability.

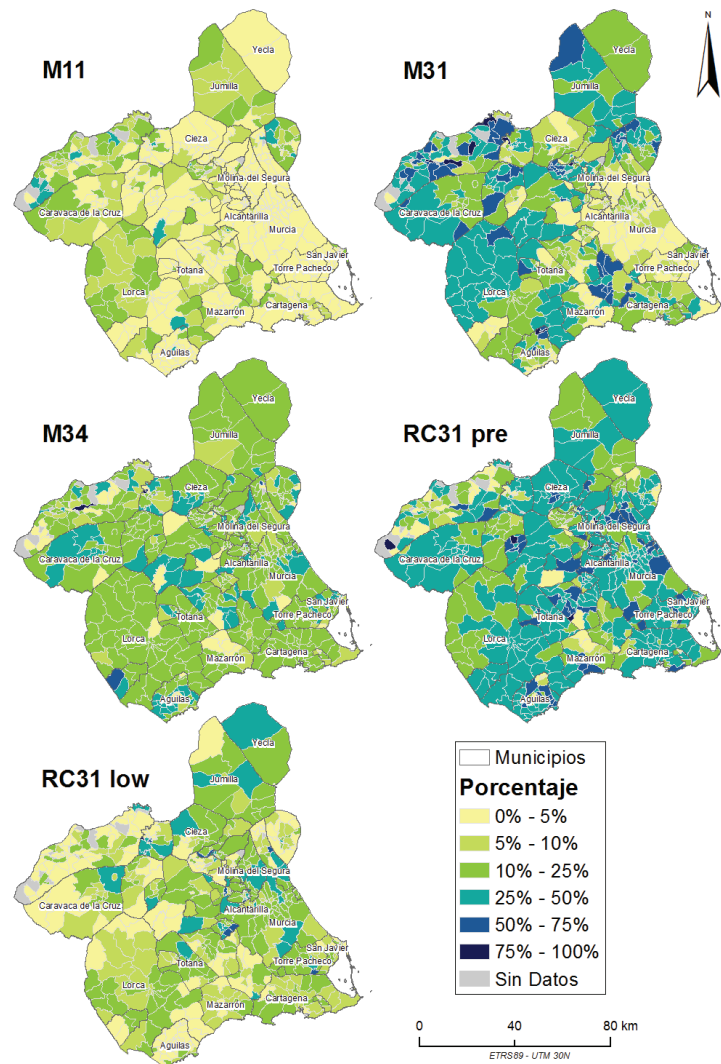


Figure 2.1: Distribution maps of the different typologies of buildings according to RISK-UE for the region of Murcia, expressing the distribution as a percentage. Figure taken from [13].

%	M11		M31		M34			RC31-pre code			RC31-low code		
	L	M	L	M	L	M	H	L	M	H	L	M	H
N ^o of floors	1-2	3+	1-2	3+	1-2	3-5	6+	1-2	3-5	6+	1-2	3-5	6+
SSRR	pre	pre	pre	low	low	low							
<1900	57		43										
1901-1920	21		71		8								
1921-1940	6		75		19								
1941-1950			9		55			36					
1951-1960			2		43			55					
1961-1970					35			65					
1971-1980					18			82					
1981-1996					12			88	100	100			
1997-2004					7						93	100	100
2004-2013					6						94	100	100

Table 2.1: Transfer matrix proposed by Patrick Murphy and employed for the assignment of typologies in the RISMUR I and II projects and in this dissertation. See [12] Vol. 3 for further detail. Typologies studied according to their year of construction and their number of floors. SSRR: level of seismic resistant design according to RISK-UE. Values in percentage (%). Cells in blank equal to 0.

2.1.2 Exposure maps

On the basis of the typologies identified and described in general terms, some interesting Lorca exposure maps regarding this dissertation are presented.

The elaboration of a Geographic Information System (GIS) of the city of Lorca that served as a support for the analysis of the seismic exposure of the city was crucial when the seismic risk studies mentioned in section 1.4.1 were developed [22]. The elaboration of said GIS engaged a great amount of work that was developed by members of the Research Group in Seismic Engineering of the Universidad Politécnica de Madrid on the basis of Cadastral information available.

In Spain, the General Directorate of Cadastre offers the possibility of downloading cadastral databases through the portal of the Electronic Headquarters of the General Directorate of Cadastre (SEC), by means of a digital certificate. Said cadastral databases provide information regarding the following features of each plot:

- Height (number of storeys)
- Area
- Year of construction
- Shape

However, in the Spanish Cadastre data, which is provided in type shapefile files, a constructive unit is not equal to a building. Therefore, it is made up of several polygons that represent elements such as the different floors of the building, the light wells, the terraces, the attics, etc.

Given that in a seismic exposure map, the study units are the buildings as individual elements, said information was debugged so as to represent each building by a single polygon per construction unit. After it, all the relevant attributes of the buildings concerning their vulnerability, i.e., height, total area and year of construction, were associated to this single polygon per construction unit. The information of the debugged GIS goes up to the year 2013.

In the seismic risk study conducted by [21], the transfer matrix elaborated by Patrick Murphy was applied so as to the Lorca GIS to classify the buildings. Once they were classified based on their year of construction and number of floors, the distribution of buildings (in percentage) was applied to the GIS at random..

On the basis of this information, the following exposure maps are developed in order to facilitate the understanding of the city of Lorca and the spatial and percentage distribution of each of the typologies presented.

List of maps of exposure and damage

- (i) **Historical evolution in relation to the the different Spanish seismic codes:** Fig. 2.2.
Map including all the buildings of Lorca depending on the year of construction.
- (ii) **Masonry typologies:** Figure 2.3.
Map including all the masonry buildings by typology.
- (iii) **Masonry typologies classified by height:** Figure 2.4.
Map including all the masonry buildings by typology and height.
- (iv) **RC typologies:** Figure 2.5.
Map including all the RC buildings by typology.
- (v) **RC typologies classified by height:** Figure 2.6.
Map including all the RC buildings by typology and height.

Furthermore, the City Council of Lorca provided the Research Group with a series of damage maps in .dwg (Autocad) format as a result of the evaluations carried out almost a month after the earthquake occurred, from May 11 to June 15. [17] analysed said information, eliminated the speculative elements and created a GIS map with the damages of the earthquake that is herein reproduced (with our format) for convenience of the reader.

- (vi) **Damages to buildings:** Figure 2.7.
Map including all the buildings highlighting their state of damage after the earthquake.

In this map, the buildings for which the Lorca City Council ceded information about their state of damage after the earthquake are highlighted. Said classification involves a triage with various colours on the basis of the quick assessment form fulfilled in the aftermath of the seismic event. The colours represent the following damage states:

- Buildings without a colour pattern (in light blue for a better comprehension of the map): buildings that do not present damage.
- Buildings in green: buildings with null or irrelevant structural damage. That is to say, when there are no cracks, fractures or buckling on the structural pillars of the building and there is no damage to thick masonry, such as accesses and accessible staircases or façades that can present a risk of collapse, etc.
- Buildings in yellow: buildings with moderate structural damage, that is, cracks, fractures and buckling in particular elements and/or in a localized way.
- Buildings in red: buildings with severe structural damage, that is, cracks, fractures and buckling in a generalised way and/or in localized elements but that entails a risk of collapse.
- Buildings in black: buildings that were declared as ruins before the seismic event.
- Building with a black star: the unique RC building collapsed during the earthquake [3] due to the presence of short columns, which means a deficient design for RC buildings in earthquake-prone areas [19].

Finally, Figure 2.8 is included in order to compare the frequencies by height of the existing four to six-storey RC buildings studied in Section 2.2.3 according to the exposure maps and those considered in the damage reports.

- (vii) **Frequencies in total RC buildings vs reports by year:** Figure 2.8.
Frequencies by height and year of construction of four to six-storey RC buildings: exposure maps versus buildings included in the reports.

612868.05

614868.05

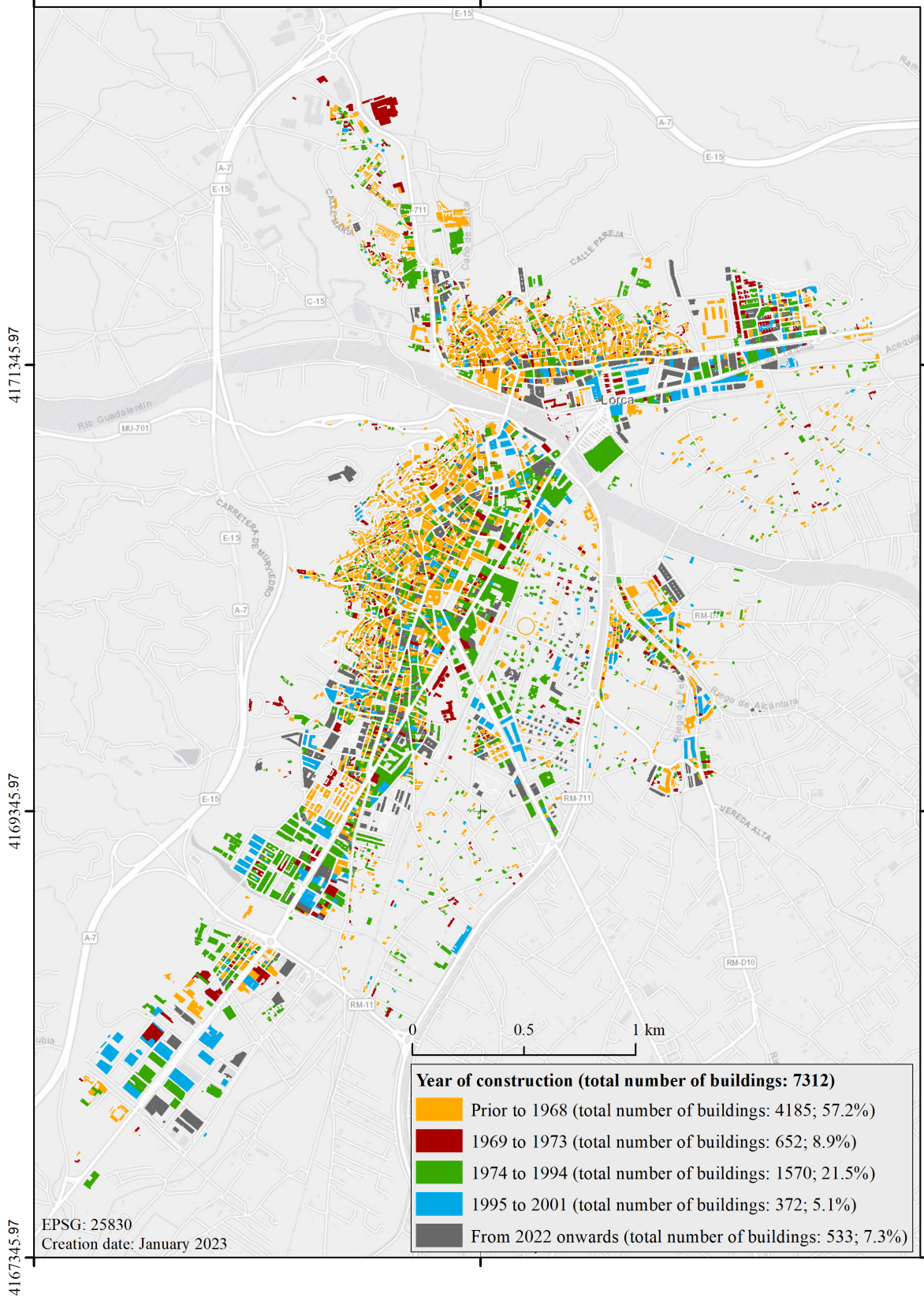


Figure 2.2: (i) **Historical evolution in relation to the appearance of the different Spanish seismic codes.** Map including all the buildings of Lorca depending on the year of construction. Recent buildings not included in the exposition map in gray.

612868.05

614868.05

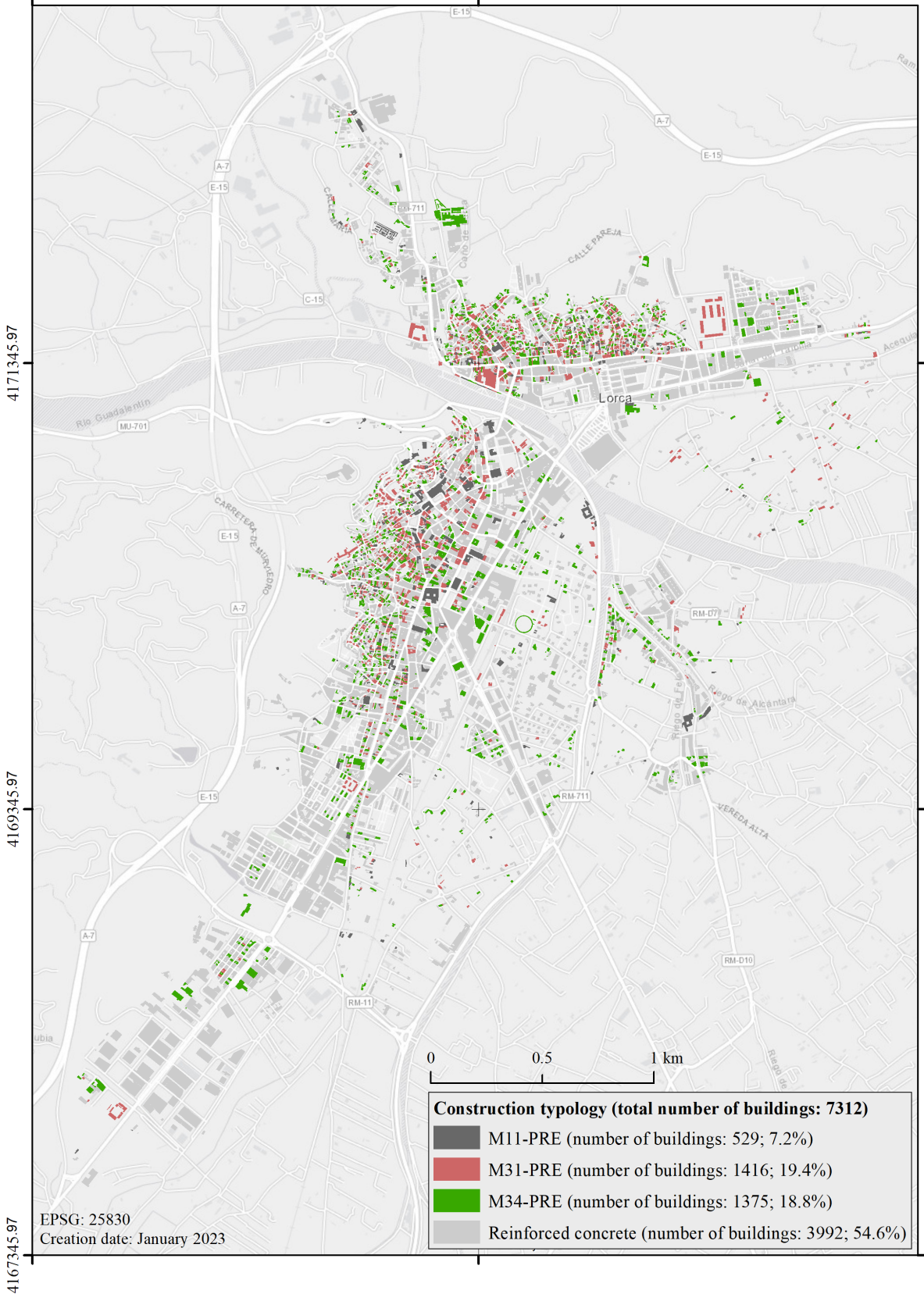


Figure 2.3: (ii) **Masonry typologies** Map including all the masonry buildings by typology.

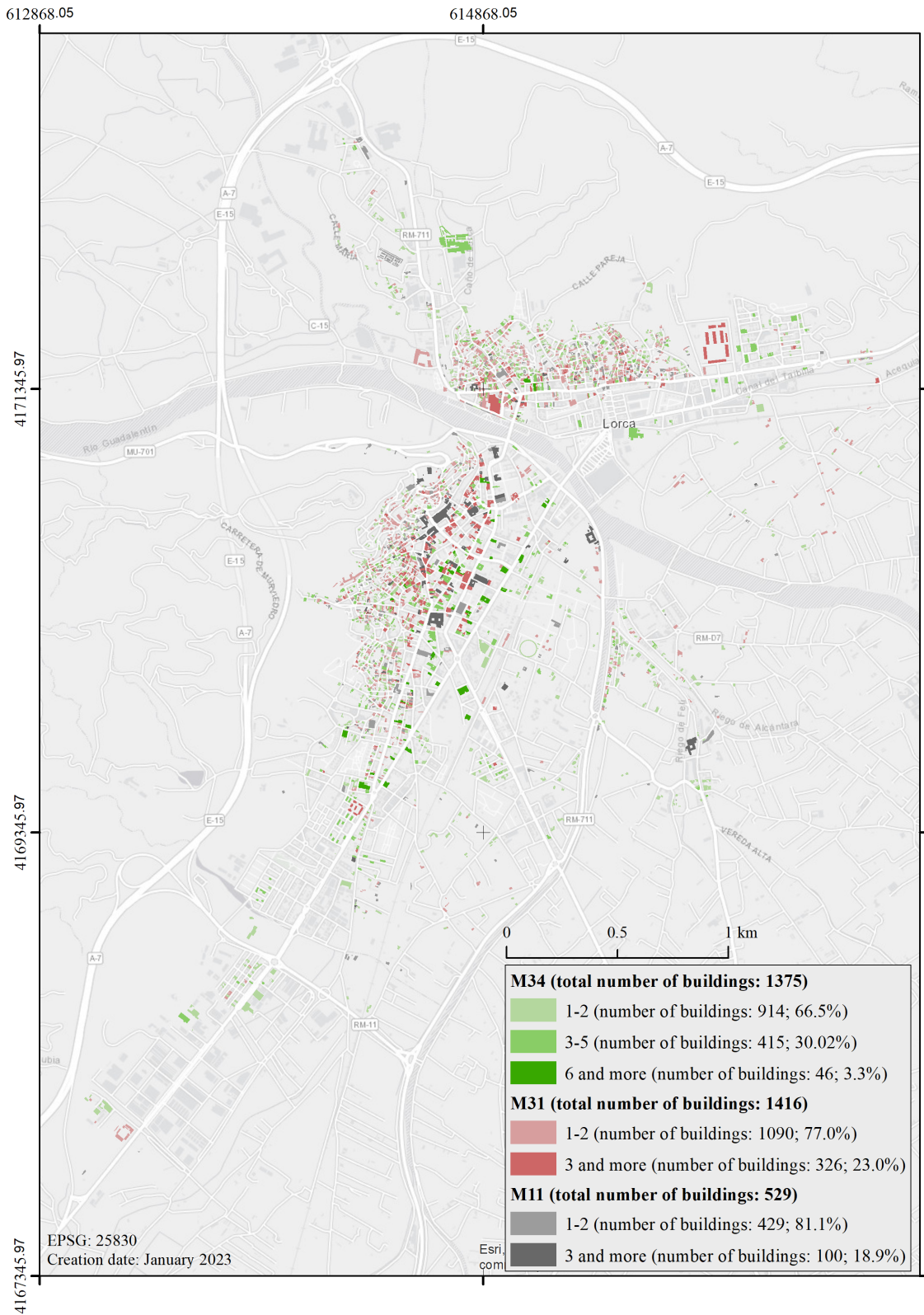


Figure 2.4: (iii) Masonry typologies classified by height Map including all the masonry buildings by typology and height.

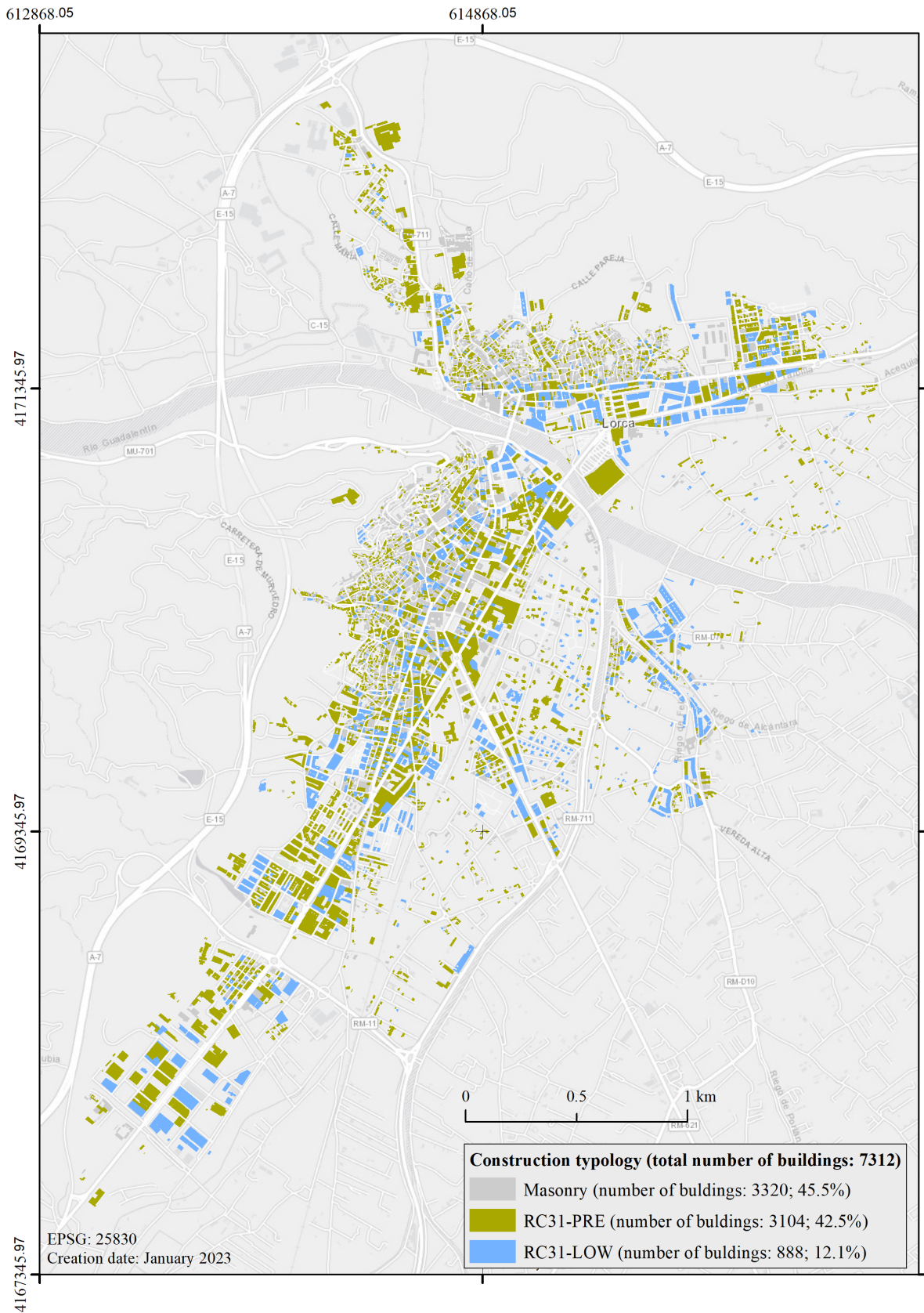


Figure 2.5: (iv) RC typologies Map including all the RC buildings by typology.

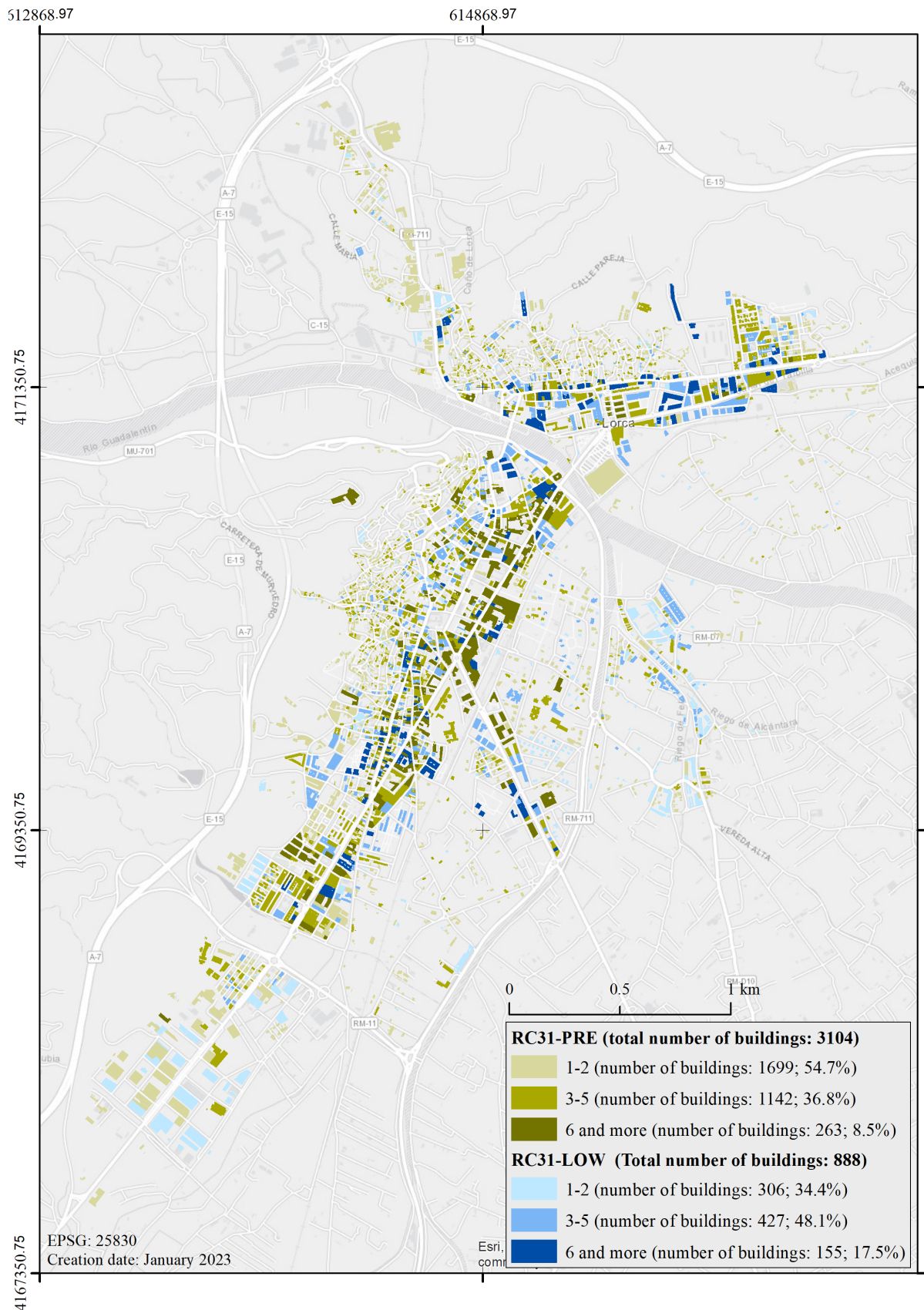


Figure 2.6: (v) RC typologies classified by height Map including all the RC buildings by typology and height.

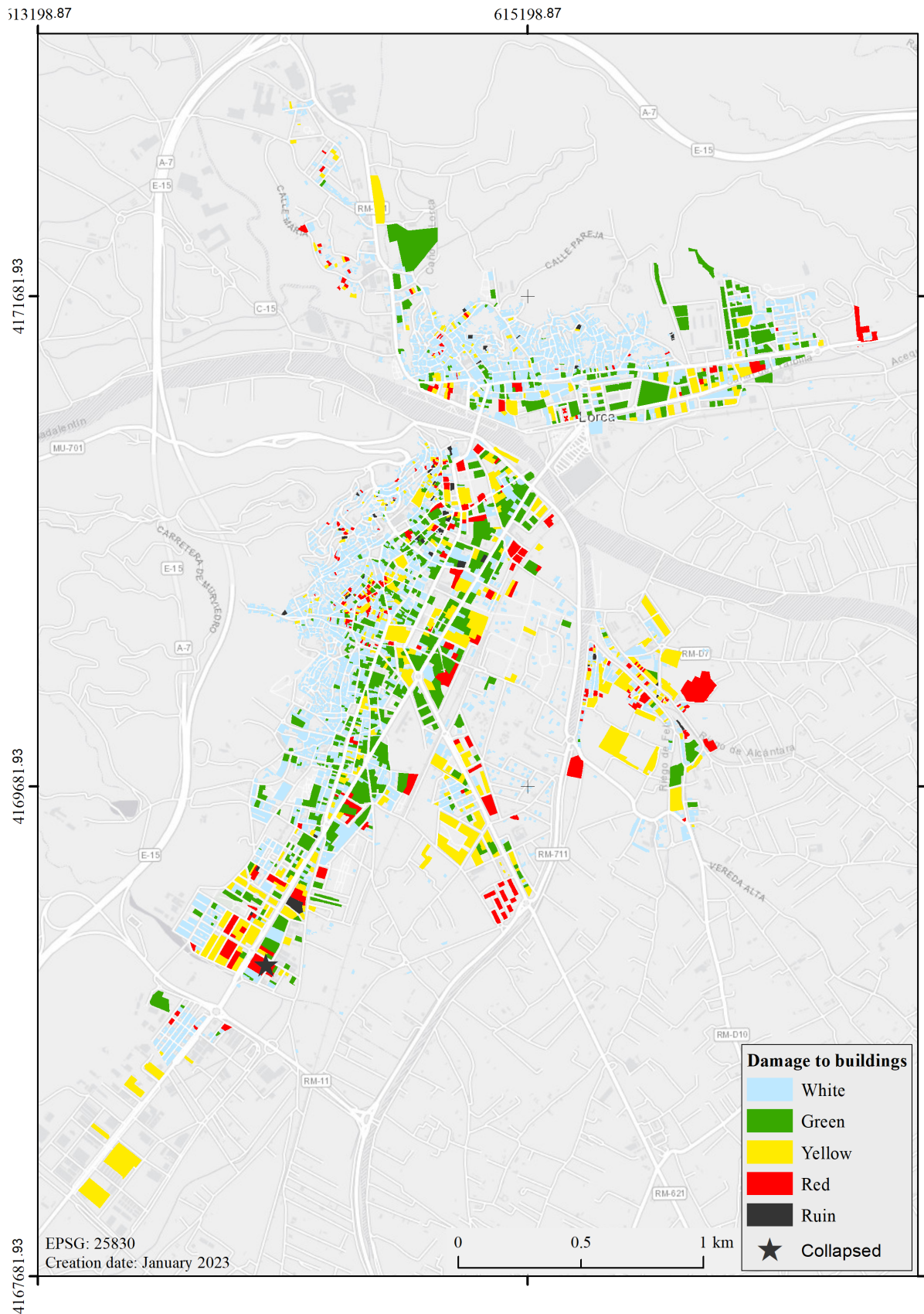
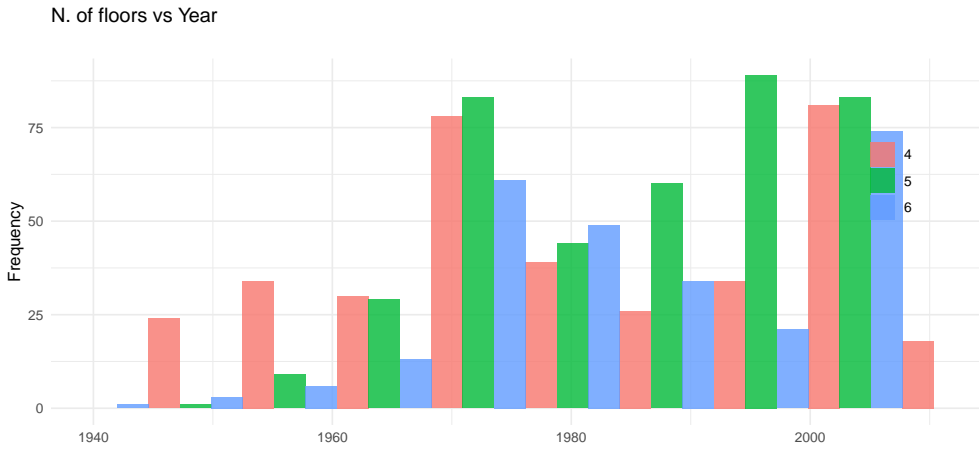
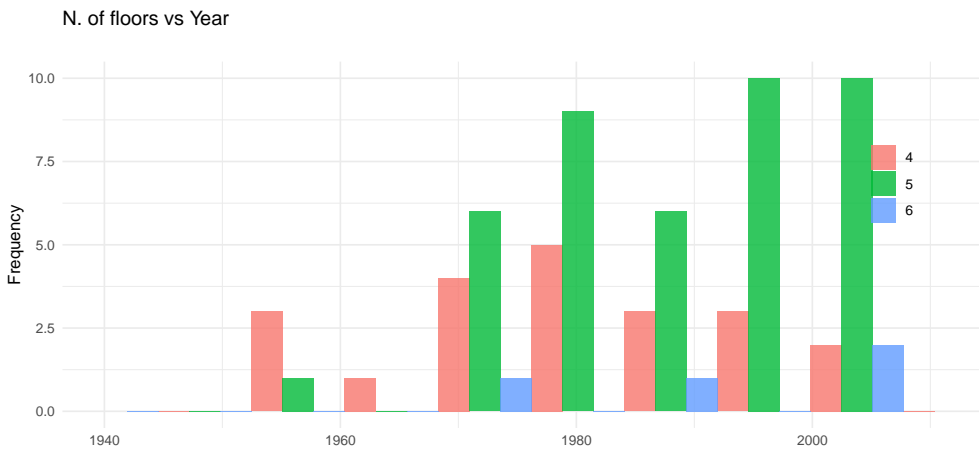


Figure 2.7: (vi) Map including all the buildings highlighting their state of damage after the earthquake.



(a) Map



(b) Reports

Figure 2.8: Total RC buildings vs reports by year

2.2 Masonry and reinforced concrete typologies

2.2.1 Reports

The typologies identified in previous risk studies and visually located in the map of Lorca were more profoundly analysed thanks to a database of more than 300 reports elaborated by AIA architects [1] just after the Lorca seism. This database includes buildings located all over Lorca which pertain to the different typologies of buildings presented in Lorca, whose unique common feature is that they were commissioned and elaborated by the same team of architects and engineers.

The reports elaborated by the experts in the aftermath of the 2011 Lorca earthquake were developed after the inspection in situ of the buildings, according to the article 1.3.3. of the Spanish regulation NCSE-02 [25] (translated from Spanish):

Any owner or community of owners, must commission a qualified technician to prepare a report analysing the consequences of the earthquake on said construction and the type of measures that, if applicable, should be adopted.

C.1.3.3. Compliance with the Standard during the useful life period.

When a high intensity earthquake occurs, a report must be made for each construction located in areas with intensity equal to or greater than VII (E.M.S. scale) in which analyze the consequences of the earthquake on said construction and the type of measures that, in their case, proceed to adopt.

The responsibility for preparing this report will fall on the technician in charge of the conservation, or, in the absence of this, on the property or operating entity, which must request the preparation of the aforementioned report to a qualified professional.

Moreover, AIA Architects provided the Research Group with all the information regarding the reparation works (budgets, layouts, constructive details, photographs ...) carried out on a great number of buildings.

2.2.2 Masonry typologies

The well-known CARTIS form ([14], [24],[16]) for seismic characterization of buildings, and GNDT form ([23]) for the seismic vulnerability assessment (both described in Sections 1.1 and 1.2.2), were fulfilled for each of the masonry typologies present in Lorca. The results are detailed in Table 2.2.

Moreover, these same typologies are studied in great depth in Chapter 4, where the capacity in terms of Spectral Acceleration (Sa) and Peak Ground Acceleration (PGA) for a number of samples is calculated and the corresponding fragility curve elaborated for M11, M31 and M34 Lorca buildings.

CARTIS form	M11 pre-code	M31 pre-code	M34 pre-code
Total floors (compressed ground floor)	1 to 2	1 to 3 (mainly 2)	1 to 3 (mainly 2)
Average height of floor [m]	2.5 to 3.5	2.5 to 3.5	2.5 to 3.5
Average height of ground floor [m]	2.5 to 3.5	2.5 to 3.5	2.5 to 3.5
Basement floors	0	0	0
Average area per floor	75	75	95
Year of construction	1880-1950	1900-1950	1940-1980
Main use	Residential	Residential	Residential
Characteristics of the masonry	Irregular without resources- rocks	Regular - low quality clay bricks	Regular - low quality clay bricks
Masonry Sack	No	No	No
Chains or Curbs Transversal connection Spurs	No	No	No
Buttresses	No	No	No
Average wall spacing [m]	3.5-4.0	4.0-5.0	4.0-5.0
Characteristics of the floors	Flexible - wood	Flexible-Semirrigid wood	Semirrigid - RC joists
Vaults	No	No	No
Mixed structures	No	No	No
Mortar	Poor quality	Low quality	Low quality - portland mortar
Porticoes, loggias and shafts	No	No	No
Average thickness of ground floor walls	40-90 (50)	40-50	30-35

Table 2.2: CARTIS form for the types identified in Lorca

M11-pre typology: rock walls + wood floor systems (Traditional)

Masonry load-bearing walls made with rounded stone or quarry rock, constituting a traditional construction in which rocks are used as basic building material, usually with a poor quality mortar (Fig. 2.9). These materials and construction techniques give rise to a heavy building with little resistance to lateral loads due to the lack of connection between vertical elements and horizontal (Fig. 2.11). The thickness of these walls is markedly higher than those which are made of bricks, from 50 to 90 cm. All the samples studied present wood floors systems with high deformability, e.g., crossbars wooden rounds (Fig. 2.10b), especially in the case of roof systems. The intermediate floor are usually composed by load-bearing structure of wood with straw and mortar board (*cañizo*), with ceramic tile finish supported on poor mortar. This constitutes the most common type during the period between 1880 and 1940, although the method was used until 1950. According to the results shown in the exposure maps, which combine Cadastral information with the transfer matrix developed by a vulnerability expert [12, Vol 3.], this constitutes the least extended typology in Lorca. In Appendix A an example of masonry building pertaining to this construction type is thoroughly detailed.

M31-pre typology: brick walls + wood flooring systems

Masonry load-bearing walls made with clay bricks of poor quality, usually with a low quality mortar. The resistance to lateral loads is also poor due to the lack of appropriate connections between horizontal and vertical elements, such as lack of ring beams. The flooring systems are made with wood joists similar to those found in the M11 typology (Fig. 2.10b). This constitute the most extended masonry typology during the period between 1900 and 1950 according to the reports. According to results shown in the exposure maps, this constitutes the most masonry extended typology in Lorca, almost a 20% of the buildings would pertain to it.

M34-pre typology: brick walls + RC flooring systems

Load-bearing unreinforced masonry walls made with brick pieces and low quality or portland mortar (Fig. 2.12) and flooring systems made with RC joists (Fig. 2.13), giving rise to a heavy building, especially due to the floors'



(a)



(b)

Figure 2.9: Type M11-pre. Traditional materials of construction in Lorca: rock walls.

weight. The thickness of the walls is markedly less with respect to those pertaining to type M11, typically from 30 to 35 cm. This constitute the most common type during the period between 1940 and 1980.



(a)



(b)



(c)



(d)

Figure 2.10: Wood flooring systems: typologies M11-pre and M31-pre



(a)



(b)

Figure 2.11: Typology M11-pre. Typical damage: disconnection between walls.



(a)



(b)



(c)



(d)

Figure 2.12: Type M31-pre and M34-pre: typical load-bearing walls in Lorca.



(a)



(b)



(c)



(d)

Figure 2.13: Type M34. Typical flooring systems in Lorca: RC joists.

2.2.3 Reinforced Concrete structure typologies

In medium seismicity areas like some regions of Europe, it is unusual for reinforced concrete (RC) structures to collapse when a medium magnitude earthquake occurs. This is due to robust earthquake resistance regulations being in place [9] and national standards that define strict criteria of quality for such constructions (e.g., [25] and [8] in the Spanish case). Nevertheless, it is quite common for their non-structural elements (NSEs) to suffer damages or collapse that provoke the fall of debris onto the public roads, and consequently, a significant number of fatalities. Additionally, current regulations are not so rigorous in relation to NSEs due to this being a field of research still in development. An instance of this fact is the case studied herein of the Lorca 2011 earthquake since the nine fatalities that occurred during its quakes were caused by the fall of debris of NSEs –solely one RC building collapsed and it did not provoke any human loss of life–.

For the aforementioned reasons, more than 300 reports documented by experts just after the 2011 Lorca earthquake have been analysed. In particular, those reports corresponding to four to six-storey RC buildings were studied in detail; as the majority of the fatalities occurred in the districts of Santiago (three), San Diego (two) and La Viña (four), of which this building type is predominant in the latter two. Moreover, see Figure 6.2 for the locations of the victims along with the four to six-storey RC buildings in the map of Lorca.

In her work Martínez-Cuevas (2014) [17] indicates that most common building types in these areas are masonry buildings consisting of one or two floors with structural and non-structural components made of masonry, reinforced concrete (RC) buildings with between two and six floors, with frame structures made of concrete and non-structural components such as infill walls and parapets made of unreinforced masonry. The RC buildings resulted to be more strongly correlated with structural damage in the type of Lorca soils (types B and C), particularly RC buildings that are between three and six floors in height, with characteristics that affect its seismic vulnerability such as vertical irregularity, setbacks on building façades (e.g., balconies), soft stories (partially enclosed) and being located either within a dense enclosed block with a central courtyard or in a clustered open block.

The present research is carried out with three objectives: to identify the most common structural and non-structural features of this type of buildings, to determine the most hazardous non-structural elements within this building typology and to reach a better understanding of their behaviour.

Within this PhD dissertation, 65 reports of buildings belonging to the four to six-storey reinforced concrete residential type have been studied. Throughout the reports, the experts detail the damage suffered by structural and NSEs. Damage to NSEs could be caused by in-plane seismic loading—which commonly affects lower floors, by out-plane – higher floors- or by a combination of both types of seismic loading –intermediate floors–.

Data provided by these technicians along with theoretical research has permitted us to characterize statistically the urban, structural and non-structural features of this building type in the case of Lorca. Added to this, the degree of damage to the buildings has been compared with the age of the buildings and the changes in the seismic Spanish regulations; revealing that, the most recent regulations have reduced the vulnerability of this building type.

Furthermore, particularly vulnerable elements and Spanish construction techniques that are inadequate for seismic areas have been identified and documented, and alternative techniques have been proposed. Unreinforced masonry chimneys, single-leaf parapet walls without reinforcing elements or stone cladding without any type of mechanical fixation fall into this category.

Additionally in Chapter 6, two actual Lorca buildings that suffered damages during this earthquake have been modelled using the Software SAP2000 according to plans, technical descriptions and graphical information available. In this way, their modes of vibration and torsion effects have been studied. Moreover, a thorough analysis of the Floor Response Spectra has been carried out by means of a Time History Analysis with the Lorca earthquake accelerograms and using the formulae proposed by several seismic codes.

Methodology and results

In order to carry out more in-depth research of the damages shown by non-structural elements for this case study, the present author have worked on the already database of more than 300 reports elaborated by experts just after the seism of Lorca. Within this information, the visual reports of 65 four to six-storey RC or mixed buildings, and the architectural plans and reparation projects of 25 of them are found.

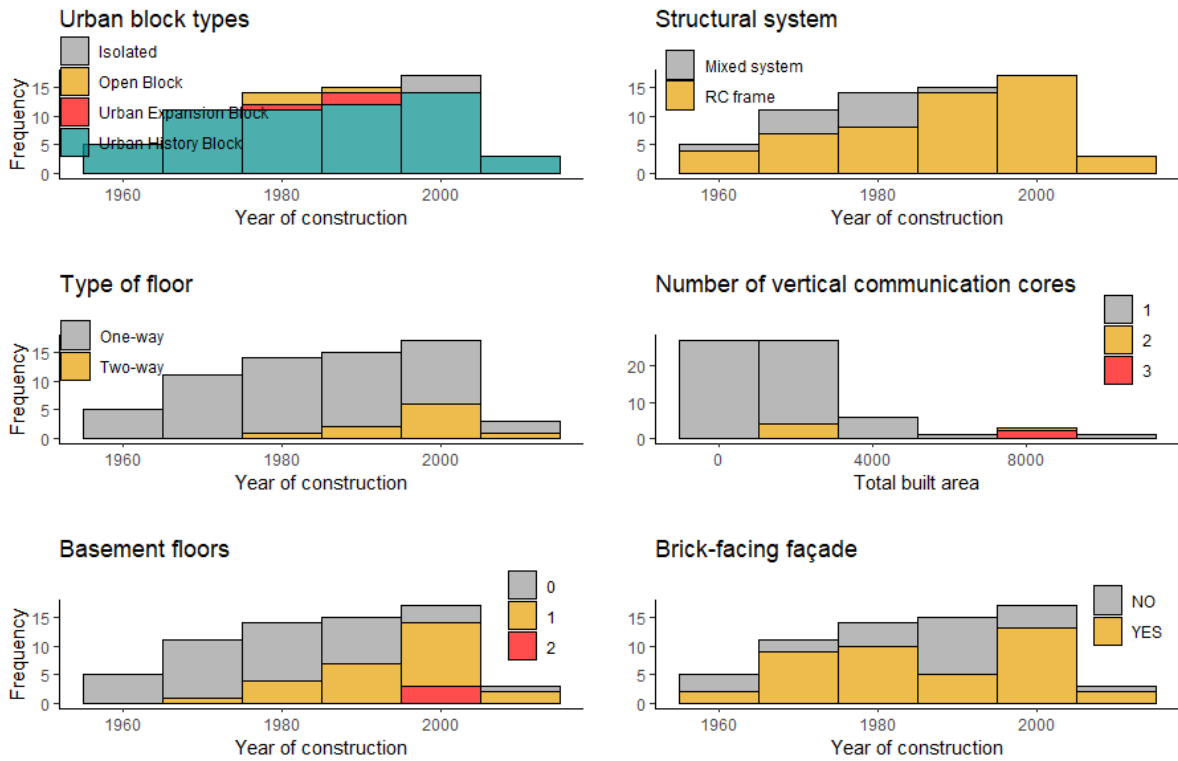
Thanks to this, throughout this work, the urban, structural and design features and the state of damage of the 65 buildings pertaining to the aforementioned building type have been statistically analysed. Furthermore, the main damages presented to them and possible improvements in the construction techniques of their elements have been documented. In relation to the graphical documentation of the reports, it is worth noting that inadequate construction techniques of non-structural elements represent a serious risk to life.

According to the reports, the majority of the buildings pertaining to the type studied were built in the four decades leading up to the Lorca seismic event (note that the gathering of the data was carried out in the year 2011).

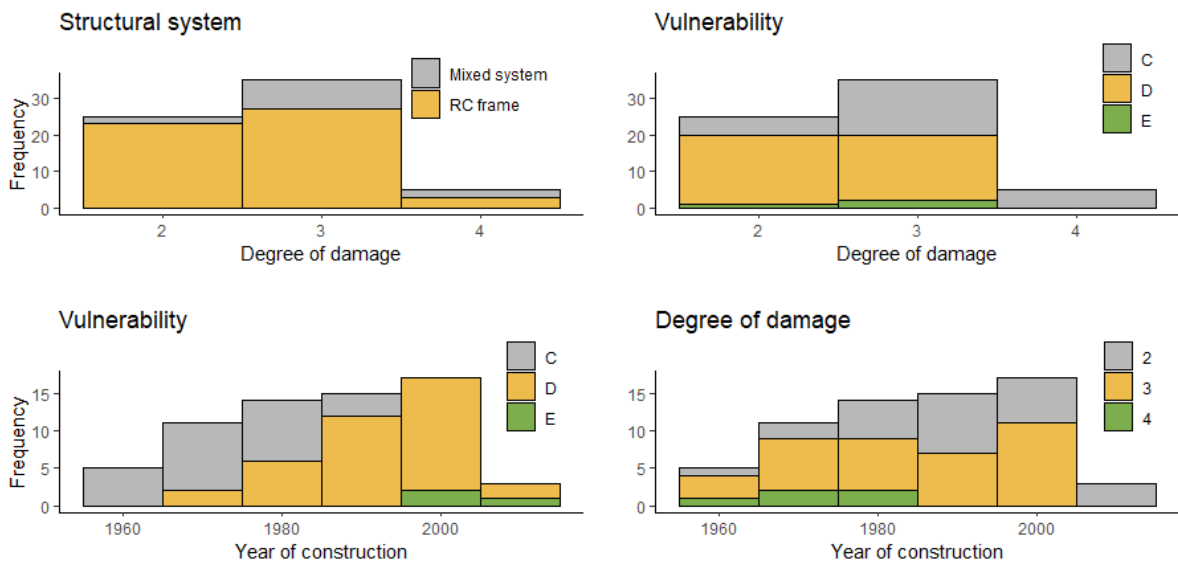
Characterisation of the features of the building type The following features of the 65 four to six-storey RC residential buildings have been studied statistically. The results are presented in Figure 2.14a:

- (i) **Urban features:** the type of block in which they are located has been characterised distinguishing between open block, isolated block, urban expansion block and urban history block. As can be seen in the top left histogram of Figure 2.14a, the majority of the buildings pertaining to this type are located within an urban history block.
- (ii) **Structural features:** their structural system and their type of floor system, namely, one-way joist floor system or two-way slab floor system (waffle slab).
- (iii) **Design features:** the total built area and the number of vertical communication cores are among the design features studied.
- (iv) **Non-structural elements features:** the number of buildings that present outer walls made of facing bricks has been studied. All the buildings documented have interior infill walls made of brick masonry. Furthermore, a widespread presence of suspended ceilings and cladding panels of different material have been noticed on the ground floor.

Lastly, the degree of damage to the buildings has been compared with some of their features, such as their age, vulnerability or structural system.



(a) Urban, design and structural features of the four to six-storey RC buildings and features of their NSE

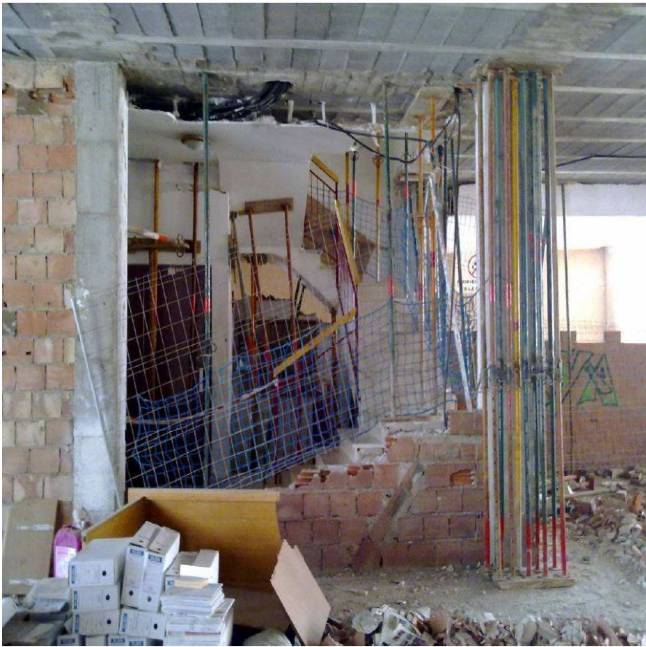


(b) Vulnerability and degree of damage of the four to six-storey RC residential buildings

Figure 2.14: Statistical analyses of four to six-storey RC residential buildings on the basis of 65 experts' reports.

Damages identified and non-structural elements potentially more vulnerable The most common damages to non-structural elements pertaining to this type of buildings during the Lorca earthquake were the following:

- **Damages to unreinforced masonry infill walls located on vertical communication cores:** a significant number of buildings presented damages to these elements. The main consequence associated with the damage to these elements is that they prevent the users of the building from being evacuated safely.



(a)



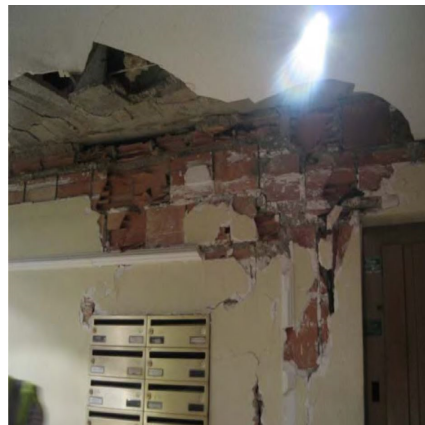
(b)

Figure 2.15: Damages to unreinforced masonry infill walls located on vertical communication cores

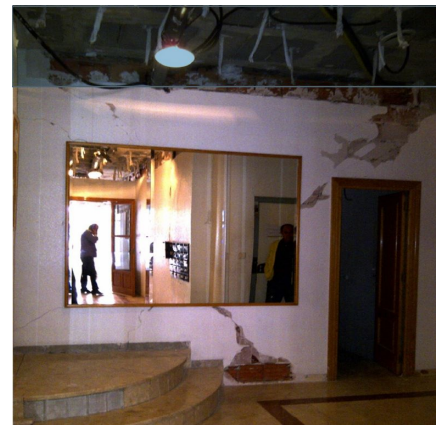
- **Damages to non-structural elements located in the common areas of the ground floor:** in the same vein as the damages to elements pertaining to the vertical communication cores, damages to these elements compromise the safety of the evacuations and in the cases of infill walls where cables and pipes run, their failure can prevent the proper functioning of the electricity and water installations. Suspended ceilings have also proved to be extremely vulnerable and hazardous elements. The majority of them show fissures and cracks after the seism, and a considerable number of them present detachments and local or global collapses.



(a)



(b)



(c)

Figure 2.16: Damages to non-structural elements located in the common areas of the ground floor

- **Damages to interior and exterior claddings panels:** the majority of the connections of the cladding panels to the exterior and interior walls were executed without any type of mechanical fixation (neither screws nor nails), trusting their adherence to the binding material, for example, cement. A type of connection that has demonstrated to be insufficient in the case of the Lorca earthquake. In some cases, the reparation projects prescribed the complete removal of the cladding panels and their substitution with a different type of panel, and in other cases, they prescribed an additional mechanical fixation for them.



Figure 2.17: Damages to interior and exterior claddings panels

- **Damages to exterior infill walls (interior and exterior façades):** on the one hand, an important number of façades has shown a lack of firm connection between the infill masonry walls (IMW) and the structural elements. In these cases, not only the detached parts represented a risk to life, but also the remaining parts. Hence, the whole element has to be removed or fixed in a better way. On the other hand, these exterior IMWs are composed by two single-leaf brick masonry walls. However, just a tiny part of them includes elements of connection between both leaves, such as steel ties; which constitute a widespread and economical improvement to their resistance against lateral forces.



Figure 2.18: Damages to exterior infill walls (interior and exterior façades)

- **Damages to interior infill walls:** the most hazardous damages to interior infill walls have been found on the ground floor, where habitually commercial units can be found. Nevertheless, the reparation of fissures and cracks provoked by exceeding internal shear forces on interior walls and the restitution of the detached ceramic tiles in bathrooms constituted a significant part of the total budget of the reparation.

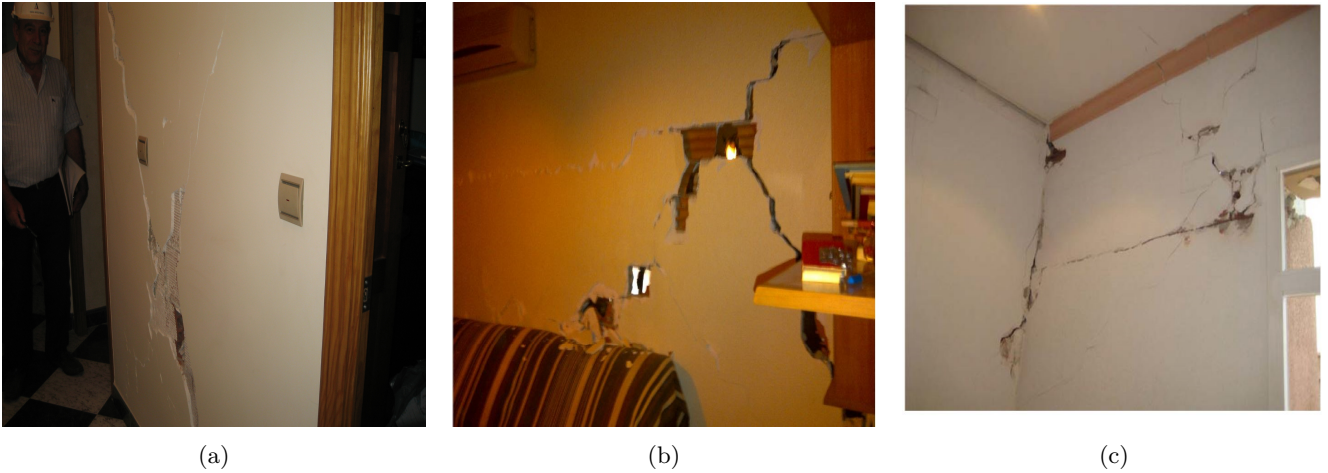


Figure 2.19: Damages to interior infill walls

- **Damages to unreinforced masonry roof parapets:** these elements have proved to be the most hazardous components of the buildings due to being the cause of the majority of the fatalities. Among the buildings studied, authors have found several complete collapses. Moreover, they present clay or stone coping pieces that, in the majority of the cases, are not firmly fixed to the parapet; resulting in an added risk. Additionally, some ledges have proved to be unable to withstand the Lorca earthquake.



Figure 2.20: Damages to unreinforced masonry roof parapets

- **Damages to unreinforced masonry roof chimneys:** a great deal of these elements, which are made of unreinforced masonry, have resulted in collapse or in such a state of degradation that had to be demolished.

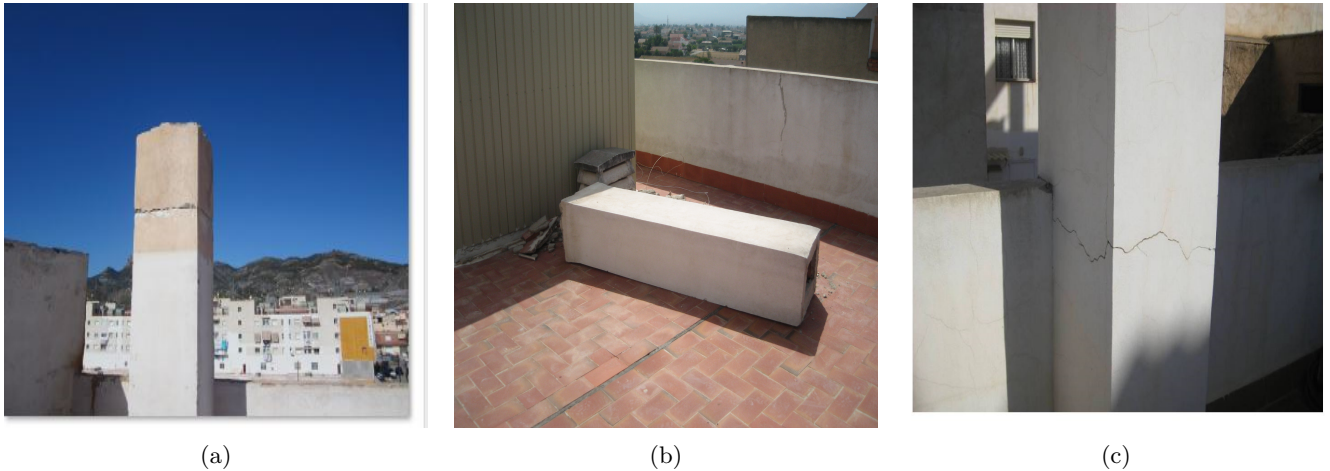


Figure 2.21: Damages to unreinforced masonry roof chimneys

Discussion

The following patterns have been observed in the previous sections concerning four to six-storey RC buildings:

- From the urban point of view, the majority of these buildings constitute urban history blocks.
- From a structural point of view, the data documented by the experts show that from the 70s to the middle of the 80s, there was a strong tendency of employing a mixed structural system in construction, which consisted of steel beams and reinforced concrete columns. A structural system that none of the buildings constructed in the XXI century presents. Moreover, figure 2.14a shows an increasing propensity towards the use of two-way joist slab floor systems, facilitating this system to become as widespread as the one-way joist floor systems in the case of the most recent buildings. Additionally, throughout the development of this study, authors have verified that the presence of conventional RC beams is not significant, since the vast majority of the buildings present wide RC beams. Lastly, the number of basement floors has increased throughout time. At the time of the seism, the majority of the buildings presented one basement floor. Additionally, it has been observed that the majority of these buildings present a unique vertical communication core, even when they comprise a large area. Moreover, in quite a number of these cases, this influential element is localised at a considerable distance from the centre of mass of the building. A fact that represents an irregularity in terms of stiffness and may lead to the emergence of global torsions. Moreover, it is commonly agreed that the Spanish vertical communication cores possess greater stiffness than the rest of the structure. Hence, consequently, a significant number of them have resulted in being heavily damaged (their structural elements as well as their non-structural elements).
- In relation to the design aspects, according to reports, 63 % of the buildings have outer walls made of facing bricks, representing the majority since the 60s. A tendency that has shown a notable increase since the year 2000.
- In relation to the general degree of damage observed, figure 2.14b shows that the oldest buildings have been classified as more vulnerable to seismic forces (vulnerability types C and D according to EMS-98), and that they have experienced major damages after the event. All the buildings built before the 70s have suffered damages of a degree equal to or greater than 3 and that none of the buildings constructed in the last quarter of the century has suffered grade 4 damage. Furthermore, the buildings of type C vulnerability are the only ones that have reached grade 4 damage. This decrease in the experimental and theoretical vulnerability may mean that the construction techniques have improved or that the latest regulations have contributed to reducing substantially the vulnerability of the buildings, as they aimed to.
- In relation to other NSEs, the damages illustrated in figures 2.15 to 2.21 indicates that the construction techniques employed in the execution of the non-structural unreinforced masonry elements, cladding panel and suspended ceilings are inadequate in seismic-prone areas. To cite some instances, in the case of parapet masonry walls, the majority of them have been constructed as a half-brick single-leaf wall, which implies that their slenderness is excessive. The slenderness of a free-standing element of a determinate size is directly correlated with its predisposition to overturn. In the cases of the IMWs, it is worth noting that a substantial part of the reports mentions a generalised disconnection of the façade walls to the structure of the buildings, which constitute a defect in the construction techniques. According to [2], problems such as the one

represented by fixing masonry façades to the structure have not yet been fully resolved in our country and the solutions used, similar throughout our geography, are not always safe. Moreover, said authors state the Lorca earthquake has only demonstrated the true risk they present.

Future lines of investigation should develop a more in-depth statistical study of the damages to NSEs, in order to assess the evolution of their construction techniques.

Furthermore, in order to design NSE properly, it is necessary to characterize their seismic demand, i.e., to estimate the accelerations or the Floor Response Spectra (FRS) at the particular location of the NSE under study. Nonetheless, at the present time (more than ten years after the Lorca earthquake), the Spanish regulation (NCSE-02,[25]) for structures located in seismic areas does not include any indication for characterizing the NSE demand.

2.3 Conclusions

In the following, the conclusions obtained from the results of this Chapter are presented.

Conclusions regarding exposure

A series of exposure maps have been contributed in order to facilitate the comprehension of the typologies presented in Lorca and their statistical and graphical distribution. In addition, a map illustrating the damages to buildings provoked by the 2011 Lorca earthquake has been provided.

Conclusions regarding masonry buildings

In relation to the masonry buildings, the CARTIS and the GNDT forms (see also Chapter 4) have been accomplished in order to reach a better characterization of the masonry buildings presented in Lorca on the basis of the experts' reports elaborated in the aftermath of the 2011 Lorca earthquake. The results present the specific features of the buildings located in the city, which are also present in a great number of urban nuclei of Spain [2].

Conclusions regarding RC buildings

Throughout the study, the main urban, structural and design features of the typology of buildings that caused the fatalities during the Lorca earthquake have been characterised. It has been ascertained that a prime example of the four to six-storey RC residential typology would be typified by a building located in an urban history block, would have a RC framed structural system with one-way joist floor system and wide beams and would have one basement floor used as parking. Moreover, it would present solely one vertical communication core, a facing brick façade composed by two single-leaf layers separated by an air gap, single-leaf masonry interior infill walls, masonry parapets and several masonry chimneys.

The most hazardous NSEs of this building typology would be: unreinforced masonry parapets and façade walls, infill walls located on staircases and suspended ceilings. Although others, like masonry chimneys, could be considered as more vulnerable. Moreover, in relation to parapets walls, the importance of slenderness has been stressed. It has been seen that a 12 cm-thick single-leaf wall was the most widely used in the area before the earthquake, despite being inadequate in seismic-prone areas. Additionally, in relation to cladding panels and brick façades, the experience has demonstrated that a firm connection is crucial, and a mechanical fixation has been recommended.

Acknowledgements

This research has been funded by the Project KUK APAHAN-RS (Reference: RTI2018-094827-B-C22): "Amenaza y Riesgo Sísmico en América Central y Sureste de España", Ministry of Science and Innovation of Spain. We thank AIA Estudio (Lorca) for providing data and building reports, in the frame of the MERISUR project (reference CGL2013-40492-R) and Alguacil for providing the synthetic accelerograms.

Furthermore, the information and assistance provided by several researchers of the Universidad Politécnica de Madrid has been indispensable. Among them, I am indebted to Sandra Martínez-Cuevas (ORCID: 0000-0002-2150-3251) and to Ligia Elena Quirós Hernández, and very specially to Rocío Romero Jarén (ORCID: 0000-0002-5919-4589).

References

- [1] AIA and Chamizo Arquitectos. *Proyectos básicos y de ejecución de rehabilitación de edificios tras el sismo de Lorca de 2011*. Professional reports elaborated after the Lorca earthquake for the buildings owners institution, 2011.
- [2] R Álvarez-Cabal, E Díaz-Pavón, and R Rodríguez-Escribano. “El terremoto de Lorca: Efectos en los edificios”. In: *Madrid, Consorcio de Compensación de Seguros, Ministerio de Economía y Competitividad* (2013).
- [3] Martha Liliana Carreño Tibaduiza et al. “Comportamiento sísmico de los edificios de Lorca”. In: *Física de la Tierra* 24 (2012), pp. 289–314.
- [4] NCSR-22. Norma de Construcción Sismorresistente (upcoming). “Consulta pública previa sobre el borrador de Real Decreto por el que se aprueba la Norma de Construcción Sismorresistente NCSR-2022. Last visit 10/05/2023”. In: (). URL: www.mitma.gob.es/el-ministerio/buscador-participacion-publica/audiencia-e-informacion-publica-sobre-el-proyecto-de-real-decreto-por-el-que-se-aprueba-la-norma-de-construccion-sismorresistente-ncsr-22.
- [5] F Dell’Acqua, P Gamba, and K Jaiswal. “Spatial aspects of building and population exposure data and their implications for global earthquake exposure modeling”. In: *Natural hazards* 68.3 (2013), pp. 1291–1309.
- [6] P.D.S.-1. Ministerio de Planificación del Desarrollo. “Decreto 3209/1974, España. Norma Sismorresistente”. In: *RD 3209/1974, Spain* (1974). URL: www.boe.es/diario_boe/txt.php?id=BOE-A-1974-1869.
- [7] P.G.S.-1. Ministerio de Planificación del Desarrollo. “Decreto 106/1969, España. Norma Sismorresistente”. In: *RD 106/1990, Spain* (1968). URL: www.boe.es/diario_boe/txt.php?id=BOE-A-1969-148.
- [8] EHE-08. “EHE-08 Comisión Permanente del Hormigón Instrucción de Hormigón Estructural”. In: *RD 1247/2008, Spain* (2008). URL: www.boe.es/eli/es/rd/2008/07/18/1247.
- [9] EN-1998. “Eurocode 8: Design of structures for earthquake resistance - Part 1 : General rules, seismic actions and rules for buildings”. In: *European Committee for Standardization, Brussels*. (2003).
- [10] Iason Grigoratos et al. “Crowdsourcing exposure data for seismic vulnerability assessment in developing countries”. In: *Journal of Earthquake Engineering* 25.5 (2021), pp. 835–852.
- [11] WILLIAM Holmes. “HAZUS-MH: Multi-hazard loss estimation methodology: Technical manual”. In: *Washington, DC: Federal Emergency Management Agency* (1999).
- [12] RISMUR I. *Estudio de Riesgo Sísmico en la provincia de Murcia (Proyecto RISMUR)*. Broadway Malyan, Grupo de Tectónica Activa y Paleosismicidad (Universidad Complutense de Madrid, UCM), Grupo de Ingeniería Sísmica (Universidad Politécnica de Madrid, UPM). 2008.
- [13] RISMUR II. *Servicio de Actualización del Análisis de Riesgo Sísmico (RISMUR) en la Región de Murcia. ETSI Topografía, Geodesia y Cartografía (Universidad Politécnica de Madrid, UPM) , Grupo de Ingeniería Sísmica (UPM)*. 2014.
- [14] Scheda CARTIS 2014. Presidenza del Consiglio dei Ministri Dipartimento della Protezione Civile of Italy. “Scheda di 1 Livello per la CARatterizzazione TIpologico-Strutturale dei comparti urbani costituiti da edifice ordinari”. In: *Available online*. (2014). URL: geoportale.comune.cavadetirreni.sa.it/file/38732/download?token=x4arE236.
- [15] Sergio Lagomarsino and Sonia Giovinazzi. “Macroseismic and mechanical models for the vulnerability and damage assessment of current buildings”. In: *Bulletin of Earthquake Engineering* 4.4 (2006), pp. 415–443.
- [16] Manuale Scheda CARTIS 2014, Progetto Reluis 2014-2016, Dipartimento della Protezione Civile, Italy. “Manuale per la compilazione della Scheda di 1 Livello per la CARatterizzazione TIpologico-Strutturale dei comparti urbani costituiti da edifice ordinari”. In: (2016). URL: <https://geoportale.comune.cavadetirreni.sa.it/file/38732/download?token=x4arE236>.
- [17] Sandra Martínez Cuevas. “Evaluación de la vulnerabilidad sísmica urbana basada en tipologías constructivas y disposición urbana de la edificación. Aplicación en la ciudad de Lorca, región de Murcia”. PhD thesis. Universidad Politécnica de Madrid, 2014. URL: oa.upm.es/30447/.
- [18] Zoran V Milutinovic and Goran S Trendafiloski. “RISK-UE: An advanced approach to earthquake risk scenarios with applications to different European towns”. In: *European Project Risk-UE* (2003).
- [19] P Murphy Corella. “Quick Field Report: Lorca Earthquake 11th May 2011”. In: *EMSC-CSM report. Available online. Last visit 10/05/2023* (2011). URL: https://www.emsc-csem.org/Files/event/221132/lorca_quickfieldreport_lowres.pdf.

- [20] Gordana Pavić et al. “Development of seismic vulnerability and exposure models—A case study of Croatia”. In: *Sustainability* 12.3 (2020), p. 973.
- [21] Ligia Elena Quirós Hernández. “Modelizaciones y análisis de sensibilidad en la evaluación integral del riesgo sísmico a escala urbana: aplicación a la ciudad de Lorca”. PhD thesis. Universidad Politécnica de Madrid, 2017. URL: oa.upm.es/48042/1/LIGIA_ELENA_QUIROS_HERNANDEZ.pdf.
- [22] Rocío Romero-Jarén, Belén Benito, and José Juan Arranz. “Testing and Application of Geospatial Techniques in Seismic Engineering”. In: *The II Geomatics Engineering Conference*. MDPI, July 2019. DOI: <https://doi.org/10.3390/proceedings2019019023>.
- [23] Regione Toscana. “Manuale per la compilazione della scheda GNDT/CNR di II livello versione modificata della Regione Toscana, Direzione Generale delle Politiche Territoriali ad Ambientali, Settore: Servizio Sismico Regionale”. In: *Progettazione Sismica* 2 (2003).
- [24] G Zuccaro et al. “La scheda CARTIS per la caratterizzazione tipologico-strutturale dei comparti urbani costituiti da edifici ordinari. Valutazione dell’esposizione in analisi di rischio sismico”. In: *Proceedings of the GNGTS* (2015).
- [25] NCSE-02. Comisión permanente de normas sismorresistentes. “España. Norma de construcción sismorresistente: Parte general y edificación”. In: *RD 997/2002, Spain* (2002). URL: www.boe.es/eli/es/rd/2002/09/27/997.
- [26] NCSE-94. Comisión permanente de normas sismorresistentes. “Norma de construcción sismorresistente: Parte general y edificación”. In: *RD 2543/1994, Spain* (1994). URL: www.boe.es/eli/es/rd/1994/12/29/2543.

Chapter 3

A methodology to assess and select fragility curves for seismic risk studies

Seismic risk studies must deal with the treatment of different types of uncertainties, whose assessment methods are still under development, such as those associated with seismic demand, or with the variability in the properties of the structural models developed and calibrated for the building portfolio of interest. Another important source of uncertainty in such studies usually is the selection of the fragility curves (FCs) for each building type, from an existing catalogue [52].

The FCs are defined as the probability of reaching or exceeding a specific damage state under earthquake excitation (see Section 1.2.1). In this respect, an inadequate selection of the FCs can mean a notably unreliable estimation of damages and losses. Therefore, the estimation of seismic risk levels for Spain or Central America may turn out to be more inaccurate when the FCs used have been developed for regions of the world with construction techniques and quality of construction materials highly dissimilar to those under study, such as North America, Italy, or other countries with a different level of investment in seismic codes or Gross Domestic Product (GDP). However, previous studies have taken this approach due to the limited availability of FCs for Central America. Moreover, the FC establishes the crucial connection between the hazard at the location and the ensuing effects on any exposed components, such as buildings [35]. Therefore, the FC can be used in community resilience frameworks [5].

Within this framework, this work proposes a methodology to assess and select FCs for seismic risk studies from a catalogue of existing proposals available in the literature. The novelty of the proposal lies in organizing practically all the variables involved according to the literature and giving them scores so that the application of the methodology provides the researcher with a quantitative and multidimensional index to rank FCs according to their adequacy to the case study. Furthermore, the methodology has been applied to the cases of San José (Costa Rica) and Murcia (Spain).

3.1 State of the art

Fragility curves have become an essential tool for seismic risk studies and vulnerability analysis. These curves allow a relationship to be established between the seismic hazard at a particular site and the effects of a ground motion on built infrastructure [43].

FCs for large-scale seismic risk assessments have been proposed for a few world regions. One of the best-known platforms available for determining building damage and loss in urban contexts is HAZUS-MH [21] for the United States. In Europe, several projects have been developed, and within this framework, a great number of fragility and vulnerability functions have been generated for different construction types. These may include these projects: RISK-UE (2001–2004) [42], [45], LESS-LOSS (2004–2007), SYNER-G (2009–2012) [7], and SERA (2017–2020) [37]. For Central America, the developed projects have analysed exposure, vulnerability, and seismic risk at a regional level or solely for some specific countries. Among the most notable projects are included RESIS II (2007–2010) [9]; Lang et al., 2009, [34]), CAPRA (2009–2015) [14], [46]; and more recently, the PREPARE II (2020–2022) project [28], [27], [29]. In South America, the main projects carried out to evaluate seismic risk in the region are SARA (2013–2015) [62], [63] and CCARA (2018) [22]. As part of the Global Earthquake Model (GEM) initiative,

hundreds of empirical and analytical fragility and vulnerability functions were collected and made publicly available through the OpenQuake-platform [37].

In this respect it is worth clarifying again that FCs specify the probabilities of exceeding a number of damage states conditional on a ground shaking intensity measure, whereas vulnerability functions establish the likelihood of loss ratio conditional on a ground shaking intensity measure [37], [63].

Some direct antecedents of the present research are the studies that developed a procedure to select suitable fragility curves by firstly assessing how well they represent the needs of the future application [36, 60, 41, 7, 11].

The work of [36] proposed qualitative evaluation criteria based on four main categories to cover fundamental categories related to capacity, demand, methodology for fragility analysis, and uncertainty. The aim of this report was to provide a set of qualitative criteria to support the selection process of the most appropriate fragility curves for the European building stock.

The study of [60] gathered expert opinion to determine which factors are most important for selecting FCs. Said study suggests a selection framework for existing functions based on nine attributes. Some of them are related to what the authors call the quality of the FCs based on the quality of inputs, the rationality of derivation procedures, and the document quality. Other attributes are concerned with the relevance of the FCs, which include the appropriateness of the damage states, building classes, and ground motion intensity measurements used in the original functions for the new application.

The framework adopted by [52] for evaluating fragility curves is based on four fundamental attributes proposed by [47]. These are the curve representativeness of the characteristics of the buildings and seismicity in the location being assessed, the quality of the inputs used to generate the FCs, the rationality of the procedures followed to construct the curves, and the documentation quality¹. The four attributes are also subdivided into evaluation criteria sets that are different for empirical and analytical FCs. Each criterion is assigned a high, medium, or low rating to facilitate the evaluation and comparison of FCs.

As part of the SYNER-G project, [7] collected, reviewed, and validated FCs against observed damage and harmonised proposals for typologies in Europe. The authors also developed software to store, harmonise and estimate the uncertainty of the FCs.

This chapter presents a method for assessing candidate FCs from an index or ranking obtained from the most pertinent dimensions and attributes, based on the suggestions and aspects established in prior studies. The previous contributions propose the series of variables that influence the adequacy of the FC to the different case studies but present rankings or rating systems more qualitative than quantitative. Therefore, the novelty of the proposal lies in organizing practically all the variables involved according to the literature and giving them scores so that the application of the methodology provides the researcher with a quantitative and multidimensional index to rank FCs according to their adequacy to the case study — an outcome for which there was no methodology available up until now —.

3.2 Select.FC: a methodology to assess and select fragility curves

The methodology herein proposed consists of the following steps. Firstly, the types of buildings under study must be identified and characterised. Secondly, a deep search for an important number of FCs in the scientific literature available must be carried out (research projects, scientific articles, graduate and post-graduate theses, conference papers, among others), focusing especially on those which characterise buildings of the types existing in the area analysed.

Thirdly, a rating index is obtained from a set of variables proposed to assess relevant aspects of the FCs identified as potential candidates for the typology under study. From this index, a classification is derived to define the FCs adequacy for each type of buildings identified (Figure 3.1). The Final Index, with a maximum value of 100 points, is obtained from a multidimensional index (Global Index) adjusted by a reduction coefficient (Building Class Similarity). The Global Index comprises two dimensions: the Technical Suitability of the FC (which includes three

¹The documentation quality attribute assesses whether the authors of the FCs provide sufficiently complete information for an independent researcher to reproduce the study ([52]).

sub-dimensions: Capacity, Fragility, and Quality) and the Suitability for the Local System. In turn, each of these dimensions and sub-dimensions comprises a set of variables that allow evaluating different aspects of FCs. The maximum score an FC can obtain in each index, dimension, sub-dimension, and variable is indicated in brackets. The score of each of the two mentioned dimensions is obtained by adding the scores assigned to all the different variables involved. Moreover, the bottom of Figure 1 shows a graphical summary (in the form of a horizontal bar) of the influence of each element involved, along with an example. In the example, the Global Index (Technical Suitability + Suitability for the Local System) sums up 78 points. Next, the reduction coefficient (green arrow) reduces the Global Index to the Final Index. This final value determines the class of the FC assessed (from A-best to F-worst), that is, its level of adequacy within the following ranges of points defined: Class A: (85, 100], class B: (65, 85], class C: (55, 65], class D: (47, 55], class E: (40, 47] and class F: (0, 40] points. Therefore, the FC used as an example is class D.

As a fourth step, the set of appropriate FCs in the highest classes for each typology under study is selected and their coherence, must be checked typology by typology and globally (between typologies), preferably with local experts, according to the level of seismic vulnerability that is expected a priori of each one. This can be done by graphing the curves together or comparing their parameters or damage exceedance probabilities for similar values of seismic action intensity. Therefore, all the curves must be expressed in the same IM.

Finally, the FCs in the highest classes for each typology that show coherence (reasonable damage exceedance probability levels in comparative terms with other typologies) are selected for each typology. If two or more curves end up classified in the same highest class for a typology, it is recommended to consolidate them into a new curve using the conflation method. This method is a probability-averaging alternative that has several benefits and none of the drawbacks of existing averaging techniques. The conflation of several input distributions is the probability distribution with density equal to the normalized product of the input densities, which optimally and unbiasedly summarizes the data ([24]). Considering that FCs are log-normal conditional cumulative probability distributions, the basic principles of conflation, derived by Hill and Miller (2011), to the special case of normally distributed (Gaussian) data have been adapted and applied in this case. Specifically, let m_i and σ_i denote the mean and standard deviation of FC_i with $i=1,2$. The mean m_p and the standard deviation σ_p of the new FC proposed for consolidation FC1 and FC2 can be calculated from Equations 3.2 and 3.2:

$$m_p = \frac{\sigma_2^2 m_1 + \sigma_1^2 m_2}{\sigma_2^2 + \sigma_1^2} \quad (3.1)$$

$$\sigma_p^2 = \frac{\sigma_2^2 \sigma_1^2}{\sigma_2^2 + \sigma_1^2} \quad (3.2)$$

3.2.1 Variable selection and evaluated dimension

The variables employed to evaluate the available FCs for a given typology were selected from among those proposed by [60], [36], and [52]. Moreover, other variables considered relevant in the FC development were included. The factors identified as central to the proposed FC selection procedure were grouped into the following three relevant dimensions:

- (i) **technical suitability**, which comprises factors related to the capacity curve from which the FC is derived, characteristics of the evaluated FC, and variables related to the quality and the general credibility of the study that proposes the analysed curve,
- (ii) **suitability for the local system** studied, and
- (iii) **building class similarity**.

Two sub-dimensions are computed from the first two dimensions to provide a quantitative assessment for each and then summed up to obtain a global index. From this last dimension, an adjustment coefficient of the global index is proposed.

Furthermore, the first dimension contributes a measure of the technical characteristics of the FCs evaluated. The second contributes a starting point for selecting FCs to include in the study from all the curves available in the literature, and the third indicates how well the curve suits a particular building type within the region. Here,

a summary of the dimensions and sub-dimensions is included for a better understanding and next each dimension and sub-dimension is thoroughly detailed. In Table 3.2 an example of application of the proposed methodology is provided.

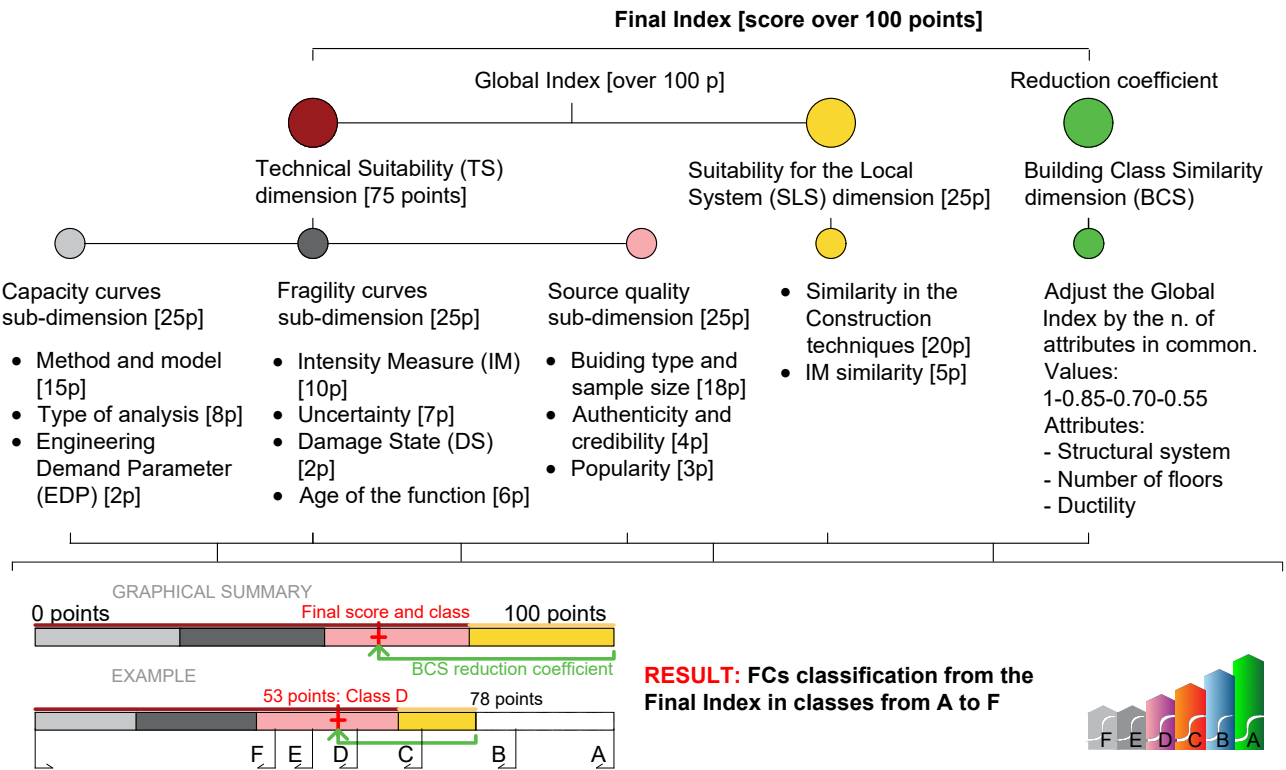


Figure 3.1: Conceptualization, dimensions, and variables of the index proposed to evaluate FCs. Maximum scores in brackets.

Technical Suitability dimension

The first dimension assessed by the technical suitability dimension comprises three sub-dimensions or blocks of variables. As shown later in the application to the case of Costa Rica, these three blocks of variables related to the capacity curves, fragility curves and quality of the source, must be evaluated as different set of variables. A best developed capacity curve in terms of technical criteria do not necessarily a most accurate fragility curve in terms of technical criteria, and the same for a major quality of the source.

Technical Suitability dimension (TS):

- Capacity Curve Block of Variables (CC BV)
 - Method and model
 - Type of analysis
 - Engineering Demand Parameter (EDP)
- Fragility Curve Block of Variables (FC BV)
 - Intensity Measure (IM)
 - Uncertainty

- Damage State (DS) thresholds
- Year of the function
- Source Quality Block of Variables (SQ BV)
 - Building type and sample size
 - Authenticity and credibility
 - Popularity

Capacity curves The first block of the Technical Suitability Dimension is related to the capacity curve, including method and model, analysis type and the engineering demand parameter considered.

Concerning the method and model found in the reviewed capacity curve, the following were identified from highest to lowest score: experimental 3D, experimental 2D, analytical 3D, analytical 2D, combined Single Degree of Freedom (SDOF) and SDOF. The SDOF option refers to a mechanical approach based on a simplified capacity curve derived from a SDOF model. The ‘combined SDOF’ would correspond to the SDOF that has also been calibrated or validated with other method; combined SDOF was used, for example, by [33].

The curves are also scored on the level of complexity of the analysis carried out for structural assessment. The types of analysis identified in the literature were grouped, in decreasing order of complexity and therefore score, as follows: (i) Nonlinear dynamic (NLDA); (ii) Nonlinear static (NLSA or Pushover); (iii) Simplified methods/direct capacity curve definition ([52]).

The last variable considered regarding the capacity curve is the engineering demand parameter (EDP), which measures the structural response obtained from the structural analysis results. The EDPs were ranked from highest to lowest as follows: inter-story drift ratio (IDR) or global inter-story drift (IDRG); maximum displacement; and roof or top displacement commonly utilised from NLSA or Pushover ([36]).

Fragility curves The second block of variables refers to characteristics directly related to the FCs evaluated, such as the IM used, the year of publication of the curve, the treatment given to the different sources of uncertainties associated with FCs, the level of popularity, and the damage thresholds considered.

The Intensity Measure (IM) is related to the quality of the information on the seismic demand used in the FC derivation process. The choice of the IM is relevant because it is the variable that connects the aspects related to the seismic hazard with the structural evaluation. A desirable IM should be practical (IM for which robust and modern Ground Motion Prediction Equations, GMPEs, are available), efficient (the structural response should exhibit a low record-to-record variability at any given level of the IM), and sufficient (relevant record-specific seismological parameters, such as magnitude, distance, epsilon, should be represented without introducing any bias in the results). The IMs were ordered from highest to lowest score as follows:

(i) Advanced intensity measures (IMs) or combination-type ground motion IMs based on $S_a(T_1)$, e.g., Critical Spectral acceleration, $S_a^c = S_a * (T_1)^{(1-\alpha)} * (S_a * (T_f)^\alpha)$, $T - f$:softened period, Critical IMs that consider the effect of the softened period $IM_{CR} = S_a * (T_1)^{(1-\alpha)} * S_a * (\sqrt[3]{R_{IM}} * T_1)^\alpha$ and $IM_{SR} = S_a * (T_1)^{(1-\alpha)} * S_a * (\sqrt{R_{IM}} * T_1)^\alpha$, where R_{IM} is a self-adaptive parameter or multiplier defined as the lateral strength required to maintain the system elastic ([39, 64]) (ii) Spectral IMs, e.g., Spectral acceleration at the first vibration period, $S_a(T_1)$, Spectral displacement at the first vibration period $S_d(T_1)$, (iii) Scalar IMs, e.g., Peak Ground Acceleration ($PGA = \max|a(t)|$), Peak Ground Displacement ($PGD = \max|d(t)|$), (iv) Discrete IMs, e.g., Modified Mercalli Intensity (MMI), European Macroseismic Scale (EMS-98) ([60]).

The year of publication of the curve captures some other relevant characteristics, such as whether the functions were derived from aged empirical data or modelled on older building types and are therefore probably less suitable for more recent seismic hazard and vulnerability analyses. The development of FCs brings with it a set of sources of variability and uncertainties that can be grouped into the following three: (i) uncertainty in the seismic demand, (ii) variability in the properties of the structural model (building-to-building uncertainty or uncertainty in capacity), (iii) uncertainty in the definition of damage thresholds ([52]). Considering this, the FCs that were derived considering the three sources of uncertainties explicitly scored higher, while the FCs derived considering only some or none of these sources of uncertainty scored lower (see Figure 3.2).

Pre-set or custom criteria can define the threshold of damage states. Defining capacities for each building provides the flexibility to tailor damage threshold values to a given building or subclass of building typologies. Alternatively, the proposed simplified formula from the literature commonly expressed as a function of yield and ultimate roof displacement, could be employed to directly estimate global damage state thresholds ([36]). Custom damage status thresholds are considered preferable to pre-established ones, as they allow the definition of thresholds to be adapted to the typology whose seismic vulnerability is being evaluated. Furthermore, it introduces capacity-demand correlations that can greatly influence the vulnerability analysis results ([36, 35]). Therefore, FCs derived from adjusted damage state thresholds are given a higher score than those obtained from pre-set damage thresholds.

Source Quality The last sub-dimension included in the Technical Suitability dimension comprises a new combined variable that evaluates the quality of source from which the FC is taken.

Firstly, it is assessed whether the capacity and fragility curves were derived from existing buildings or from building prototypes and the size of the sample of buildings used. It is expected that the larger the sample size, the greater the precision and the possibility of generalising the results obtained to the typology evaluated.

The second variable included in this fourth dimension refers to the authenticity and credibility of the study from which the fragility curve was derived. To assess this characteristic, the type of publication in which the analysed FC is found is considered. Those FCs from published scientific articles or doctoral theses, for example, are therefore understood to have higher credibility (and therefore a higher score) than those derived from a conference paper, master's or degree final projects, or unpublished reports.

The last variable of this third block measures the popularity of the FCs, that is, the number of times the function was used for seismic risk assessments. For this, the number of citations in Google Scholar presents the study in which the evaluated FCs was used as a proxy variable that captures the use of the FCs although imperfect, it is easier to measure: (i) High, when it presents more than 50 citations or from a big source data; (ii) Medium, when it has been cited between 10 and 50 times; and (iii) Low, when less than 10 times.

These last block of variables could be more subjective than those included in the other dimensions and sub-dimensions. However, several authors propose considering them to evaluate FCs ([60, 59, 36, 41, 7]). As these variables present a degree of subjectivity, relatively low scores were assigned to them, so they do not determine the final classification of the FCs. In this way, the robustness of the method is maintained; that is to say, the class of the curve will not be affected by small variations from the assumptions of these subjective variables.

Suitability for the Local System Dimension

In the second dimension, the suitability for the local system seeks to assess the level of adequacy of the FCs evaluated for the typologies analysed and the study to be carried out based on the following variables: similarity in construction techniques and IM similarity.

Suitability for the Local System Dimension (SLS):

- Similarity in Construction Techniques
- Intensity Measure (IM) similarity

Similarity in the construction techniques is assessed based on the geographical applicability in the case of some typologies, such as masonry, and on the criteria of the researcher for the high-rise reinforced concrete and steel typologies as these typologies are more standardized globally and are likely to be built by foreign engineers. The similarity in the expertise of the engineers that usually work in the country and in the level of compliance of the buildings with good-practice codes regarding seismic-resistant design could be reasonable parameters so that the researcher can assess this variable in the case of high-rise buildings. The geographic applicability assesses whether the curve evaluated was derived for the locality, state or country of the typology under investigation or was obtained for another country in the same subregion, in the same region, or from another region. It is assumed that the functions derived from the typologies of the country itself will share similar characteristics, such as building design, construction materials, and building practices [60]. In this case, the definition of country or state, region, and subregion is associated with the main factors determining the construction techniques and existing typologies in a zone. Specifically, the construction typologies are mainly influenced by climate, sociocultural factors, income per capita, level of technological advancement and seismic-resistant regulation development, as well as its degree of application [12]. Therefore, a country or state is considered to be one delimited by political or natural borders that

share the four factors. A sub-region comprises one or several neighboring countries or states with similarities in at least three of the above-mentioned factors. A region comprises one or several neighboring countries or states that share similarities in at least two factors. In the case study, Costa Rica is considered a country, Central America is the subregion, and Latin America is the region. Thus, an FC not for a country or area in Latin America is classified as outside the region.

The IM similarity captures the suitability between the IM of the FC and that corresponding to the hazard information ([60]). Therefore, the FC will be ranked according to whether its IM matches the IM included in seismic hazard information or according to how easily the IM can be translated into the IM needed based on the hazard information. Based on Stone et al. (2017) [60], the degree of similarity between the intensity measurement (IM) of the FC and that of the seismic hazard information and, therefore, the difficulty in converting one into the other is expressed in the high, medium, and low scores of Figure 3.2 in the following way: (i) the high score is assigned when both IMs coincide, (ii) the medium score is assigned when they are similar but not the same, but the conversion does not introduce a significant source of uncertainty; this is the case when one of the IMs is pseudo-acceleration (Sa), and the other pseudo-displacement (Sd) and (iii) the low score is assigned when the dissimilarity between the two IMs is high, and the conversion introduces a high uncertainty, as occurs between the discrete IMs (MMI, EMS-98, for example) or scalar IM (PGA or PGD) and the rest.

Building Class Similarity coefficient

Building Class Similarity (BCS): a reduction coefficient

The third dimension refers to the similarity between the building class of the candidate functions and the building class of the function that must be applied. To evaluate this similarity, the number and type of common attributes between both building classes are considered. In particular, the basic attributes and those that can be considered more important in view of the seismic vulnerability of the examined typology are lateral load-resisting system, number of stories, ductility, year of construction, and compliance with seismic regulations. It must be pointed out that the FC must correspond to a typology of the same material as the one analysed. Given the importance of the number of common attributes between the building class studied and the one for which the evaluated FC has been derived, this dimension is the most weighted one for determining the FC suitability through an adjustment coefficient of the global index.

Figure 3.1 indicates the attributes relevant to this dimension and its score according to the material of the FCs under study. For all the typologies analysed, the FCs must be selected to present the same material of lateral load resisting system and height range (low, medium, high)² among those corresponding to the same building class. The height range is considered a basic attribute in selecting the candidate, as the natural period of vibration of a building is highly conditioned by its height and is a crucial property for assessing the seismic base shear, which is controlled by its mass and stiffness. As the height of the building increases, its mass increases but its overall stiffness decreases. The natural period of the building therefore grows ([10]). Moreover, the empirical formulas used, for example in construction codes, to estimate the fundamental time period of buildings are generally expressed as a function of the height of the building ([31]).

In the cases of the masonry, reinforced concrete, wood, and steel typologies, a score from minimum to maximum is assigned in this coefficient when the FC of the candidate building class shares from one to all the following attributes for which information is generally available: the structural system, the number of floors, and the ductility. This ranking system avoids giving more value to the FCs of the candidate typologies that do not share the first basic attributes and others considered important for seismic vulnerability in the analysed building class. In that case, neither candidate FCs will receive more scores when they share other attributes or constructive features that differ from those previously mentioned for each material.

A score assigned to each of the dimensions and variables analysed (Figure 3.3) considers the comparative importance of each to determine the suitability of the curve analysed based on the framework for FC evaluations proposed by [60], [36], [17] and [52].

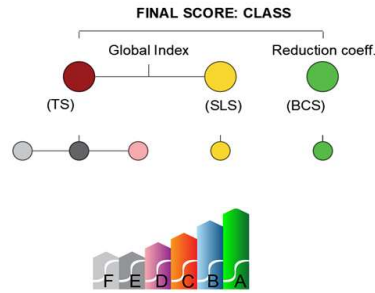
²Following the definition of the height ranges proposed in [21], the height of a building is considered low when it has one to three stories, mid when it has four to seven stories, and high when it has eight or more stories.

Number of attributes in common	Score	Type of attributes in common by typology				
		REIN-FORCED CONCRETE	MASONRY	STEEL	WOOD	INFORMAL/PRECARIOUS
None beyond basic attributes to qualify as candidate FC	0.55	Similar primary construction material (RC) and height range	Similar primary construction material (masonry) and height range	Similar primary construction material (steel) and height range	Similar primary construction material (wood) and height range	Informal/precarious and similar height range
One shared attribute*	0.70	(+1)Structural system (LLRS):	(+1)Structural system (LLRS):	(+1)Structural system (LLRS):	(+1)Structural system (LLRS).	(+1)Similar material.
Two shared attributes*	0.85	walls, frames, dual.	unreinforced, reinforced	frames, frames with steel	(+1)Similar material.	(+1)Identical number of floors.
Three or more shared attributes*	1.00	(+1)Identical number of floors. (+1)Ductility. (+1)Other.	confined, confined. (+1)Identical number of floors. (+1)Ductility. (+1)Other.	brace, steel light frames. (+1)Similar material. (+1)Ductility. (+1)Identical number of floors. (+1)Other.	(+1)Ductility. (+1)Identical number of floors. (+1)Other.	(+1)Other.

Table 3.1: Attributes considered and their corresponding scores for the adjustment coefficient related to building class similarities. Note: Height ranges: low, 1 to 3 stories; mid, 4 to 7 stories; and high, 8 or more stories (based on [21]). *When the typology studied and that of the FC present one, two, or three, or more of any of the attributes listed, it receives a score of 0.70, 0.85, or 1, respectively, in this dimension.

TECHNICAL SUITABILITY DIMENSION														
Subdimension	Score	Candidate FC			Subdimension	Score	Candidate FC			Subdimension	Score	Candidate FC		
		DH	CAL	VV			DH	CAL	VV			DH	CAL	VV
CAPACITY CURVES	25				FRAGILITY CURVES	25				QUALITY	25			
Method and model	15				Intensity measure (IM)	10				Building type and sample size	18			
Experimental 3D	15				Advanced IM	10				EB>10 and PR probabilistic	18	X		X
Experimental 2D	12	X			Spectral acceleration or displacement	8	X			PR and Sample=1	14			X
Analytical 3D	9				Scalar IM (PGA, PGD)	6		X	X	EB and Sample=5-10	10			
Analytical 2D	6		X		Discrete IM (MMI, EMS-98)	0				EB and Sample=1-5	6			
Combined SDOF	3			X	Sources of uncertainty considered	7				EB and Sample=1	0			
SDOF	0				3 sources considered	7	X		X	Authenticity and Credibility	4			
Type of analysis	8				1 or 2 sources considered	5		X		High	4	X		X
Nonlinear Dynamic Analysis (NLDA)	8	X	X	X	No source considered	0				Medium	2		X	
Nonlinear Static Analysis (NLSA)	4				DS thresholds	2				Low	0			
Simple	0				Customised	2	X		X	Popularity (citations)	3			
EDP	2				Preset	0		X		High (50+ Big source data)	3			X
IDR	2	X	X		Years of the function	6				Medium (10- 50)	1			
IDR global	2			X	<3 years	6				Low (<10)	0	X		X
Maximum displacement	1				3-5 years	5	X	X	X	Total	22	20	21	
Roof displacement	0				5-10 years	4								
Total	22	22	16	13	10-20 years	2								
					older	0								
					Total	22	22	16	20					

SUITABILITY FOR THE LOCAL SYSTEM DIMENSION			
Subdimension	Score	Candidate FC	
		DH	CAL VV
Similarity in Construction techniques	20		
Country	20	X	X
Subregion	15		
Region	10		X
Out of the region	0		
IM similarity	5		
High, equal IM	5	X	X X
Medium, different IM	3		
Low	0		
Total	25	25	15



GLOBAL INDEX			
	Score	Candidate FC	
		DH	CAL VV
Technical suitability	66	52	54
Suitability for the local system	25	25	15
TOTAL	91	77	69
ADJUSTMENT COEF. BY BUILDING CLASS SIMILARITY			
Number of common attributes	Score	Candidate FC	
		DH	CAL VV
3 or more attributes	1.00	X	
2 attributes	0.85		X X
1 attribute	0.70		
0 attributes	0.55		
FINAL INDEX	91	66	59
CLASS		A	B C

GEM Description of candidate FC	Author	Acronym
MCR+CBH/LWAL+DUC/HEX:2/IRRE/FN	Diego Hidalgo (2017)	DH
MR/LWAL+DUC/HEX:2 and MCF/LWAL+DUC/HEX:2	Calderón and Silva (2019)	CAL
MCF/LWAL+DUC/HEX:2	Villar Vega (2017)	VV

Figure 3.2: Dimensions, variables, and categories of the index to evaluate FCs and their corresponding weights. Moreover, an example of the evaluation of three FCs in the case of two-story reinforced confined masonry buildings of Costa Rica.

Note: SDOF: Single Degree of Freedom, IDR: inter-story drift ratio, PGA: Peak Ground Acceleration, PGD: Peak Ground Displacement, EMS-98: European Macroseismic Scale, SB: Specific building, BPR: Building prototype. The 3 sources of uncertainty of FC parameters are: (i) uncertainty in the seismic demand, (ii) uncertainty in the capacity of the building, (iii) uncertainty in the definition of damage thresholds ([52, 7])

Classification: Class A: (85, 100], Class B: (65, 85], Class C: (55, 65], Class D: (47, 55], Class E: (40, 47] and Class F: (0, 40] points.

3.2.2 Practicality of the methodology

A clear advantage in terms of practicality of the subdivision into dimensions is that some dimensions need not be particularised for each specific area or structural system (see Figure 3.3). In other words:

- The technical dimension is independent of the area under study or the type studied, i.e., it depends only on the method used to elaborate the FCs. Therefore, once done for a specific FC, the said value is valid for any seismic risk study. Moreover, this is the most time-consuming dimension.
- The local system dimension depends only on the features of the town/city/area under study. The said value is therefore valid for any structural type within the area.
- The building class similarity reducing coefficient is the only dimension that must be particularised for any structural type according to its attributes (material, structural system, number of floors and ductility).

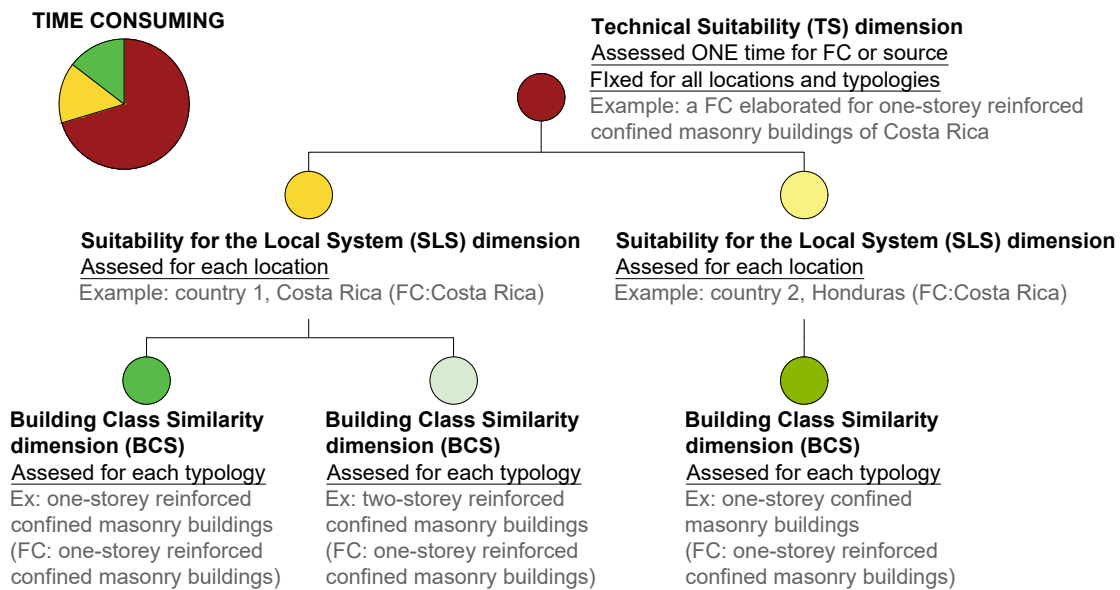


Figure 3.3: Conceptualization and example of applicability of the different dimensions defined for the methodology.

3.2.3 Classification of fragility curves

Once the FCs have been assessed and points assigned to each curve, the curves are classified (Figure 3.1) to give a rapid and clear idea of the adequacy of each curve to the study under development. Said sorting in classes is based on the methodology of classification that stems from the field of energy consumption, which is already present in several fields such as structural engineering ([38, 40]).

In the classification, each colour and letter represent a level of adequacy to describe classes or categories that differ in their assessment qualitatively rather than quantitatively. In this framework, FCs of Class A are those whose total score is higher than 85, Class B corresponds to FCs with a total score higher than 65, Class C to those higher than 55, D to those higher than 47, E to those higher than 40, and Class F to all other FCs with a total score under 40. The values assigned to the consecutive steps have been defined considering 85% the value of the step immediately above (Class A: (85, 100] points; Class B: (65, 85]; Class C: (55, 65]; Class D: (47, 55]; Class E: (40, 47], Class F: (0, 40] points) .

After that, the curves are drawn, and those pertaining to the highest-scored classes are highlighted by type and state of damage. Also, if considered pertinent, the FCs for different types can be drawn together.

At this point, if most of the FCs with higher scores for a particular type resemble each other, this consensus is an additional indicator of suitability. The resemblance between the FCs can be easily analyzed visually from the graph that represents them jointly. It is also possible to determine the similarity between the FCs by comparing

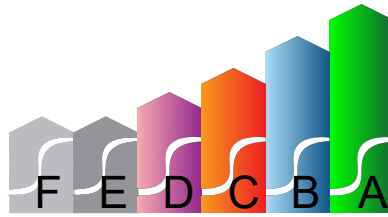


Figure 3.4: Fragility curves classification.

their parameters (median or mean and standard deviation) or the corresponding damage exceedance probabilities for similar values of intensity of the seismic movement. Nonetheless, the evaluation tool must be assisted by the criteria of local experts, as they may establish whether the results are coherent between different typologies.

Therefore, the methodology can be considered a tool that permits a well-founded evaluation of the FCs available in the literature, whose suitability of results or output would depend on the quality of the inputs and the knowledge of the local experts involved.

In order to facilitate the evaluation of the different curves selected, a spreadsheet has been included as additional material [6].

3.3 Application to the case of Costa Rica

Firstly, the methodology has been calibrated and tested via the application to the case of Costa Rica. Later, it is applied to the case of Spain.

The selection of San José, capital of Costa Rica, as the case study to calibrate the proposal is motivated by these reasons: several well-known and comprehensive seismic risk studies have been carried out in the last decades in the region; and the buildings typologies of this country include types extended all over the world (such as RC buildings) and typologies that are almost specific of the area (like reinforced confined masonry buildings). These two characteristics of Costa Rica are key for a consistent calibration of the proposal.

The GEM building taxonomy, [57] and [12], is used to characterize the typologies of FCs evaluated according to their attributes in a uniform classification scheme.

3.3.1 The Costa Rica case study

Central America is one of the greatest seismic hazard zones in the world. Additionally, it is a region characterised by a high physical and social vulnerability [48]. The most common types of buildings in the area are adobe, unreinforced masonry, and wooden ones [13]. According to the literature assessment and the comments from the local engineers, there is ineffective enforcement of contemporary seismic laws, which unavoidably results in a stock of buildings that is quite vulnerable [13]. It has been precisely the combination of these two negative factors that has caused an extremely high number of fatalities and economic losses in the past when a seismic event has occurred.

The most destructive earthquake in the history of Central America occurred in Guatemala in 1976, when the Motagua-Polochic Fault caused an earthquake with a magnitude of surface levels of M_s 7.5 [8]. This earthquake left a balance of more than 22700 deaths and close to 76000 injuries and generating losses of around 1.1 trillion dollars, representing 18% of Gross National Product (GNP) at that time [18] and [20]. In April 1991, an Mw 7.7 earthquake devastated the Caribbean region of Costa Rica and Panama. And, in September 1992, an earthquake off the coast of Nicaragua caused the worst tsunami in the region. More recently, two earthquakes affected El Salvador on January 13 and February 13, 2001, in which more than 1000 people lost their lives [8], [51]. Moreover, more recently, the Cinchona earthquake occurred in Costa Rica (MW 6.2) on January 8, 2009, seriously affecting rural populations and hydroelectric works [49], [8].

For that reason, in the last few decades, several seismic risk studies have been carried out to identify the vulnerability of the existing buildings and the potential economic costs that a strong-motion earthquake could cause

in the region [28, 34, 46]. Moreover, the research studies being performed aim to introduce mitigation measures such as the retrofitting of buildings or the improvement of the regulations in force.

The case of Costa Rica is a very interesting example within Central American countries. A significant number of specific vulnerability studies have been carried out in the country (see Tables 3.2, 3.3 and 3.4), and its seismic codes are notably advanced and detailed, which has led to a significant decrease in poor-quality construction techniques in formal buildings that comply with current planning and building regulations. Nevertheless, these inadequate techniques continue to be predominant among the most disadvantaged sectors of the population of other countries of Central America. Within this framework, FCs for several types of buildings in San José de Costa Rica have been assessed by applying the new methodology proposed in this article, based on a multidimensional index developed to evaluate FCs from a broad set of variables, which involves comparisons between the FCs proposed available.

In Costa Rica, the National Insurance Institute (INS) requested that the first relevant study regarding vulnerability be carried out on a national scale [54]. In the study, the dwellings were classified into seven types according to wall materials, seismic design, and the state of the building. The materials considered were adobe, concrete, reinforced masonry, and steel and wood frameworks. The study concluded that under seismic actions, on the Modified Mercalli Intensity (MMI) scale ³, the typologies that suffer a higher percentage of damage are adobe, construction with low-quality materials, and reinforced concrete structures without seismic design [4].

In 2003, the seismic risk was evaluated in the San José Metropolitan Area (AMSJ) [53]. In this area, six types of basic structural systems were identified depending on the material of the load-bearing walls: masonry, a combination of masonry and wood, wood, precast concrete, waste material, and others (bahareque and adobe). Moreover, based on the criteria of specialists, 152 typologies were generated for the vulnerability analysis using the HAZUS methodology. The quantification of human losses due to damage to buildings was based on spatial distribution and structural typology utilising the Global Earthquake Safety Initiative (GESI) methodology. This study was completed by [58], which analysed the seismic vulnerability of reinforced and confined masonry housing structures of one and two floors in a pilot area of the Central Valley.

The construction sequence and system present key differences between confined masonry and reinforced concrete frames with masonry infill walls. In confined masonry construction, the masonry walls carry the seismic loads, while the reinforced concrete confining elements are used to confine individual walls. The confining elements are effective in enhancing the stability and integrity of the masonry walls for in-plane and out-of-plane earthquake loads by confining damaged masonry walls, as well as in enhancing the strength and ductility of masonry walls under lateral earthquake loads, which improves their earthquake performance. Reinforced and confined masonry, also known as integrally reinforced masonry, is one of the most used composite materials used in Costa Rica to construct one- or two-story single-family homes, thanks to its good acoustic, thermal, and humidity insulation. The use of ductile steel as reinforcement placed vertically and horizontally provides better quality, durability, and resistance to lateral loads of the constructions [23].

Likewise, in addition to the seismic vulnerability analyses carried out for Costa Rica in the RESIS II, CAPRA ([61]), and PREPARE ([27] and [28]) projects, several research studies have developed capacity and fragility curves for different building typologies. Tables 3.2, 3.3 and 3.4 summarise the main references and characteristics of these studies.

3.3.2 Results and discussion

In the following, the results for San Jose (Costa Rica) of the application of the methodology elaborated to assess fragility curves are presented.

The work developed by [32] presents an analysis of the type of buildings included in the catalogue of exposure of Costa Rica, considering the total building stock, that is, constructions of all uses (residential, commercial, etc.): 20 types of buildings within which MRC (reinforced confined masonry) and MCF (confined masonry), RC (reinforced concrete), S (steel), W (wood) and informal constructions are included. Among the most relevant ones according to their frequency, the following typologies have been considered for the application of the methodology proposed to San José of Costa Rica:

³Note that MMI is a discrete IM that, today, is not much used in vulnerability and seismic risk studies as it presents some deficiencies that have been overcome by other IMs considered more appropriate, such as spectral pseudo-acceleration.

Author(s)	Study year	Project type	Study type	Geogr. area studied	Institutions involved	Analysed Variable(s)	Vulnerability assessed by FC? Source of FC
Typologies analysed							
Sauter and Shah[54]	1978	National	Project: Earthquake Insurance Study	Costa Rica	Instituto Nacional de Seguros (INS), Comisión Nacional de Emergencias (CNE)	Material, structural system, year of construction	Yes. FCs given in MMI values.
Montoya (2002)[44]	2002	National	PhD dissertation	Cartago	Geo-Information Science and Earth Observation (ITC) (PhD dissertation)	Material, structural system, height, number of floors, type of foundation	Yes. FCs given in MMI values
Climent et al., (2003)[16]	2003	Regional	Capacity Building for Natural Disaster Reduction for Guanacaste Central America	Cañas (Province of Guanacaste)	Centre of Prevention of Disasters of America Central (CEPRE- DENAC), UNESCO, International Institute for Geoinformation Science and Earth Observation (ITC)	Qualitative and preliminary analysis of seismic vulnerability	No. A qualitative and preliminary analysis of the vulnerability of buildings is carried out.
Lang et al., (2009) [34]	2009	Regional	Project: RESIS II	Costa Rica	Norwegian Seismic Array (NORSAR), Universidad Politécnica de Madrid, Universidad de Costa Rica (UCR), CEPREDENAC	Material, structural system, height, level of code compliance.	Yes. FCs are obtained from different sources.
Evaluación de Riesgos Naturales America Latina (ERN), (2009) [14]	2009	Regional	Project: CAPRA (Probabilistic Risk Assessment)	San José	Evaluación de Riesgos Naturales de América Latina (ERN), Ingeniería Técnica y científica Ltda. (ITEC), Centro Internacional de Métodos Numéricos en Ingeniería (CIMNE), World Bank, Interamerican Development Bank	Structural system and number of floors	No. Vulnerability is analysed using the physical and human loss vulnerability functions.
Structural masonry, simple masonry, wood, concrete frames							

Table 3.2: Principal studies and projects on seismic vulnerability in Costa Rica. [Table 1/3]

Author(s)	Study year	Project type	Study type	Geogr. area studied	Institutions involved	Analysed Variable(s)	Vulnerability assessed by FC? Source of FC
Miyamoto International, (2020) [28]	2016	Regional	Project: PREPARE	San José	USAID, Miyamoto Inc.	International Material, LLRS and height	Yes. Adaptation of the FCs proposed by FEMA (2001) [3]
Typologies analysed							
Hidalgo-Leiva (2017) [23]	2017	National	PhD dissertation	-	Universidad Politécnica de Cataluña	Material, structural system	Yes. Own FCs for both typologies analysed.
Reinf. and confined masonry known as "Integrally reinf. masonry".							
Calderón (2018) [19]	2018	National	Graduate Thesis	Cartago	University of Costa Rica (UCR)	Material, structural system, height, number of floors, type of foundation	Yes.
Cold Rolled Steel Frame (2–3 storeys), steel with structure IMF, OMF, SMF (4 storeys), steel with structure IMF, OMF, SMF (10 storeys), steel with SCBF (4–10 storeys), reinf. concrete dual structure (4–7 storeys, 8–18 storeys), reinf. concrete with frame (4–7 storeys), reinf. concrete wall structure (6–8, 9–18 storeys), masonry with wall structure (2 storeys), reinf. concrete with dual structure (4–10 storeys), reinf. concrete with frame structure (6–10 storeys).							
Calderón and Silva (2019) [13]	2019	National	Project: earthquake Model (GEM)	Global Costa Rica	Instituto Geográfico Nacional (IGN), Banco Central de Costa Rica (BCCR), Cámara de la Construcción (C.C.C), Colegio Federado de Ingenieros y Arquitectos de Costa Rica (CFIA), Instituto Nacional de Estadística y Censo (INEC), University of Costa Rica (UCR)	Material, structural system, ductility, height, year of construction	Yes. Own FCs for ductile confined masonry and precast reinforced concrete structures and FCs for other typologies are from Villaverde et al. (2017) [62].
Conf. masonry, wall system, (low to high ductility and 1–6 storeys, Post 1980); reinf. masonry, wall system (low to high ductility and 2–12 storeys, post-1980); wall system (none to high ductility, 1-storey, pre-1980); informal unknown non-ductile 1-storey unknown; precast conc., wall system, (low to high ductility, 1-storey, post 1980); reinf. concrete, frames (low to high ductility, 1–6 storeys, post-1980); wood, wall system, (none to low ductility, 1–2 storeys, Pre 1980); reinf. concrete, dual system (low to high ductility, 3–6 storeys, post-1980); reinf. concrete, wall system, (low to high ductility, 6–12 storeys, post-1980); precast conc., wall system (low to high ductility, 2–3 storeys, post-1980); unreinf. masonry, wall system (non-ductile, 1-storey); unreinf. masonry, adobe blocks, wall system (non-ductile, 1-storey); steel, cold form steel members, frames (low to high ductility, 1-storey); steel, hot-rolled steel members, frames (low to high ductility, 1–2 storeys); wood unknown, post and beam, low, 1 storey; heavy wood, wall system (high ductility, 1–2 storeys).							

Table 3.3: Principal studies and projects on seismic vulnerability in Costa Rica [Table 2/3].

Author(s)	Study year	Project type	Study type	Geogr. area studied	Institutions involved	Analysed Variable(s)	Vulnerability assessed by FC? Source of FC
Typologies analysed							
Esquivel-Salas (2020)[32]	2020	National	Master Thesis	Área metropolitana de San José	Laboratorio de Ingeniería Sísmica (LIS) de la UCR y German Research Centre for Geosciences (GFZ-GeoForschungsZentrum)	Material, structural system, number of storeys, structural regularity	Yes. FCs given in MMI values
<p>Regular rigid reinf. and confined masonry, flexible confined and reinf. masonry, confined masonry, reinf. concrete with dual system (1–5 storeys, 6–11 storeys and more than 11 storeys), reinf. concrete with infilled frame (1–5 storeys), reinf. concrete with moment frame (1–5 storeys, 6–11 storeys and more than 11 storeys), wood with moment frame (1–2 storeys), wood with wall system (1–2 storeys), structural steel with moment frame (1 storey), cold-rolled steel members with moment frame (1–5 storeys), hot-rolled steel members with moment frame (1–5 storeys), informal (1 storey).</p>							
Climent et al., (2003)[16]	2021	Regional	Research Paper	Costa Rica	Global Earthquake Model Foundation, University Fernando Pessoa, Universidad de Nicaragua, Universidad de Panamá, Universidad de Costa Rica, Universidad Mariano Gálvez de Guatemala, Universidad de El Salvador	Material, structural system (LLRS), ductility, stories, capacity	Yes. FCs from Martins and Silva (2020) [37].
<p>Wood and light wood members with shear wall LLRS (low and moderate ductility, 1–2 storeys); wood and wattle and daub with shear wall LLRS (low ductility, 1 storey); unreinf. masonry with shear wall LLRS (low ductility, 1–2 storeys), unreinf. masonry and adobe blocks with shear wall LLRS (low ductility, 1–2 storeys); reinf. masonry with shear wall LLRS (low, moderate and high ductility, 1–3 storeys); confined masonry with shear wall LLRS (non-ductile, moderate and high ductility, 1–3 storeys); reinf. concrete with moment frame LLRS (non-ductile and with high ductility), reinf. concrete with moment frame LLRS with soft storeys (non-ductile, 2 storeys); reinf. concrete with infilled frame LLRS (low, moderate and high ductility, 1–3 storeys and 4–6 storeys); reinf. concrete with dual frame LLRS (high ductility, 6–12 storeys); steel and hot-rolled steel members with braced frame LLRS (moderate ductility with 1 storey and high ductility with 6–12 storeys), steel and cold-formed steel members with moment frame LLRS (low, moderate, and high ductility, 1 storey), waste/other materials with unknown LLRS (low ductility, 1 storey)</p>							

Table 3.4: Principal studies and projects on seismic vulnerability in Costa Rica. [Table 3/3]

- (i) **Two-storey, reinforced confined masonry with wall system:**
MRC+CBH/LWAL/HEX:2/IRRE/FN (38.7% of total built area),
- (ii) **One-storey, reinforced confined masonry with wall system:**
MRC+CBH/LWAL/HEX:1/IRRE/FC (24.8% of total built area),
- (iii) **More than eleven-storey reinforced concrete with dual system:**
(RC/LDUAL/HBET:11+/IRRE/FC)(6.9% of total built area),
- (iv) **One to five-storey reinforced concrete with wall system:**
RC/LWAL/HBET:5,1/IRRE/FC (3.3% of total built area),
- (v) **One to five-storey reinforced concrete with dual system:**
RC/LDUAL/HBET:5,1/IRRE/FC (2.5% of total built area).

In particular, the RC types have been selected in a way that permits a comparative assessment of the methodology, depending on the number of floors of buildings with the same structural system and the structural system itself, either dual or just with shear walls.

For each of these types, several FCs have been selected and scored. As an example, we will show the most extended type: two-storey reinforced confined masonry with wall system (see Figure 3.2).

The FCs selected for comparison have been taken from very different sources: big sources of data, such as HAZUS or GEM, regional or national seismic risk projects, scientific articles, PhD studies, and final master projects. Among these databases, the references used for Costa Rica consider the FCs included in the following works and developed or adapted from other sources by the researchers specified (see Tables 3.5, 3.6 and 3.7 for more detail): [28, 34, 21, 19, 32, 13, 37, 62, 15, 4].

Tables 3.5, 3.6 and 3.7 show the scores for FCs assessed in the case of Costa Rica following the methodology proposed. Particularly, the results of the following cases are shown graphically in detail in Figure 3.5:

- a (i) Two-storey, reinforced confined masonry with wall system (MRC+CBH/LWAL/HEX:2/IRRE/FN) and
- (ii) One-storey, reinforced confined masonry with wall system (MRC+CBH/LWAL/HEX:1/IRRE/FC);
- b (i) One to five-storey reinforced concrete with dual system (RC/LDUAL/HBET:5,1/IRRE/FC) and
- (ii) One to five-storey reinforced concrete with wall system (RC/LWAL/HBET:5,1/IRRE/FC).

The candidate curves for the first two typologies (Figure 3.5a) are:

- FC1: MRC+CBH/LWAL+DUC/HEX:1/IRRE/FN by Calderón (2018) based on Hidalgo-Leiva (2017);
- FC2: MRC+CBH/LWAL+DUC/HEX:2/IRRE/FN by Calderón (2018) based on Hidalgo-Leiva (2017);
- FC3: MR/LWAL+DUC/HEX:1 by Calderón and Silva (2019);
- FC4: MR/LWAL+DUC/HEX:2 by Calderón and Silva (2019);
- FC5: MR/LWAL+DNO/HEX:1 by Calderón and Silva (2019);
- FC6: MCF/LWAL+DUC/HEX:1 by Villar-Vega et al. (2017).

In the case of the one to five-story reinforced concrete with wall system and dual system (Figure 3.5b), only the following FCs developed in Central America or used as inputs in previous seismic risk studies were analyzed:

- FC1: RC+CIP/LDUAL/HBET:4,7 by Calderón (2018) based on Labarca (2006) and Ávila (2011);
- FC2: RC+CIP/LDUAL/HBET:11,6 by Esquivel-Salas (2020) based on Calderón (2018);
- FC3: RC+CIP/LWAL/HBET:1,3 by Lang et al. (2019);
- FC4: RC+CIP/LWAL/HBET:4+ by Miyamoto International (2016);
- FC5: RC/LDUAL+DUC/HEX:5 by Martins and Silva (2020);
- FC6: RC/LDUAL+DNO/HEX:5 by Martins and Silva (2020).

The first bar for each FC shows the value of the global index and its component dimensions: those included in the technical suitability dimension (the three dimensions related to the capacity curve, the fragility curve, and the general quality of the study) and the suitability for the local system dimension. The second and third bars show the final index value for each typology corrected according to the building class similarity coefficient. As previously mentioned, this coefficient adjusts the global index, evaluating the similarity between the typology under study and the one for which the FC evaluated was built or proposed. The horizontal lines in each figure show the thresholds set for each of the seven classes proposed to classify the FC according to its score in the final index score.

As can be seen in the mentioned Figure, the application of the methodology proposed renders it very easy to identify the most appropriate FC for a particular structural type (Figure 3.5a). Moreover, it reveals the cases where the FCs assessed are not suitable and where more FCs should be included in the catalogue, or where efforts in the development of an enhanced FC for a particular type should be focused (Figure 3.5b — One to five-storey reinforced concrete with dual system). Furthermore, the aspects in which the curves present greater efficiencies or deficiencies are quickly identifiable.

It is worth mentioning that in the case of the one to five-storey reinforced concrete with dual system (Figure 3.5b), only FCs developed in Central America or used as inputs in previous seismic risk studies were analysed.

Therefore, according to the results of the methodology, the quest for FCs should continue to include FCs developed for the same building type all over the world. It is worth mentioning that construction techniques present fewer differences between countries in the case of RC buildings, mostly medium- or high-rise than in the case of masonry dwellings, mostly low-rise.

In Figure 3.6, scores for each dimension and sub-dimensions of all the FC tested are graphed from the highest to the lowest final score. This graph shows that the different sub-dimensions and dimensions present distinct results, and there is no clear or strong correlation between all of them. This fact suggests that the variables included in the index capture different aspects related to the FC evaluated; therefore, the dimensionality (quantity of variables) of the index should not be reduced.

Given that most of the variables in the proposed index refer to the three dimensions of the technical suitability dimension, evaluating the degree of existing correlation between them is of interest. Furthermore, as previously mentioned, the technical dimension depends on the process used to elaborate the FC and is independent of the typology studied or the area under investigation. As a result, the value is applicable to all seismic risk studies once it has been completed for a particular FC. Figure 3.6 graphically presents the correlation matrix between these dimensions calculated from the scores obtained for the fragility curves evaluated in the case of Costa Rica. Similar to what is observed in Figure 3.7, the estimated coefficients indicate low levels of correlation between the three dimensions. This result again suggests that the aspects valued concerning the capacity curve, the fragility curve, and the quality of the study that proposes them provide different information that, for the reasons previously stated in Section 3.2.1, must be considered when assessing a FC for a given typology.

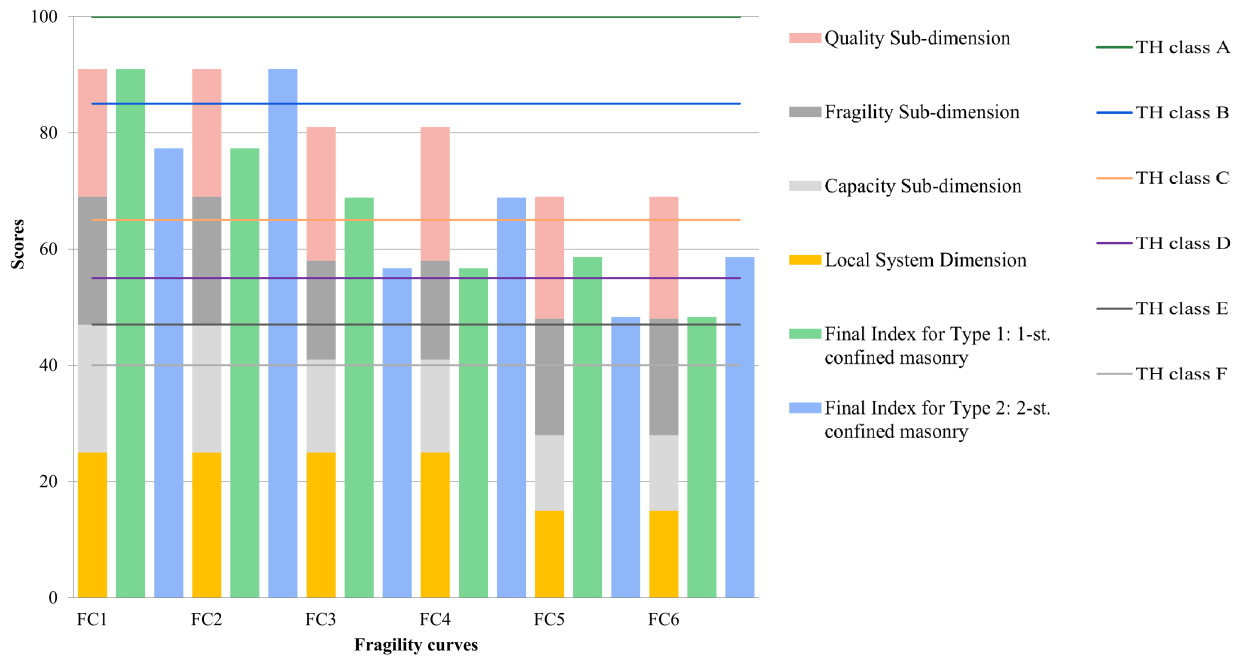
This classification gives rise to the following figures, in which the different fragility curves have been represented. All the FCs have been graphed into the same IM to facilitate the comparison. The IM selected to represent the FCs is PGA, since it is the most widely used, and it allows the alteration of the original curve developed by the different researchers to be avoided. Moreover, the seismic risk studies usually give as outputs seismic hazard maps in PGA or S_a , while other IM such as S_d cannot be applied without an intermediate step, the calculation of the performance point, which hinders their comparison. The regulation in force in Costa Rica [2, 1] and the performance point identification method [56] have been employed for the conversion of the IM.

The FCs have been represented in a manner that permits the differentiation into damage states (DS) and classes. Moreover, in the cases in which there are two different FCs in the highest class, the method called conflation has been applied for consolidating data from these different FCs.

A specific FC has been established as the most suitable one in the following cases:

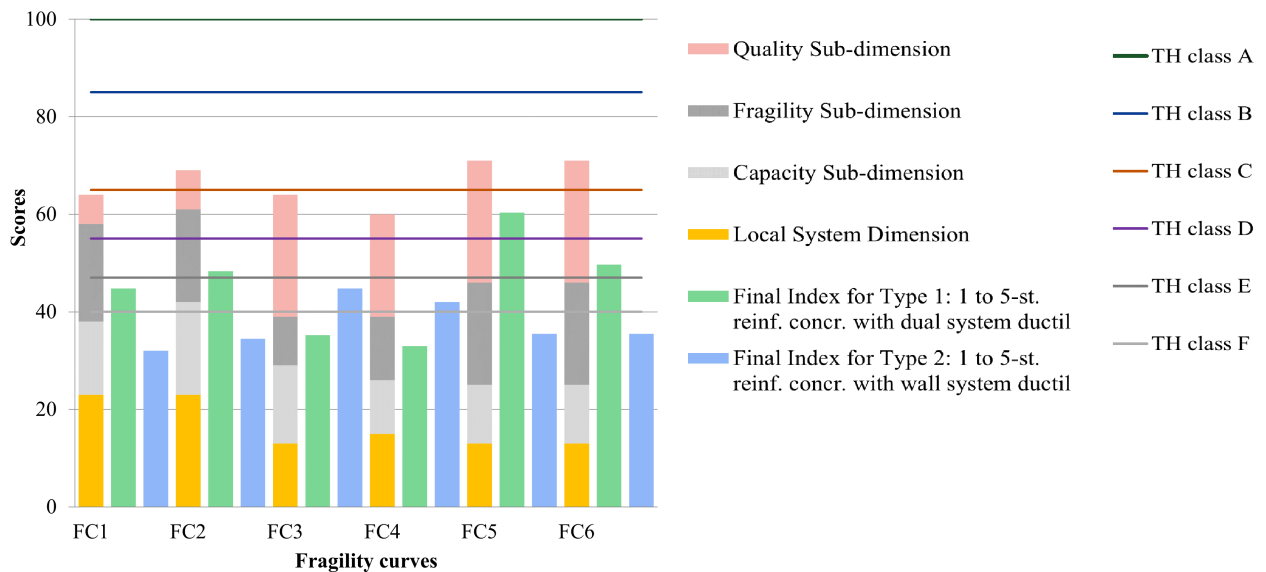
- (i) For one-storey, reinforced confined masonry with wall system typology:
 - (A) MRC+CBH/LWAL+DUC/HEX:1/IRRE/FN, E. Calderón (2018) based on Hidalgo-Leiva (2017)
- (ii) For two-storey, reinforced confined masonry with wall system typology:
 - MRC+CBH/LWAL+DUC/HEX:2/IRRE/FN, E. Calderón (2018) based on Hidalgo-Leiva (2017)

Scores for Types 1 and 2 of reinforced confined masonry



(a) Results for the case of Two-storey, reinforced confined masonry with wall system (MRC+CBH/LWAL/HEX:2/IRRE/FN) and One-storey, reinforced confined masonry with wall system (MRC+CBH/LWAL/HEX:1/IRRE/FC). FC1: MRC+CBH/LWAL+DUC/HEX:1/IRRE/FN by Calderón (2018) based on Hidalgo-Leiva (2017); FC2: MRC+CBH/LWAL+DUC/HEX:2/IRRE/FN by Calderón (2018) based on Hidalgo-Leiva (2017); FC3: MR/LWAL+DUC/HEX:1 by Calderón and Silva (2019); FC4: MR/LWAL+DUC/HEX:2 by Calderón and Silva (2019); FC5: MR/LWAL+DNO/HEX:1 by Calderón and Silva (2019); FC6: MCF/LWAL+DUC/HEX:1 by Villar-Vega et al. (2017). (See Tables 3.5, 3.6).

Scores for Types 1 and 2 of 1 to 5-story reinforced concrete



(b) One to five-story reinforced concrete with dual system (RC/LDUAL/HBET:5,1/IRRE/FC) and wall system (RC/LWAL/HBET:5,1/IRRE/FC). FC1: RC+CIP/LDUAL/HBET:4,7 by Calderón (2018) based on Labarca (2006) and Ávila (2011); FC2: RC+CIP/LDUAL/HBET:11,6 by Esquivel-Salas (2020) based on Calderón (2018); FC3: RC+CIP/LWAL/HBET:1,3 by Kappos and Panagopoulos (2008); FC4: RC+CIP/LWAL/HBET:4+ by Miyamoto International (2016); FC5: RC/LDUAL+DUC/HEX:5 by Martins and Silva (2020); FC6: RC/LDUAL+DNO/HEX:5 by Martins and Silva (2020). (See Table 3.7).

Figure 3.5: Example of application: Costa Rica. Note: TH (ThresHold) class refers to the threshold for each specified class.

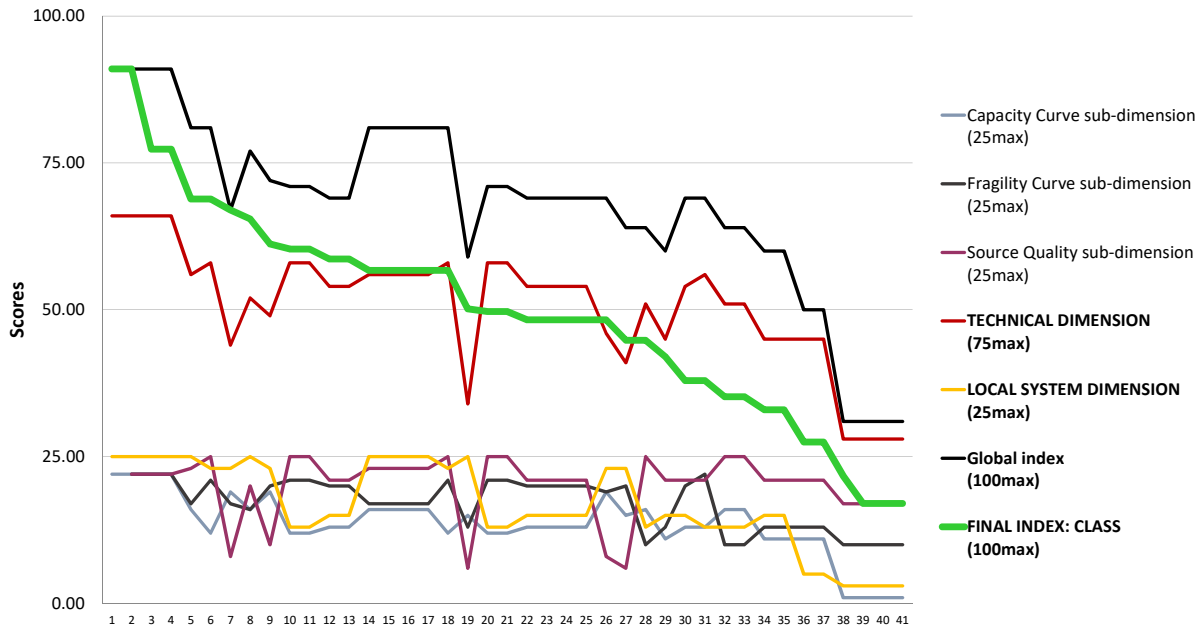


Figure 3.6: Comparison of the scores of the different sub-dimensions and dimensions for the FC evaluated.

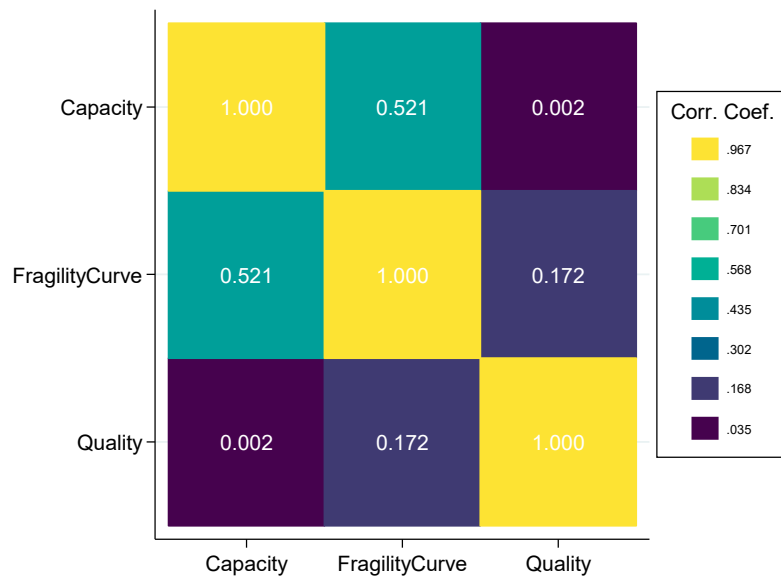


Figure 3.7: Correlation matrix between the sub-dimensions of the technical suitability dimension for FC of Costa Rica.

- (iii) For more than eleven-storey reinforced concrete with dual system typology: A ponderation of these two FCs applying the conflation method for consolidating data from different probability distributions:
 - (B) RC+CIP/LDUAL/HBET:11+, Esquivel-Salas (2020) based on E. Calderón (2018)
 - (B) RC/LDUAL+DUC/HEX:11, Martins and Silva (2020).

Whereas for the following two cases, the methodology has identified the need for further research.

- (iv) For one to five-storey reinforced concrete with wall system typology.
- (v) For one to five-storey reinforced concrete with dual system typology.

To this must be added the cases of RC buildings subject to different irregularities that also require a reliable

FC for evaluating their compounded seismic vulnerability [50]. There are other issues to consider when dealing with RC structures as, for example, the type of non-linearity by which the response is characterised [55].

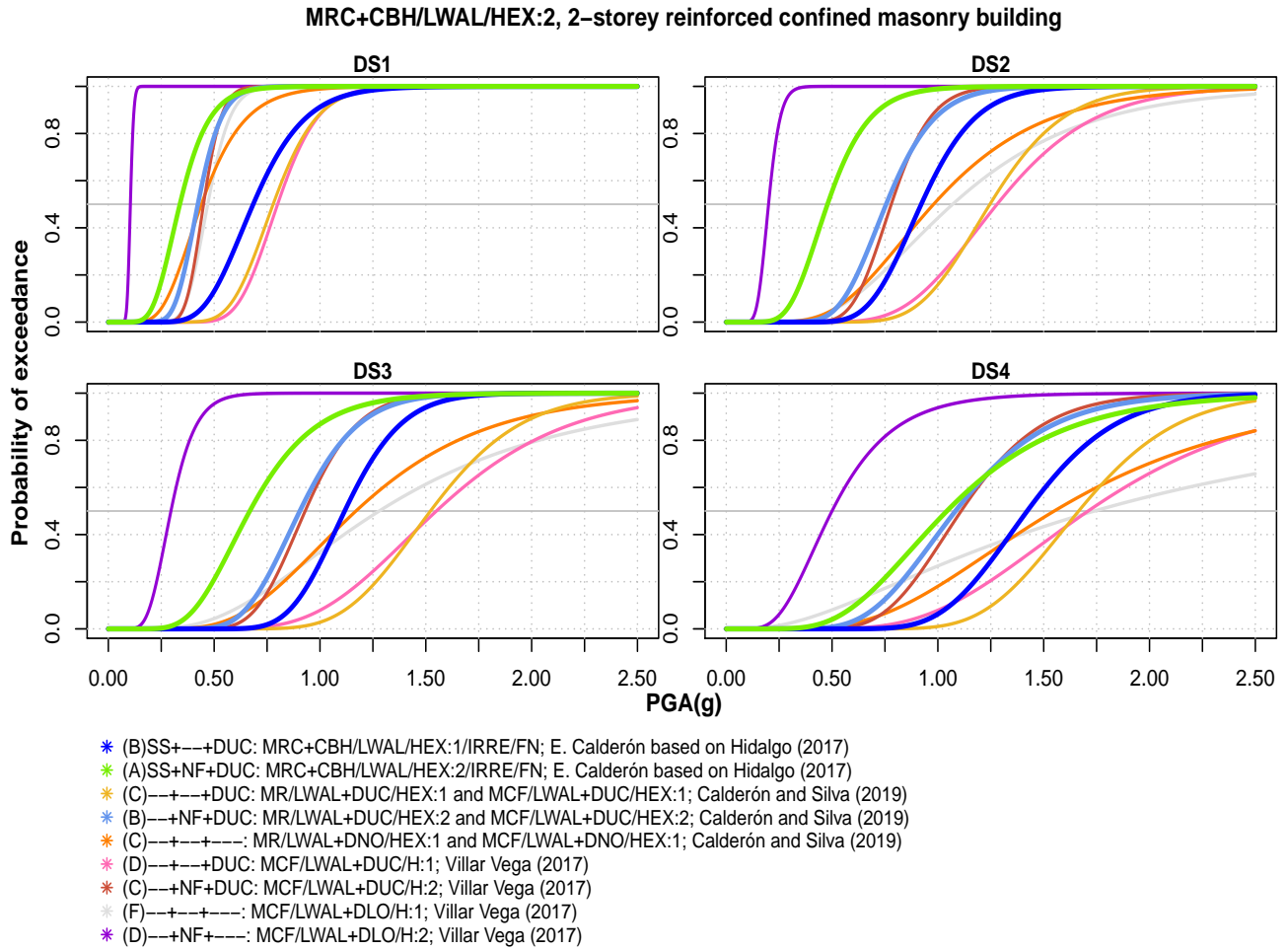


Figure 3.8: Fragility curves evaluated in the study: MRC+CBH/LWAL/HEX:2, 2-storey reinforced confined masonry building.

Note: DS: Damage State. DS1-4: Slight - Moderate - Severe damage - Collapse. (X): Class of the curve, also differentiated by colours. Attributes: SS - Structural System, NF - Number of floors and DUC - ductility. Acronyms for the attributes regarding Building Class Similarity dimension: SS - Structural System, NF - Number of floors and DUC - ductility. When the acronym of a specific attribute or several of them (connected by the "+" symbol) appear into the legend is because said attribute can be considered equal for both typologies, the typology for which the FC was elaborated and the studied typology. Otherwise, its absence (symbolized by"—") means that said attribute is not equal for both typologies.

Author of candidate FC	Description of candidate typology according to taxonomy	CC BV	FC BV	SQ BV	TS	LS	Global index	BCS Coef.	Final index	Class
MRC+CBH/LWAL+DUC/HEX:1(One-story, reinforced confined masonry with wall system ductile)										
(Calderón, 2018) based on Hidalgo-Leiva (2017)	MRC+CBH/L-WAL+DUC/HEX:1/IRRE/FN	22	22	22	66	25	91	1.00	91	A
(Calderón, 2018) based on Hidalgo-Leiva (2017)	MRC+CBH/L-WAL+DUC/HEX:2/IRRE/FN	22	22	22	66	25	91	0.85	77	B
(Calderón and Silva, 2019)	MR/LWAL+DUC/HEX:1 and MCF/LWAL+DUC/HEX:1	16	17	23	56	25	81	0.85	69	B
(Calderón and Silva, 2019)	MR/LWAL+DUC/HEX:2 and MCF/LWAL+DUC/HEX:2	16	17	23	56	25	81	0.70	57	C
(Calderón and Silva, 2019)	MR/LWAL+DNO/HEX:1 and MCF/LWAL+DNO/HEX:1	16	17	23	56	25	81	0.70	57	C
(Villar-Vega et al., 2017)	MCF/LWAL+DUC/HEX:1	13	20	21	54	15	69	0.85	59	C
(Villar-Vega et al., 2017)	MCF/LWAL+DUC/HEX:2	13	20	21	54	15	69	0.70	48	D
(Villar-Vega et al., 2017)	MCF/LWAL+DNO/HEX:1	13	20	21	54	15	69	0.70	48	D
(Villar-Vega et al., 2017)	MCF/LWAL+DNO/HEX:2	13	24	21	58	13	71	0.55	39	F
Miyamoto International (2006)	MR+MOC/LWAL/HBET:3,1	11	13	21	45	5	50	0.55	28	F
Cattari et al. (2004)	MR+MOC/LWAL/HBET:3,1	1	10	17	28	3	31	0.70	21	F
Cattari et al.(2004)	MCF+MOC/LWAL/HBET:3,1	1	10	17	28	3	31	0.55	17	F

Table 3.5: Scores and final class for FCs assessed for some building typologies in Costa Rica following the methodology proposed. CC BV: Capacity Curve Block of Variables(BV), FC BV: Fragility Curve BV, SQ BV: Source Quality BV, TS: Technical Suitability dimension, LS:local System dimension, BCS: Building Class Similarity. References: [28, 34, 21, 19, 32, 13, 37, 62, 15, 4, 30].

Author of candidate FC	Description of candidate typology according to GEM taxonomy	CC BV	FC BV	SQ BV	TS	LS	Global index	BCS Coef.	Final index	Class
MRC+CBH/LWAL+DUC/HEX:2 (Two-story, reinforced confined masonry with wall system ductile)										
(Calderón, 2018) based on MRC+CBH/L- Hidalgo-Leiva (2017)	WAL+DUC/HEX:1/IRRE/FN	22	22	22	66	25	91	0.85	77	B
(Calderón, 2018) based on MRC+CBH/L- Hidalgo-Leiva (2017)	WAL+DUC/HEX:2/IRRE/FN	22	22	22	66	25	91	1.00	91	A
(Calderón and Silva, 2019)	MR/LWAL+DUC/HEX:1 and MCF/LWAL+DUC/HEX:1	16	17	20	56	25	81	0.70	57	C
(Calderón and Silva, 2019)	MR/LWAL+DUC/HEX:2 and MCF/LWAL+DUC/HEX:2	16	16	20	52	25	77	0.85	65	B
(Calderón and Silva, 2019)	MR/LWAL+DNO/HEX:1 and MCF/LWAL+DNO/HEX:1	16	17	23	56	25	81	0.70	57	C
(Villar-Vega et al., 2017)	MCF/LWAL+DUC/HEX:1	13	20	21	54	15	69	0.70	48	D
(Villar-Vega et al., 2017)	MCF/LWAL+DUC/HEX:2	13	20	21	54	15	69	0.85	59	C
(Villar-Vega et al., 2017)	MCF/LWAL+DNO/HEX:1	13	20	21	54	15	69	0.55	38	F
(Villar-Vega et al., 2017)	MCF/LWAL+DNO/HEX:2	13	20	21	54	15	69	0.70	48	D
Miyamoto International (2006)	MR+MOC/LWAL/HBET:3,1	11	13	21	45	5	50	0.55	28	F
Cattari et al. (2004)	MR+MOC/LWAL/HBET:3,1	1	10	17	28	3	31	0.55	17	F
Cattari et al.(2004)	MCF+MOC/LWAL/HBET:3,1	1	10	17	28	3	31	0.55	17	F

Table 3.6: Scores and final class for FCs assessed for some building typologies in Costa Rica following the methodology proposed. CC BV: Capacity Curve Block of Variables(BV), FC BV: Fragility Curve BV, SQ BV: Source Quality BV, TS: Technical Suitability dimension, LS:local System dimension, BCS: Building Class Similarity. References: [28, 34, 21, 19, 32, 13, 37, 62, 15, 4, 30].

Author of candidate FC	Description of candidate typology according to GEM taxonomy	CC BV	FC BV	SQ BV	TS	LS	Global index	BCS Coef.	Final index	Class
RC+CIP/LWAL+DUC/ HBET:11+ (More than eleven-story reinforced concrete with dual system ductile)										
Calderón(2018) based on Hidalgo-Leiva(2017) and Bravo(2002)	RC+CIP/LDUAL+DUC/HBET:18,8	19	20	10	49	23	72	0.85	61	C
Esquivel-Salas (2020) based on Calderón (2018)	RC+CIP/LDUAL/HBET:11+	19	17	8	44	23	67	1.00	67	B
Kappos and Panagopoulos (2008)	RC+CIP/LWAL/HBET:8+	16	10	25	51	13	64	0.55	35	F
Miyamoto International (2016)	RC+CIP/LFM/HBET:4+	11	13	21	45	15	60	0.55	33	F
Martins and Silva (2020)	RC/LDUAL+DUC/HEX:11	12	21	25	58	23	81	0.85	69	B
Martins and Silva (2020)	RC/LDUAL+DNO/HEX:11	12	21	25	58	23	81	0.70	57	C
RC+CIP/LDUAL+DUC/ HBET:5,1 (One to five story reinforced concrete with dual system ductile)										
Calderón (2018) based on Labarca (2006) and Ávila (2011)	RC+CIP/LDUAL/HBET:4,7	15	20	6	41	23	64	0.70	45	E
Esquivel-Salas (2020) based on Calderón (2018)	RC+CIP/LDUAL/HBET:11,6	19	19	8	46	23	69	0.70	48	D
Kappos and Panagopoulos (2008)	RC+CIP/LWAL/HBET:1,3	16	10	25	51	13	64	0.55	35	F
Miyamoto International (2016)	RC+CIP/LWAL/HBET:4+	11	13	21	45	15	60	0.55	33	F
Martins and Silva (2020)	RC/LDUAL+DUC/HEX:5	12	21	25	58	13	71	0.85	60	C
(2020)	RC/LDUAL+DNO/HEX:5	12	21	25	58	13	71	0.70	50	D
RC+CIP/LWAL+DUC/ HBET:5,1 (One to five story reinforced concrete with wall system ductile)										
Esquivel-Salas (2020) based on Calderón (2018)	RC+CIP/LWAL/HBET:5,1	15	13	6	34	25	59	0.85	50	D
Kappos and Panagopoulos (2008)	RC+CIP/LWAL/HBET:3,1	16	10	25	51	13	64	0.70	45	E
Miyamoto International (2016)	RC+CIP/LWAL/HBET:1,3	11	13	21	45	15	60	0.70	42	E
Martins and Silva (2020)	RC/LWAL+DUC/HEX:1	12	21	25	58	13	71	0.85	60	C
Martins and Silva (2020)	RC/LWAL+DNO/HEX:1	12	21	25	58	13	71	0.70	50	D

Table 3.7: Scores and final class for FCs assessed for some building typologies in Costa Rica following the methodology proposed. CC BV: Capacity Curve Block of Variables(BV), FC BV: Fragility Curve BV, SQ BV: Source Quality BV, TS: Technical Suitability dimension, LS:local System dimension, BCS: Building Class Similarity. References: [28, 34, 21, 19, 32, 13, 37, 62, 15, 4, 30].

MRC+CBH/LWAL/HEX:1, 1-storey reinforced confined masonry building

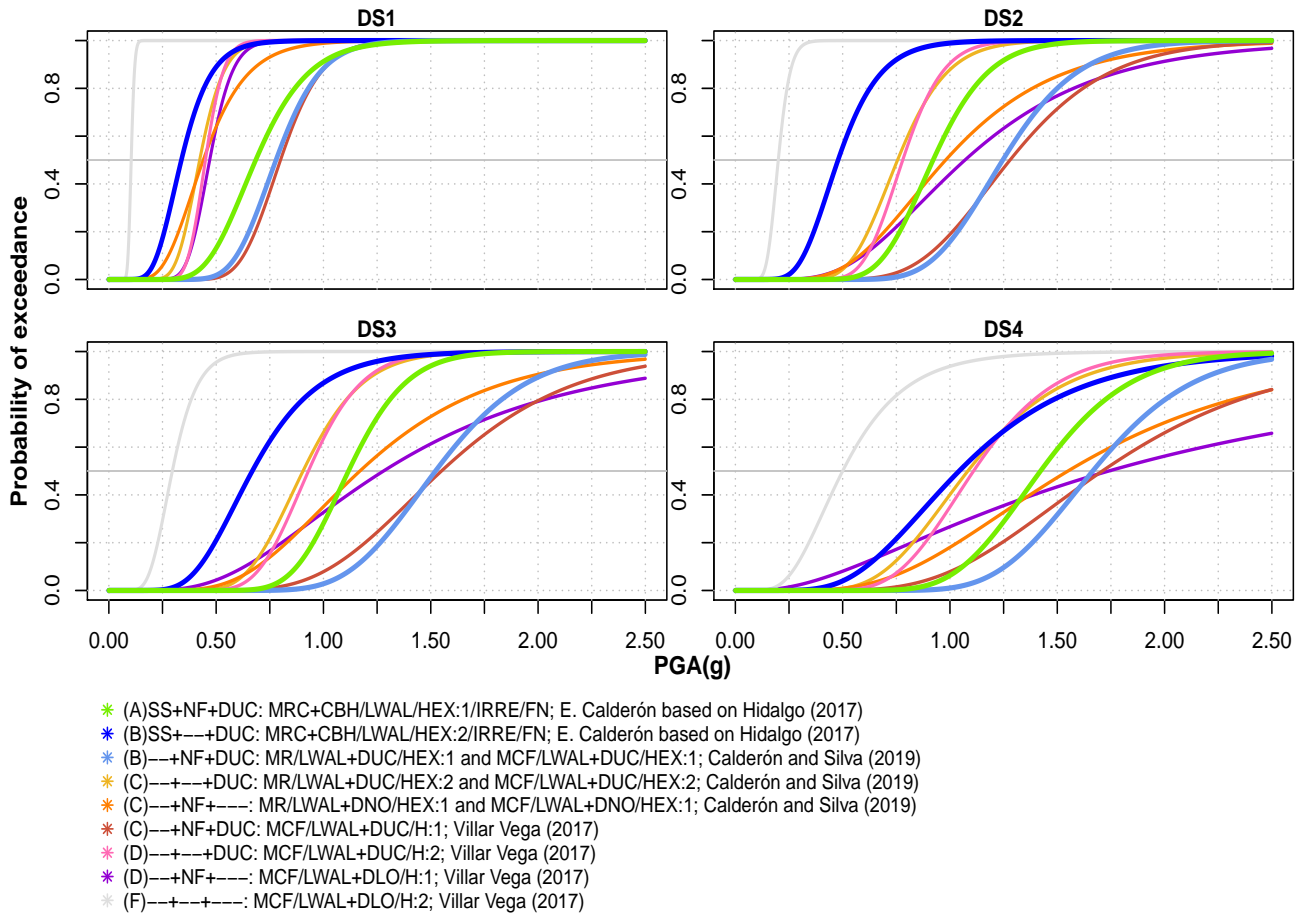


Figure 3.9: Fragility curves evaluated in the study: MRC+CBH/LWAL/HEX:1, 1-storey reinforced confined masonry building.

See Figure 3.8 for label descriptions.

3.4 Application to the case of Lorca

Herein, the application of the methodology to the case of Lorca is presented.

Concerning the state of the art of Lorca buildings' characterisation of vulnerability, in Section 1.4.1 of the State of the Art Chapter the successive seismic risk studies carried out in Lorca up until now are listed and detailed. It is worth noting also herein that among them just the RISMUR II project [26] employs FCs to characterise the buildings' vulnerability. In this Section, said FCs are assessed together with new FCs developed for within this PhD dissertation (see Chapter 4) for Lorca masonry buildings.

The typologies employed here to characterise exposure of Lorca are the same described in previous Chapters (see Section 2.1.1). In particular, those are most extended all over the city: M11L-pre, M31L-pre, M34L-pre, RC31L-pre, RC31M-pre and RC31M-low. The sum up of all these typologies corresponds to a 78.0 % of the Lorca building stock.

- (i) **One to two-storey rubble stone and/or fieldstone masonry with wall system (wood flooring system) [M11L-pre]:**
MUR/LWAL/BET:2,1/IRRE/RWO1/FW99(5.9%)
- (ii) **One to two-brick masonry with wall system (wood flooring system) [M31L-pre]:**
MUR+CL99/LWAL/HBET:2,1/IRRE/RWO1/FW99 (14.9%),

RC+CIP/LWAL+DUC/HBET:11+, >11-storey RC with dual system ductil

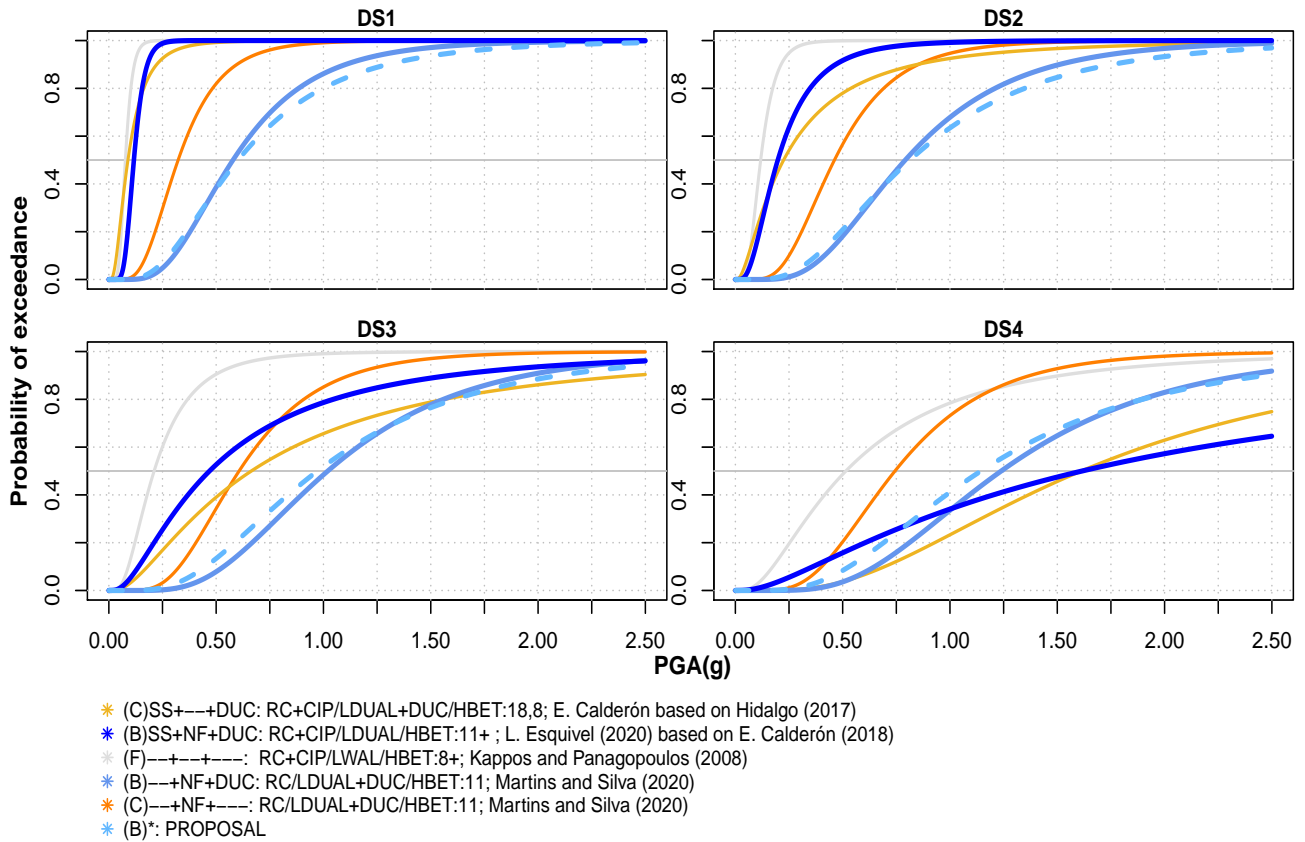


Figure 3.10: Example of fragility curves evaluated in the study: RC/LDUAL/HBET:11+/IRRE/FC, more than eleven-storey reinforced concrete with dual system.

See Figure 3.8 for label descriptions. (X)*PROPOSAL (dotted line curve): FC proposed by the authors, result of a consolidation of the FCs in the best class with the conflation method.

- (iii) **One to two-brick masonry with wall system (RC flooring system) [M34L-pre]:**
MUR+CL99/LWAL/HBET:2,1/IRRE/RC99/FC99 (12.5%),
- (iv) **One to three-storey reinforced concrete with frame system (pre-code) [RC34L-pre]:**
RC/LFINF /HBET:3,1/IRRE/FC/DNO (23.2%),
- (v) **Three to five-storey reinforced concrete with frame system (pre-code) [RC31M-pre]:**
RC/LFINF /HBET:5,3/IRRE/FC/DNO (15.6%),
- (vi) **Three to five-storey reinforced concrete with frame system (low-code) [RC31M-low]:**
RC/LFINF /HBET:5,3/IRRE/FC (5.8%).

The FCs evaluated for said typologies are the following. Table 3.8 shows the results.

-Those corresponding to said typologies employed in the RISMUR II project. In it, the FCs were taken from different authors: Lagomarsino and Giovinazzi (2006) [33] in the case of masonry buildings, and from HAZUS-MH [25] in the case of reinforced concrete buildings.

-Those FCs developed in this PhD dissertation for the specific masonry buildings of Lorca (see Chapter 4).

The results of the application of the proposed methodology for the FCs employed in the RISMURII project, finished in 2014, have revealed that today they can be considered class D or E, and therefore, there is a wide margin of improvement according to the actual state of the art. As a consequence, on the one hand, FCs for Lorca masonry buildings have been elaborated and contributed, see Chapter 4. Said contributed FCs herein result to be class B

RC+CIP/LWAL+DUC/HBET:5,1, 1 to 5 storey RC with wall system ductil

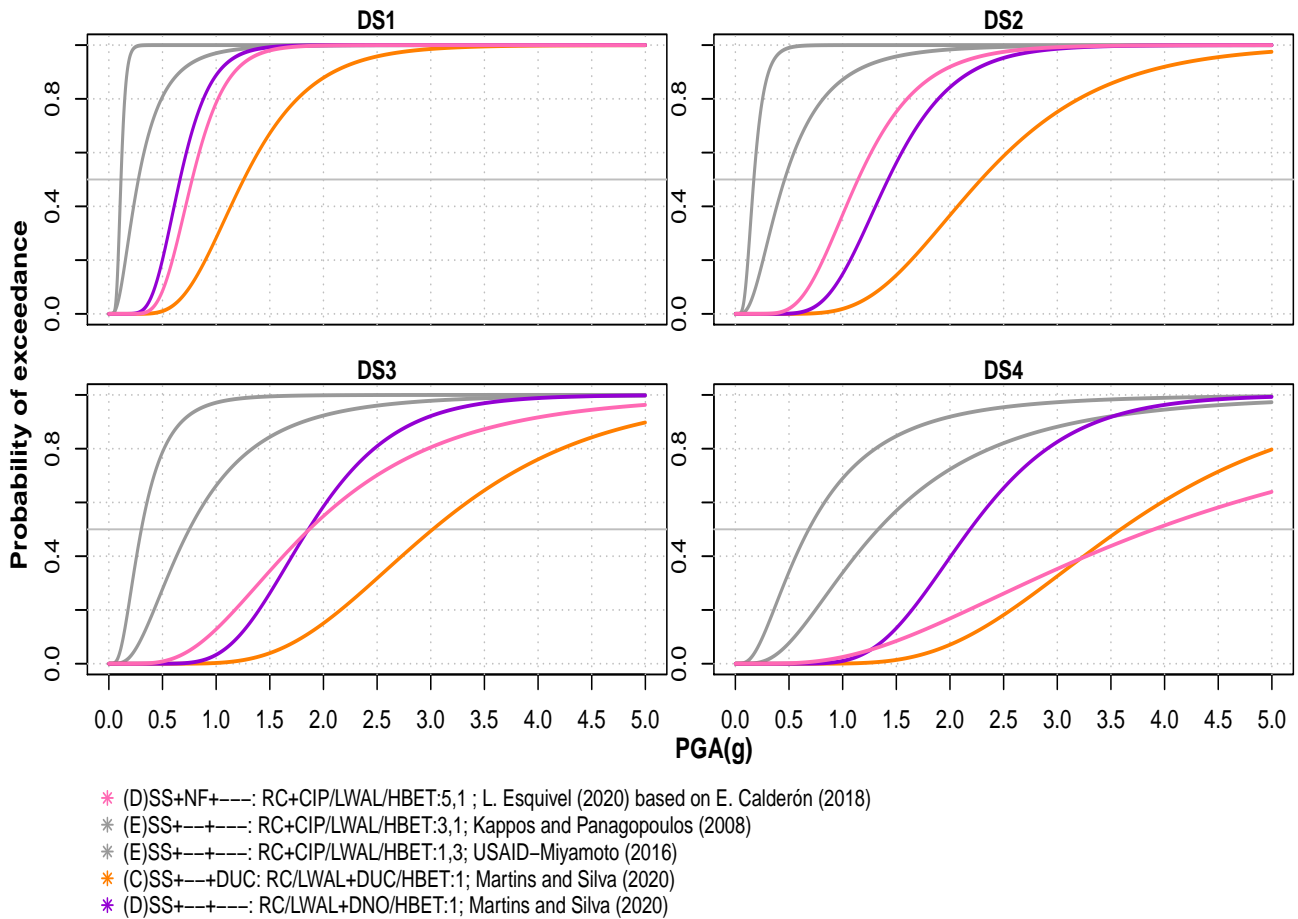


Figure 3.11: Example of fragility curves evaluated in the study: RC/LWAL/HBET:5,1/IRRE/FC, One to five-storey reinforced concrete with wall system.

See Figure 3.8 for label descriptions.

according to the methodology, which means they are deemed as significantly more adequate. This result seems sensible as the FCs elaborated for this research considered the specific characteristics of Lorca buildings and for their elaboration, a more recent methodology has been employed. On the other hand, in the case of RC buildings, further search for FCs among those available in the literature is recommended, since the structural and design characteristics of RC buildings are commonly more similar between regions than those of masonry buildings. This is due to in the past it was customary to use materials available close to the specific region for the construction of masonry buildings and the lack of applying any rules far from those considered as good practices in the area.

3.5 Conclusions and future lines of research

In this chapter, a methodology for assessing seismic fragility curves is presented. This method permits the well-founded selection of the most appropriate fragility curves for a particular type of building in a specific seismic-prone area for seismic risk studies from a set of curves available in the literature. A series of specific criteria are proposed to facilitate the creation of a rational ranking of FCs in terms of adequacy. The assessment process is based on several variables divided into three key dimensions: technical suitability, suitability for the local system, and building class similarity. The novelty of the proposal, therefore, lies in organizing all the variables involved according to the literature in a practical way and giving them scores so that the application of the methodology provides the researcher with a classification of the assessed FCs according to their adequacy to the area under study. The results have proven to be robust in the application case of reinforced confined masonry in Costa Rica because small changes in the score of the variables involved in the multidimensional index do not significantly affect the classes

Author of candidate FC	Description of candidate typology according to GEM taxonomy	CC BV	FC BV	SQ BV	TS	LS	Global index	BCS Coef.	Final index	Class
MUR/LWAL/BET:2,1/IRRE/RWO1/FW99 (One to two-storey rubble stone and/or fieldstone masonry with wall system (wood fl. s.))										
Lagomarsino and Giovanazzi (2006)	MUR/LWAL/BET:2,1/RWO1/FW99	4	10	21	35	20	55	1.00	55	D
PhD diss. Navas-Sánchez (2023), Chapter 4	MUR/LWAL/BET:2,1/IR-RE/RWO1/FW99	10	25	14	49	25	74	1.00	74	B
MUR+CL99/LWAL/BET:2,1/IRRE/RWO1/FW99 (One to two-brick masonry with wall system (wood fl. s.))										
Lagomarsino and Giovanazzi (2006)	MUR+CL99/LWAL/-BET:2,1/RWO1/FW99	4	10	21	35	20	55	1.00	55	D
PhD diss. Navas-Sánchez (2023), Chapter 4	MUR+CL99/LWAL/BET:2,1/IR-RE/RWO1/FW99	10	25	14	49	25	74	1.00	74	B
MUR+CL99/LWAL/HBET:2,1/IRRE/RC99/FC99 (One to two-brick masonry with wall system (RC fl. s.))										
Lagomarsino and Giovanazzi (2006)	MUR+CL99/LWAL/H-BET:2,1/RC99/FC99	4	10	21	35	20	55	1.00	55	D
PhD diss. Navas-Sánchez (2023), Chapter 4	MUR+CL99/LWAL/HBET:2,1/IR-RE/RC99/FC99	10	25	14	49	25	74	1.00	74	B
RC/LFINF /HBET:3,1/IRRE/FC/DNO (One to three-storey reinforced concrete with frame system (pre-code))										
HAZUS-MH	RC/LFINF/HBET:3,1/DNO	11	13	21	45	5	50	0.85	42	E
RC/LFINF/HBET:5,3/IRRE/FC/DNO (Three to five-storey reinforced concrete with frame system (pre-code))										
HAZUS-MH	RC/LFINF/HBET:5,3/FC/DNO	11	13	21	45	5	50	0.85	50	E
RC/LFINF /HBET:5,3/IRRE/FC (Three to five-storey reinforced concrete with frame system (low-code))										
HAZUS-MH	RC/LFINF/HBET:5,3/FC	11	13	21	45	5	50	1.00	50	D

Table 3.8: Scores and final class for FCs assessed for some building typologies in Costa Rica following the methodology proposed. CC BV: Capacity Curve Block of Variables(BV), FC BV: Fragility Curve BV, SQ BV: Source Quality BV, TS: Technical Suitability dimension, LS:local System dimension, BCS: Building Class Similarity. References: [33], [25] and Chapter 4 of this PhD dissertation. fl. s. = flooring system

RC+CIP/LDUAL+DUC/HBET:5,1, 1 to 5 storey RC with dual system ductil

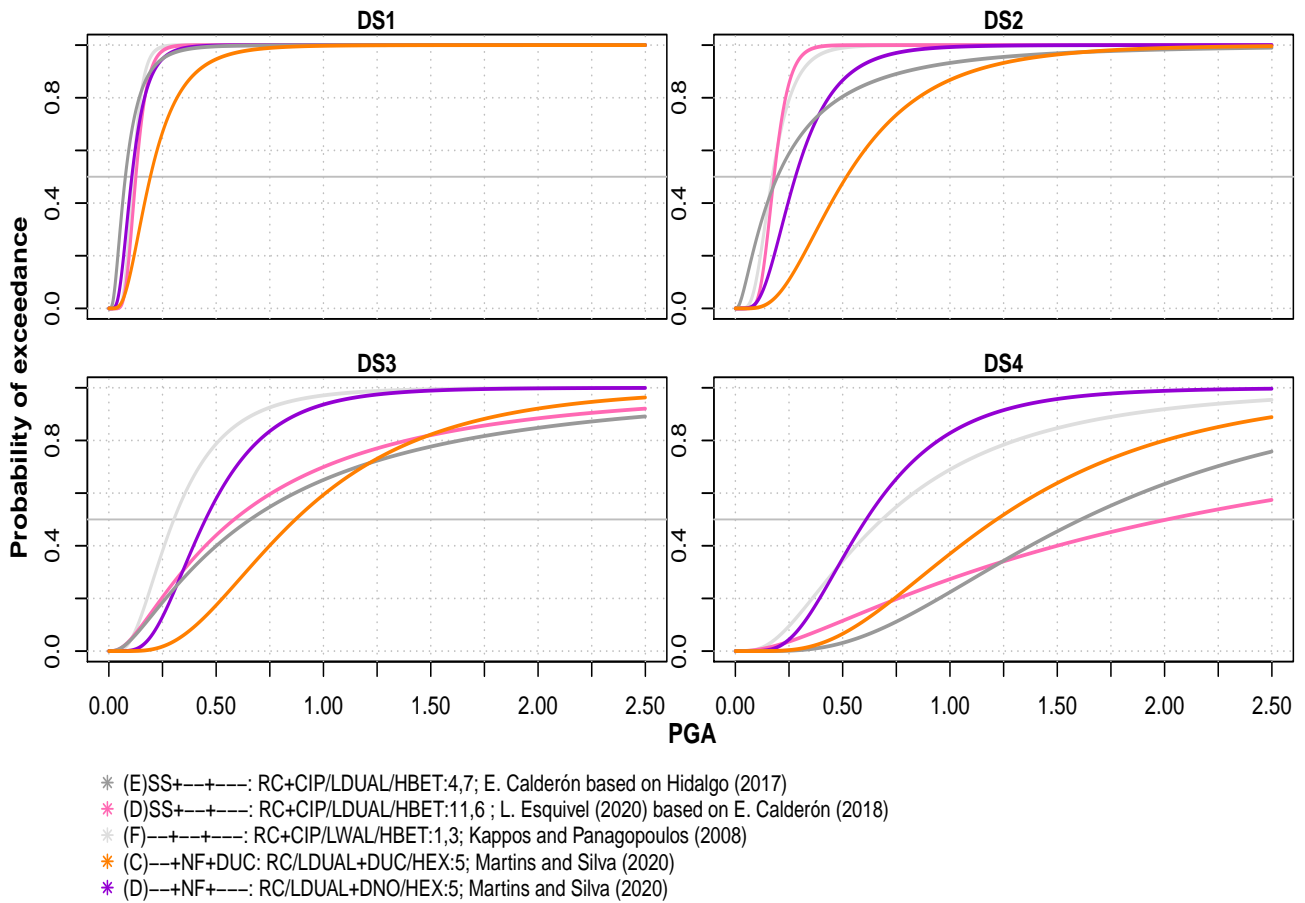


Figure 3.12: Example of fragility curves evaluated in the study: RC/LDUAL/HBET:5,1/IRRE/FC, one to five-storey reinforced concrete with dual system.

See Figure 3.8 for label descriptions. (X)*PROPOSAL (dotted line curve): FC proposed by the authors, result of a consolidation of the FCs in the best class with the conflation method.

in which the FCs evaluated were classified.

Moreover, the proposed methodology permits the reliability level of the FC obtained to be identified depending on the class the curve was classified into as a consequence of its score. Therefore, it allows the adequacy related to the selected FC to be established and to reduce the uncertainty or error involved in that selection, which is a subject that the researchers should consider in seismic vulnerability and risk studies.

In addition, the classification together with a systematised representation of the FCs allow the researcher to easily compare results and draw conclusions. For example, in the cases of one and two-story reinforced confined masonry with ductile wall systems of Costa Rica, the candidate FCs analyzed show different variations in terms of PGA depending on the dissimilar attribute they present with respect to the Costa Rican typology. Moreover, in the case of two-storey reinforced confined masonry with ductile wall system, however, the curves pertaining to higher classes seem to yield more conservative values than the other curves.

Furthermore, the proposed index can be broken down into its three dimensions and component variables, allowing the researcher to recognise those aspects in which each of the evaluated FCs has obtained better and worse scores. In addition, in this way, a researcher can weigh differently the dimensions or variables in the case of his or her study that requires them. Another possible use of a quantitative assessment of the different dimensions evaluated in the FCs examined is to use these scores to obtain a weighted average of the different FCs classified in the higher classes from a logical tree in which those scores act as weighting elements.

Additionally, when the FC introduced as inputs are insufficient or their scores too low, the method allows the identification of possible future lines of research in seismic vulnerability, as has been the case of Costa Rica one to five-storey reinforced concrete with dual system and with a RC wall system. In the same line, in the case of Spain, the results concerning the FCs employed in the RISMURII project, finished in 2014, have revealed that necessity of search for or elaboration of more adequate and updated FCs according to the current state of the art. This has given rise to Chapter 4, in which specific FCs for Lorca masonry buildings have been contributed.

Besides, a open database with an increasing number of FC evaluated is being created in order to facilitate the selection for future seismic risk studies.

Future lines of research to improve the methodology should perform a formal survey of a greater number of experts in the field aiming to widen the consensus in relation to the scores assigned to the different components of the proposed index. Moreover, the Fuzzy Analytic Hierarchy Process (AHP) can be implemented in said results in order to improve the variables involved and the scores given to the variables of the methodology. The Fuzzy AHP method involves weighting criteria of variables for evaluating FC using pairwise comparison based on expert opinions and evaluation scores. By capturing both subjective and objective assessment measures, AHP can reduce bias in decision-making. Furthermore, in many practical cases, the uncertainty and imprecision of different expert criteria can be challenging. To address this, the Fuzzy AHP method integrates fuzzy sets theory by using fuzzy numbers for pairwise comparison instead of real numbers to handle the impreciseness of human judgments.

Finally, it is worth noting that the methodology presents the advantage of being flexible enough to admit the implementation of new dimensions, sub-dimensions or variables, such as one in which it can be evaluated whether or not the FC has been calibrated with post-earthquake observations.

References

- [1] CFIA 2010. *Código sísmico de Costa Rica, 2010, 4 ed. Cartago, Costa Rica*. Colegio Federado de Ingenieros y de Arquitectos de Costa Rica. Editorial Tecnológica de Costa Rica, 2011, 2010.
- [2] CFIA 2014. *Código sísmico de Costa Rica. Revisión 2014. Cartago, Costa Rica*. Colegio Federado de Ingenieros y de Arquitectos de Costa Rica. Editorial Tecnológica de Costa Rica, 2018, 2014.
- [3] FEMA. Hazus-MH 2.1. “Advanced Engineering Building Module (AEBM). Technical and User’s Manual”. In: *Federal Emergency Management Agency (FEMA). Washington, DC* (2001).
- [4] Calderón A. *Análisis de riesgo para el sector residencial costarricense por zona sísmica. San José de Costa Rica*. Pavia: Università Degli Studi di Pavia, 2017.
- [5] Ahmed U Abdelhady, Seymour MJ Spence, and Jason McCormick. “Risk and fragility assessment of residential wooden buildings subject to hurricane winds”. In: *Structural Safety* 94 (2022), p. 102137.
- [6] *Additional Spreadsheet for assessing fragility curves according to Navas-Sánchez (2023)*. URL: drive.upm.es/s/CkRK7INpKX28zmA.
- [7] Kaynia Amir et al. “Guidelines for deriving seismic fragility functions of elements at risk: Buildings, lifelines, transportation networks and critical facilities”. In: (2013).
- [8] MB Benito et al. *Amenaza sísmica en América Central. Entinema, 28004 Madrid*. Tech. rep. ISBN 978-84-8319-474-4, 2010.
- [9] María Belén Benito et al. “A new evaluation of seismic hazard for the Central America region”. In: *Bulletin of the Seismological Society of America* 102.2 (2012), pp. 504–523.
- [10] Shrikant R Bhuskade and Samruddhi C Sagane. “Effects of various parameters of building on natural time period”. In: *Int J Eng Res Technol* 6.4 (2017), pp. 2278–0181.
- [11] Luigia Binda et al. “Vulnerability analysis of the historical buildings in seismic area by a multilevel approach”. In: *Asian Journal of Civil Engineering (Building and Housing)* (2006).
- [12] Svetlana Brzev et al. *GEM building taxonomy (Version 2.0)*. Tech. rep. GEM Foundation, 2013.
- [13] Alejandro Calderón et al. “Toward a uniform earthquake loss model across Central America”. In: *Earthquake Spectra* 38.1 (2022), pp. 178–199.

- [14] Omar Darío Cardona et al. “CAPRA—comprehensive approach to probabilistic risk assessment: international initiative for risk management effectiveness”. In: *Proceedings of the 15th world conference on earthquake engineering. Available online (last visit 10/05/2023)*. Vol. 1. 10. 2012. URL: http://www.iitk.ac.in/nicee/wcee/article/WCEE2012_0726.pdf.
- [15] S Cattari et al. “Un modello meccanico per l’analisi di vulnerabilità del costruito in muratura a scala urbana”. In: *Proceedings of XI Convegno Nazionale “L’ingegneria sismica in Italia”, Genova, Italy (2004)*.
- [16] A Climent et al. “Amenaza sísmica y vulnerabilidad física en la ciudad de Cañas, Guanacaste, Costa Rica”. In: *Capacity Building for Natural Disaster Reduction (CBNDR), Regional Action Program for Central America (RAPCA)*. ITC. 2003.
- [17] European Commission et al. *Seismic fragility curves for the European building stock : review and evaluation of existing fragility curves*. Publications Office, 2016. DOI: [doi/10.2788/586263](https://doi.org/10.2788/586263).
- [18] Ian Davis. “Shelter after disaster”. In: *Shelter after disaster*. 1978, pp. 127–127.
- [19] Calderón E. *Curvas de fragilidad según el método del espectro de capacidad para tipologías estructurales definidas en el Código Sísmico de Costa Rica*. Universidad de Costa Rica, 2018.
- [20] AF Espinosa. “The Guatemalan Earthquake of February 4, 1976”. In: *US Geol. Surv. Prof. Pap 1002 (1976)*, p. 90.
- [21] ELEM Fema-Nibs. “HAZUS Technical Manual”. In: *Federal Emergency Management Agency and National Institute of Building Sciences, Washington, DC, USA (2003)*.
- [22] J Garcia et al. “Assessing earthquake hazard in the Caribbean and Central America within the CCARA Project”. In: *Seismology of the Americas meeting: Latin American and Caribbean Seismological Commission. Seismological Society of America, Miami, FL, May*. 2018, pp. 14–17.
- [23] Diego Hidalgo Leiva. “Análisis estructural probabilista orientado a evaluación del daño sísmico con aplicaciones a tipologías constructivas empleadas en Costa Rica”. PhD thesis. Universitat Politècnica de Catalunya, 2017. URL: tdx.cat/handle/10803/405589.
- [24] Theodore P Hill and Jack Miller. “How to combine independent data sets for the same quantity”. In: *Chaos: An Interdisciplinary Journal of Nonlinear Science* 21.3 (2011), p. 033102.
- [25] WILLIAM Holmes. “HAZUS-MH: Multi-hazard loss estimation methodology: Technical manual”. In: *Washington, DC: Federal Emergency Management Agency (1999)*.
- [26] RISMUR II. *Servicio de Actualización del Análisis de Riesgo Sísmico (RISMUR) en la Región de Murcia. ETSI Topografía, Geodesia y Cartografía (Universidad Politécnica de Madrid, UPM) , Grupo de Ingeniería Sísmica (UPM)*. 2014.
- [27] Miyamoto International. *Citywide assessment of earthquake risks in San Salvador, El Salvador*. El Salvador, 2002.
- [28] Miyamoto International. *Fase I: Evaluación de los riesgos de terremotos. San José en función de pérdidas de vidas humanas*. Universidad de Costa Rica, 2016.
- [29] Miyamoto International and USAID. *Programa de Reducción de Riesgo Sísmico en la Ciudad de Guatemala*. Guatemala, 2021.
- [30] Panagopoulos GK Kappos A. *Development of Analytical Seismic Vulnerability Functions for the WHE-PAGER Project Phase 2*. Colorado, USA, 2008.
- [31] Oh-Sung Kwon and Eung Soo Kim. “Evaluation of building period formulas for seismic design”. In: *Earthquake engineering & structural dynamics* 39.14 (2010), pp. 1569–1583.
- [32] Esquivel-Salas LC. *Inventario de edificaciones del Cantón de San José para el caso específico de amenaza sísmica utilizando el método de mapeo ambiental rápido*. Universidad de Costa Rica, 2020.
- [33] Sergio Lagomarsino and Sonia Giovinazzi. “Macroseismic and mechanical models for the vulnerability and damage assessment of current buildings”. In: *Bulletin of Earthquake Engineering* 4.4 (2006), pp. 415–443.
- [34] Dh. Lang et al. *Reducción de riesgo sísmico en Guatemala, El Salvador y Nicaragua con Cooperación Regional a Honduras, Costa Rica y Panamá*. Kjeller. NORISAR, 2009.
- [35] R Maio et al. “Review of fragility curves for seismic risk assessment of buildings in Europe”. In: *Proceedings of the 16th World Conference on Earthquake Engineering, Santiago, Chile. Available online (last visit 10/05/2023)*. 2017, pp. 9–13. URL: <http://www.wcee.nicee.org/wcee/article/16WCEE/WCEE2017-3283.pdf>.

- [36] Rui Maio and Georgios Tsionis. “Seismic fragility curves for the European building stock: Review and Evaluation of Existing Fragility Curves. Ispra.” In: *Brussels: JRC Technical Report, European Commission* (2015).
- [37] Luís Martins and Vítor Silva. “Development of a fragility and vulnerability model for global seismic risk analyses”. In: *Bulletin of Earthquake Engineering* 19.15 (2021), pp. 6719–6745.
- [38] Claudio Mazzotti et al. “Una metodologia speditiva per la valutazione di vulnerabilità sismica di edifici in muratura e calcestruzzo armato [A simplified method for seismic vulnerability assessment of masonry and reinforced concrete buildings]”. In: *Progettazione Sismica* 4.2 (2013), pp. 95–112. DOI: [10.7414/PS.4.2.95-112](https://doi.org/10.7414/PS.4.2.95-112).
- [39] Sameh SF Mehanny. “A broad-range power-law form scalar-based seismic intensity measure”. In: *Engineering Structures* 31.7 (2009), pp. 1354–1368.
- [40] Quisco Mena. “Towards a structural efficiency classification system”. In: *Structures*. Vol. 26. Elsevier, 2020, pp. 298–310.
- [41] Abdelghani Meslem et al. “Uncertainty and quality rating in analytical vulnerability assessment”. In: *Proceedings of the 2nd European Conference on Earthquake Engineering and Seismology (2ECEES)*. The European Association for Earthquake Engineering, 2014, pp. 1–12. URL: <https://discovery.ucl.ac.uk/id/eprint/1471790/>.
- [42] Zoran V Milutinovic and Goran S Trendafiloski. “RISK-UE: An advanced approach to earthquake risk scenarios with applications to different European towns”. In: *European Project Risk-UE* (2003).
- [43] Stylianos Minas, Carmine Galasso, and Tiziana Rossetto. “Preliminary investigation on selecting optimal intensity measures for simplified fragility analysis of mid-rise RC buildings”. In: *2nd European Conference on Earthquake Engineering and Seismology (2ECEES), Istanbul, Turkey*. European Association for Earthquake Engineering (EAEE), 2014, pp. 24–29.
- [44] Lorena Montoya. “Urban disaster management: A case study of earthquake risk assessment in Cartago, Costa Rica”. In: *ITC Publication Series No. 96, 2 December. Enschede: International Institute for Geo-Information Science and Earth Observation (ITC)* (2002).
- [45] P Mouroux et al. “The European RISK-UE project: an advanced approach to earthquake risk scenarios”. In: *Proc. of the 13th World Conference on Earthquake Engineering*, 2004.
- [46] Cardona OD. *Informe técnico ERN-CAPRA-T1-3. Propuesta de indicadores y funciones de vulnerabilidad en Honduras. México, DF*. ERN, 2009.
- [47] K Porter. *GEM vulnerability Rating System, GEM global vulnerability estimation methods consortium*. 2011.
- [48] Adolfo Quesada-Román and Daniela Campos-Durán. “Natural disaster risk inequalities in Central America”. In: *Papers in Applied Geography* just-accepted (2022), pp. 1–15.
- [49] Barquero P. R. “El terremoto de Cinchona del Jueves 8 de Enero deL 2009”. In: *Revista Geológica de América Central* 40.40 (2009), pp. 91–95. DOI: [10.15517/rgac.v0i40.4188](https://doi.org/10.15517/rgac.v0i40.4188).
- [50] Pathmanathan Rajeev and S Tesfamariam. “Seismic fragilities for reinforced concrete buildings with consideration of irregularities”. In: *Structural Safety* 39 (2012), pp. 1–13.
- [51] William I Rose, Julian J Bommer, and Ciro A Sandoval. “Natural hazards and risk mitigation in El Salvador: An introduction”. In: *SPECIAL PAPERS-GEOLOGICAL SOCIETY OF AMERICA* (2004), pp. 1–4.
- [52] Tiziana Rossetto et al. “Evaluation of existing fragility curves”. In: *SYNER-G: Typology definition and fragility functions for physical elements at seismic risk*. Springer, 2014, pp. 47–93.
- [53] L.A. Salas Alvarado. *Evaluación del riesgo sísmico en edificaciones residenciales del Área metropolitana de San José en función de pérdidas de vidas humanas*. Universidad de Costa Rica, 2003.
- [54] Franz Sauter. *Estudio de seguro contra terremoto*. Instituto Nacional de Seguros, 1978.
- [55] MIJ Schotanus et al. “Seismic fragility analysis of 3D structures”. In: *Structural Safety* 26.4 (2004), pp. 421–441.
- [56] Lin Shibin et al. “Performance-based methodology for assessing seismic vulnerability and capacity of buildings”. In: *Earthquake engineering and engineering vibration* 9.2 (2010), pp. 157–165.
- [57] Vitor Silva et al. “A building classification system for multi-hazard risk assessment”. In: *International Journal of Disaster Risk Science* 13.2 (2022), pp. 161–177.

- [58] Luis Carlos Solórzano Arias. “Vulnerabilidad sísmica de estructuras de viviendas de uno y dos pisos en una zona piloto del Valle Central”. In: *san José: Universidad de Costa Rica* (2005).
- [59] H Stone et al. “A review of seismic vulnerability assessments in Central America”. In: *Society of Earthquake and Civil Engineering Dynamics*. Society for Earthquake and Civil Engineering Dynamics (SECED). 2015, pp. 1–10.
- [60] H Stone et al. “On the use of existing seismic fragility and vulnerability functions”. In: *16th World Conference on Earthquake (WCEE)*, pp. 9–13. URL: <https://www.wcee.nicee.org/wcee/article/16WCEE/WCEE2017-2092.pdf>.
- [61] Marco Valente et al. “Historical masonry building aggregates: advanced numerical insight for an effective seismic assessment on two row housing compounds”. In: *Engineering Structures* 190 (2019), pp. 360–379.
- [62] Mabé Villar-Vega et al. “Development of a fragility model for the residential building stock in South America”. In: *Earthquake Spectra* 33.2 (2017), pp. 581–604.
- [63] Catalina Yepes-Estrada et al. “Modeling the residential building inventory in South America for seismic risk assessment”. In: *Earthquake Spectra* 33.1 (2017), pp. 299–322.
- [64] Yantai Zhang et al. “Selection of Ground Motion Intensity Measures in Fragility Analysis of a Mega-Scale Steel Frame Structure at Separate Limit States: A Case Study”. In: *Buildings* 12.10 (2022), p. 1530.

Chapter 4

Vulnerability of Lorca masonry buildings: fragility curves

The elaboration of appropriate fragility curves that characterise the vulnerability of the specific buildings located in an area is crucial for developing advanced seismic risk studies. In Section 3.4, it has been shown that the fragility curves employed in the RISMURII project (2014) [10] carried out in Murcia can be improved by elaborating fragility curves with more recent methods and using as samples buildings with the specific features of those present in Lorca. The method herein employed contributes fragility curves stemmed as class B for the Lorca masonry buildings, as the mentioned Section shows.

Within this context, this Chapter involves the calculation of the fragility curves for the residential masonry typologies of Lorca, by means of the application of a simplified method, named RE.SIS.TO. in the following, to estimate their seismic vulnerability and the Monte Carlo method to account for its variability. These typologies are those detailed in section 2: M11, M31 and M34. Moreover, those particularly studied, with a number of storeys between one and three floors are shown in Figure 4.1 and 4.2, differentiated by height and topology. As the figures and percentages shown in the map legend illustrate, these are extremely extended typologies within Lorca.

The information about residential unreinforced masonry buildings studied in order to characterise their fragility curves have been taken from the database of reports described in section 2.2.1 by experts in the aftermath of the 2011 Lorca earthquake.

4.1 Methodology

The seismic assessment of buildings can be performed via design and performance methods, which at the same time can be simple and fast or complex and profound. The selection of the appropriate method among those available depends on the objective of the researcher or engineer. In the following, the main purposes of design and performance evaluations are briefly exposed.

- The design evaluations are aimed at understanding if a building stays upright considering its weight and imposed load according to the seismic regulation in force.
- The performance evaluations are aimed at understanding the behaviour of a building in the event of an earthquake and, in particular, at determining the seismic resistance of a building. Several procedures of dynamic verification can be found within the literature, for example, simplified evaluations, expeditious evaluations such as RE.SIS.TO.[17], those included within the NTC18 regulation [20] and the conventional methods.

All these evaluations have a normative reference or a scientific research behind and they differ from each other in the depth of the study, the time required to carry it out and the economic value it entails.

Within all these possibilities, an expeditious method, RE.SIS.TO is selected according to the information available and the objective of our study, to provide fragility curves suitable for a seismic risk study of Lorca. Moreover, the simplified method of dynamic evaluation RE.SIS.TO has been developed and it is widely used in some Italian academic institutions like the UNIBO; which means that for Spain, a country that present notable similarities

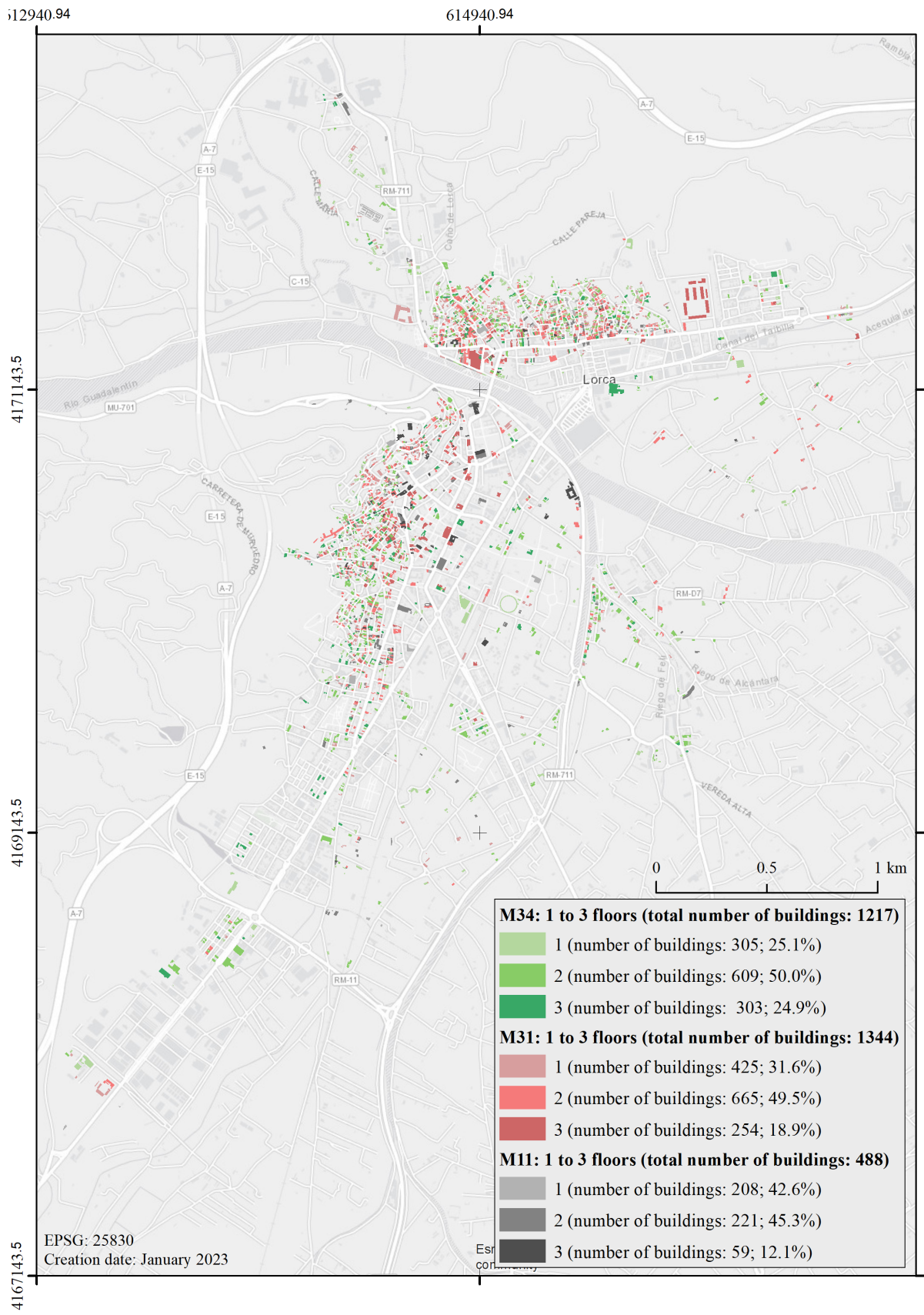


Figure 4.1: Studied masonry typologies. Map including all the typologies of masonry buildings considered in this study: 1 to 3-storey M11, M31 and M34 buildings. Heights distinguished by colours.

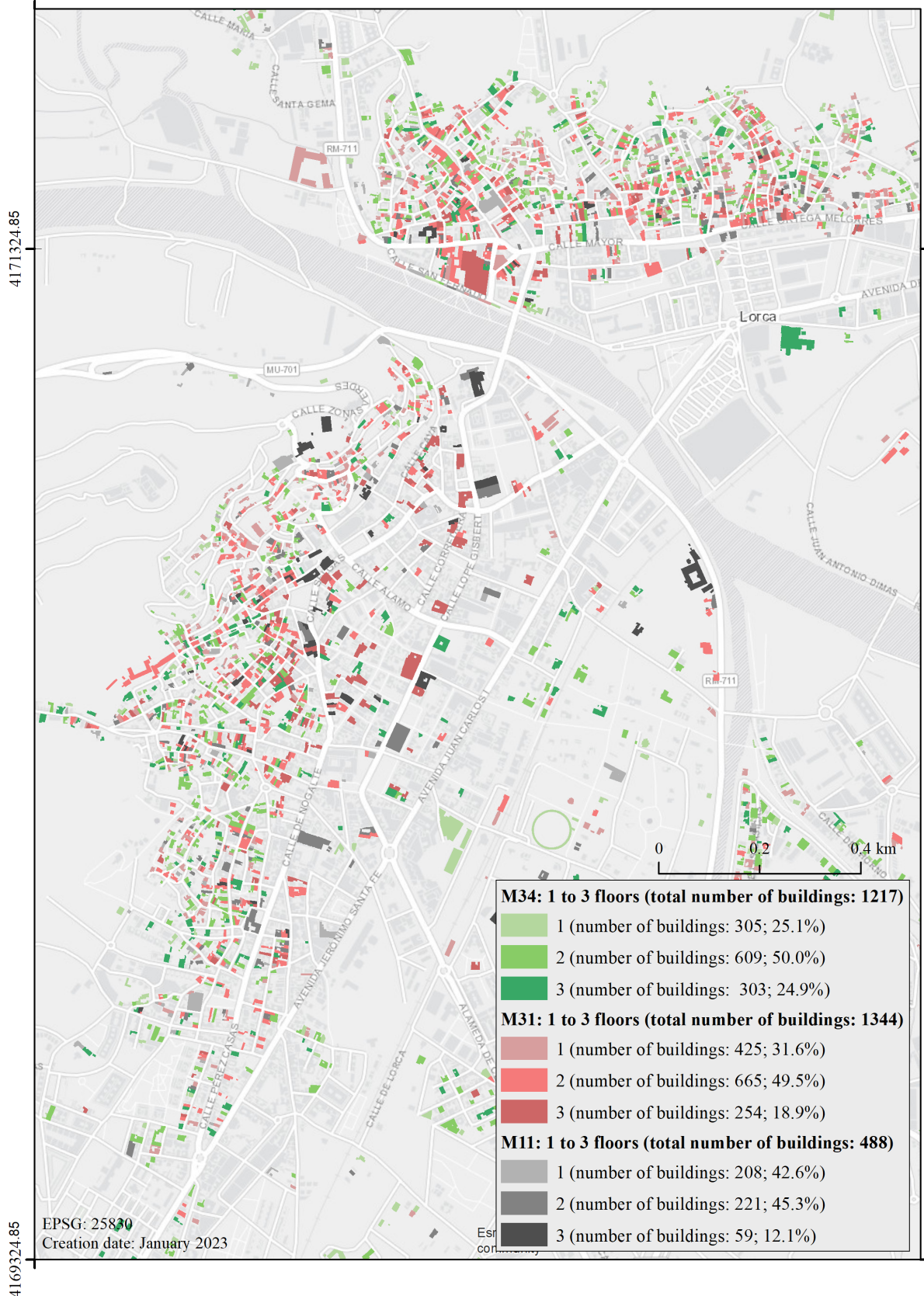


Figure 4.2: Studied masonry typologies. Zoom of the map including all the typologies of masonry buildings considered in this study: 1 to 3-storey M11, M31 and M34 buildings. Heights distinguished by colours.

in the construction techniques with Italy, is appropriate, and its applicability clearly covers the characteristics of the buildings that are under study.

4.2 A simplified method: RE.SIS.TO[®]

The RE.SIS.TO method for the vulnerability assessment of existing buildings was born referring to the seismic hazard of the Italian territory, in order to improve the immediacy of perception of the seismic vulnerability results. This methodology is fully described in [17]. Some of the most important aspects of it are detailed here, as convenience to the reader since the paper is in Italian. The methodology can be also found as an App in the official webpage,[22]

The RE.SIS.TO acronym derived from the Total Seismic Resistance (*REsistenza SISmica TOTale* in Italian). The method aims to frame within macro categories the vulnerability that presents a large scale of reinforced concrete or masonry buildings in presence of the seismic actions foreseen in the site. Therefore, its main purpose is to provide a fast tool able to comparatively assess the critical status of buildings, thus allowing the identification of an order of interventions priority to reduce vulnerability in the area. This definition of classes of vulnerability (the priority ranking) determines the degree of necessity of improvement interventions and seismic retrofitting required by each set of buildings based on their characteristics. Next, based on the results of these expeditious methods, some seismic risk studies may provide further investigation on particular buildings. However, there is no possibility of conducting these deepened evaluations on the large scale at the early stages because they require considerable financial and time resources and a great amount of data.

The procedure leads to the definition of the Spectral Acceleration of collapse $S_{a,c}$ and, as a consequence, of the Peak Ground Acceleration of collapse, PGA_c . Both, the $S_{a,c}$ and the PGA_c are the intensity measurements used in the seismic hazard maps, which implies that with the conjunction of capacity ($S_{a,c}$ or PGA_c) and demand (hazard map) the safety index can be calculated.

The $S_{a,c}$ is obtained through a procedure that involves, firstly, the evaluation of the building shear resistance, floor by floor by making use of simplified mechanical considerations. (Similar approaches have been proposed before as in [15], or [12], applied in [13]). Later, the calibration of this value by means of the use of expert judgment in order to take into account the actual complexity of the construction under consideration is recommended.

That is to say, at a certain point, it is necessary to step from the theoretical calculation scheme to the actual conditions of the building; which may indicate possible structural problems identified during inspections that influence the global vulnerability. Although, in any case, the constructive details do not have to be analyzed thoroughly since the method is expeditious. The step in terms of capacity from solely considering the shear resistance results to the actual situation is done by making use of a reductive coefficient, obtained from the parameters contained in the vulnerability sheets of the “Gruppo Nazionale per la Difesa dai Terremoti” (GNDT 1994) [28].

Therefore, the information requested by the method mainly relates to the geometry of the buildings under study, an estimate of the types of materials used in structures and a simplified load analysis.

The values already reduced by the coefficient that accounts for the expert judgment are then compared with vulnerability ranges proposed in the RE.SIS.TO simplified classification. This gives rise to the buildings to be classified within five homogeneous categories according to their seismic vulnerability level, and thus for intervention criticality. The membership in a category is graphically given by a chromatic scale that uses colors from red to green. Thus, finally, the method assigns a class that could vary from A (low vulnerability) to E (high vulnerability), depending on the ratio between the capacity and the demand in terms of ground acceleration. Eventually, in the presence of notable critical elements, the technician expertise must intervene and reassign a pejorative class with respect to the ones resulting from the PGA ratio.

In summary, the method consist of three subsequent phases, which in turn are divided in steps:

- 1) Phase 1: Research of technical information, in order to obtain a reliable picture of the actual condition of the building.
 - Phase 1a: Knowledge level of the building from documents
 - Phase 1b: In-situ investigation

- 2) Phase 2: Evaluation of the seismic vulnerability of the system, meant as the seismic acceleration that leads to the collapse of the building or, in other terms, the peak ground acceleration corresponding to the Life Safety Limit State (SLV) for the building.
 - Phase 2a: Assessment of the seismic demand
 - Phase 2b: Computation of shear resistance of walls in the two directions
 - Identification of resisting areas and total weight
 - Computation of shear force for each floor
 - Computation of external action (shear)
 - Identification of building's critical floor
 - Phase 2c: Masonry quality coefficient C_{rid} - Complete the GNDT II Level Form
 - Estimate of the actual shear resistance of the building
 - Computation of the pseudo-acceleration corresponding to structural collapse
 - Calculation of the peak-ground acceleration of collapse
- 3) Phase 3: RE.SIS.TO comparison between peak ground acceleration of the building and in-situ demand in terms of acceleration, to assess the safety level of the building. Classification according to the safety levels (see Figure 4.3).

4.2.1 Phase 1) Geometric Survey

The first phase of the analysis, consists in the research of technical information, in order to obtain a picture of the likely actual state of the building. In order to carry out this step, it is important to define the knowledge level of the building. The knowledge of the historical constructions is a prerequisite for a reliable evaluation of seismic safety and for the identification of possible critical weaknesses. In existing structures it is a fundamental aspect to identify the original building features and the changes or damages that occurred over time due to anthropic changes, aging of materials or caused by natural events. Therefore, the initial step concerns an extensive analysis of historical documentation of the original project, if available, (for old simple constructions the projects often do not exist), and the other possible further projects that have followed over time, in order to establish the various construction phases and transformations.

The definition of the knowledge level is also based on: the geometrical survey of the building and of each structural element, such as slabs, roofs, stairs, vaults, etc.; on the survey of the distribution of damages and cracks; and finally the material typologies in order to obtain the strength of the masonry panels from the strength values of their constituent materials, which are bricks and mortar. For the identification of the material, can be recommendable to remove the plaster of one or two parts of the masonry wall apparatus in order to verify the typology, while the mechanical properties are assigned on the basis of the tables in the “Circolare delle NTC del 2 Febbraio 2009, n.617.” [19]

In-situ investigations are also valuable to obtain more information that will allow the formation of a complete picture of the building's actual state. These steps can be executed in just one day due to the fastness of this method, and have to be performed with people aware of the building status. This operation is composed of different possible actions such as the realization of a photographic survey, the definition of the position and the dimensions of the resisting elements, the identification of the openings, the distinction of the structural/nonstructural elements, the inspection of the floor and roof type and finally the analysis of the deterioration status of the building. It is also important to inspect the connection quality of floors and masonry walls trying to understand how transversal walls are connected to the external ones, and how bricks are placed in the corners. Another aspect to be defined is the masonry quality including the quality of mortar joints and their thickness.

All those aspects are not directly taken into account in calculations, but they will be considered by the technician's judgment by applying some reduction coefficients. The knowledge level of existing structures is related to confidence factors, which are used to reduce the mean values of material properties for the definition of structural capacity. When the value of the confident factor is low, that means a high knowledge level and high design strength and vice versa.

Furthermore, the seismic vulnerabilities will be taken into account, developing the RE.SIS.TO spreadsheet and in particular, in the section regarding the GNDT II level form [26], in which all the main parameters that could influence the vulnerability of the structure, are defined and weighted.

In the case of the Lorca buildings, the phase of the Geometric Survey is carried out by means of a intense analysis of the reports that the experts provided of the state of the buildings in the aftermath of the events. As mentioned before, these reports provide the description of the building, the structural elements and materials and the state of damage. Furthermore, they include the partial or global collapses caused by the Lorca 2011 earthquake, providing information about the local vulnerabilities that the buildings presented.

4.2.2 Phase 2) Shear resistance

The procedure to calculate the shear resistance depends on the structural material of the buildings under study, since masonry and reinforced concrete structures exhibit different collapse mechanisms. For that reason, RE.SIS.TO provides two different definitions of the resistant model. Herein, the method is applied only masonry buildings, for that reason just this resistant model is described.

In both cases, the computation of the shear resistance is performed by a specific procedure and later, a reduction coefficient (C_{rid} , *Coefficiente riduttivo* in Italian) is applied in order to consider other factors such as the geometrical configuration, irregularities or non-structural elements.

The resisting shear is evaluated for each floor, $V_{r,i}$, and compared with the stressing shears of each floor, $V_{s,i}$, obtained applying a load distribution to the structure of equivalent static forces obtained considering a unitary spectral acceleration [5]. The ratios between said $V_{r,i}$ and the corresponding $V_{s,i}$ define the structural performance of the individual floors of the building in terms of accelerations on structural masses [4]. The different relationships like this obtained allow to identify the weakest story (the one with the minimum value of this ratio) and to define the resistance of the building in spectral acceleration terms, S_a .

However, this acceleration value is strongly conventional, since it does not consider the real complexity of the construction under consideration. The adjustment of the conventional capacity to a realistic value is done by using of ten of the eleven contained parameters in the II level seismic vulnerability sheet (GNDT, 1994); only the Conventional Resistance parameter is excluded (no. 3), as it calculates the resistant capacity of the building, which has been previously assessed as aforementioned. The parameters are used to obtain a reduction factor of the strength of the building, determined with the mechanical criterion described above.

Table 4.1 shows the ten parameters, e.g., each of which are associated with four classes of vulnerability, four scores, and the weight of parameter over the others. It is recalled that, despite having excluded the third parameter, numbering in Table 4.1 remains the same as that of the vulnerability spreadsheet GNDT (1994). The weights of the parameters 5, 7, 9, are variable quantities, and as such, they must be recalculated for each building.

N.	Parameter	Score A	Score B	Score C	Score D	Weight
1	Type and organization of the resistant system	0	5	20	45	1.5
2	Quality of the resistant system	0	5	25	45	0.25
4	Location of the building and foundations	0	5	25	45	0.75
5	Horizontal structural elements	0	5	15	45	VAR
6	Plan configuration	0	5	25	45	0.5
7	Elevation configuration	0	5	25	45	VAR
8	Maximum distance between walls	0	5	25	45	0.25
9	Roof system	0	15	25	45	VAR
10	Non-structural elements	0	0	25	45	0.25
11	State of conservation	0	5	25	45	1.00

Table 4.1: Parameters, vulnerability classes, scores and weights of the GNDT seismic vulnerability sheets II level for masonry buildings

Once the vulnerability classes of the building have been defined in accordance with the compilation manual of the seismic vulnerability sheet II level GNDT of the Tuscany Region, each one of the i -th parameter in the table will match a score, p_i , and a weight, w_i . Therefore, for each parameter the following product is obtained:

$$K_i = p_i * w_i \quad (4.1)$$

The reduction factor C_{rid} is determined through the report:

$$C_{rid} = \prod_{i=1}^{10} \left(1 - \alpha \cdot \frac{K_i}{K_{pegg}} \right) \quad (4.2)$$

where K_{pegg} is the summation of K_i in the worst class (all parameters in class D) and α is a coefficient that allowed the calibration of the method. When this parameter varies, it allows the establishment of the lower bound (all parameters in class D) of the range of variation of the reduction coefficient, C_{rid} . The upper limit (all parameters in class A), on the other hand, it is fixed and is equal to the unit. For further information about the lower limit of the reduction factor, C_{rid} , see the paper [17].

The collapse pseudo-acceleration, reduced using the C_{rid} coefficient, therefore, turns out to be:

$$S_{a,c} = C_{rid} \cdot S_a \quad (4.3)$$

Finally, to define the intensity of the earthquake to which the structure can stand without collapsing in terms of Peak Ground Acceleration, it is necessary to transform the spectral value of the acceleration, $S_{a,c}$, in value of the maximum acceleration of the ground, PGA_c . Taking into account that the spectral acceleration value computed is a linear static type of value, the relationship between $S_{a,c}$ and PGA_c can be established based on the modal participation factor, the coefficient of spectral amplification, a coefficient that accounts for the capacity of dissipation of the structure and a factor that takes into account the ductility of the structure [5].

4.2.3 Phase 3) Comparison between acceleration and demand

The main objective of the methodology is an expeditious comparison between acceleration and demand. For that reason, in order to improve the ease of interpretation of the results, a simplified classification called RE.SIS.TO® (acronym of Total Seismic Resistance) is defined by the Authors of the methodology. This classification provides a immediate perception of the results of the analysis. Moreover, the assessed buildings are framed within of five homogeneous categories per level of seismic vulnerability, and therefore for intervention criticality. Membership in a category is returned graphically using a chromatic scale (using colors from red to green) and also the intervals of the ratio between capacity and demand for each class (Figure 4.3). According to this, a class from I (the best) to V (the worst) is initially assigned to each building.

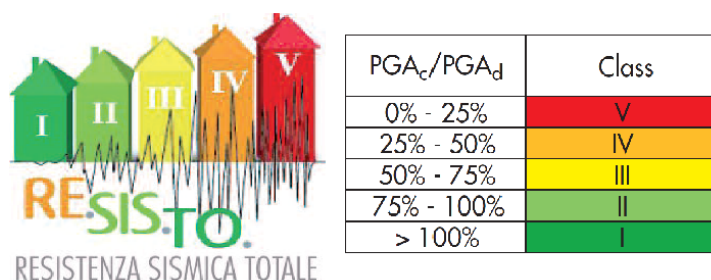


Figure 4.3: Colour scale of the classes and RE.SIS.TO® logo and ranges of the capacity-demand ratio

Any local vulnerabilities that have emerged from the inspections, which can represent weaknesses in the behavior of the structure under earthquake but have not been adequately valued in the previous analysis phase, come into play at this stage. Specifically, in the presence of considerable critical elements in a building, this building could be recognized as a higher class, from I to V, (therefore pejorative) to that resulting from ratio of PGA only. According to [17], this allows to evaluate, though in a simplified way, some local phenomena, among others aspects. For example, the local phenomena of out-of-plane of masonry walls collapse, great scarcity of stirrups in the pillars (if known), irregularities particularly serious geometric or structural, etc.

Based on the procedure described, building heritage at a large territorial scale may be classified quickly and it will be possible to reason in terms of intervention criticality. If particular building results in V-Class, for example, it will take priority over all others and be therefore among the first ones on which the checks required by current regulations and on which any interventions will be planned local repair and/or seismic improvement.

Later, depending on experts criteria, it could be useful to carry out the appropriate checks/interventions for all the remaining strategic buildings, following the order of the RE.SIS.TO® Classes (therefore following the order of Classes IV, III, II, I).

4.3 Buildings' features and seismic vulnerabilities

The geometric survey was conducted on an architectural basis provided by the Lorca experts that was carried out directly in the aftermath of the earthquake. The collected data was elaborated for a total of 50 masonry buildings, from which includes 20 all the data necessary to performed the seismic assessment according to the RE.SIS.TO method.

Specifically, these reports includes plans, sections, technical details, materials and a detailed description of the damages presented as a consequence of the seismic event. Moreover, this data provides the improvements necessary in order to make the building safe according to the experts' judgment or in some cases the declaration of technical ruin of the building because the budget of reparation overcomes the 50% of the value of a new building with similar characteristics (Art. 224 [18]).

4.3.1 Buildings' features

The main vulnerabilities from a seismic point of view have been identified from the analysis of the photographic survey and writings included in the reports. These are:

- Poor connections between vertical and horizontal structural elements
- Nonexistence or inefficiency of wood tie-beams
- Thrusting roofs that push on moderate/poor quality masonry
- Slenderness of pillars and walls
- Excessive deformability of the slabs
- Irregularities in masonry texture
- Absence of load sharing elements such as ring beams
- Long and heavy structural roof elements
- Disconnections between roof structural elements

A great number of the damages exhibited by the masonry buildings after the 2011 Lorca earthquake were due to the lack of good construction techniques and to the poor material quality of some of the bearing walls or foundations characteristics. These were considered by the experts in the seismic improvement interventions carried out for repairing the buildings. In particular:

- Extended lack of monolithism due to poor connections between horizontal and vertical elements such as ring beams.
- Roofs without seismic design. As a consequence, there were a significant number of buildings whose roof resulted in collapse and consequently had to be completely substituted.
- A reduced number of buildings presented inadequate foundations that had to be improved in the reparation project.
- Generalized disconnections between perpendicular walls in buildings constructed using the M1, type of material.

4.4 Characterization of the seismic vulnerability by means of the RE.SIS.TO® method

This paragraph details the rapid assessment of the seismic vulnerability level that has been performed on the aforementioned buildings of Municipality of Lorca before the 2011 Lorca earthquake. The assessments described

below are mainly of a global nature, i.e., relative to the masonry building like a whole; but also involve some aspects of a local nature, i.e., relative to the local collapse mechanisms of some macro elements considered particularly vulnerable, such as roofs. The analysis is aimed at the process of acquiring structural knowledge and the seismic vulnerability of the building. Knowledge of the state of the building assumes fundamental importance in the evaluation of the building's safety checks and in the design of any subsequent seismic adaptation and improvement interventions.

For the local assessments, some simple considerations were made based on the accelerations at the base and on the conformation of the structural elements. The following tools were used for the global assessments:

- the fulfillment of the level II CNR-GNDT form [28];
- the use of the expeditious methodology for the Assessment of Seismic Vulnerability, developed by the Interdepartmental Center for Industrial Building and Construction Research - University of Bologna (UNIBO);
- the use of the RE.SIS.TO® classification.

In Appendix B, an example of the application of the methodology RE.SIS.TO to a building of Lorca (identification (ID): m3) is included.

4.4.1 Capacity estimate

The expeditious methodology RESISTO was used to estimate the building's resistant capacity to horizontal actions. The methodology leads to the definition of a building collapse spectral acceleration ($S_{a,c}$) and collapse ground acceleration (PGA_c) through the evaluation of its resistant shear, floor by floor.

In this subsection, firstly, these values are evaluated using simplified mechanical considerations and, later, are appropriately adjusted to take into account the actual complexity of the construction in question, considering that, as mentioned before, the transition from the theoretical calculation scheme to the real conditions of the building takes place using a C_{rid} coefficient obtained starting from the parameters contained in the seismic vulnerability sheets of II level of the GNDT form [28]. This procedure can also highlight possible structural criticalities identified during inspections but not analyzed in detail. Thus, the method allows the performance of an evaluation of the aspects characterized by greater empiricism according to methodologies recognized at the Italian national level and already applied on several occasions.

Assessment of the floor shear resistance and pseudo-acceleration

In this section, the procedure for assessing the shear resistance is thoroughly described.

The capacity to resist shear forces of the generic i -th floor (each floor is identified by the unitary "i" index) must be assessed by adopting the following procedure. Firstly, two directions of reference for the building, x and y , have to be chosen. Next, the areas of the horizontal sections of the various resistant elements (masonry walls) must be quantified as follows:

$$A_{x,i} = \sum_{n=1}^{NM_{x,i}} A_{x,n,i} \quad A_{y,i} = \sum_{n=1}^{NM_{y,i}} A_{y,n,i} \quad (4.4)$$

where: $A_{x,n,i}$ and $A_{y,n,i}$ are the areas of the n -th resistant masonry wall belonging to the i -th floor in the x and y directions, respectively; $NM_{x,i}$ and $NM_{y,i}$ indicate the number of resistant elements (masonry walls) of the i -th floor in the x and y directions, respectively.

Once the resisting areas are calculated, it is fundamental to perform the Load Analysis, evaluating each element in the buildings that can contribute masses to the inertial force. Therefore, the analysis of the loads is carried out to evaluate the load q_i per unit of the surface corresponding to the generic i -th floor, taking into account the SLV State Limit.

SLV combination of seismic loads according to EN-1998:

$$\Sigma G_{k,j} + \psi_{E,i} \cdot Q_{k,i} \quad (4.5)$$

Seismic combination:

$$\sum_{j \geq l} G_{kj} + P + A_{Ed} + \sum_{i \geq l} \psi_{2,i} Q_{k,i} \quad (4.6)$$

Where:

G : Permanent actions acting during the nominal life of the construction, whose variation in intensity over time is so small and slow that they can be considered as constant over time. Three main permanent actions are defined within the category of this action: G1, G2 and P. G1 represents the self-weight of all structural elements; instead, G2, is defined as the self-weight of the non-structural ones; and P is the pretension and precompression actions, which in our specific case, have been considered equal to 0 ($P = 0$).

Q : Variable actions acting on the structure or structural element, with instantaneous values that could result different over time. Those actions are divided into long-term and short-term actions. Q_{kj} represents the combination of variable actions, Q_{K1} the dominant variable action and Q_{K2}, Q_{K3}, \dots the variable actions that may act simultaneously with the dominant one. The variable actions are then combined with the combination coefficients ψ_{0j}, ψ_{1j} e ψ_{2j} .

Therefore, the loads are the self-weight of structural and non-structural elements multiplied by 1 and the use loading multiplied by 0.3 ($\psi_{2,i} = 0.3$ for residential buildings).

The self-weight of the different types of flooring systems found in the buildings is detailed in Table 4.2. A slightly different value has been assigned to the flooring systems that are slightly dissimilar to those shown in the table. Nonetheless, the table is always taken as a reference.

Type	Joists	Filling	Other	Constructive
Roof-W	Wood beam	Cañizo	Suspended ceiling	roof tiles
Total: 2.45	0.45	0.75	0.25	1.00
Intermediate floor-W	Wood beam	Cañizo	Suspended ceiling	Flooring
Total: 3.45	0.45	0.75	0.25	2.00
Roof-RC	Prestress concrete joists		Suspended ceiling	roof tiles
Total: 5.25	3.00		0.25	2.00
Intermediate floor-RC	Prestress concrete joists		Suspended ceiling	Flooring
Total: 5.25	3.00		0.25	2.00

Table 4.2: Values of loads per unit area of each floor [kN/m^2]. FS = flooring system. W= wood, Cñ =“Cañizo” (straw and canes joint with plaster), RC= Reinforced Concrete.

Then, the q_i load per unit of surface area is:

$$q_i = \frac{(A_{x,i} + A_{y,i}) \cdot h_i}{A_{tot,i}} \cdot p_{m,i} + p_{s,i} \quad (4.7)$$

where h_i and A_{tot} , are, respectively, the height and the total floor area covered, $p_{(m,i)}$ is the specific weight of the masonry (taken from the Circular table), $p_{(s,i)}$ is the permanent load per unit of floor area.

The total weight of the i-th floor W_i is given by the following relationship:

$$W_i = q_i \cdot A_{tot,i} \quad (4.8)$$

while the average normal compression stress, σ_0 , acting on the masonry walls of the same floor, will be equal to the ratio between the weight of the floors above and the total area of the resistant elements of the floor in question:

$$\sigma_{0,i} = \frac{\sum_{k=i}^N W_k}{A_{x,i} + A_{y,i}} \quad (4.9)$$

where N is the number of floors of the building.

The resistant shear of the i-th plane, $V_r(i)$, is then evaluated using the following formula:

$$V_{r,i} = A_{\min,i} \cdot \tau_r \cdot \sqrt{1 + \frac{\sigma_{0,i}}{1.5 \cdot \tau_r}} \quad (4.10)$$

where $A_{(\min, i)}$ is the lesser of $A(x, n, i)$ and $A(y, n, i)$, τ_r is the average tangential resistance of the masonry.

It is possible to compare the resistant shear at all planes, $V_{r,i}$, with the demanding shear, $V_{s,i}$, obtained by applying to the structure distribution of equivalent static forces obtained by considering a unit spectral acceleration (parameterization). In analytical terms, the force to be applied to the generic mass of the i -th floor of the building is given by the following relationship:

$$F_i = 1g \cdot \frac{W}{g} \cdot \frac{z_i \cdot W_i}{\sum_{j=1}^N z_j \cdot W_j} \quad (4.11)$$

where z_i , W_i , z_j , W_j are, respectively, the height with respect to the foundation plane and the weight of the i -th and j -th floor, g is the acceleration of gravity and W is the total weight of the building:

$$W = \sum_{i=1}^N W_i \quad (4.12)$$

The stressing shear of the generic i -th floor is equal to the sum of the forces applied to the higher floors:

$$V_{s,i} = \sum_{k=1}^N F_k \quad (4.13)$$

To determine the calculation values, a confidence factor $CF = 1$ and a safety factor $\gamma_m = 1$ are considered. The reason is that the objective is not designing a building, but knowing its capacity as realistic as possible.

Calculation of the Reductive Coefficient (C_{Rid})

The adjustment of the conventional capacity to a realistic value is carried out using ten of the eleven parameters contained in the level II seismic vulnerability sheet [28]; only the parameter that calculates the resistant capacity of the building is excluded (Parameter n ° 3), as it has already been evaluated. The parameters are used to obtain a reduction coefficient of the building resistance. The individual parameters are analyzed, indicating for each of them the class to which they belong in accordance with the manual for compiling the level II GNDT seismic vulnerability sheet of the Tuscany Region [26].

(No. of Class) of each parameter In the following, the Class Parameters are described.

(1) Type and organization of the resistant system The first parameter expresses the ability of the structure to behave as a box, through the detection of the presence and effectiveness of the masonry connections. The organization of the vertical structural elements is evaluated, without considering the materials and characteristics of the masonry: the most important factor to consider is the presence of efficient connections between orthogonal walls to ensure the box behaviour of the building.

In order to evaluate the bonding between the orthogonal walls, it is necessary to investigate the quality and the manufacturing of the masonry, verifying that the dimensions of the brick or stone elements, arranged alternately along the height of the wall, are such as to affect the entire wall thickness and not only a part thereof. The four classes are defined as follows:

- Class A/B: Constructions built following a seismic design, regular, with rigid slabs, reinforced concrete ring beams at each floor, well-connected vertical structural elements, concrete or steel lintels, steel chains in vaults and arches;
- Class C: Medium quality of the connections between vertical structural elements, rigid slabs, concrete ring-beams, inefficient steel chains;
- Class D: Absence of ring-beams and steel chains, no connections between vertical structural elements, deformable slabs.

In the buildings of Lorca, the following criteria have been established:

- A With seismic resistant design, regular, rigid flooring system, ring beams (There are no samples pertaining to this class, they do not appear until 1994, when the NCSE-94 [31] regulation came into force)

- B RC slabs (with deficient reinforcement) and masonry brick walls
- C Masonry with flooring systems made of wood
- D Masonry of deficient quality and deformable flooring systems

(2) Quality of the resistant system The parameters influencing the classification of the building are:

- The type and homogeneity of material: quality of bricks/blocks and mortars;
- The texture typology: regularity, the shape of the blocks and their dimensions throughout the wall;
- Transversal connections between wall leaves (“diatoni”).

To identify the class of the masonry under investigation the following procedure based on three levels of knowledge is carried out. A letter that defines a specific characteristic has to be assigned to each level.

The classes could be defined as follows:

- Class A/B: Masonries with homogeneous elements, with a good texture and good quality mortars (to superficial scratch);
- Class C: Irregular masonries, with a decent texture, average quality mortars (to superficial scratch);
- Class D: Masonries with the presence of rounded elements or with consistent voids, insufficient transversal connections(‘diatoni’), poor quality mortars (to superficial scratch).

1. First level: Wall facing type

2. Second level: Wall texture

- Ao = Organized wall texture

- Ad = Disorganized wall texture

3. Third level: Mortar quality

- Mb = Good, Cement or hydraulic mortar

- Mc = Poor, Inconsistent or mealy mortar

The following criteria have been established for the buildings under study:

- A Perforated or hole clay bricks with mortar of high quality (There are no samples pertaining to this class, they do not appear until 1994, when the NCSE-94 [31] regulation came into force)
- B Perforated or hollow clay bricks
- C Clay brick and irregular masonry or just irregular masonry of average quality
- D Poor quality masonry

(3) Resistance This parameter has already been evaluated in section 4.4.1.

(4) Location of the building and foundations The fourth parameter expresses a synthetic evaluation of both the location of the building, in relation to the ground of the surrounding area, and the foundations, in relation to the type of soil and to the differences of the laying surface.

The parameter defines the influence of the soil and the foundations on earthquake response of the structure. Some aspects should be considered:

- The consistency of the soil;
- The slope of the soil;
- The presence of foundations at different levels;
- Unbalanced pressures of the embankments.

The four possible classes are defined as follow:

- Class A: Buildings on bedrocks or on non-thrusting loose soils, with slopes lower than 10% and $\Delta_h = 0$;
- Class B: Buildings on bedrocks or on non-thrusting loose soils, with slopes lower than 30% and $\Delta_h < 1m$;
- Class C: Buildings on non-thrusting or thrusting loose soils, with slopes lower than 50% and/or $\Delta_h < 1m$;
- Class D: Buildings on non-thrusting or thrusting loose soils with slopes greater than 50% and/or $\Delta_h > 1m$.
For the assignment of the class it refers to the worst case condition.

(5) Horizontal structural elements This parameter expresses the horizontal elements role in order to have a good box behavior, by means of good connections to vertical walls and high stiffness of the flooring in its plane.

In dividing into classes the various buildings, the following requirements are taken into account:

- High stiffness for the deformation in its plane which means good connections between building elements;
- Effective connections between the resisting vertical elements;
- High difference in resistance and stiffness between the building floorings and masonry.
- In the case of different horizontal structural types in the same building, for the assessment of the building class, it is necessary to refer to the worst flooring condition.

The four classes are the followings:

- Class A: RC slabs, precast or cast in-situ RC slabs with hollow blocks, corrugated metal sheets and concrete, vaults with steel chains or consolidated; Connections between structural elements (ring beams, connections between timber beams and between timber beams and masonry walls,...)
- Class B: Similar to Class A both for the structural typologies and connections but not everywhere in the building;
- Class C: Precast or cast in-situ, non-reinforced concrete slabs with hollow blocks , vaulted ceilings, masonry vaults. Efficient connections, as for class A;
- Class D: Deformable slabs, as for Class C. Buildings with horizontal elements of any nature poorly connected to the walls. Absence of ring beams, limited support length at the end of the beams. Pay attention to heavy slabs realized on vertical elements characterized by poor-quality masonry.

In the buildings of Lorca, the following criteria has been established:

- A Rigid RC slabs with adequate reinforcement (There are no samples pertaining to this class, they do not appear until 1994, when the NCSE-94 [31] regulation came into force)
- B Semirigid RC beam, self-supporting joists with inadequate reinforcement
- C Semirigid wood flooring system (beams or joists made of wood) without ring beams
- D Deformable wood slabs of deficient quality without ring beams

(6) Plan configuration The seismic behavior of a building also depends on the building plan itself. This parameter takes into account the plan configuration and, therefore, the regularity of the building (see Figure 4.4). A regular configuration is associated to a better seismic behavior of the construction. The parameters β need to be defined.

The four classes are described below:

- Class A: Buildings with $\beta_1 \geq 80$ and $\beta_2 \leq 10$;
- Class B: Buildings with $60 \leq \beta_1 \leq 80$ and $10 < \beta_2 \leq 20$;
- Class C: Buildings with $40 \leq \beta_1 < 60$ and $20 < \beta_2 \leq 30$;
- Class D: Buildings with $\beta_1 < 40$ and $\beta_2 > 30$.

The values of β_1 and β_2 are studied for each particular building.

(7) Elevation configuration In the case of masonry buildings, especially old ones, the main cause of irregularities in elevation are mainly associated to the presence of porticoes or towers with a significant mass, balconies and roof terraces. It takes into account the regularity in elevation of the building (see Figure 4.5). Porticoes built in adherence to the perimeter walls of the main building should be excluded. The presence of porticoes is reported as the percentage ratio between the porch plan surface and the floor total surface. It is possible to substitute the ratio in terms of mass with the ratio in terms of covered surface.

The four classes referring to the configuration in elevation parameter are:

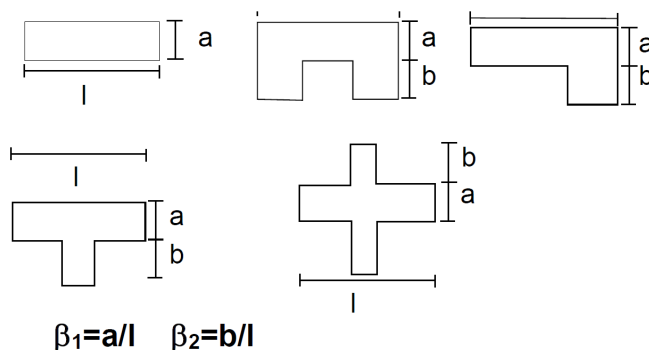


Figure 4.4: Different plan configurations. (GNDT II Level Form)

- Class A: Buildings with a uniform or decreasing distribution of the masses or of the resisting elements in elevation. Differences in plan between floors less than 10%;
- Class B: Buildings with porticos less than 10%, and differences in plan between floors less than 20%. Towers with a height less than 10%;
- Class C: Buildings with porticos less than 20% and/or differences in plan between floors less than 20%. Towers with a height less than 40%;
- Class D: Buildings with porticos greater than 20% and towers with a height greater than 40%.

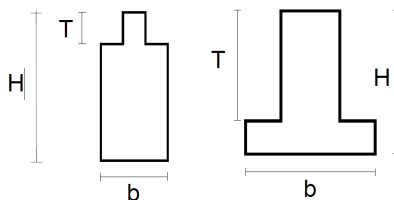


Figure 4.5: Different elevation configurations. (GNDT II Level Form)

The values of the distribution of the masses are studied for each particular building.

(8) Maximum distance between walls With this parameter, the presence of walls (partitions excluded) intersected by transverse walls, able to constitute an effective constraint on the considered sections, is taken into account. The presence of the orthogonal walls contrasts the onset of the failure mechanisms related to overturning of the plane of the concerned wall.

An effective constraint includes a strong bonding between the wall and the bracing wall. The effectiveness of the constraint also depends on the wall structure and on the presence of openings in the vicinity of the corner. The classes are defined in terms of the most unfavorable ratio of the distance between the transverse walls and the considered wall thickness.

The four classes are:

- Class A: Buildings with ratio distance/thickness of the transversal wall lower than 15;
- Class B: Buildings with ratio distance/thickness of the transversal wall between 15 and 18;
- Class C: Buildings with ratio distance/thickness of the transversal wall between 18 and 25;
- Class D: Buildings with ratio distance/thickness of the transversal wall greater than 25.

(9) Roof system The factors which influence the seismic behavior of the building are the typology and the weight of the roof. In particular the additional elements to be considered are:

- The classification of thrusting or non-thrusting roofs;
- The presence of ring beam connecting the roof and the vertical walls;
- The presence of steel ties;
- The permanent load;
- The support length.

The thrusting feature of a roof favors, during the earthquake, the out-of-plane collapse of the wall thrust and the ones below it, due to the increase of the thrust exerted under normal conditions.

The heaviness affects adversely in that it determines the rise of high inertia forces that can overcome the resistance of the walls of bad quality.

The identification of a specific class for a certain parameter is then determined as a function of the thrusting action of the structural type of building roof.

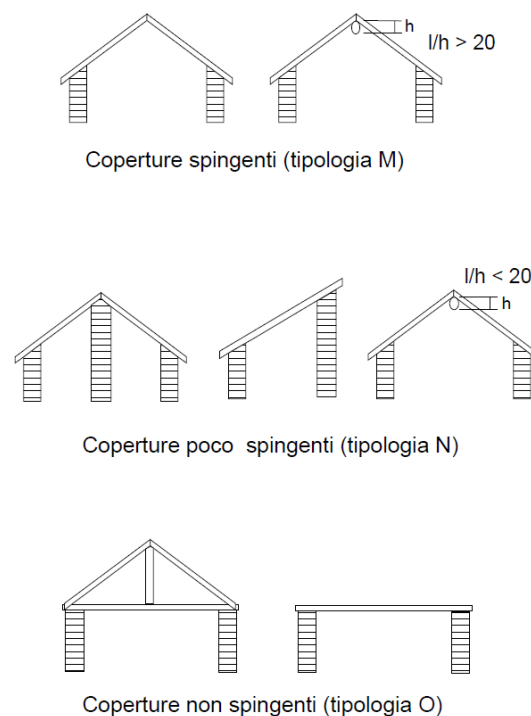


Figure 4.6: Different plan configurations. (GNDDT II Level Form)

- Class A: Rigid, non-thrusting roof with ring-beams and/or steel or timber chains.
- Class B: Rigid, non-thrusting roof, without ring-beams and/or steel or timber chains or without efficient connections. Rigid, low-thrusting roof with ring-beams and/or chains.
- Class C: Non-thrusting, brittle roof, without efficient connections and without a slab. Rigid, low-thrusting roof, not well connected. Rigid, thrusting roof with ring-beams and/or chains.
- Class D: Rigid, thrusting roof without ring-beams and/or chains. Heavy roof positioned over poor-quality masonry walls.

(10) Non-structural elements This parameter takes into account the presence of elements that may produce damages to people or things, such as cornices and window frames. They should be identified even if they are secondary elements in the vulnerability assessment of the building.

The classes are defined as follows:

- Class A/B: Buildings without attachments, cornices, false ceilings and chimneys well connected, balcony integrated with the structure;

- Class C: Buildings with window fixtures not well connected, false ceilings covering big surfaces but not well connected;
- Class D: Buildings with chimneys close to the perimeter of the roof and not well connected, dangerous attachments, balcony without efficient connections, heavy false ceilings.

(11) State of conservation The classes are defined according to the state of conservation of the building, considering the diffusion of damages throughout the structures and the width of cracks.

The classes are defined as follows:

- Class A: Buildings in good conditions without damages;
- Class B: Buildings with slight damages, such as fissures, not diffused;
- Class C: Buildings with medium gravity damages (2 to 3mm);
- Class D: Buildings with significant damages and walls deviating from the vertical direction.

Scores Once the vulnerability classes related to the building in question have been defined, in accordance with the manual for compiling the level II GNDT seismic vulnerability sheet of the Tuscany Region [26], the generic i -th parameter will uniquely correspond to a single score, p_i , and a weight w_i . Therefore, for each parameter the product is evaluated, $K_i = p_i * w_i$.

The same products must be evaluated in the hypothesis that the building in question has all the parameters in class D (the worst):

$$K_i(D) = p_i(D) \cdot w_i \quad (4.14)$$

All the latter must then be added to obtain the sum, K_{pegg} :

$$K_{pegg} = \sum_{i=1}^{10} K_i(D) \quad (4.15)$$

The reduction coefficient C_{rid} is determined through the following relationship:

$$C_{rid} = \prod_{i=1}^{10} \left(1 - \alpha \cdot \frac{K_i}{K_{pegg}} \right) \quad (4.16)$$

when this parameter changes, the lower limit (all parameters in class D) of the range of variation of the reduction coefficient, C_{rid} , is established. The upper limit (all parameters in class A), on the other hand, is fixed and is equal to unity. Using recognized reference methodologies ([5] and [4]), α has been defined in such a way as to provide a lower limit for the reduction coefficient, C_{rid} , equal to 0.60.

The previously determined spectral acceleration is reduced by means of the C_{rid} coefficient:

$$S_{a,c} = C_{rid} \cdot S_a \quad (4.17)$$

The values of the $S_{(a,c)}$ and PGA_c for the all the buildings studied classified according to its type are included in Table 4.3 and in Fig. 4.7a. Moreover, in addition to the calculation of $S_{a,c}$ and PGA for the weakest direction, these quantities are also evaluated for the less vulnerable direction for research purposes concerning the unpredictable directionality of the seismic event (see Section 4.4.2).

Calculation of the Peak Ground Acceleration (PGA_C)

To determine the earthquake intensity which the structure can withstand without collapsing, it is necessary to transform the spectral acceleration values in the maximum ground acceleration (PGA_c).

Said transition, from pseudo-acceleration ($S_{a,c}$) to ground acceleration leading to collapse of the structure PGA_c , is established by the following relationship [[6]]:

M11	$S_{(a,c)}[g]$	$PGA_c[g]$	M31	$S_{(a,c)}[g]$	$PGA_c[g]$	M34	$S_{(a,c)}[g]$	$PGA_c[g]$
m1	0.073	0.091	m6	0.146	0.183	m12	0.145	0.181
m2	0.060	0.075	m7	0.224	0.280	m13	0.109	0.136
m3	0.034	0.045	m8	0.086	0.108	m14	0.070	0.088
m4	0.076	0.095	m9	0.477	0.477*	m15	0.118	0.148
m5	0.067	0.084	m10	0.167	0.209	m16	0.097	0.121
-	-	-	m11	0.144	0.180	m17	0.184	0.230
-	-	-	-	-	-	m18	0.085	0.085*
-	-	-	-	-	-	m19	0.164	0.205
-	-	-	-	-	-	[M34]	-	-
-	-	-	-	-	-	m20	0.367	0.459

Table 4.3: Values of $S_{(a,c)}[g]$ and $PGA_c[g]$ for all the buildings under study. X*: buildings with one floor. [M34]: type M34 with steel pillars

$$PGA_c = \frac{S_{a,c}}{\alpha_{PM} \cdot \alpha_{AD} \cdot \alpha_{DT} \cdot \left(\frac{1}{\alpha_{DUC}}\right)} \quad (4.18)$$

where:

α_{PM} is the modal participation coefficient: 0.80 for buildings with more levels and 1.00 Buildings with one level;
 α_{AD} is the spectral amplification coefficient: equal to 2.5;
 α_{DT} is a coefficient that takes into account the dissipative phenomena: 0.80 Otherwise – No masonry resisting infill contribution and 1.00 if the masonry resisting infill contribution is significant with respect to the one of the principal resisting system;
 α_{DUC} is the behaviour factor: equal to 2 for masonry structures.

The values assumed for these parameters are listed in Table 4.4:

Coefficients	Values
α_{PM}	0.8
α_{AD}	2.5
α_{DT}	0.8
α_{DUC}	2.0

Table 4.4: values of $\alpha_{PM}, \alpha_{AD}, \alpha_{DT}$ and α_{DUC} for the buildings under study

Therefore, for building with varios levels $PGA_c = S_{a,c} * 1.25$ and for buildings with just one level, $PGA_c = S_{a,c}$.

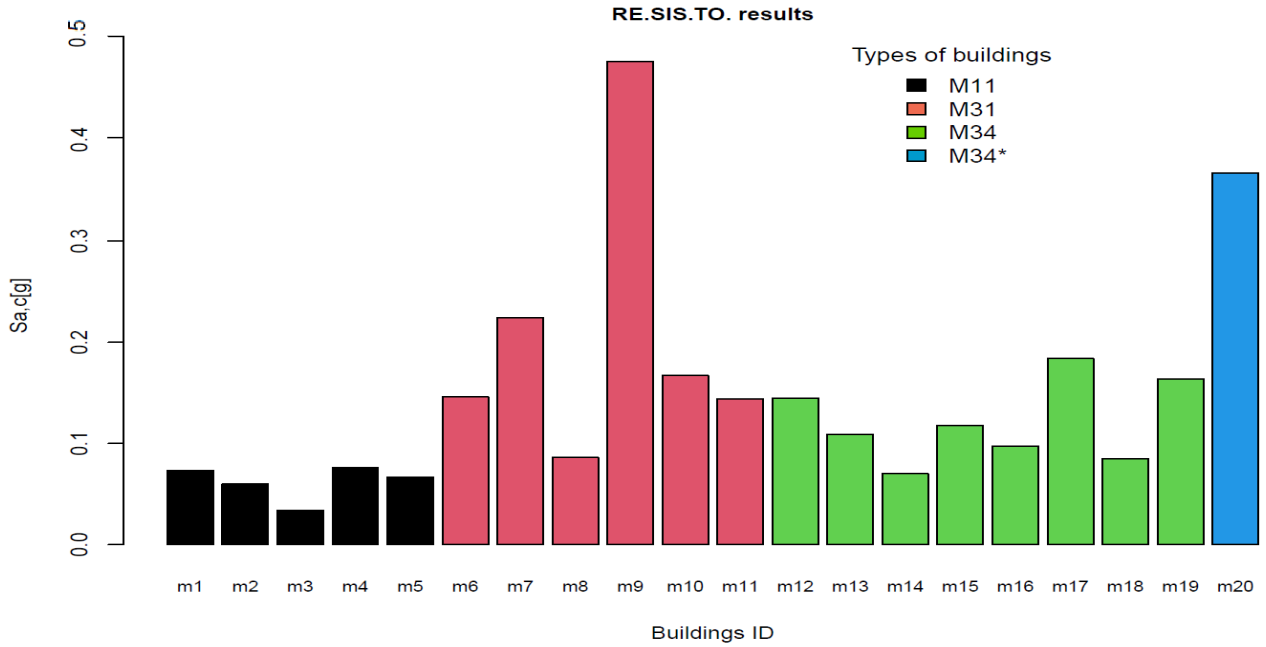
Moreover, the relation between the PGA_c and other parameters such as the year of construction, the number of floors and the surface area per floors is studied (Fig. 4.8).

The graphs included in 4.8 do not reflect a clear tendency for most of the parameters studied.

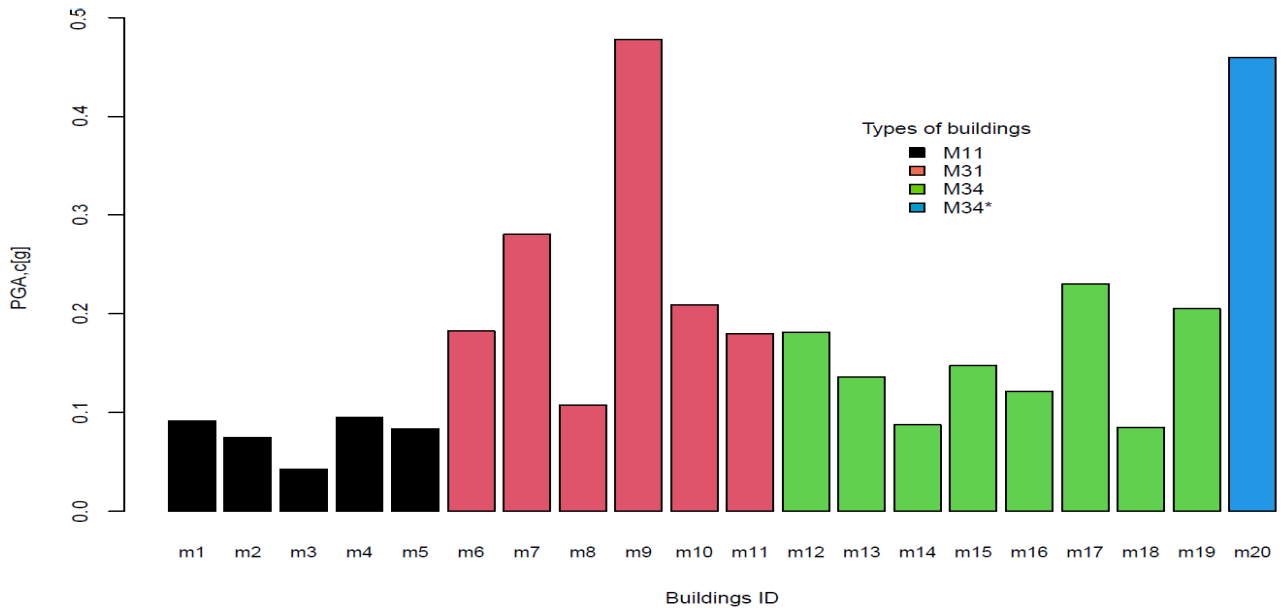
In Fig 4.9a the capacity of the buildings in PGA_c is organised according to their number of floors above ground. As said figures reflects, for the types M11 and M34, the capacity is stable independently of the number of floors, whereas for the type M31 this parameter constitutes an aspect that could be taken into account in the development of the fragility curves.

4.4.2 Variability depending the seismic directionality

The directionality of the ground motion ia a relevant aspect to consider for the calibration of fragility curves (FCs), as the results of [29] show. For that reason, the seismic vulnerability in the most favorable direction of the ground motion for the building is also studied. In this context, it is worthwhile mentioning the assignment of the x and y axis of the buildings correspond to the main directions of the building resisting walls.



(a) $S_{a,c}$ of all the buildings under study



(b) PGA_c of all the buildings under study

Figure 4.7: Resistance of all the buildings under study

The most favorable direction for each building from those considered principals (x and y), has been analysed floor by floor obtaining the results shown in Table 4.5 and Figure 4.9b.

In Figure 4.10, a deeper analysis of the $S_{(a,c)}$ of the buildings is performed. In Fig. 4.10a, a clear relationship between the maximum and the minimum $S_{(a,c)}$ can be established: a linear regression ($S_{(a,c,max)} = 1.4186 * S_{(a,c,min)} + 0.0363$) reaches a low quadratic error ($r^2=0.8899$) just overlooking an abnormal point [$x=0.097, y=0.7$].

Moreover, in Fig. 4.10b, the strong correlation between the ratio of the resistant area and the total surface area of the most unfavorable floor $A_{(r,max)}/A_{(r,min)}$ and the ratio $S_{(a,c,max)}/S_{(a,c,min)}$ taking into account the directionality is illustrated. explicar el parrafo superior

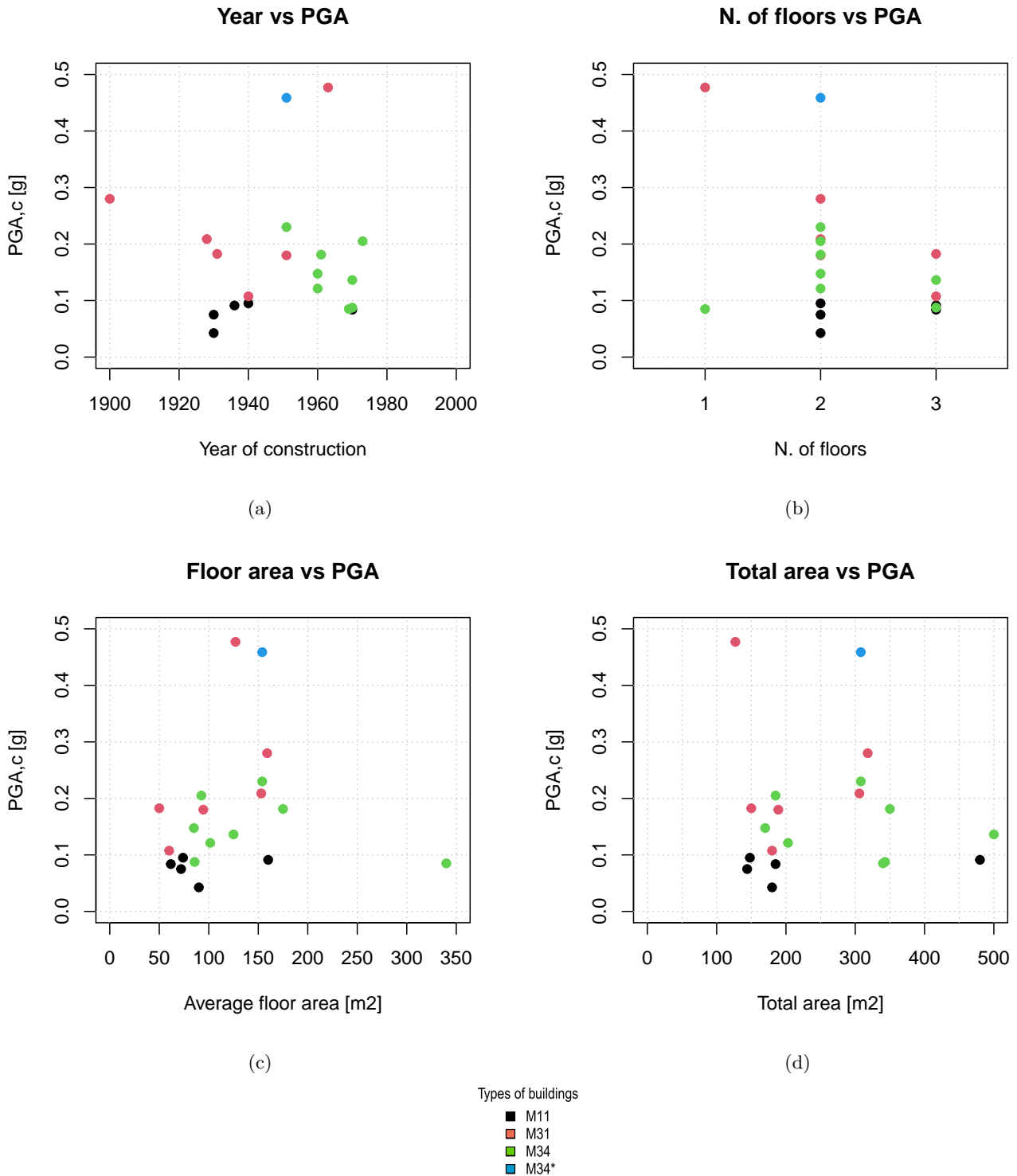
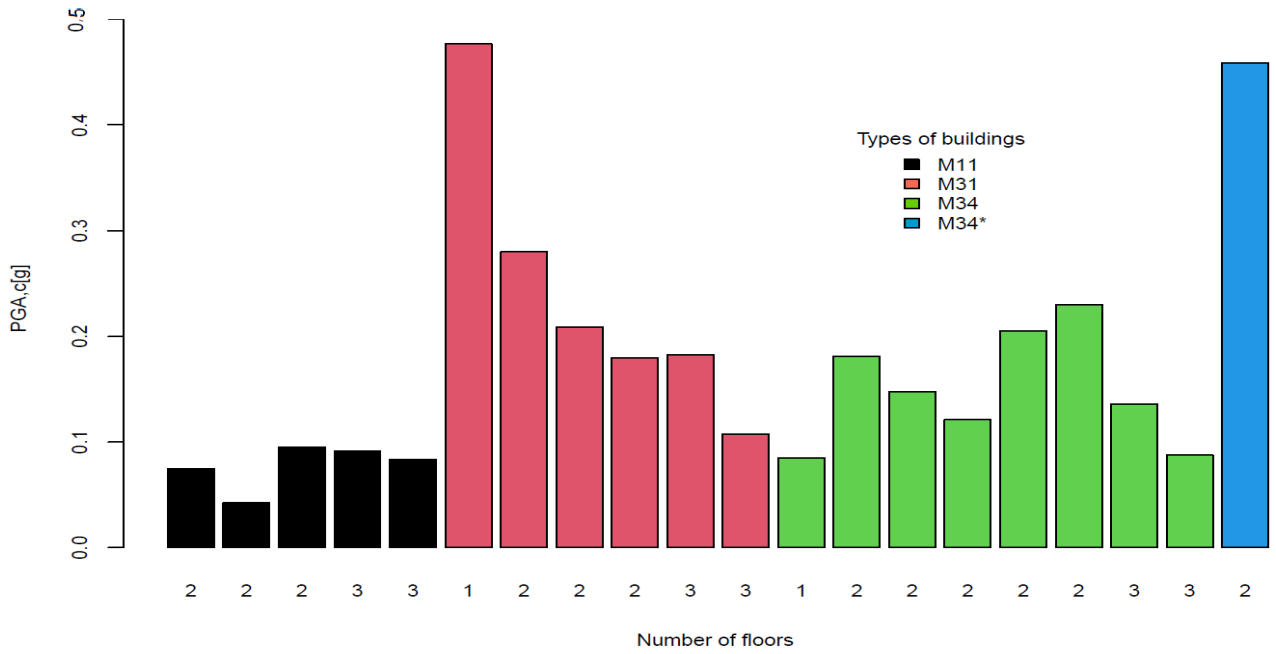
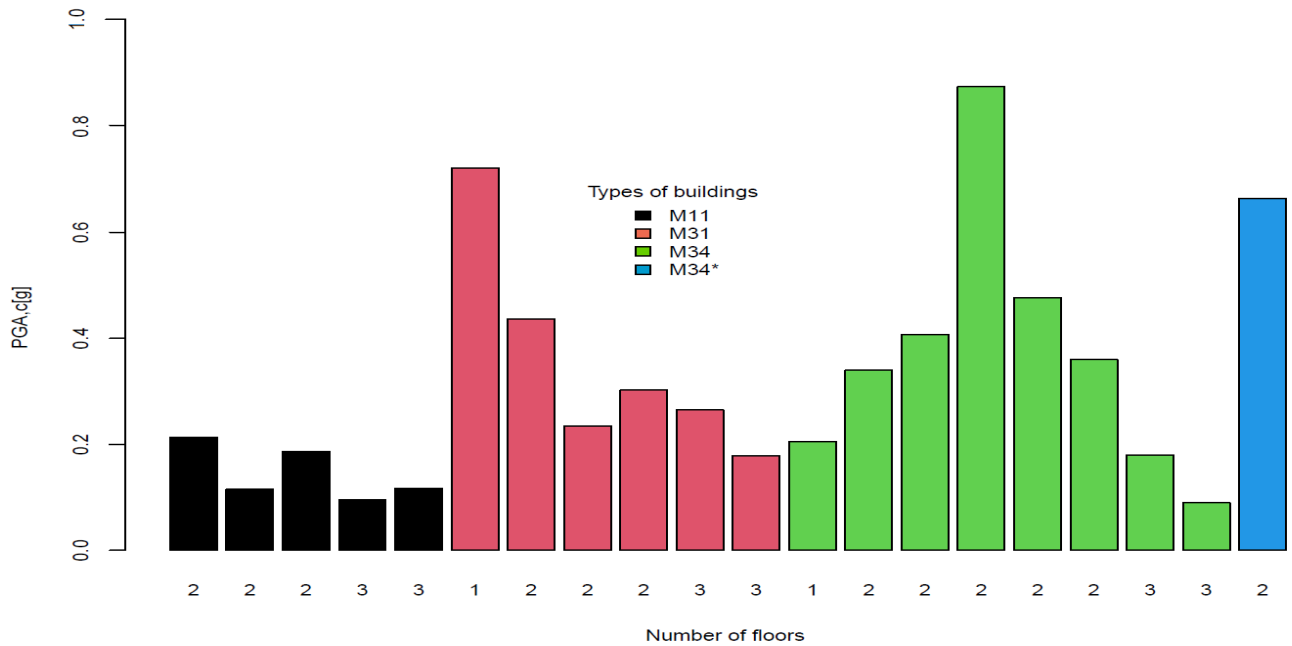


Figure 4.8: Relationship between a number of parameters studied and the PGA_c of all the buildings under study



(a) PGA_c of all the buildings under study considering the number of floors in the most unfavorable direction



(b) PGA_c of all the buildings under study considering the number of floors in the most favorable direction

Figure 4.9: Vulnerability of all the buildings under study

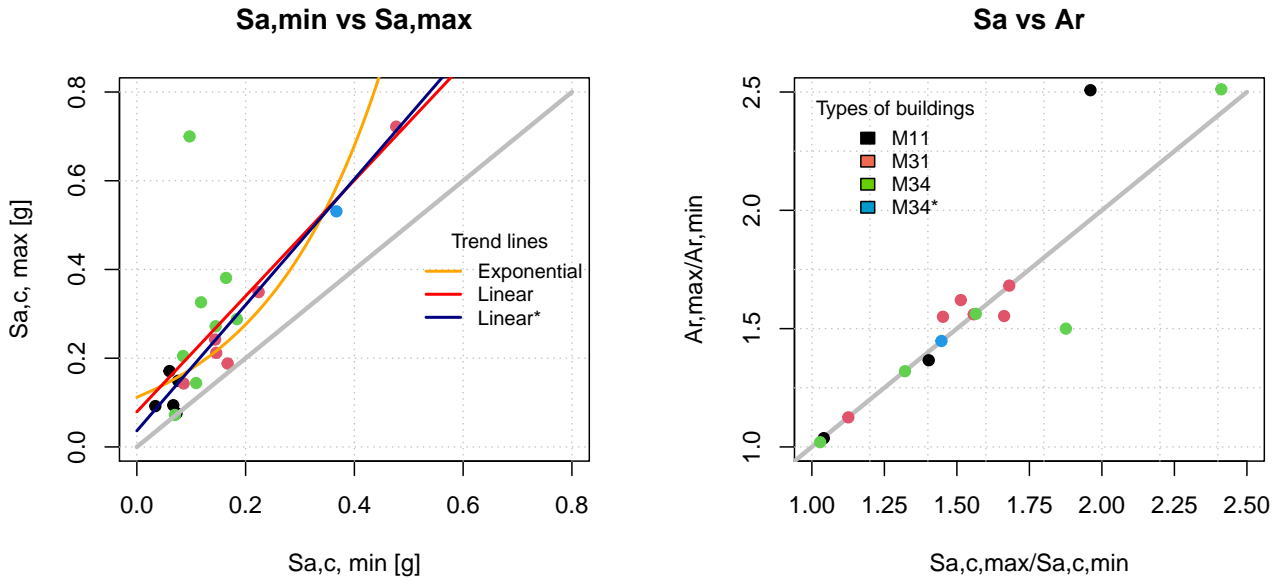
4.4.3 Demand estimate

The demand assessment of the Lorca buildings will be performed using as a reference the European regulation and the procedures established on it. In addition, this method will be compared with the Italian regulation, location where the methodology was developed and is more widely used.

The seismic demand is calculate on the basis of the seismic hazard of the specific region, which, on its part, is indicated on the seismic hazard maps developed for a specific period of return.

M11	$S_{(a,c)}[g]$	$PGA_c[g]$	M31	$S_{(a,c)}[g]$	$PGA_c[g]$	M34	$S_{(a,c)}[g]$	$PGA_c[g]$
m1	0.212	0.265	m6	0.144	0.115	m12	0.772	0.618
m2	0.092	0.115	m7	0.072	0.058	m13	0.094	0.075
m3	0.149	0.1863	m8	0.012	0.094	m14	0.188	0.150
m4	0.076	0.2176	m9	0.143	0.114	m15	0.700	0.560
m5	0.094	0.1368	m10	0.326	0.261	m16	0.193	0.154
-	-	-	m11	0.149	0.119	m17	0.288	0.230
-	-	-	-	-	-	m18	0.157	0.1256
-	-	-	-	-	-	m19	0.164	0.205
-	-	-	-	-	-	[M34]	-	-
-	-	-	-	-	-	m20	0.367	0.459

Table 4.5: Values of $S_{(a,c)}[g]$ and $PGA_c[g]$ for all the buildings under study in the most favorable direction. X*: buildings with one floor. [M34]: type M34 with steel pillars



(a) Relationship between $S_{(a,c,max)}$ and $S_{(a,c,min)}$ taking into account the directionality. Max= most favorable direction, min= most unfavorable direction-Trend lines: Exponential: $0.1121\exp(4.5044x)$, $r2=0.5097$; Linear: $1.305x+0.0791$, $r2=0.5446$; Linear*: $1.4186x+0.0363$, $r2=0.8899$ (without the abnormal point $[x=0.097,y= 0.7]$)

(b) Relationship between the ratio of the resistant area and the total area of the most unfavorable floor $A_{(r,max)}/A_{(r,min)}$ and the ratio $S_{(a,c,max)}/S_{(a,c,min)}$ taking into account the directionality. Max= most favorable direction, min= most unfavorable direction

Figure 4.10: Relationship between the maximum and the minimum Sa_c of all the buildings under study

Italian, Spanish and European procedures

At the present time, the procedures provided by the Italian, Spanish and European regulations to establish the seismic demand present some differences.

In the case of assessing Italian buildings, the seismic actions applicable to the buildings have to be evaluated according to the Italian Building Code, the Decree of the Minister of Infrastructure on February 20, 2018, [20] and the [14]. Whereas, in the case of Spain, the code applicable is NCSE-02 [30]. Furthermore, the European regulation, EN-1998 [7], is applicable to both countries.

In all cases, in order to define the seismic action it is necessary to define the reference period, the probability of exceeding it and the returning period, which takes into account the limit state considered, and the class of building.

In the following, the procedure to characterise these parameters is detailed. The Italian regulation is always used as key reference since it is the most up-to-date according to the State of the Art and the more recent one.

Reference period, V_R

The reference period is the reference life of the building, for which the return period is calculated.

The Italian regulation establishes a relation of the seismic actions to a reference period V_R which is obtained, for each type of construction, by multiplying the nominal life V_N by the coefficient of use C_U :

$$V_R = V_N * C_U \quad (4.19)$$

The value of the use coefficient C_U is defined according to the use class, as shown in Table 4.6:

Class of use	Coefficient C_U
I	0.7
II	1.0
III	1.5
IV	2.0

Table 4.6: Coefficient C_U according to each class of use

Note that if $V_R \leq 35$ years, V_R should be consider equal to 35 years.

In the presence of seismic actions, the buildings are divided into the use following classes of use, with reference to the consequences of an interruption of operations or a possible collapse:

- **Class I:** Buildings that are infrequently occupied such as agricultural buildings.
- **Class II:** Buildings whose use involves average occupation and activity, without dangerous contents to the environment and without essential public and social functions. Industries with activities that are not dangerous for the environment. Bridges, infrastructural works, road networks that do not fall under Class of Use III or Class of Use IV, railway networks whose disruption would not cause emergency situations. Dams whose collapse would not cause significant consequences.
- **Class III:** Buildings whose use involves significant occupation. Industries with contents that could damage the environment. Inter-urban road networks that do not fall under Class of Use IV. Bridges and railway networks whose disruption leads to emergency situations. Dams whose eventual collapse would cause significant consequences.
- **Class IV:** Buildings with important public or strategic functions, also with reference to the management of civil protection in the event of a disaster. Industries with activities that are particularly dangerous for the environment. Road networks of type A or B, as per Ministerial Decree 5 November 2001, n. 6792, "Functional and geometric rules for road construction" [25], and type C when belonging to routes connecting between provincial capitals not also served by type A or B roads. Bridges and railway networks of critical importance for the maintenance of communication routes, particularly after a seismic event. Dams forming part of aqueducts and related to power plants.

The studied buildings fall into the Class II.

The nominal life of a structure, V_N , is understood as the number of years in which the structure, provided it is subject to ordinary maintenance, must be able to be used for the purpose for which it is intended. The nominal life of the different types of works is that shown in the table and must be specified in the project documents.

In this case, the buildings pertain to type 2, $V_N = 50$ years.

Therefore, the reference period according to the Italian regulation is $V_R = V_N * C_U = 50$ years. Table 4.8 summarizes all the parameters involved.

Type of construction	V_N (in years)
1. Provisional constructions Structures under construction	≤ 10
2. Ordinary constructions, bridges, infrastructures and dams of small size or of normal importance	≥ 50
3. Major or essential constructions, bridges, infrastructures and dams of large dimensions or strategic importance	≥ 100

Table 4.7: Coefficient V_N according to the type of construction

Summary of parameters	
Class	II
C_U	1.0 (Class II)
V_N	Type 2 (≥ 50)
V_R	50 years

Table 4.8: Summary of main parameters

Probability of exceeding the limit for S_a during the reference period, P_{V_R} The probabilities of exceeding the reference period, P_{V_R} , has to be referred according to regulation in order to identify the seismic action acting in each of the limit states considered, which are shown in Table 4.9:

Limit states	P_{V_R} : Probability of exceeding S_a during V_R
SLS, Serviceability Limit States:	
SLO, Operativity	81
SLD, Damage Limit	63
ULS, Ultimate Limit States:	
SLV, Life Saving	10
SLC, Collapse Prevention	5

Table 4.9: Probability of exceeding the limit for S_a during the reference period according to the limit state under study

If the protection against the operating limit states is of priority importance, the P_{V_R} values given in the table must be reduced according to the degree of protection to be achieved. As the buildings analyzed does not need to fulfill this condition, the value are not reduced.

According to its authors, the limit state used for the application of RESISTO is the Life Safety State, SLV.

Return period, T_R The return period is the inverse of the annual probability of exceedance, which is the average number of years it takes to get an exceedance.

The corresponding return period T_R must be estimated according to Eq. 4.20:

$$T_R = -\frac{V_R}{\ln(1 - P_{V_R})} = -\frac{C_U \cdot V_N}{\ln(1 - P_{V_R})} \quad (4.20)$$

Therefore, the returning period for the buildings under study is $T_R(ULS, SLV) = 475$ "years" when applying the Italian regulation.

On its part, the European regulation states that the values to be assigned to the P_{V_R} or T_R for use in a State can be found in the Spanish national annex within the own document. The recommended values are $P_{NCR} = 10$ and $T_{NCR} = 475$ years for prevention of collapse limit state.

Seismic actions

In the case of the Italian buildings, the necessary values for the determination of the seismic actions are estimated according to Annexes A and B to the Decree of Minister of Infrastructure January 14, , published in the S.O. to the Official Gazette of February 4, 2008, n.29 [19], and any subsequent updates.

The parameters a_g, F_0, T_C^* involved in this calculus, can be defined as follows:

a_g : The peak ground acceleration at the location of the building

F_0 : The maximum value of the amplification factor of the spectrum in horizontal acceleration

T_C^* : The reference value for determining the start period of the constant velocity segment of the accelerating spectrum horizontal

In the cases under study, buildings located in Spanish region of Murcia (municipality of Lorca), the latest hazard maps developed for the Spanish territory are considered (see [21]). Said values are not available up to date in the regulation in force. Nonetheless, the information that the Italian regulation provides is more complete than the latest Spanish hazard maps.

In this respect, it is worth detailing that for Spain there are two hazard maps available. The former is included in the NCSE-02 seismic regulation currently in force [30]. The latter is the hazard map that can be found on the National Institute Geographic (IGN) web [9] and in the book [21], which has been developed in collaboration between the Universidad Politécnica de Madrid (UPM) and the IGN institution in 2015. This map incorporates more advanced techniques of hazard assessment as a consequence of the fact that it was commissioned after the Lorca's 2011 earthquake; a seismic event that, as mentioned along this dissertation, exhibited larger peak ground accelerations and spectra than those predicted by the regulation in force, specially for short-period buildings [1, 24], such as unreinforced masonry buildings of from one to three storeys. Despite the fact that, in general, it increases the a_g values all over the country and consequently will improve the safety of the buildings, up until date it does not have become compulsory. Nonetheless, a new regulation is under development [3] cite the state at the moment.

Peak Ground Acceleration, PGA_d The Peak Ground Acceleration (PGA_d), which determines the design seismic action, depends on the type of soil, the importance of the building under study (classes of use, Table 4.6) and the maximum reference acceleration.

With respect to the soil and building characteristics the Italian, European and Spanish regulations in force—NTC08, EN1998 and NCSE-02 respectively— provide different assessment criteria. In the following, the criteria of these regulations and the seismic hazard maps are described.

Soil Category In order to obtain the seismic response, it is necessary to evaluate the effect of local site response by defining reference Soil Categories (A,B,C,D,E).

In Italy, this is done according to the national regulation, NTC Table 3.2.II. In Spain, this is detailed below in the case of the new hazard maps.

The results of a geotechnical test for the determination of the subsoil category are not available. However, it can be established according to the seismic site classification map for Lorca (Fig. 4.11) elaborated by [16]:

On the one hand, the areas located far from the city center constitute the two predominant bedrock areas in Lorca city were not exposed to high levels of damage. Namely, the areas on the south-westernmost part of Lorca city, close to the Sierra de Las Estancias hill, have the best soil conditions corresponding to EC8 site class A. And in the northernmost part of Lorca city, close to the Sierra La Tercia hill, the soil condition belongs to the EC8 category of B1.

On the other hand, a large area of Lorca city is classified as EC8 site class B2 – in which is located the main damaged district of La Viña. Also, the seismic site classification map points out that the other severely damaged districts, such as La Alberca and La Alameda districts, are located in areas with unconsolidated Holocene materials, corresponding to the EC8 site class C.

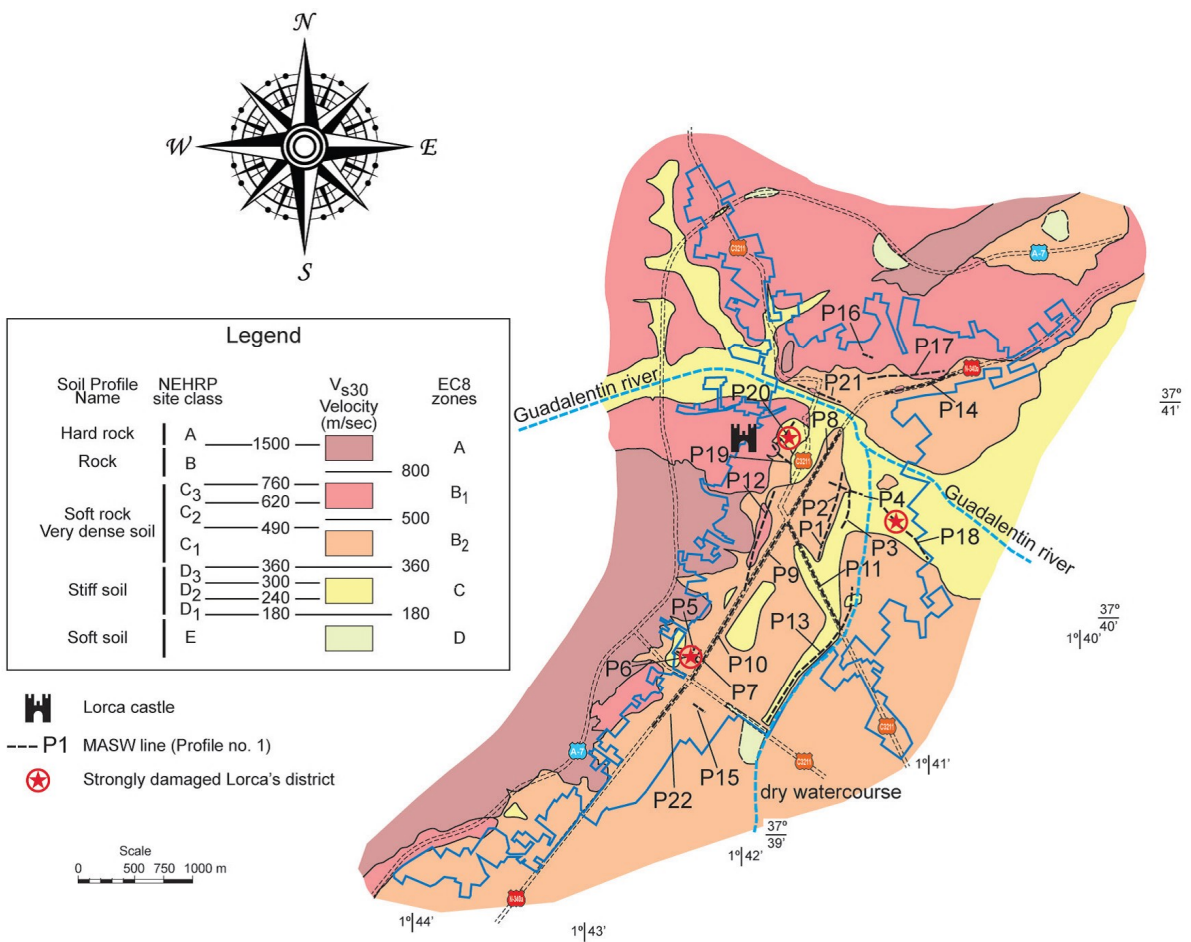


Figure 4.11: Vs30 map of Lorca city following criteria from the EC8 and NERRP site class codes (Holzer et al. 2005; NEHRP 2001; EN 1998). (Credits: Figure 11, [16])

Therefore, the soil type B is considered as the predominant in the area of analysis, Lorca Centre, which according to EN-1998 [7] consists in:

- Deep deposits of dense or medium-dense sand, gravel or stiff clay with thickness from several tens to many hundreds of meters ($V_{s,30} = 360 - 800m/s$, $N_{SPT} > 50$ and $c_u > 250KPa$).

Additionally, there is an reduced area with Soil type C, which consists in:

- Deep deposits of dense or medium-dense sand, gravel or stiff clay with thickness from several tens to many hundreds of metres ($V_{s,30} = 180 - 360m/s$, $N_{SPT} = 15 - 50$ and $c_u = 70 - 250KPa$).

Additionally, according to NCSE-02 [30], the type considered is defined as Type II:

- Highly fractured rock, dense granular or hard cohesive soils. Speed of propagation of transverse elastic or shear waves, $750m/s > VS > 400m/s$.

For the city of Lorca, the values established by each hazard map for the Seismic Demand, PGA_d are the described below.

The a_g or directly the PGA_d values have been obtained from the the maps illustrated in Fig 4.12a ([30]) and Fig. 4.12b [9] extracted from its respective references. Nevertheless, these figures are not easily comparable, as they were obtain employing different methodologies and establishing different types of soils of reference: soil II in the case of the NCSE-02 map and soil I in the case of the IGN maps. Soil II consist in highly fractured soils, dense granular or hard cohesive soils and soil I in rock.

Demand estimate according to different proposals In the following, the PGA_d is estimated according to the criteria established by the two regulations applicable to Spain, NCSE-02 and EN-1998, and the two seismic hazard maps available, that included in the NCSE-02 and that developed by the IGN and the UPM institutions.

NCSE-02 maps For the residential building, the PGA parameter could be defined as follow according to the NCSE-02's procedure, in which the design acceleration is determined by means of Eq. 4.21.

$$a_c = S \cdot \rho \cdot a_b \quad (4.21)$$

According to the maps included in NCSE02, $a_b(NCSE02) = 0.12g$ [30], with parameter $K=1.0$ for a return period of 500 years.

Where the parameter K constitutes a coefficient of contribution that takes into account the influence of the different types of earthquakes expected, near-field or far-field earthquakes, in relation to the seismic hazard of each point.

The reference acceleration given in NCSE-02 by the already mentioned basic seismic acceleration a_b (NCSE-02, art. 2.1) conditions, according to its value, the risk coefficient r , the ground coefficient C and the ground amplification coefficient S , which is used to determine the design acceleration (as defined in NCSE-02, art 2.2).

- For $\rho \cdot a_b \leq 0.1g$

$$S = \frac{C}{1.25}$$

- For $0.1g < \rho \cdot a_b < 0.4g$

$$S = \frac{C}{1.25} + 3.33 \left(\rho \cdot \frac{a_b}{g} - 0.1 \right) \left(1 - \frac{C}{1.25} \right)$$

- For $0.4g \leq \rho \cdot a_b$

$$S = 1.0$$

Resulting for a soil Type II according to NCSE02 ($C=1.3$), a $PGA_d(NCSE - 02)$ or $a_c(T = 0)$ equals to:

$$T = 0 : PGA_d(NCSE - 02) = a_c = S \cdot \rho \cdot a_b = 1.037 \cdot 1 \cdot 0.12g = 0.124g \quad (4.22)$$

NCSE-02 and new maps However, when the newest and more precise hazard maps want to be applied, as the new maps substantially modifies the reference acceleration, which now corresponds to the maximum ground acceleration in a standard soil (Type I according to EN-1998), it is necessary to modify the coefficient S . Therefore, in the case of taking the $PGA(T_R = 475)$ as the reference acceleration obtained in the new map, referenced to a type I soil, the new ground amplification coefficient S to be applied will be given by the following criterion:

- For $\rho \cdot a_r \leq 0.1 \text{ g}$

$$S = C$$

- For $0.1 \text{ g} < \rho \cdot a_r < 0.4$

$$S = 1 + 3.33(1 - C) [(\rho \cdot a_r / \text{g}) - 0.4]$$

- For $0.4 \text{ g} \leq \rho \cdot a_r$

$$S = 1.0$$

Where:

C is the ground coefficient, dependent on the geotechnical characteristics of the soil (NCSE-02, art. 2.4)

a_r the new reference acceleration $PGA(T_R = 475)$.

Resulting a $PGA_d(\text{NCSE} - 02)$ or $a_c(T = 0)$ equals to:

$$T = 0 : PGA_d(\text{NCSE} - 02) = a_c = S \cdot \rho \cdot a_b = 1.2 \cdot 1 \cdot 0.19\text{g} = 0.228\text{g} \quad (4.23)$$

EN1998 and new maps To conclude, according to EN-1998, the regulation applied through this document for the sake of consistency, the PGA_d depends is determined following Eq. 4.24 and 4.25.

The value of design acceleration for a soil type A corresponds to:

$$a_g = \gamma_I \cdot a_{gR} \quad (4.24)$$

where:

γ_I ponders the importance of the building, being 1 for buildings of normal importance, as is the case; and a_{gR} is the reference acceleration of the ground for a soil type A.

The value of the PGA_d or $S_e(T=0)$, which defines the elastic spectrum for horizontal loads, is determined as:

$$0 \leq T \leq T_B : S_e(T) = a_g \cdot S \cdot \left[1 + \frac{T}{T_B} \cdot (\eta \cdot 2, 5 - 1) \right] \quad (4.25)$$

where:

- S is a coefficient that depends on the type of soil, being in this case equal to 1.2 (soil type B);
- T is the period of the building under study, in this case, it is considered to be 0;
- T_B is the period that defines the end of the first branch of the spectrum;
- ν is a coefficient that depends on the damping of the structure.

Therefore, the $PGA_d(\text{EN1998})$ is:

$$T = 0 : S_e(T) = \gamma_I \cdot a_{gR} \cdot S \cdot 1 = 1 \cdot 0.19\text{g} \cdot 1.2 \cdot 1 = 0.228\text{g} \quad (4.26)$$

Summary of results for the seismic demand A summary of results derived from the application of the different regulations and seismic hazard maps available is included in Table 4.10.

Regulation and hazard map	PGA_d
NCSE-02 and maps in force	0.124g
NCSE-02 and new hazard maps (IGN and UPM)	0.228g
EN-1998 and new hazard maps (IGN and UPM)	0.228g

Table 4.10: PGA_d : Demand of Peak Ground Acceleration according to the different regulations and the seismic hazard maps applicable to Lorca.



Figure 4.13: Buildings classification according to the RESISTO method.

4.4.4 Vulnerability and comparison Demand—Capacity

In this section, the RE.SIS.TO classification of all the buildings is performed.

4.4.5 RE.SIS.TO classification

In order to improve the perception of the analysis results, the simplified RESISTO classification, described in Section 4.2.3, is here applied.

The quantitative values obtained from the comparison between peak ground acceleration of the building and in-situ demand in terms of acceleration, are used to assess the safety level of the building. Those values are compared with vulnerability ranges proposed in the RE.SIS.TO simplified classification. A chromatic scale helps to identify the right class to which the building belongs. The scale uses colors from red to green, where obviously, the red color corresponds to the worst class, instead the green color refers to the better class. Initially a class is assigned, and it could vary from I (low vulnerability) to V (high vulnerability), depending on the ratio between the capacity and the demand, in terms of ground acceleration. If considerable critical elements are present, the technician expertise is needed, and this judgment could change the class to a higher class (so pejorative), with respect to the ones resulting from the PGA ratio.

PGA_c/PGA_d	Class of resistance
0%- 25%	V
25%- 50%	IV
50%- 75%	III
75%- 100%	II
> 100%	I

Table 4.11: Summary of parameters for the building taken as an example

Figure 4.14 shows the results for all the buildings studied. The results clearly illustrate the fact that the M11 typology is the most vulnerable one. Moreover, a significant number of the buildings (8/20) are consider classes IV or V. It is worth mentioning that the PGA used as demand for said comparison is that provided by the most recent Spanish hazard maps (0.228g).

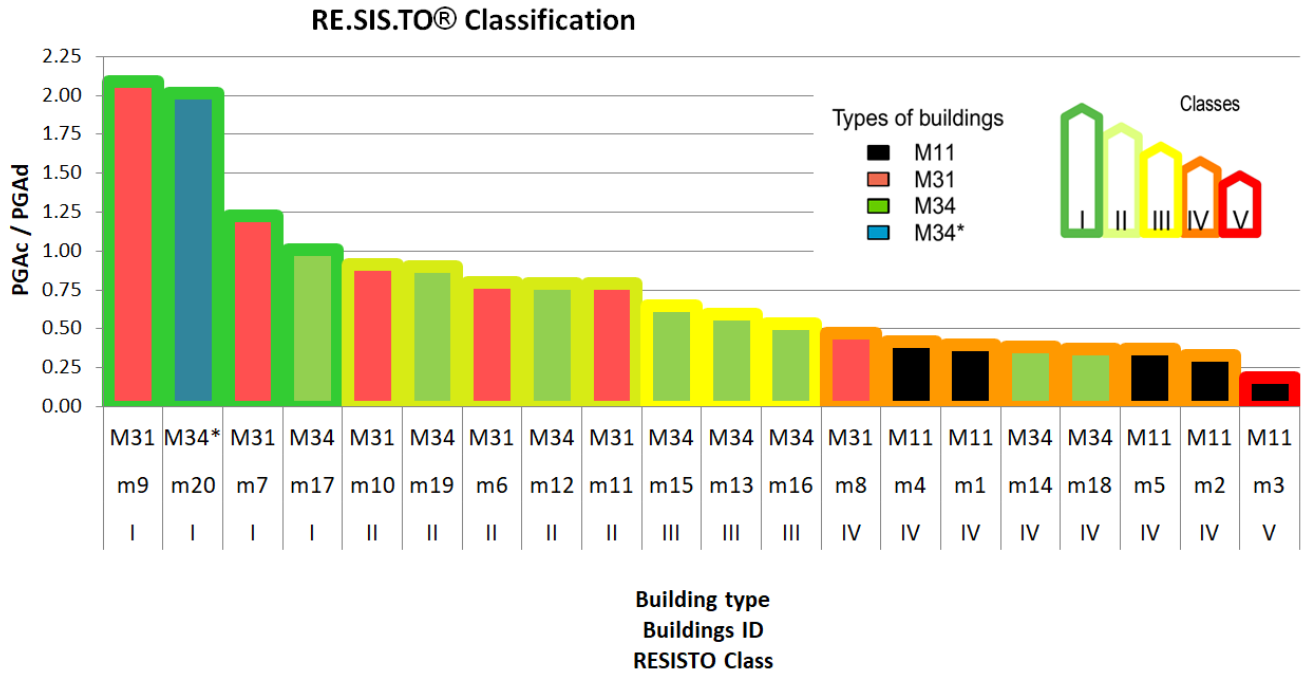


Figure 4.14: Buildings classification according to the RESISTO method.

4.4.6 Possible interventions

To obtain that the building is able to withstand the seismic actions established in the latest seismic hazard maps, it will be necessary to intervene in almost all the buildings, except from m9, m20, m7 and m17 (Fig. 4.14).

In Fig. 4.15, the parameters influencing their vulnerability according to the RE.SIS.TO. method are statistically studied. According to the results, the worst class of vulnerability, type D, is the most present in Parameter 8 (maximum distance between walls, section 4.4.1). This means that some transversal walls or elements should be added to the longest walls, in order to reduce their tendency to out-of-plane failure mechanism, that also reduce their capacity against in-plane loads.

With respect to parameter 3 (Shear Resistance, section 4.4.1), the solution is to increase the resistance area or increase the shear strength τ_0 of the walls involved. For some of said buildings, particularly those with lesser capacity, the later solution is insufficient because they have also shown local vulnerabilities in the roof system (a number of them presented roof system local collapses after the Lorca earthquake).

4.5 Fragility curves of the masonry typologies of the municipality of Lorca

The methodology that must be apply to develop FC should depend on the objective of each FC. In this research, these three cases are contemplated:

- **Life saving and regulation case:** Assessment of the capacity and quality of the design of a particular typology with respect to the demand established in the latest seismic hazard maps developed. In this case, the FCs should consider the worst case in term of resistance, as the objective is to ensure that the building is capable of withstanding the seismic event no matter its direction. (*FC for $S_{a,c}$ minimum*)
- **Current seismic risk studies case:** Development of fragility curves for seismic risk studies in which the hazard and exposure maps do not consider the direction of the seismic source in conjunction with the direction of the building. In this case, the most realistic fragility curve is the one that considers a ponderation of the FC obtained for each direction. A proposal to ponder this is presented. (*Unique FC for $S_{a,c}$*)
- **Future line of development of seismic risk studies:** Development of fragility risk studies in which the

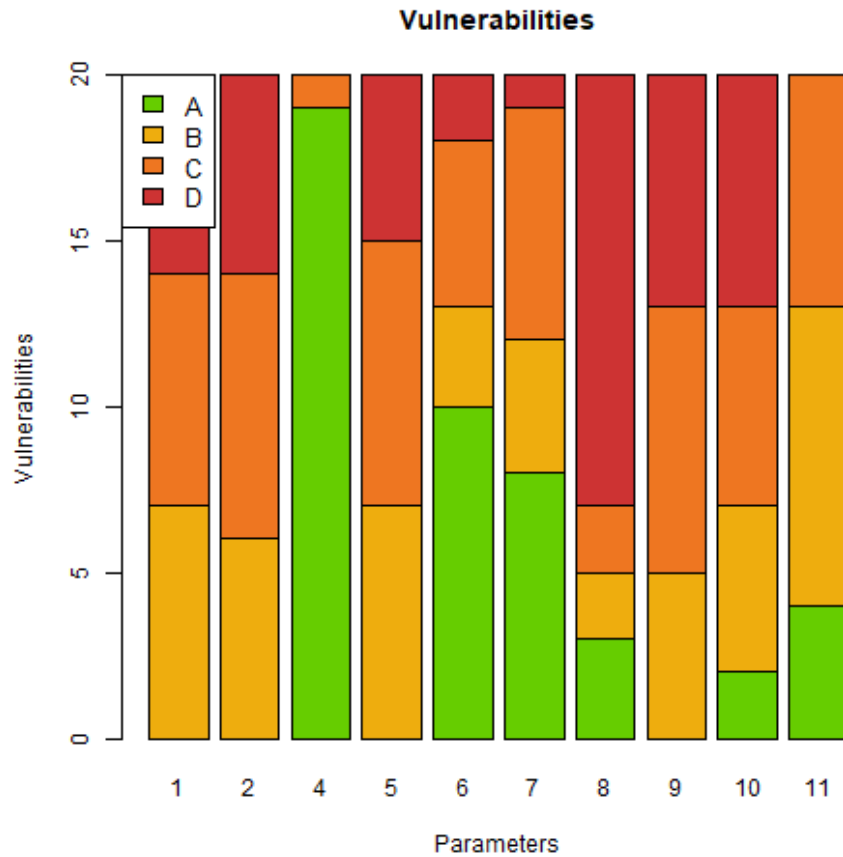


Figure 4.15: Type of vulnerability for each of the studied parameters (see Table 4.1). Parameters:

1. Type and organization of the resistant system;
2. Quality of the resistant system;
4. Location of the building and foundations;
5. Horizontal structural elements;
6. Plan configuration;
7. Elevation configuration;
8. Maximum distance between walls;
9. Roof system;
10. Non-structural elements;
11. State of conservation.

seismic sources and the direction of the buildings are well characterised. This fact permits the evaluation of the effects of the earthquake considering directionality. In this case, all the FCs are useful, those developed for both main directions and the FC developed to consider statistically the directionality in a unique FC. (*FCs for $S_{a,c}$ minimum, $S_{a,c}$ maximum and Unique FC for $S_{a,c}$*)

The tool that was used for the construction of all the fragility curves is the Monte Carlo method, passing through the definition of the response surfaces of each building typology with respect to significant structural parameters.

4.5.1 Methodology to develop the fragility curves

In order to define the fragility curves upon collapse of the prevalent masonry typologies, it is necessary to extend the data available, identifying relationships between the selected Intensity Measurement found for the M11, M31 and M34 buildings in question and the most significant mechanical/ geometric characteristics.

Firstly, it is necessary to define a reliable trend of variation of a specific characteristic starting from the available data. After that, it is possible to simulate the result in terms of the selected Intensity Measurement, in this case

$S_{a,c}$, exploiting the relationship obtained which is configured as a response surface of the building typology in question. At this point, the Monte Carlo method is applied to produce a sufficiently large number of possible combinations of variables. Finally, a log-normal distribution is adjusted to the results for each one of the type of buildings.

The Monte Carlo method

Many quantitative problems in science, engineering, and economics are nowadays solved via statistical sampling on a computer. Such Monte Carlo methods can be used in three different ways: (1) to generate random objects and processes in order to observe their behavior, (2) to estimate numerical quantities by repeated sampling, and (3) to solve complicated optimization problems through randomized algorithms. [11].

Therefore, the Monte Carlo simulation consists in the application of a series of algorithms to reproduce and numerically solve a problem in which several random variables are involved, but for which there is little known starting data. In practice, the Monte Carlo method is based on the fact that a direct analytical solution to the problem, that is, one that allows to directly explicit the link of the output that is to be obtained with the input data, may be too burdensome or perhaps impossible.

Hence, the problem is solved numerically by means of numerical simulations, producing a sufficiently large number N of possible combinations of the values that the input variables can assume, and calculating the relative output on the basis of the equations of the model. To construct each of the N combinations, a value is randomly generated (ie 'extracted') for each input variable, in accordance with the specified probability distribution and respecting the correlations between variables. Repeating this procedure N times (with N sufficiently large to allow statistically reliable results, making the intrinsic error of the method 'negligible'), a N independent values of the output variable are obtained, which therefore represent a sample of the possible values that can be assumed by the output. The sample can be studied with statistical analysis techniques to estimate the descriptive parameters, reproduce frequency histograms, and numerically derive the trends of the output distribution functions.

The main feature of these techniques is to evaluate a certain quantity of output through parameters such as mean ν , variance σ^2 and correlation of a certain probability distribution. Furthermore, the goodness or otherwise of the Monte Carlo simulation strongly depends on the assumptions underlying the model and on the equations, provided as inputs, which express the mathematical relationships between the input and output variables.

In Monte Carlo probabilistic simulations, the method of generating the statistical sample is of particular importance: the sampling method used, in fact, directly affects not only the goodness of the results obtained but above all the computational efficiency of the entire process. The sampling method is required not only to produce a statistically representative sample of the statistical population examined but also, in order to optimize the computational efficiency of the probabilistic simulation, to maintain a good representativeness of the sample as its size decreases. The simplest and most intuitive sampling method is based on the purely random or more properly pseudo-random generation of the elements of the sample itself.

To improve the efficiency of the Monte Carlo method, more refined sampling methods can be used that generate the individuals making up the statistical sample following appropriate criteria that ensure their representativeness even for small sizes.

The sampling applied in this research is based on random extractions of parameters appropriately selected as representative of the different types of masonry, and significant for the simplified analysis RE.SIS.TO. applicable on a large scale. The extractions are carried out considering log-normal variables of the parameter A_r/A_t and τ_0 , calibrated on the representative data of the buildings studied in the selected building practices. This selection of variables is founded on previous works (see [23] and [27]).

The following paragraphs show the construction of the fragility curves by means of the Monte Carlo method [2] for the different topological classes. Moreover, a manner of considering the unpredictable directionality of the seismic actions in the construction of the FCs is studied and a simplified proposal to do so provided.

Definition of response surface for each typology

In order to define the fragility curves upon collapse of the three main types of masonry in the Municipality of Lorca (M11, M31 and M34) it is necessary to extend the data available, identifying the relationships between the selected Intensity Measurements found for the buildings under examination and the most significant mechanical / geometric characteristics. In this case, the $S_{a,c}$ is defined as the most appropriate Intensity Measurement as the latest hazard maps developed in Spain incorporate the hazards in this magnitude and because the RESISTO method provides the PGA_c as a magnitude derived from the primitive $S_{a,c}$. In total, a sample of 19 building is considered:

- 5 buildings [from m1 to m5] for M11;
- 6 buildings [from m6 to m11] for M31;
- and 8 buildings [from m12 to m19] for M34 (m20 has not been included as it is not completely representative of the typology).

Firstly, a reliable variation trend of a specific characteristic had been defined starting from the available data for each direction (Table 4.12 and 4.14).

After that, in order to simulate the result in terms of $S_{a,c}$, a response surface of the building type in question is elaborated as a possible relationship between the variables involved (see Figures 4.17, 4.18 and 4.19 and Table 4.14).

To determine a single correlation function of $S_{a,c}$ with the structural parameters of resistant area on total area (A_r/A_t) and average shear strength $\tau_0[N/mm]$, multiple linear regression models were applied. The variable $y = S_{a,c}$ is the 'response variable', which is dependent on the variables $x_1 = \tau_0$ and $x_2 = A_r/A_t$ (called 'independent or predictive variables').

$x_2 = A_r/A_t$ were already detailed in Sections 4.4.1 and 4.4.2 and can be described as follows. $A_{r,min}$ and $A_{r,max}$ are the resistant area of the walls in either direction of the two main orthogonal considered, specifically, the one corresponding to the story with the minimum resistant capacity in terms of $S_{a,c}$. A_t is the floor area corresponding to the floor with the resistant area considered for $A_{r,min}$ and $A_{r,max}$.

Two different correlation functions have been adopted, of increasing complexity, depending on the number of data available for each type:

Equation A: for typologies M11, M31 and M34:

$$y = \beta_1 + \beta_2 x_1 + \beta_3 x_2 \quad (4.27)$$

Equation B: for typologies M31 and M34:

$$y = \beta_1 + \beta_2 x_1 + \beta_3 x_2 + \beta_4 x_1 x_2 \quad (4.28)$$

In which:

- β_1 is the intercept, that is the value of y when all the values x_i are all equal to zero;
- β_2, β_3 are the coefficients of the first and second characteristics respectively;
- β_4 is the coefficient of the interaction term $x_1 x_2$.

The purpose of multiple linear regression is to determine the best plane or curved surface, which intercepts the starting data and, to do so, it is necessary to estimate the regression coefficients β for each adopted function.

Thanks to a processing with a script in the Matlab environment (Mathworks), [23], the following functions have been obtained for the three prevalent types: for each type, the calculation procedure described up to now has been differentiated into three cases depending on the direction of the building considered in terms of capacity:

- (i) **Minimum capacity case:** $S_{a,c,min}$ the case defined in start from the parameters corresponding to the smaller $S_{a,c}$ (called 'minimum');
- (ii) **Maximum capacity case:** $S_{a,c,max}$ the case corresponding to the maximum value of $S_{a,c}$ (called 'maximum');

(iii) Case considering the seismic directionality: $S_{a,c,unique}$ the case corresponding to a unique FC that ponders the unpredictable direction of the earthquake.

In the following, the results obtained for the maximum and minimum capacity cases, (i) and (ii), and the methodology proposed to obtain the inputs for the case in which the directionality is considered, (iii), and its results are detailed.

Minimum and maximum capacity cases [(i) and (ii)] The results obtained for the minimum and maximum cases, illustrate the fact that in general the $S_{a,c}$ increases as the ratio A_r/A_t increases.

Directionality case [(iii)] A method to develop a unique FC that ponders the minimum and maximum cases is proposed in order to take into account in an statistical manner the unpredictable direction of the earthquake. Moreover, it is compared with the results of the application of the conflation method to ponder two statistical distributions.

Conflation method The method called conflation is a probability-averaging alternative that has several benefits and none of the drawbacks of existing averaging techniques. The conflation of several input distributions is the probability distribution with density equal to the normalised product of the input densities, which optimally and unbiasedly summarises the data [8]. Considering that FCs are log-normal conditional cumulative probability distributions, the basic principles of conflation, derived by [8], to the special case of normally distributed (Gaussian) data have been applied. This methodology considers that both directions would be equally probable in terms of earthquake directionality.

Proposal for pondering the minimum and maximum cases The proposal herein exposed is based on mathematical considerations and on the primal parameters involved in the calculus of the FCs (τ_0 , A_r and $S_{a,c}$). From this three parameters, τ_0 does not depend on the seismic directionality but just on the characteristics of the building; however, A_r is a variable that clearly depends on the directionality and determines the capacity to withstand the earthquake, i.e. $S_{a,c}$. For that reason, our proposal establishes a manner of defining a resistance area ($A_r, unique$) that ponders the unpredictable directionality of the earthquake and give rise to a $S_{a,c, unique}$ that can serve as a base for the construction of the FCs.

Then, our objective can be described as finding a manner of pondering the fact that in each direction, each building presents a different A_r —being especially remarkable $A_{r,minimum}$ and $A_{r,maximum}$ —, and that all directions must have the same weight in the ponderation.

The herein proposed way of doing said ponderation is based on the fact that, mathematically, the areas of a circle and an ellipse are the sums of all their radius weighted by the length of one half of the corresponding arch, proportional to the same radius. Then, let us pose the following geometrical figures (see Fig. 4.16 for conceptualization and colours): two circles with radius $A_{r,minimum}$ (blue) and $A_{r,maximum}$ (green) respectively; and an ellipse with the same two values for its radius, $r_1 = A_{r,minimum}$ and $r_2 = A_{r,maximum}$ (maroon). Then, we can define a new circle (orange) whose area is equal to that of the ellipse described. Consequently, this new circle (orange) will have a radius ($A_r, unique$) that ponders the weight of the resistant areas according to the elliptical model for all directions in an equiprobable manner. Equations (4.29), (4.30) and (4.31) summarise the mathematical basis.

$$Area_{ellipse} = \pi * r_1 * r_2 = \pi * A_{r,min} * A_{r,max} \quad (4.29)$$

$$Area_{circle,unique} = \pi * A_{r,unique}^2 \quad (4.30)$$

$$Radius_{circle,unique} = A_{r,unique} = \sqrt{A_{r,min} * A_{r,max}} \quad (4.31)$$

Finally, we have to apply the methodology RE.SIS.TO. employing the found value for the resistant area $A_r = A_{r,unique} = r_{circle}$ of equal area to the ellipse (orange) for A_r for each of the floors; obtain the $S_{a,c, unique}$ for each building; and use the Monte Carlo method and response surfaces for the elaboration of the FCs. As previously described, the unique inputs required to elaborate the FCs with this procedure are the values of τ_0 , A_r for each of

ID	τ_0	A_r/A_t	A_r/A_t	$S_{a,c}$	$S_{a,c}$	A_r	A_r	A_r	A_r/A_t	$S_{a,c}$
		min	max	min	max	min	max	unique	unique	unique
M11										
m1	15	0.098	0.102	0.073	0.076	21.60	22.40	22.00	0.100	0.073
m2	15	0.045	0.113	0.060	0.171	3.80	7.90	6.84	0.080	0.094
m3	15	0.069	0.217	0.034	0.092	4.20	2.60	7.55	0.124	0.053
m4	15	0.075	0.151	0.076	0.149	6.50	16.30	9.36	0.108	0.098
m5	15	0.097	0.132	0.067	0.094	17.20	23.50	20.57	0.116	0.078
M31										
m6	30	0.133	0.207	0.146	0.212	8.00	12.40	9.92	0.165	0.169
m7	42	0.057	0.090	0.224	0.349	13.20	20.60	16.49	0.072	0.262
m8	20	0.063	0.097	0.086	0.143	4.70	7.30	6.47	0.086	0.109
m9	65	0.035	0.057	0.477	0.722	2.90	4.70	3.69	0.045	0.566
m10	20	0.083	0.094	0.167	0.188	16.00	18.00	16.97	0.088	0.172
m11	30	0.047	0.079	0.144	0.242	4.40	7.40	5.71	0.061	0.172
M34										
m12	65	0.017	0.034	0.145	0.272	3.40	5.10	4.74	0.024	0.190
m13	20	0.039	0.052	0.109	0.144	5.00	6.60	5.75	0.045	0.120
m14	20	0.049	0.050	0.070	0.072	5.00	5.10	5.05	0.050	0.070
m15	40	0.027	0.067	0.118	0.326	2.40	5.80	4.04	0.045	0.179
m16	65	0.028	0.205	0.097	0.700	2.70	19.50	7.26	0.076	0.226
m17	30	0.019	0.042	0.085	0.205	4.30	10.80	7.98	0.035	0.139
m18	65	0.022	0.041	0.164	0.381	2.30	8.60	4.18	0.040	0.272
m19	65	0.041	0.026	0.184	0.288	3.20	5.00	4.00	0.033	0.218

Table 4.12: Main features of the buildings studied in relation to the development of FCs. Parameters denoted with the word *unique* make reference to the Directionality Case (iii).

- τ_0 in kN/m^2 ;

- $A_r/A_{t,min}$ or max or *unique* without units. $A_{r,min}$ and $A_{r,max}$ are the resistant area of the walls in either direction of the two main orthogonal considered, specifically, the one corresponding to the story with the minimum resistant capacity in terms of $S_{a,c}$. A_t is the floor area corresponding to the floor with the resistant area considered for $A_{r,min}$ and $A_{r,max}$. $A_{r,unique}$ is the A_r calculated according to the proposal to consider the seismic directionality (Eq. 4.31), and A_t the floor area for which has been calculated;

- $S_{a,min}$ or max or *unique* in g .

* In some cases, the worst floor is not the same when considering the x and y directions. For that reason, in these cases, it may occur that $A_{r,min}$ is greater than $A_{r,max}$, or, $A_r/A_{t,min}$ is greater than $A_r/A_{t,max}$ or $A_r/A_{t,unique}$. This is for example the $m3$ building case. In these situations, $A_{r,max}$ has not been considered the area of greater value because, for coherence, it must correspond with the value that relates to the maximum resistant capacity in terms of $S_{a,c}$

the floors and the results in terms of $S_{a,c}$ of each of the buildings.

Therefore, employing the radius $A_r, unique$ in the methodology RESISTO, we will obtain a $S_{a,c, unique}$ in which the direction of the earthquake is statistically evaluated. Nevertheless, this proposal can be improved, but represent a first approximation in a straightforward manner of considering the uncertainty of the seismic directionality for a expeditious methodology. That is to say, a methodology whose objective is to assess a large scale of buildings about which we have limited information in a reasonable amount of time.

Definition of the fragility curves of the structural typologies prevalent in the Municipality

Once the regression coefficients and therefore the function y —as a function of the ratio of resistant area to total area A_r/A_t and the average shear strength τ_0 — are obtained, the fragility curves were elaborated using the Monte-carlo method.

The sampling applied is based on random extractions from log-normal variables of A_r/A_t and τ_0 calibrated on the representative data of the buildings analyzed in the case study, i.e. random extractions of the two selected

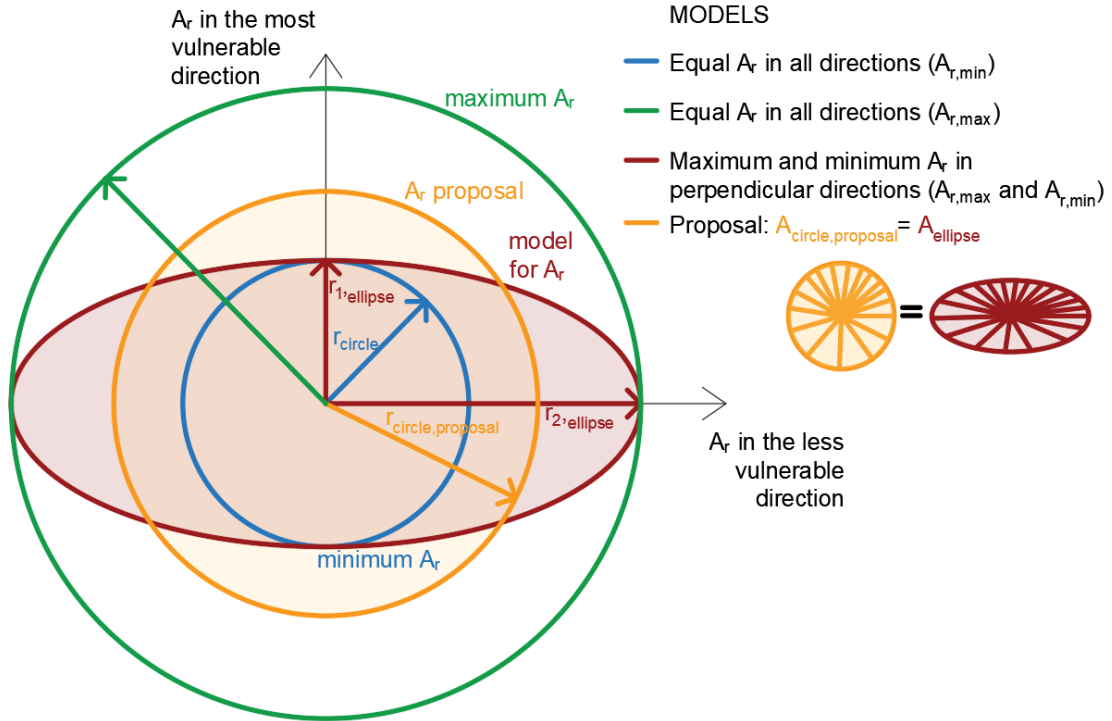


Figure 4.16: Conceptual schema of the proposal basis.

structural parameters that influence the seismic behavior of the masonry. Therefore, log-normal distributions of A_r/A_t and τ_0 have been implemented, centered on the average values of the available data. To do this, the mean μ and the standard deviation σ values associated with each parameter are provided in Table 4.14 for each type of buildings. These values shown in the table have been calculated with respect to the logarithmic values of the quantities A_r/A_t and τ_0 , in order to avoid the extraction of negative area values, which would have been meaningless. 100.000 random extractions of pairs of values of A_r/A_t and τ_0 were defined to calculate the respective $S_{a,c}$ starting from the response surfaces, for each type.

Once the response surfaces were defined, the computed high number of $S_{a,c}$ (capacity) was compared with a set of random values of $S_{a,d}$ (demand), so as to calculate the cumulative number of simulated buildings that reach collapse ($S_{a,c} < S_{a,d}$), for each structural type. The points obtained were interpolated with cumulative log-normal functions, whose trends are shown below, with the respective mean and standard deviation values, in which the blue points represent the values obtained with the Monte Carlo method (Figures 4.20, 4.21 and 4.22).

For each prevailing type, the relationships that bind the $S_{a,c}$ were calculated with the ratio between the % of resistant masonry area at the base of the buildings, and total area in plan of the building (A_r/A_{tot}) (Fig. 4.17, 4.18 and 4.19). Moreover, the $S_{a,c}$ trend is studied as a function of the shear strength of the masonry (τ_0), which significantly affects the result of the RE.SIS.TO.

In Table 4.13 are shown the values of the parameters obtained for equations A (eq. 4.27) and B (eq.4.28) for each typology.

4.5.2 Results

In the following Figures and Tables the results in terms of response surfaces, Monte Carlo results and FCs are referenced as convenience for the reader.

- Response surfaces:
 - Figures: M11 (Fig. 4.17), M31 (Fig. 4.18) and M34 (Fig.4.19).
 - Tables: Table 4.13.

Coefficients for eqS. A (4.27) and B (4.28)				
Type	β_1	$\beta_2 (x_1)$	$\beta_3 (x_2)$	$\beta_4 (x_1x_2)$
M11				
Min, Eq. A	$8.47 \cdot 10^{-18}$	2.58130	0.30385	-
Max, Eq. A	$1.16 \cdot 10^{-17}$	9.23850	-0.15524	-
Proposal, Eq. A	$4.28 \cdot 10^{-17}$	9.84964	-0.66881	-
M31				
Min, Eq. A	-0.01117	7.11445	-0.36770	-
Max, Eq. A	-0.01233	11.24271	-0.62651	-
Min, Eq. B	-0.02356	8.08899	0.40982	-33.77520
Max, Eq. B	-0.01675	11.56366	-0.45769	-7.07231
Proposal, Eq. B	-0.01966	9.37360	0.00315	-22.0945
M34				
Min, Eq. A	0.01133	1.82754	0.85165	-
Max, Eq. A	-0.04406	3.87319	2.38075	-
Min, Eq. B	0.00280	3.04394	1.77262	-61.36444
Max, Eq. B	-0.01008	3.36363	1.24352	18.43153
Proposal, Eq. B	0.00426	3.25308	0.89333	-8.65751

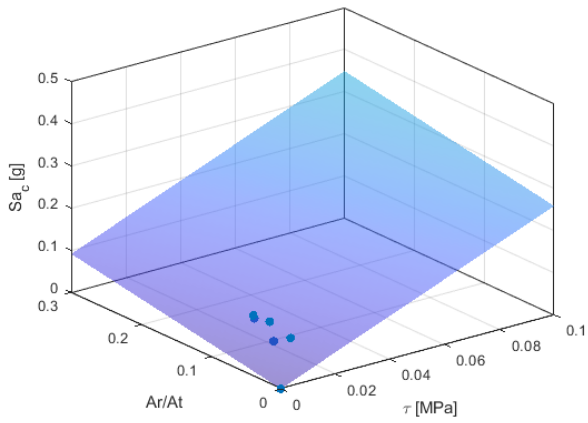
Table 4.13: Summary of coefficients of the response surfaces.

- Monte Carlo results:
 - Figures: M11 (Fig. 4.20), M31 (Fig. 4.21) and M34 (Fig.4.22).
- FC results:
 - Figures: Figs. 4.23, 4.24 and 4.25.
 - Tables: Tables 4.14 and 4.15.

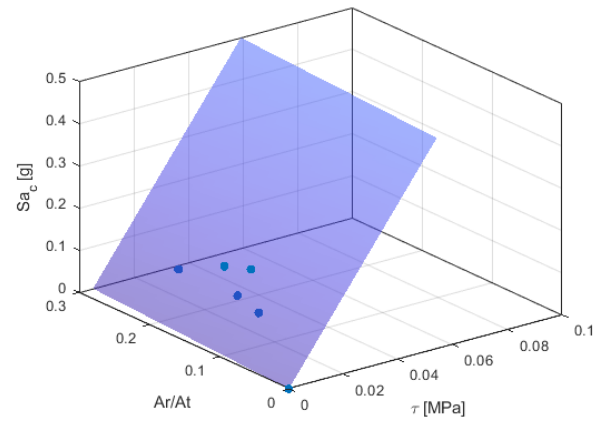
With respect to the resulting FC for different directions, it must be mentioned that:

- The low standard deviation value obtained in the FCs resulting from the application of the conflation method is due to the fact that it considers that, by combining data from two or more distributions, you have more information. Therefore, the variance or standard deviation of the resulting new distribution is expected to be smaller. In these cases, especially for the M11 typology, the conflation results do not seem sensible. This fact can be due to the assumption of the data from each of the distributions being combined are independent or arise from independent studies, which strictly speaking. they are not completely independent.

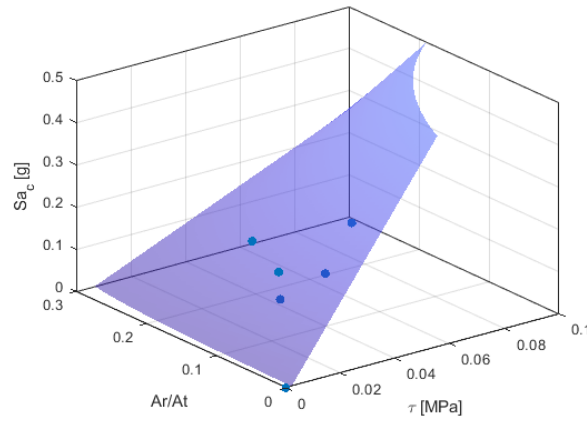
- The results for the proposed manner of including the earthquake directionality ($A_r, unique \rightarrow S_{a,c}, unique \rightarrow RESISTO \rightarrow FCs$) give raise to results that seems sensible and can be applied in seismic risk studies.



(a) M11, minimum Sa_c , equation type A

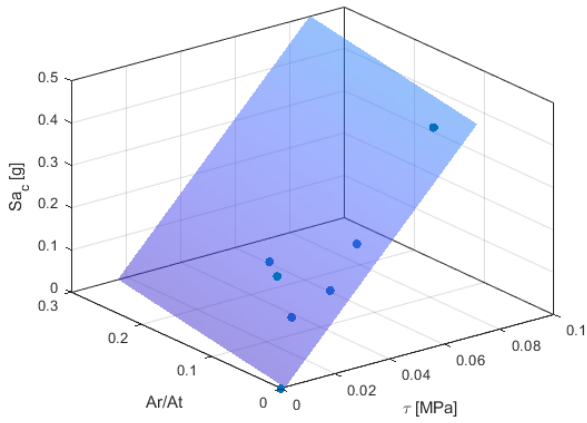


(b) M11, maximum Sa_c , equation type A

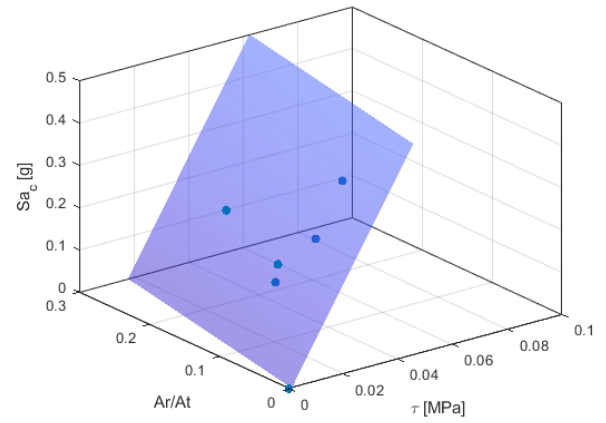


(c) M11, unique FC according to the proposed method (Sa_c , equation type A)

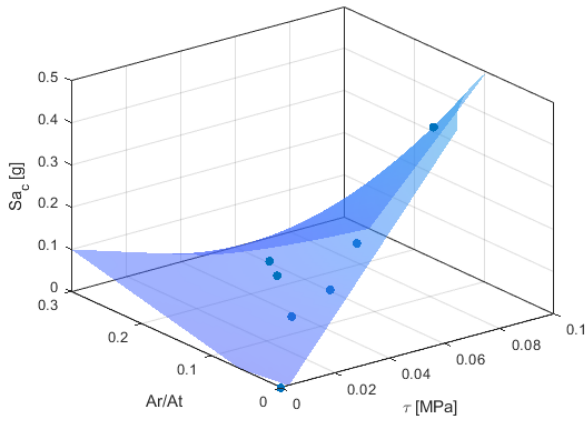
Figure 4.17: M11: Calibration of the response surfaces parameters for the different cases considered



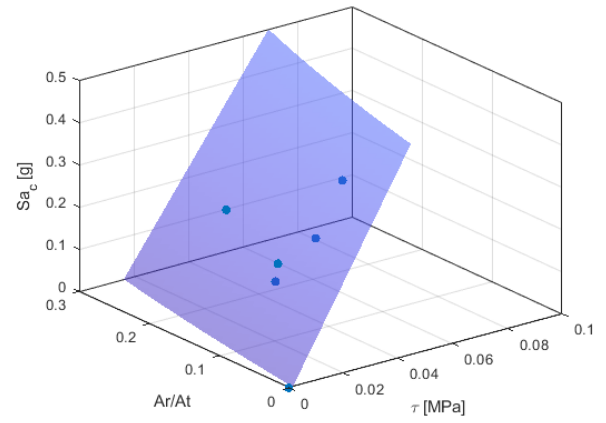
(a) M31, minimum Sa_c , equation type A



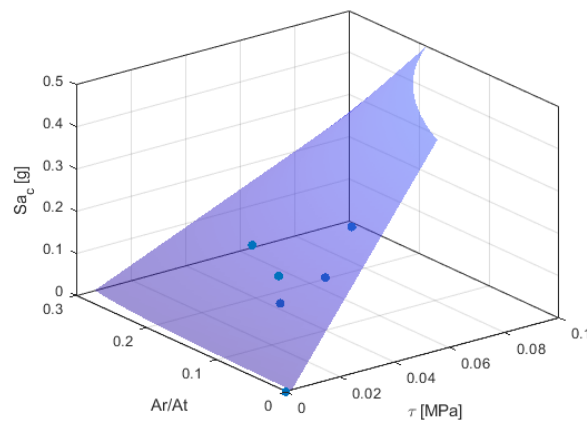
(b) M31, maximum Sa_c , equation type A



(c) M31, minimum Sa_c , equation type B

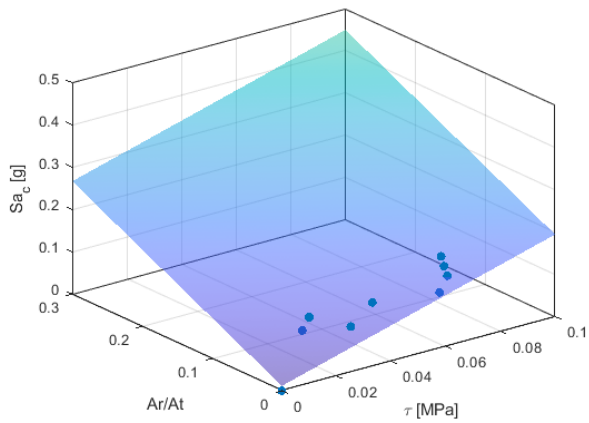


(d) M31, maximum Sa_c , equation type B

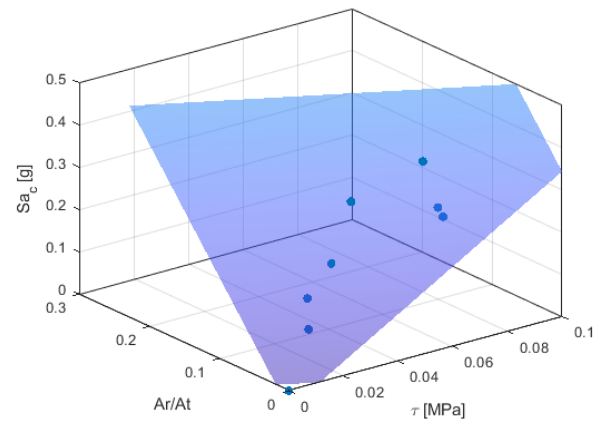


(e) M31, unique FC according to the proposed method (Sa_c , equation type B)

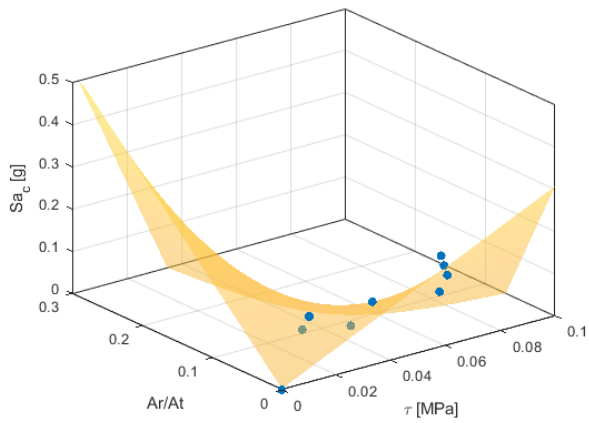
Figure 4.18: M31: Calibration of the response surfaces parameters for the different cases considered



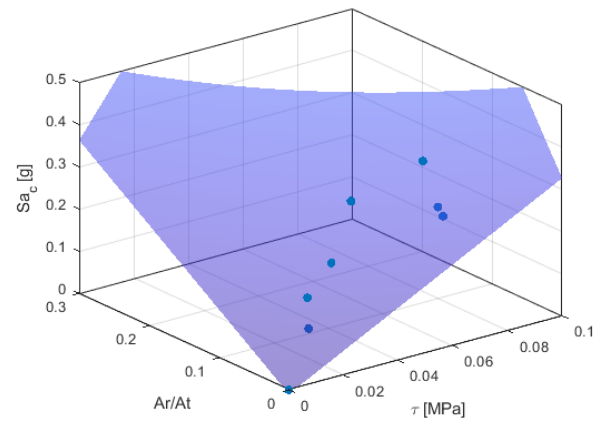
(a) M34, minimum Sa_c , equation type A



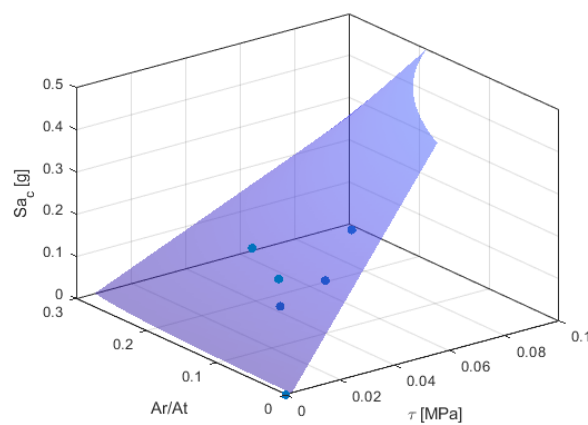
(b) M34, maximum Sa_c , equation type A



(c) M34, minimum Sa_c , equation type B

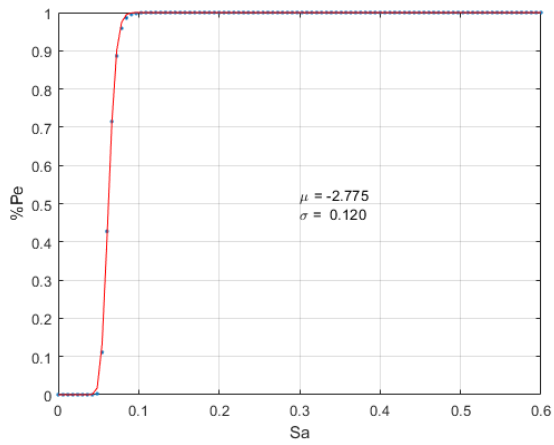


(d) M34, maximum Sa_c , equation type B

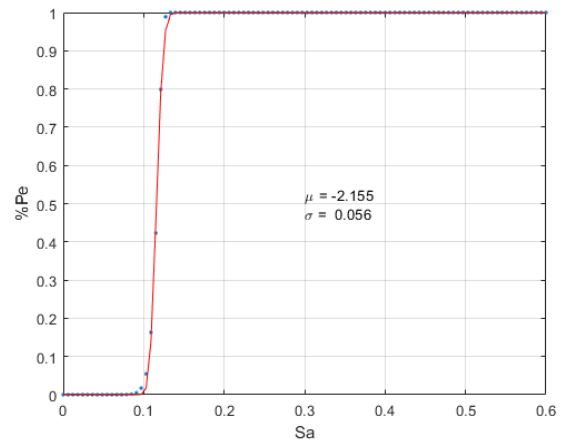


(e) M34, unique FC according to the proposed method (Sa_c , equation type B)

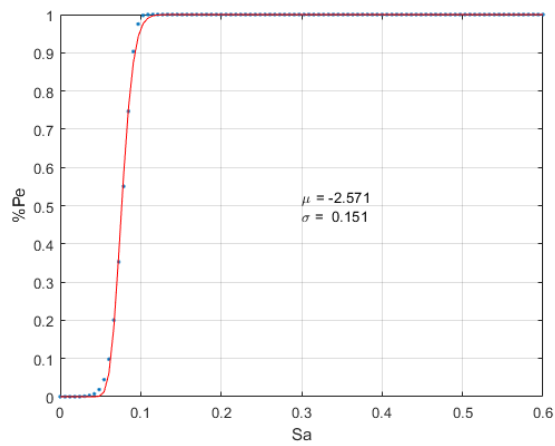
Figure 4.19: M34: Calibration of the response surfaces parameters for the different cases considered



(a) M11, minimum Sa_c , equation type A

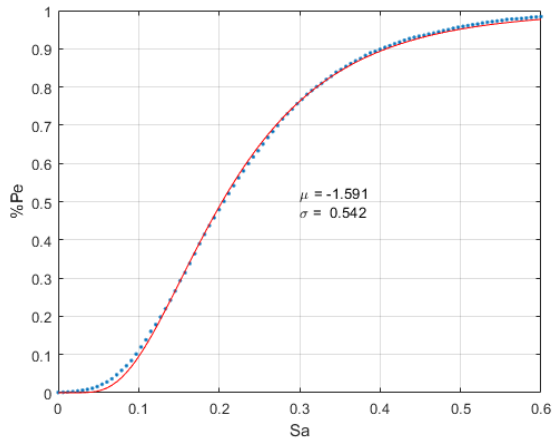


(b) M11, maximum Sa_c , equation type B

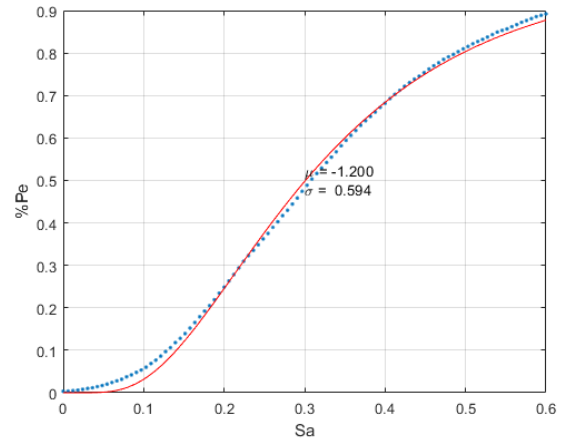


(c) M34, minimum Sa_c , equation type B

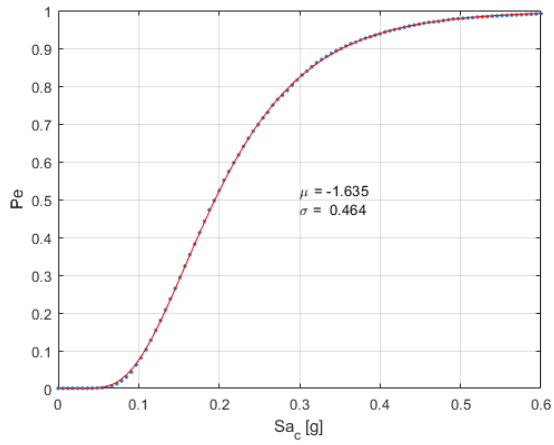
Figure 4.20: M11: Calibration of the FC for the different cases



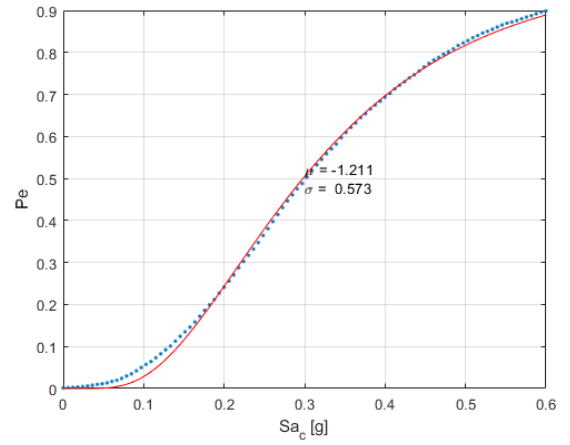
(a) M31, minimum Sa_c , equation type A



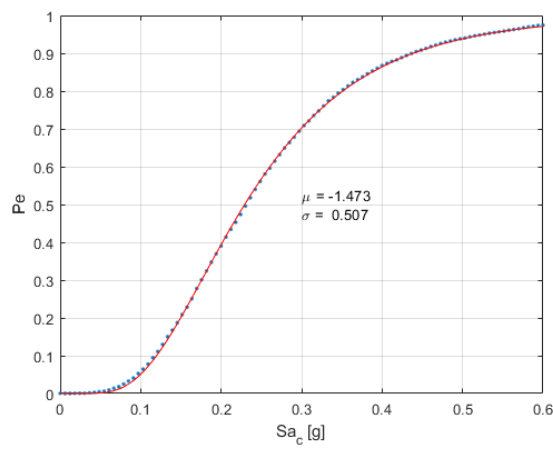
(b) M31, maximum Sa_c , equation type A



(c) M31, minimum Sa_c , equation type B

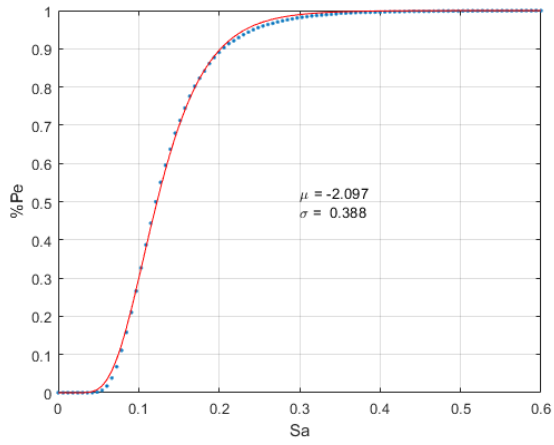


(d) M31, maximum Sa_c , equation type B

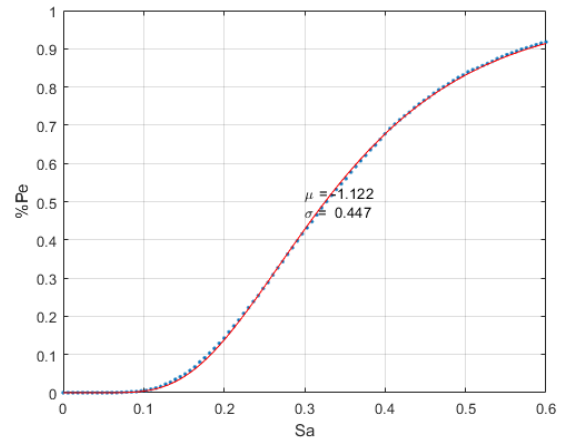


(e) M34, unique FC according to the proposed method (Sa_c , equation type B)

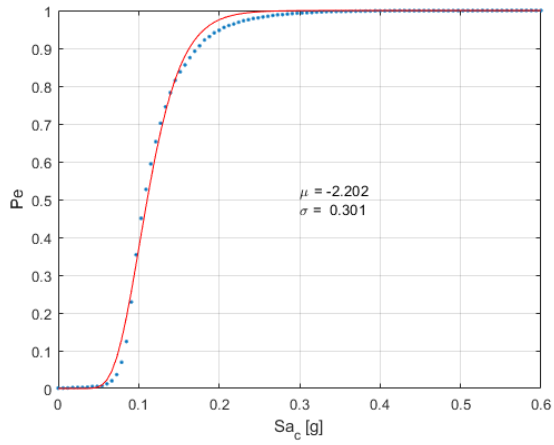
Figure 4.21: M31: Calibration of the FC for the different cases



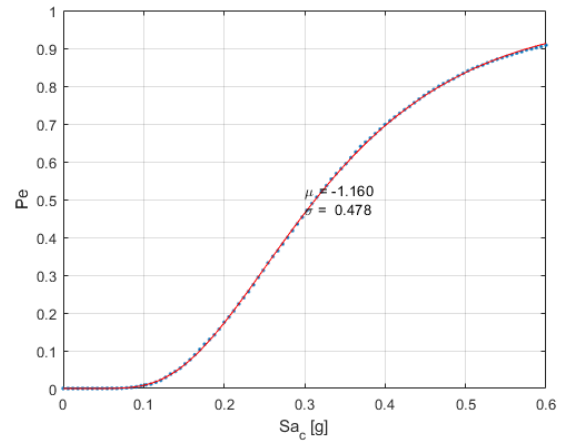
(a) M34, minimum Sa_c , equation type A



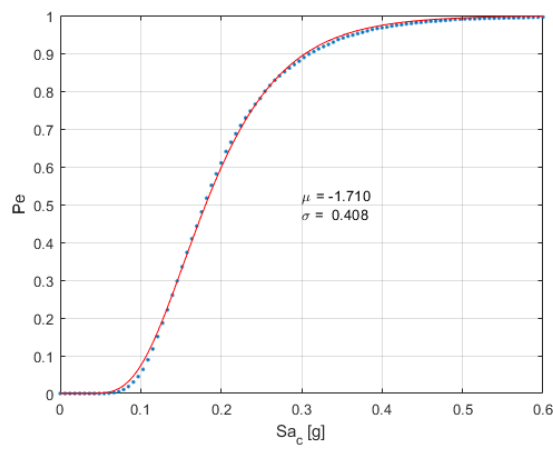
(b) M34, maximum Sa_c , equation type A



(c) M34, minimum Sa_c , equation type B

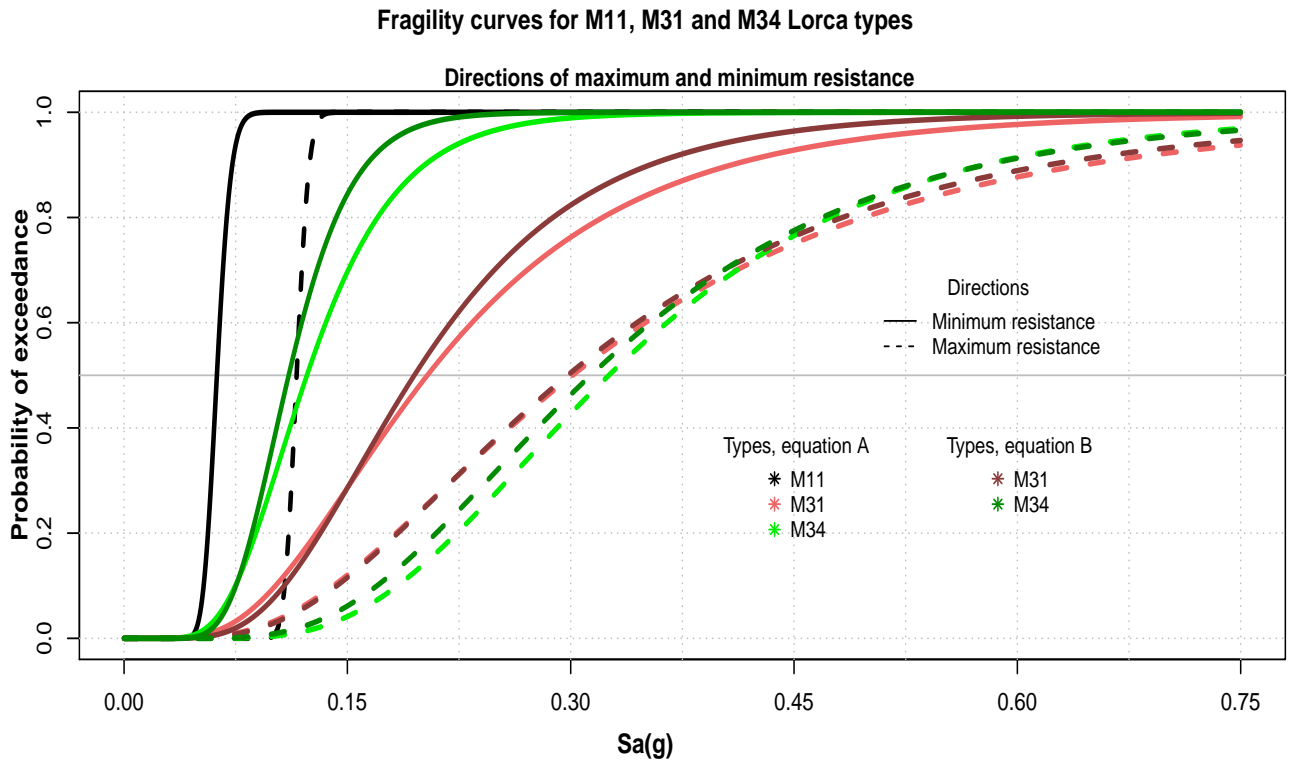


(d) M34, maximum Sa_c , equation type B

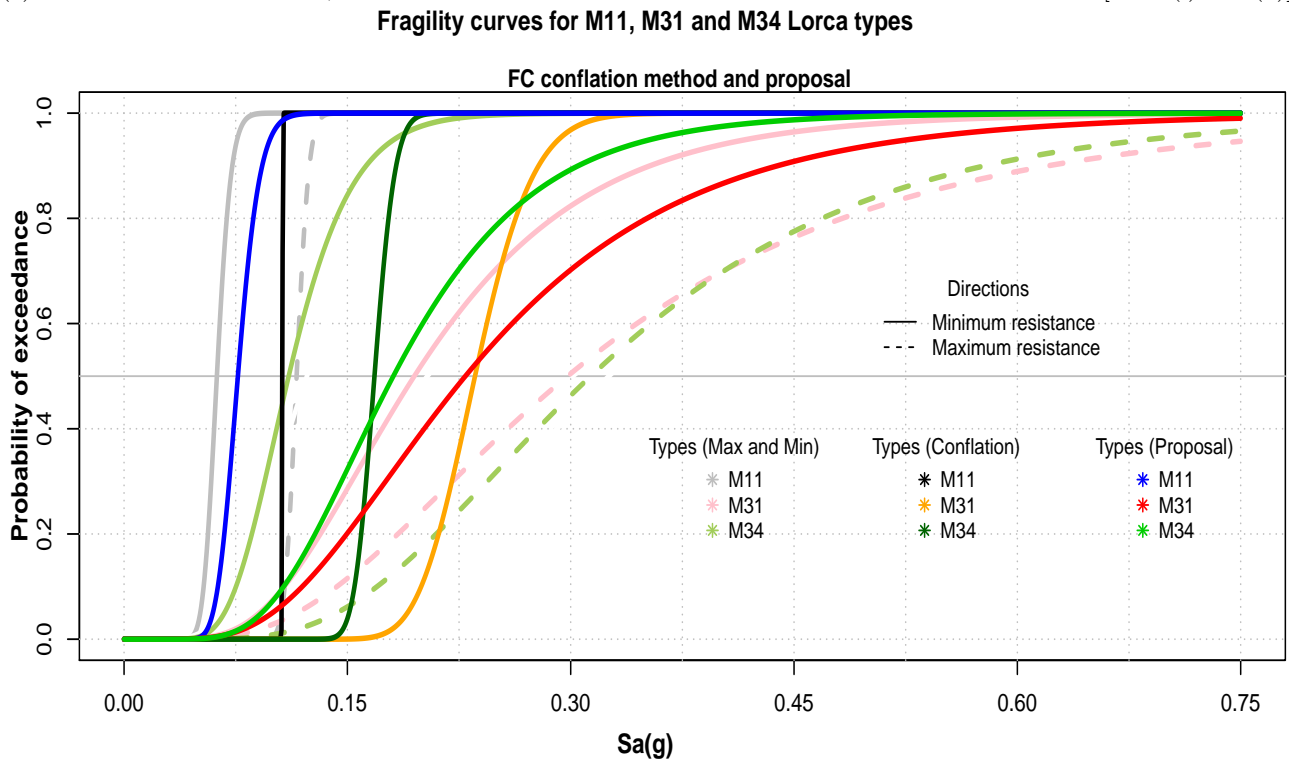


(e) M34, unique FC according to the proposed method (Sa_c , equation type B)

Figure 4.22: M31: Calibration of the FC for the different cases



(a) Obtained FCs for the M11, M31 and M34 in the directions of maximum and minimum resistance [cases (i) and (ii)]



(b) Obtained FCs for the M11, M31 and M34 by means of the application of the conflation method and the proposal elaborated in this dissertation for the case in which the seismic directionality is considered [case (iii)]

Figure 4.23: Fragility curves in Sa_c for the different cases: (i) Minimum capacity, (ii) Maximum capacity and (iii) case considering the seismic directionality. (See Fig. 4.24 for a better interpretation of results).

Fragility curves for M11, M31 and M34 Lorca types

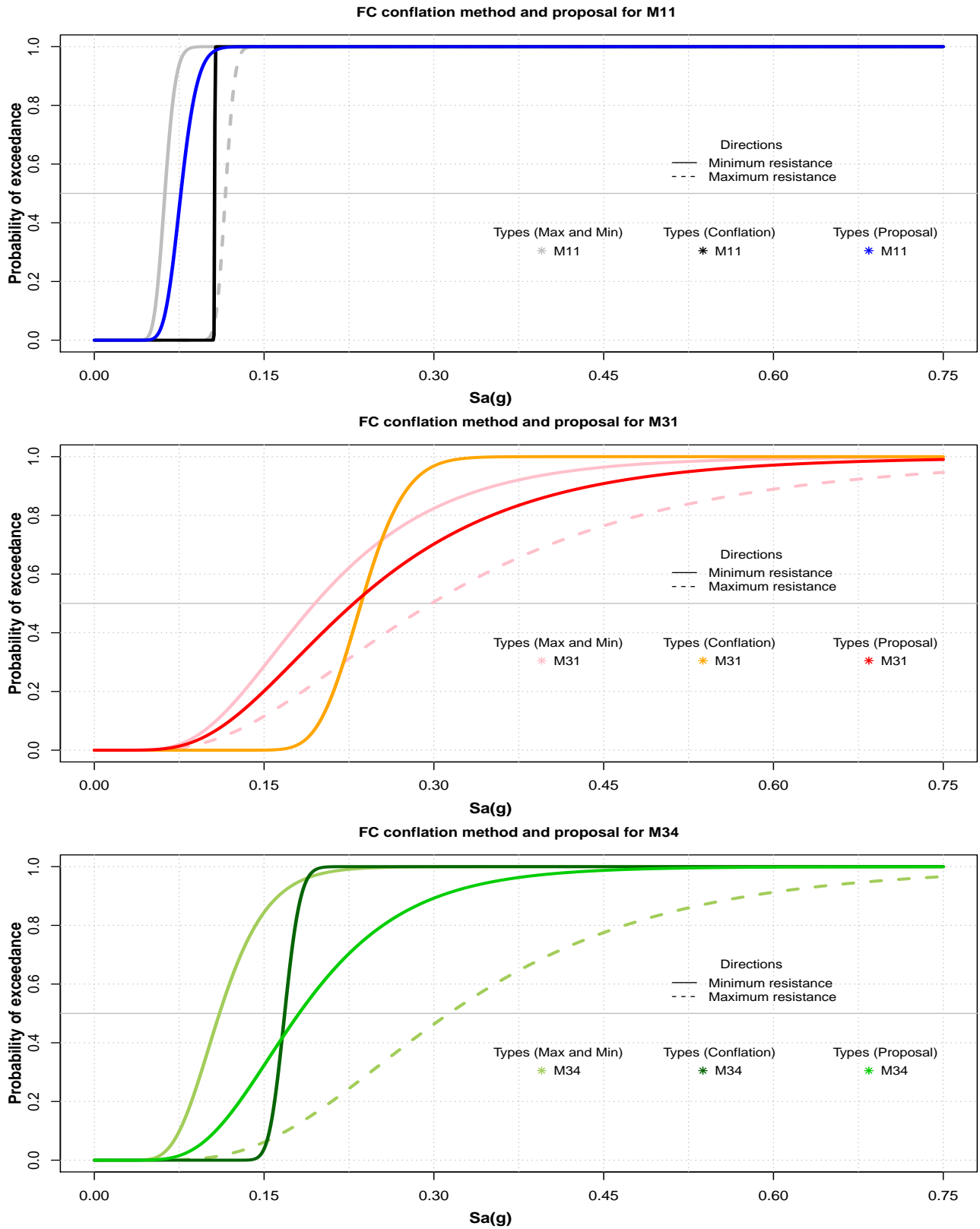


Figure 4.24: Fragility curves typology by typology in Sa_c for the different cases: (i) Minimum capacity, (ii) Maximum capacity and (iii) case considering the seismic directionality. Top: typology M11; center: typology M31; bottom: typology M34

	Buildings data		FC for both directions	
	A_r/A_t	τ_0	FC (eq.A)	FC (eq.B)
M11				
M11, min S_a				
σ	0.07662	0.01500	0.06235	-
μ	0.32029	0.00000	0.12000	-
M11, max S_a				
σ	0.14286	"	0.11590	-
μ	0.29427	"	0.05600	-
M31				
M31, min S_a				
σ	0.06982	0.03458	0.20372	0.19495
μ	0.46263	0.45428	0.54200	0.46400
M31, max S_a				
σ	0.10389	"	0.30119	0.2978
μ	0.42396	"	0.59400	0.57300
M34				
M34, min S_a				
σ	0.02844	0.04625	0.12282	0.11058
μ	0.35344	0.53151	0.38800	0.30100
M34, max S_a				
σ	0.07096	"	0.32563	0.31348
μ	0.54388	"	0.44700	0.47800

Table 4.14: Summary of parameters. Buildings data: median and standard deviation of the parameters used as inputs of the Monte Carlo procedure, A_r/A_t and τ_0 . FC for both directions: values of the median and standard deviation of the FC resulting from the application of the procedure for each typology in both directions (FC represented in Figs. 4.23 and 4.24).

	Unique FC for both directions		
	Data A_r/A_t proposal	FC (Proposal)	FC (conflation)
M11, S_a			
σ	0.10548	0.07646	0.10633
μ	0.16569	0.15100	0.00258
M31, S_a			
σ	0.08624	0.22924	0.23572
μ	0.43838	0.50700	0.13003
M34, S_a			
σ	0.04344	0.18087	0.16819
μ	0.33881	0.40800	0.06488

Table 4.15: Summary of parameters. Unique FC for both directions: values of the median and standard deviation of the FC resulting from the application of the procedure for each typology according to the proposal (FC represented in Figs. 4.23, 4.24 and 4.25). Conflation applied to Model B Equation for the Cases of M31 and M34.

4.6 Conclusions and future line of development of seismic risk studies

This work has contributed FCs for the masonry typologies present in the Municipality of Lorca (M11, M31 and M34). Said FCs can also be applied for Spanish cities with similar techniques of construction, for example, the region of Murcia and the south of Spain. The different analyses carried out along with the FCs developed have revealed the M11 typology is the most vulnerable one.

Furthermore, a method to compute the unpredictable direction of the seismic event has been proposed so as to develop a unique FC for seismic risk studies when the expeditious method RESISTO is applied.

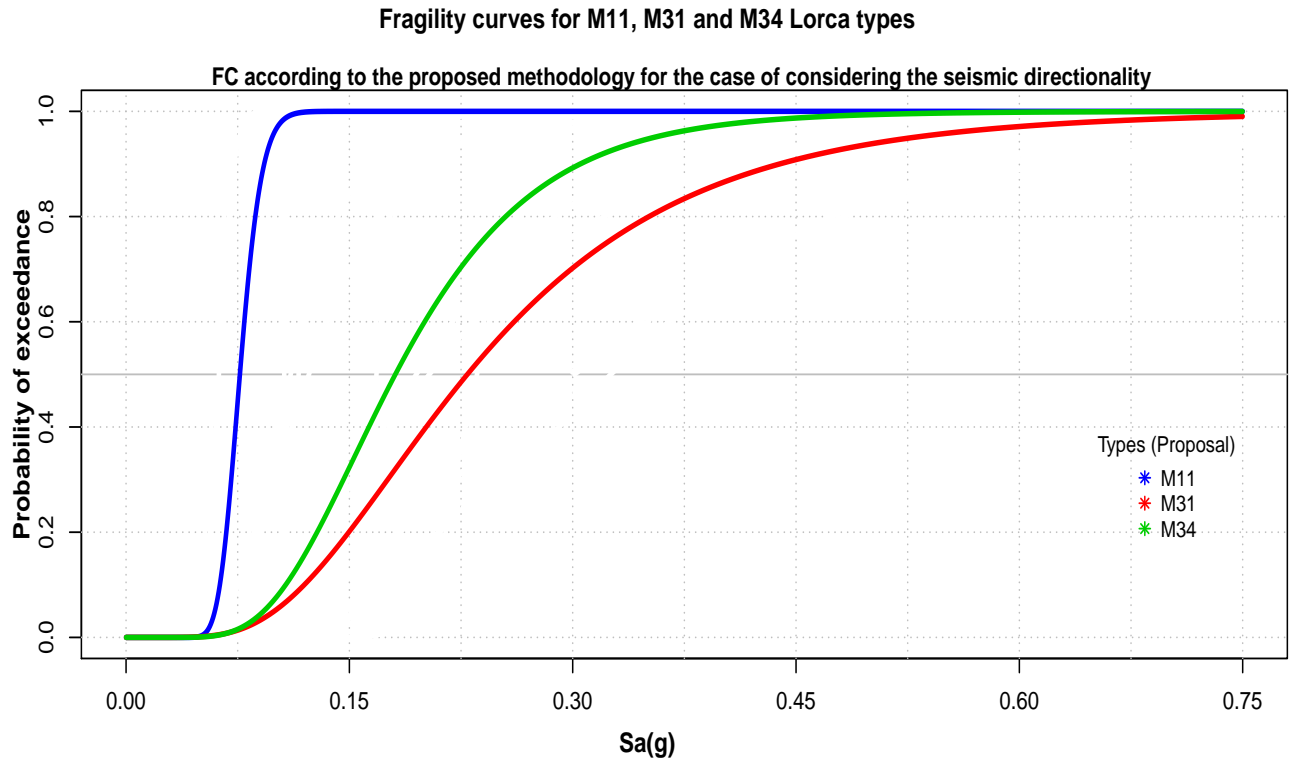


Figure 4.25: Fragility curves in Sa_c for the (iii) case: considering the seismic directionality according to the proposed methodology.

Future seismic risk studies and some current ones incorporate exposure maps that include the location of the different seismic sources and the position of the buildings for which the researcher wants to analyse the vulnerability and predict the possible level of damage suffered. This means that the FCs that account for the directionality will permit the development of seismic risk scenarios more accurately, with the consequent improvement in emergency management and the prevention of fatalities and economic losses.

References

- [1] Belén Benito Oterino et al. “El Terremoto de Lorca (2011) en el contexto de la peligrosidad y el riesgo sísmico en Murcia.” In: *Física de la Tierra* 24 (2012), pp. 255–287.
- [2] Ding-Geng Chen and John Dean Chen. *Monte-Carlo simulation-based statistical modeling*. ICSA Book Series in Statistics. Springer, 2017. ISBN: 978-981-10-3306-3,978-981-10-3307-0.
- [3] NCSR-22. Norma de Construcción Sismorresistente (upcoming). “Consulta pública previa sobre el borrador de Real Decreto por el que se aprueba la Norma de Construcción Sismorresistente NCSR-2022. Last visit 10/05/2023”. In: (). URL: www.mitma.gob.es/el-ministerio/buscador-participacion-publica/audiencia-e-informacion-publica-sobre-el-proyecto-de-real-decreto-por-el-que-se-aprueba-la-norma-de-construccion-sismorresistente-ncsr-22.
- [4] M Dolce and C Moroni. “La valutazione della Vulnerabilità e del Rischio Sismico degli Edifici Pubblici mediante le procedure VC e VM”. In: *Progetto SAVE, Atti di Dipartimento, vol 4* (2005).
- [5] M Dolce et al. “Valutazione della vulnerabilità sismica di edifici scolastici della Provincia di Potenza”. In: *Atti del XI Convegno Nazionale L’Ingegneria Sismica in Italia, Genova* (2004).
- [6] Mauro Dolce and Daniela Di Bucci. “National Civil Protection Organization and technical activities in the 2012 Emilia earthquakes (Italy)”. In: *Bulletin of earthquake engineering* 12.5 (2014), pp. 2231–2253.
- [7] EN-1998. “Eurocode 8: Design of structures for earthquake resistance - Part 1 : General rules, seismic actions and rules for buildings”. In: *European Committee for Standardization, Brussels*. (2003).

- [8] Theodore P Hill and Jack Miller. “How to combine independent data sets for the same quantity”. In: *Chaos: An Interdisciplinary Journal of Nonlinear Science* 21.3 (2011), p. 033102.
- [9] IGN, 2015. Developed by IGN and UPM. Last visit 08/02/2022. URL: <https://www.ign.es/web/mapas-sismicidad>.
- [10] RISMUR II. *Servicio de Actualización del Análisis de Riesgo Sísmico (RISMUR) en la Región de Murcia. ETSI Topografía, Geodesia y Cartografía (Universidad Politécnica de Madrid, UPM) , Grupo de Ingeniería Sísmica (UPM)*. 2014.
- [11] Dirk P Kroese and Reuven Y Rubinstein. “Monte carlo methods”. In: *Wiley Interdisciplinary Reviews: Computational Statistics* 4.1 (2012), pp. 48–58.
- [12] P.B. Lourenço and J.A. Roque. “Simplified indexes for the seismic vulnerability of ancient masonry buildings”. In: *Construction and Building Materials* 20.4 (May 2006), pp. 200–208. DOI: [10.1016/j.conbuildmat.2005.08.027](https://doi.org/10.1016/j.conbuildmat.2005.08.027).
- [13] P.B. Lourenço et al. “Simplified indexes for the seismic assessment of masonry buildings: International database and validation”. In: *Engineering Failure Analysis* 34 (Dec. 2013), pp. 585–605. DOI: <https://doi.org/10.1016/j.engfailanal.2013.02.014>.
- [14] MIT-19. “Istruzioni per l’applicazione dell’«Aggiornamento delle «Norme tecniche per le costruzioni»», 21 gennaio”. In: *Decreto Ministeriale del Ministero delle Infrastrutture e dei Trasporti* 7 (2019).
- [15] Guido Magenes and GiamMichele Calvi. “In-plane seismic response of brick masonry walls”. In: *Earthquake Engineering and Structural Dynamics* 26 (1997), pp. 1091–1112.
- [16] P Martínez-Pagán et al. “Shear-wave velocity based seismic microzonation of Lorca city (SE Spain) from MASW analysis”. In: *Near Surface Geophysics* 12.6 (2014), pp. 739–750.
- [17] Claudio Mazzotti et al. “Una metodologia speditiva per la valutazione di vulnerabilità sismica di edifici in muratura e calcestruzzo armato [A simplified method for seismic vulnerability assessment of masonry and reinforced concrete buildings]”. In: *Progettazione Sismica* 4.2 (2013), pp. 95–112. DOI: [10.7414/PS.4.2.95-112](https://doi.org/10.7414/PS.4.2.95-112).
- [18] Comunidad Autónoma de la Región de Murcia. “Decreto Legislativo 1/2005, de 10 de junio, Ley del Suelo de la Región de Murcia”. In: *DL 1/2005* (2005).
- [19] NTC08. “Norme tecniche per le costruzioni”. In: *Decreto Ministeriale del Ministero delle Infrastrutture e dei Trasporti* 14 (2008).
- [20] NTC18. “Aggiornamento delle Norme tecniche per le costruzioni, 20 febbraio”. In: *Decreto Ministeriale del Ministero delle Infrastrutture e dei Trasporti* 42 (2018).
- [21] IGN Actualización de Mapas de Peligrosidad. “Sísmica en España 2012”. In: *Instituto Geográfico Nacional (IGN): Madrid, Spain* (2013), p. 127. DOI: [10.7419/162.05.2017](https://doi.org/10.7419/162.05.2017).
- [22] RESISTO Project website. Last visit 23/03/2022. URL: <https://www.resistoproject.com/en/what-is-resisto-project/>.
- [23] Valentina Rapagnetta. “Studio comparativo di analisi speditive con metodo RE.SIS.TO. e di analisi statiche non lineari eseguite con software 3Muri per la valutazione della fragilità di edifici in muratura nel comune di Maranello (MO).” Tesi di laurea. University of Bologna, Scuola de Ingegneria e Architettura, 2021.
- [24] X Romão et al. “Field observations and interpretation of the structural performance of constructions after the 11 May 2011 Lorca earthquake”. In: *Engineering Failure Analysis* 34 (2013), pp. 670–692.
- [25] Functional S.O. n.5 and geometric standards for road construction. “Gazzetta Ufficiale 04/01/2002 n.3.” In: *Ministerial Decree n. 6792, 5/11/2001* (2001).
- [26] Regione Toscana. “Manuale per la compilazione della scheda GNDT/CNR di II livello versione modificata della Regione Toscana, Direzione Generale delle Politiche Territoriali ad Ambientali, Settore: Servizio Sismico Regionale”. In: *Progettazione Sismica* 2 (2003).
- [27] UR7 UNIBO: Marco Savoia (coordinatore), Lucia Praticò, Elena Simoni, Gianluca Salamida. “Definizione di curve di fragilità dei comparti CARTIS in muratura del comune di Maranello”. In: *Progetto ReLUIS* (2021).
- [28] GNDT Scheda di Esposizione e Vulnerabilità. “e di Rilevamento Danni di Primo Livello e Secondo Livello (Muratura e Cemento Armato)”. In: *Gruppo Nazionale per la Difesa dai Terremoti: Rome, Italy* (1994).
- [29] Maria Zucconi, Marco Bovo, and Barbara Ferracuti. “Fragility Curves of Existing RC Buildings Accounting for Bidirectional Ground Motion”. In: *Buildings* 12.7 (2022), p. 872.

- [30] NCSE-02. Comisión permanente de normas sismorresistentes. “España. Norma de construcción sismorresistente: Parte general y edificación”. In: *RD 997/2002, Spain* (2002). URL: www.boe.es/eli/es/rd/2002/09/27/997.
- [31] NCSE-94. Comisión permanente de normas sismorresistentes. “Norma de construcción sismorresistente: Parte general y edificación”. In: *RD 2543/1994, Spain* (1994). URL: www.boe.es/eli/es/rd/1994/12/29/2543.

Chapter 5

Capacity of non-structural elements of RC buildings. A model for the characterisation of the out-of-plane behaviour of URM walls

Observations made after recent seismic events have shown that out-of-plane (OOP) failure of unreinforced masonry (URM) elements probably constitutes the most serious hazard to life in the case of several types of buildings. Among them are, for instance, masonry buildings and reinforced concrete buildings with unreinforced non-structural elements. On the one hand, façade walls and gables of historical masonry buildings are prone to separation and out-of-plane collapse as in the recent past it was not customary to firmly connect them to horizontal structures or transverse walls [10]. On the other hand, in areas of medium overall seismicity, falling debris of parapets, infill panels or ledges from reinforced concrete buildings to the public road is frequent and hazardous. As mentioned before, the nine fatalities caused by the 2011 Lorca earthquake were due to this latter phenomenon [23]. Fig. 5.1 illustrates this fact.

As a result of this, several studies have been conducted aiming to assess the OOP seismic response of URM elements. This has led to the development and use of various approaches, ranging from simple kinematic based analytical models to complex numerical simulations aimed to represent the behaviour of cantilever or infill panels. However, the majority of the practical, simplified approaches are based on experimental tests and consequently they can be considered robust solely in a limited range of cases: walls similar to those tested.

Within this framework, the present work proposes an analytical approach, which is used to characterise the linear and non-linear OOP seismic response of cantilever URM walls. Its significance derives from the fact that it is only based on theoretical principles and its accuracy has been demonstrated via comparison with very different experimental tests reported in the literature. Which means that our approach is valid for any wall, provided that its boundaries and loadings correspond with those of the proposal. From a practical point of view, it is also of interest because we have included a simplified trilinear version aimed especially at practitioners.

The contributions provided are organised as follows: Section 5.1 provides the state of the art. Section 5.2 presents the methodology: model and initial assumptions, detailed justification of the theoretical basics and discussion on the most significant parameters (subsection 5.2.1). Criteria used for the elaboration of the trilinear simplification of the curves; the resultant regression formulae; and equations to characterise the fundamental period and energies of the walls according to different models (subsection 5.2.2). Section 5.3 proves the capability of the model via comparison with very different experimental tests reported in the literature, and with other proposals and seismic codes. Finally, Section 5.4 presents conclusions and future lines of investigation.

5.1 State of the art

In the 1960s, Housner [24] demonstrated that rocking walls do not have a unique natural period. This evidence led to the execution of an increasing number of intense experimental and analytical studies aiming to adequately characterise the OOP seismic behaviour of these elements. These studies established the fact that cantilever and



Figure 5.1: Parapet wall collapsed during the 2011 Lorca earthquake. Author: Antonio Tomás, Universidad Politécnica de Cartagena

simply-supported walls subjected to one-way OOP bending can perform satisfactorily even when the seismic forces have overcome the maximum threshold (e.g., [40, 14, 27]). As a result of these findings, at present, the displacement-based philosophy is highly regarded within the scientific community for the seismic assessment of these kind of structures.

In this respect, it should be noted that the response of cantilevers and simply-supported walls is essentially different because of its strong dependency on boundary conditions. For instance, thick simply-supported walls with vertical loads or concrete frames on their top, can develop a beneficial arching actions in this direction, that cantilevers cannot. Furthermore, the interaction between infills and structural frames can cause the infills to be subjected to inter-storey drift (in-plane) and inertial (OOP) forces simultaneously [4, 3, 8, 32]. Nevertheless, the behaviour of both URM elements presents significant similarities, mainly related with the comparison between their actual load-displacement capacity curve and the same curve derived from a simpler modelling by means of rigid blocks under rotation.

Parapets and non-bearing façades that are poorly connected to the transversal structural elements (lack of box-type behaviour) can be considered to behave like a cantilever wall [10, 13, 25]; whereas the behaviour of an unreinforced masonry infill (IMW) located on concrete framed structures can be assimilated as a simply-supported wall [12].

The most significant experimental studies regarding flexible cantilever URM walls subjected to OOP loading and their contributions to the field are presented in Table 5.1. Furthermore, the force-displacement ($F-d$) idealisations proposals available to date are listed in Table 5.2. It is worth mentioning that a great number of these idealisations are based on the experimental studies mentioned in Table 5.1 and that the most common simplification of the complete curve consist in a trilinear version of it.

In contrast to these published approaches, our proposal to construct the capacity curves derives from well-known theoretical considerations: linear and non-linear constitutive laws of the materials and mathematical relationships between loads, internal forces and displacements, including second order effects. Furthermore, the robustness of our approach is demonstrated by the common agreement between its results and those of four experimental test specimens with very different characteristics ([26, 19, 11, 18]). This excellent agreement demonstrates that its

Studied by	URM samples and OOP tests	Subject studied Contributions
Lam et al.,(1995) [26]	1 clay building brick parapet wall. Initial displacement and impulsive tests.	The accuracy of various simplified methods used to determine the OOP behaviour of URM cantilever by means of a MEF model calibrated with the dynamic properties obtained from the tests. Highlights the difficulties of predicting the response of URM cantilever walls.
Shi et al.,(2008) [36]	Single walls, walls with returns and cells using a Structural Testing Multi-Axis Shaking Table. Pseudo-static tests.	The analysis of the influence of geometric conditions and connections conditions on OOP collapse mechanisms. Concludes OOP damage mechanism is determined by corners configurations, the most crucial parameter for OOP load factor. Validates the FaMIVE numerical procedure [10].
Shawa et al.,(2012) [35]	A U-Shape assemblage (CM) from a wider campaign. 34 shaking table tests using four recorded accelerograms.	The influence of transversal walls on the cantilever collapse mechanism. Reflects the existence of a significant dynamic reserve of stability provided that the wall behaves monolithically. Provides data for the assessment of discrete element methods and SDOF models.
Ferreira et al.,(2015a) [18]	6 full-scale sacco stone masonry walls. Surface load and a horizontal load-line at the top.	Sacco stone masonry walls' behaviour with and w/o pre-compression. Concludes that the walls presented large displacement capacities and that their capability to dissipate energy is highly influenced by their pre-compression state. Reports a ratio of maximum stability displacement-thickness of around 60%. Provides data for the Ferreira's approach to elaborate four-branch capacity curves [17].
Giaretton et al.,(2016) [19]	13 full-scale solid clay brick wall. Dynamic loading using a shaking table.	The dynamic behaviour of URM walls by means of experimental tests. Provides a comparison of results with procedures and codes available. Concludes not only that cracking acceleration depends on the parapet height and mortar strength but also that maximum top displacement prior to collapse depends on parapet thickness, height and mortar properties.
Degli et al., (2017) [11]	3 mock-ups of traditional irregular stone masonry panels. Static and dynamic tests.	The reliability of rigid block and constant equivalent viscous damping assumptions Highlights the need to consider the initial elastic stiffness to represent best the walls' behaviour, rather than classic rigid block models. Concludes that actual damping is higher than that related to elastic impacts only.

Table 5.1: Most significant experimental studies regarding flexible cantilever URM walls subjected to OOP loading and their contributions to the field. CM= Cantilever Mechanism, SDOF= Single Degree of Freedom.

Contributed by	Scope	Proposal
Doherty et al.,(2002) [14]	CM and SSW	A trilinear capacity curve based on nonlinear rigid-body analysis in conjunction with experimentally determined empirical parameters or ratios. Validated by means of static and dynamic tests in the case of SSW [22].
D'Ayala et al., (2005) [15]	CM, among others	A four-branch idealised force-displacement relationship for a wide range of façades. Evaluates the strength capacity by the equilibrium limit analysis and defines the capacity curve by estimating the elastic period and a rational value for ductility.
Shawa et al.,(2012) [35]	U-Shape assemblages (CM)	A trilinear moment-rotation curve based on the explicit formulation of the equation of motion, which combines: rocking models with three-branch moment-rotation laws and an indented hinge. Validated with experimental THA.
Derahkshan et al.,(2013) [12]	CM and SSW	An analytical approach which improves that of Doherty [14]. Research into the influence of horizontal crack height, masonry compressive strength and diaphragm support stiffness.
Lagomarsino et al.,(2015) [25]	CM and MBM	Bilinear and trilinear capacity curves of flexible URM walls and multi-block mechanisms, and the definition of related damages.
Ferreira et al.,(2015b) [17]	CM	A four-branch curve for sacco stone masonry walls on the basis of simplified analytical formulae that includes experimentally derived parameters from previous tests ([18]).
Godio and Beyer (2019) [21]	CM and SSW	A trilinear curve based on a mechanical model ([20]) which considers the deformability of the walls and nonlinear geometric effects. Validated via shaking table tests.

Table 5.2: Force-displacement ($F - d$) idealisations proposals available to date, including fundamentals and main characteristics. CM= Cantilever Mechanism, SSW = Simply Supported Walls, MBM= Multi-Block Mechanisms.

plausibility is stable for any wall that can be assimilated into a single leaf cantilever wall; in contrast to proposals such as those of Doherty or Ferreira, in which the robustness decreases as the characteristics of the element studied deviates from those of the experimental test samples on which they have been calibrated.

Furthermore, unlike these approaches, our model considers the geometric characteristics and the mechanical properties of the wall.

In addition, the application of our simplified trilinear version of the approach is as simple as the other proposals, since its key points can be obtained from the formulae (Fig. 5.8) provided in section 5.2.1. These formulae are posed by using solely non-dimensional relationships between variables, seeking to use the most relevant between the different parameters. This results in our approach avoiding problems with units in dimensional constants, such as those noted in [3, pg. 2226] in relation to the comparison between the reviewed models for the response of simply-supported walls.

Finally, several tests have shown that rocking walls or parapets, due to their softening behaviour, may become unstable prematurely [38]; hence, full utilisation of the substantial post-cracking OOP displacement capacity is risky.

5.2 Methodology

The proposed methodology aims to extend and improve the performance assessment of cantilever URM walls subjected to OOP seismic loading. In this respect, this work contributes a number of straightforward formulae to elaborate the simplified trilinear capacity curve of these elements, accounting for its geometrical and mechanical properties. Moreover, it provides several expressions to characterise their energies and fundamental periods accurately.

To reach these formulae, firstly, we have elaborated an analytical model based on theoretical principles capable of characterising the non-linear OOP behaviour of these types of elements in terms of acceleration and displacements. Later, we have developed the trilinear simplification of the resulting theory-based curves, which fulfills energy conservation and minimum squared error criteria. Lastly, we have characterised the energies and fundamental periods of the walls after an in-depth discussion about the formulation of different models. Furthermore, as it will be shown in the following section, the resulting formulae have also permitted us to validate our analytical approach

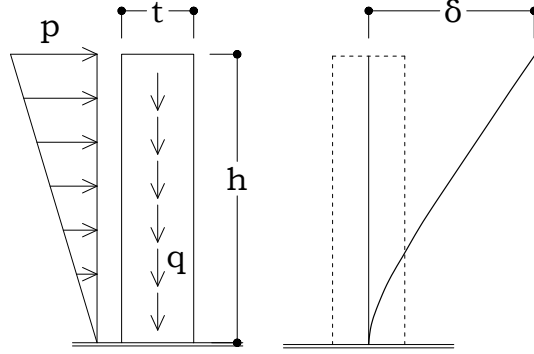


Figure 5.2: 1-m wide cantilever wall subjected to triangularly distributed OOP loading. δ : top displacement.

with published experimental tests.

5.2.1 Analytical approach

The current study aims to deepen the relationship between the OOP seismic loading applied to a cantilever wall and the displacement derived from it. For that reason, the laws of the external and internal forces and those of the material of a typified element will be established. After that, the best manner of representing the variables involved, action and demand, will be analysed, concluding with some examples of the results of the approach.

First, the response of a 1 m wide cantilever wall subjected to seismic OOP loading (Fig. 5.2) with its features parameterised is studied in-depth.

In order to approximate the second-order response derived from the $P - \Delta$ effect, we have considered that the horizontal capacity is the resultant capacity from the first-order analysis of the flexible block minus that which the wall loses due to the $P - \Delta$ effect, considering it as if it were a rigid block.

The first-order laws of horizontal loads p , vertical loads q , axial forces N , shear forces V and bending moments M are immediate:

$$p = 2\alpha mg \frac{z}{h^2} \quad (kN/m) \quad (5.1)$$

$$q = mg \frac{1}{h} \quad (kN/m) \quad (5.2)$$

$$N = mg \left(1 - \frac{z}{h}\right) \quad (kN) \quad (5.3)$$

$$V = \alpha mg \left(1 - \left(\frac{z}{h}\right)^2\right) \quad (kN) \quad (5.4)$$

$$M = \frac{\alpha mgh}{3} \left(1 - \frac{z}{h}\right)^2 \left(2 + \frac{z}{h}\right) \quad (kNm) \quad (5.5)$$

where h is the height of the wall, t its thickness, m its total mass and αmg the acting horizontal load triangularly distributed for the situation of interest, are the primary variables of the problem. Moreover, z is the height considered and α represents the acceleration applied in dimensionless terms.

Thus, the eccentricity of the load can be deduced by:

$$e = \frac{M}{N} = \alpha h \frac{(1 - \zeta)(2 + \zeta)}{3} \quad (m); \quad \zeta = \frac{z}{h} \quad (5.6)$$

Cracking reduces the useful section of the element when the eccentricity is higher than the maximum achievable

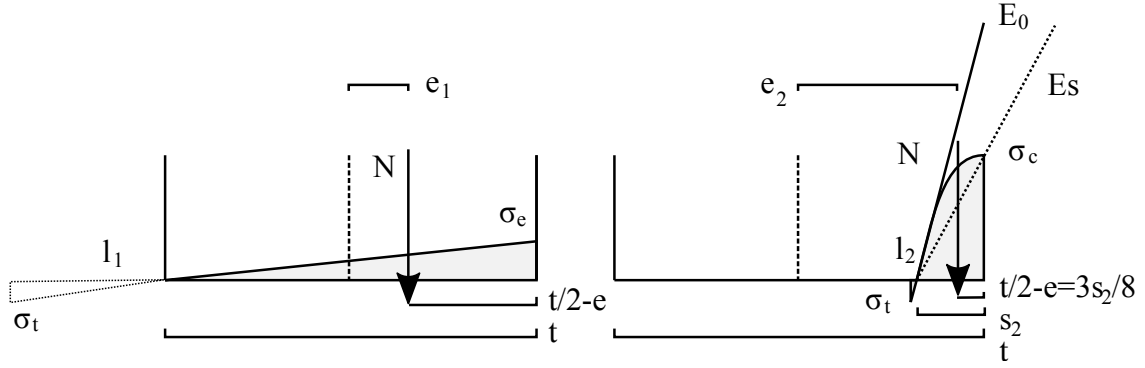


Figure 5.3: Eccentricities and limit stresses corresponding to the elastic and collapse models of behaviour.

eccentricity within the elastic range $e_e = \frac{t}{6}$. Horizontal cracking lines appear up to a relative height limit, ζ_l , from which the section can be considered uncracked, i.e., with elastic behaviour.

$$\frac{e_e}{t} = \frac{1}{6} = \frac{2}{6} \alpha \frac{h}{t} (1 - \zeta_l)(2 + \zeta_l) \quad (5.7)$$

$$\zeta_l = \sqrt{\frac{9}{4} - \frac{1}{2\alpha\lambda} - \frac{1}{2}}; \quad \lambda = \frac{h}{t}. \quad (5.8)$$

where λ represents the slenderness of the wall.

Hence, above the ζ_l level the section can be considered uncracked and below the ζ_l level the section will either be cracked or not, depending on its tensile strength. It is worth noting that for low lateral loads or low slenderness, no section will neither crack, nor experience tensile stress, being in this case

$$\zeta_e = 0 \implies \alpha\lambda \leq \frac{1}{4} \quad (5.9)$$

Moreover, cracked sections are considered to possess an effective thickness t_{ef} that is strictly assimilated to the compressed thickness plus an uncracked tensile amplitude of effective length l , characteristic of the type of masonry and state —gradient— of existing stresses. This effective length l accounts for the distance between fissures and for a specific localised tensile capacity in that small region.

$$t_{ef} = 3 \left(\frac{t}{2} - e \right) + l \quad (m) \quad (5.10)$$

where l is discussed next.

One possible way to address the problem, perhaps more efficient than others, consists in interpolating between two easy to recognise extreme behaviours. On the one hand, the limit of eccentricity that corresponds to the elastic model; and on the other hand, the limit of resistance corresponding to the overturning condition —non-linear model of collapse— (Fig. 5.3). In the latter case, the parabolic law of stresses has been defined considering a secant stiffness at the fracture point, E_s , equal to 0.5 the initial tangent stiffness, E_0 . A rule consistent with criteria that regulations established for the characterisation of this material. For instance, [39] establishes a recommended value of 0.6 for limit analysis.

In both cases, there are potentially uncracked tensioned lengths. Both limits will have secant stiffness modules between which the values corresponding to the case analysed will be placed. Moreover, the crushing and cracking strengths that limit the stresses —compressive σ_c and tensile σ_t stresses— are characteristics of the material. Finally, N and e , ($e_1 \leq e \leq e_2$) constitute the load and its eccentricity.

Furthermore, in both limit cases, a significant parameter can be deduced: at the elastic limit, the minimum necessary stress σ_e to reach that state; at the point of collapse, the thickness s required to support the load N .

Having, therefore, for given values of N, e and for a given material characterized by its mechanical properties

σ_c , σ_t and E_0 , the following sequence:

$$s_2 = \frac{3}{2} \frac{N}{\sigma_c} \quad (m); \quad (5.11)$$

$$e_1 = \frac{t}{6}; \quad (m); \quad (5.12)$$

$$e_2 = \frac{t}{2} - \frac{3s_2}{8} \quad (m); \quad (5.13)$$

$$l_1 = \frac{\sigma_t}{\sigma_e} t \quad (m); \quad (5.14)$$

$$l_2 = \frac{\sigma_t}{2\sigma_c} s_2 \quad (m); \quad (5.15)$$

$$\eta = \frac{e_2 - e_1}{e_2 - e_1}; \quad (5.16)$$

$$s = \eta t + (1 - \eta) s_2 \quad (m); \quad (5.17)$$

$$l = \eta l_1 + (1 - \eta) l_2 \quad (m); \quad (5.18)$$

$$E_s = \eta E_0 + (1 - \eta) \frac{E_0}{2} = (1 + \eta) \frac{E_0}{2} \quad (kN/m^2) \quad (5.19)$$

where $\eta \in [0, 1]$ is a measure of the “ proximity ” to the elastic state. As a result, the deformed shape of the element can be plotted.

Stiffness of the cracked section relative to the elastic nominal stiffness In this section, the effective stiffness $E_s I_{ef}$ is compared with the nominal stiffness EI via comparison of the resulting top displacements derived from the two hypotheses

- EI of the uncracked section
- $E_s I_{ef}$ of the cracked section below ζ_l

In respect to the uncracked section, the following sequence of functions is obtained:

$$M(z), \quad (5.20)$$

$$c(z) = \frac{M(z)}{EI}, \quad (5.21)$$

$$\theta(z) = \int_0^z \frac{M(z)}{EI} dz, \quad (5.22)$$

$$\delta(z) = \int_0^z \theta(z) dz, \quad (5.23)$$

with

$$\theta = \frac{\alpha h^2 mg}{12EI} (\zeta^4 - 6\zeta^2 + 8\zeta) \quad (rad) \quad (5.24)$$

$$\delta = \frac{\alpha h^3 mg}{60EI} (\zeta^5 - 10\zeta^3 + 20\zeta^2) \quad (m) \quad (5.25)$$

where θ is the slope and δ the deflection, whose maximum value —the elastic deflection δ_{el} — is obtained for $z = h, \zeta = 1$:

$$\delta_{el} = \frac{11}{60} \frac{\alpha h^3 mg}{EI} \quad (m) \quad (5.26)$$

A straightforward version of this expression can be obtained by considering: $mg = \rho \lambda t^2$, being ρ the specific weight; $\rho \times 1 \times t = q$, being q the weight per unit of the wall surface area; and $I = t^3/12$.

$$\frac{\delta_{el}}{h} = \frac{11}{5} \alpha \lambda \lambda^2 \frac{q}{E} \quad (5.27)$$

Conversely, if the cracked stiffness is accounted for, there will be two laws with these ranges of applicability: $[0, \zeta_l]$ and $[\zeta_l, 1]$, for the potentially cracked and uncracked sections respectively. In the first region E_s and I_{ef} depends on the compressed thickness and on the uncracked tensile amplitude l . The secant modulus E_s is deducible

from 5.19, and the effective inertia I_{ef} relative to the initial inertia I , in the first instance, can be approximated by:

$$0 \leq \frac{I_{ef}}{I} = \left(\frac{t_{ef}}{t}\right)^3 = \left(3\left(\frac{1}{2} - \frac{e}{t}\right) + \frac{l}{t}\right)^3 = \left(\frac{3}{2} - \alpha\lambda(1-\zeta)(2+\zeta) + \frac{l}{t}\right)^3 \leq 1, \quad (5.28)$$

where the effective thickness t_{ef} is estimated according to the compressed region obtained by considering a triangular linear law plus a segment under tension given by 5.18.

A more rigorous estimate for t_{ef} is given by

$$t_{ef} = s + l \leq t \quad (m) \quad (5.29)$$

with s and l given by 5.17 and 5.18. However, the Expr. 5.28 is ideal for the following reflection, and the difference between results is negligible.

This expression has a maximum threshold when the eccentricity is close to half the thickness of the element. A threshold which corresponds to the limit of the equilibrium, which is reached when, for $\zeta \geq 0$, Expr. 5.30 is fulfilled.

$$\frac{I_{ef}}{I} = 0 \implies \frac{3}{2} - \alpha\lambda_l(1-\zeta)(2+\zeta) + \frac{l}{t} = 0 \quad (5.30)$$

Thus, the condition corresponding to an uncracked tensile amplitude of nil effective length ($l = 0$) can be set as a reference:

$$\lambda_l \approx \frac{3}{4\alpha} \quad (5.31)$$

$$\lambda_l \alpha \leq \frac{3}{4} \quad (5.32)$$

Taking into account the laws mentioned above for E_s and I_{ef} , the laws of rotations and deflections accounting for cracking can be determined. The curvature would be $c = M/E_s I_{ef}$ and the deflection would be $\delta = h^2 \int d\zeta \int c d\zeta$. An expression that can be determined numerically, and related to the corresponding displacement when cracking is not considered in the model (Expr. 5.26) for the conditions of slenderness and lateral loads described by the β parameter, being $\beta = \alpha\lambda$, the product of the slenderness by the base shear factor.

The parameter β results to be fundamental in the study of the behaviour of cantilever walls, because the eccentricity e relative to the thickness t only depends on the relative dimension considered ζ and the parameter mentioned, as can be deduced from 5.6.

When the meaning of the Expr. 5.9 and 5.32 are examined, it is noticeable that:

$$\beta = \alpha\lambda; \begin{cases} 0 \leq \beta \leq 0.25 : & \text{wall in the elastic state} \\ 0.25 < \beta < 0.75 : & \text{cracking bellow } \zeta_l, \\ 0.75 \leq \beta : & \text{collapse.} \end{cases} \quad (5.33)$$

The curvature in the cracked regions c_{cr} is

$$c_{cr} = \frac{1}{h} \frac{q}{E_s} \frac{4\beta\lambda^2(1-\zeta)^2(2+\zeta)}{\tau(\zeta, \beta, l/t)^3} \quad (1/m) \quad (5.34)$$

where it can be used either 5.28 or, preferably, as it will be done later, 5.29 in order to establish $\tau(\zeta, \beta, l/t) = t_{ef}/t$. In uncracked regions, when $\zeta \geq \zeta_l$ (see 5.8) the curvature is

$$c_{unscr} = \frac{1}{h} \frac{q}{E} 4\beta\lambda^2(1-\zeta)^2(2+\zeta) \quad (1/m) \quad (5.35)$$

Moreover, when considering cracked regions the E will be equal to E_s (secant stiffness corresponding to the state of deformation reached), instead of $E = E_0$ (tangent stiffness of the masonry), the value associated with uncracked

regions. Therefore,

$$c = \Phi\gamma; \quad (5.36)$$

$$\Phi = \frac{4\beta\lambda^2q}{Eh}; \quad \gamma(\zeta, \dots) = \frac{(1-\zeta)^2(2+\zeta)}{\varphi(\zeta, \dots)}, \quad (5.37)$$

$$\begin{cases} \zeta < \zeta_l & ; \varphi = \frac{E_s}{E} \tau(\zeta, \beta, l/t)^3 \leq 1 \\ \zeta \geq \zeta_l & ; \varphi = 1 \end{cases} \quad (5.38)$$

where $\tau = t_{ef}/t$ expresses the relationship between the effective and the total thickness, derived from 5.29. As both the rotation and the deflection are null in origin,

$$\theta = \Phi h \int \gamma(\zeta, \dots) d\zeta \quad (5.39)$$

$$\delta = \Phi h^2 \int d\zeta \int \gamma(\zeta, \dots) d\zeta \quad (5.40)$$

whose maximum is reached when, $\zeta = 1$:

$$\delta_{\text{fis}} = \Phi h^2 \int_0^1 d\zeta \int \gamma(\zeta, \dots) d\zeta = \mu(\dots) \delta_{\text{el}}. \quad (5.41)$$

The function $\varphi = \varphi(\zeta, \dots)$ depends on β , on the relationship $E_s/E = E_s/E_0$ (5.19), as well as on l/t (5.18)¹. Therefore the dependencies result as follows: $\varphi(\zeta, \beta, \lambda, q/\sigma_c, \sigma_t/\sigma_c)$, $\gamma(\zeta, \beta, \lambda, q/\sigma_c, \sigma_t/\sigma_c)$ and $\mu(\beta, \lambda, q/\sigma_c, \sigma_t/\sigma_c)$.

It is worth noting that the loading term q —superficial— acts as a horizontal as well as a vertical force; a force whose effect on the vertical stresses depends on the height considered as load height. And, therefore, on a fraction of the height h , which implies a linear dependency on the slenderness λ when the terms relative to the thickness are used. So $\mu = \mu(\beta, (\lambda q)/\sigma_c, \sigma_t/\sigma_c)$ is the expression actually obtained.

Resulting that the multiplying factor μ necessary to determine the maximum deflection, relative to the uncracked element (Eq. 5.26) is

$$\frac{\delta_{\text{fis}}}{\delta_{\text{el}}} = \mu \left(\beta, \frac{\lambda q}{\sigma_c}, \frac{\sigma_t}{\sigma_c} \right) = \frac{20}{11} \int_0^h d\zeta \int \gamma(\zeta, \dots) d\zeta \quad (5.42)$$

It is interesting to consider the significance of the non-dimensional parameter $\lambda q/\sigma_c$:

$$\frac{\lambda q}{\sigma_c} = \frac{\lambda t}{\sigma_c/\rho} = \frac{h}{\sigma_c/\rho} \quad (5.43)$$

which expresses the quotient between the height of the masonry and a characteristic length of the material, $\sigma_c/\rho = \mathcal{A}$, which in other publications has been called “material structural scope”, see [30] equation (1.4) and associated explanations.

The resulting relative deflection values are plotted in Fig. 5.4. This relationship can be interpreted in each case as the inverse of the average stiffness of the cracked element in relation to the original elastic nominal stiffness.

In the same way, the deformed shape of the wall centre-line (relative to the maximum elastic deflection) is plotted for an intermediate condition in the range of interest for the parameter $(0.25 - \beta - 0.75)$ $\beta = 0.5$. In the figure, the wall centre-line shows an easily assimilated behaviour with that of a piece with a hinge very close to its base, although not exactly on it (represented in dashed line).

Table 5.3 shows the typical values of several properties of a wide range of Italian masonry materials (Table C.8.5.I, NTC 2018, NTC [28]). Values that are also used as a reference in other Southern European countries [37, 7, 34] and on other continents, [33]. Hence, it gives an order of the magnitudes of the fundamental variables involved.

¹Although the development is not shown, for documentation purposes it can be mentioned that: $l/t = n/d$ with $n = n_1 + n_2$, $n_1 = (12\beta\zeta^2 + (33 - 36\beta)\zeta + 24\beta - 33)\lambda q/\sigma_c$, $n_2 = 16\beta(\zeta + \zeta^2) + 24 - 32\beta$, $d = (16 - 27(1 - \zeta)\lambda q/\sigma_c) \sigma_c/\sigma_t$. Besides, s/t such that $t_{ef}/t = s/t + l/t$ results to be $s/t = m/d$ with $m = m_1 + n_2$, being $m_1 = (24\beta\zeta^3 - (39 - 72\beta)\zeta + 48\beta - 39)\lambda q/\sigma_c$. Finally, $E_s/E_0 = (1 + o/d)/2$, with identical d , and being $o = 16\beta(\zeta + \zeta^2) - 27(1 - \zeta)\lambda q/\sigma_c + 24 - 32\beta$.

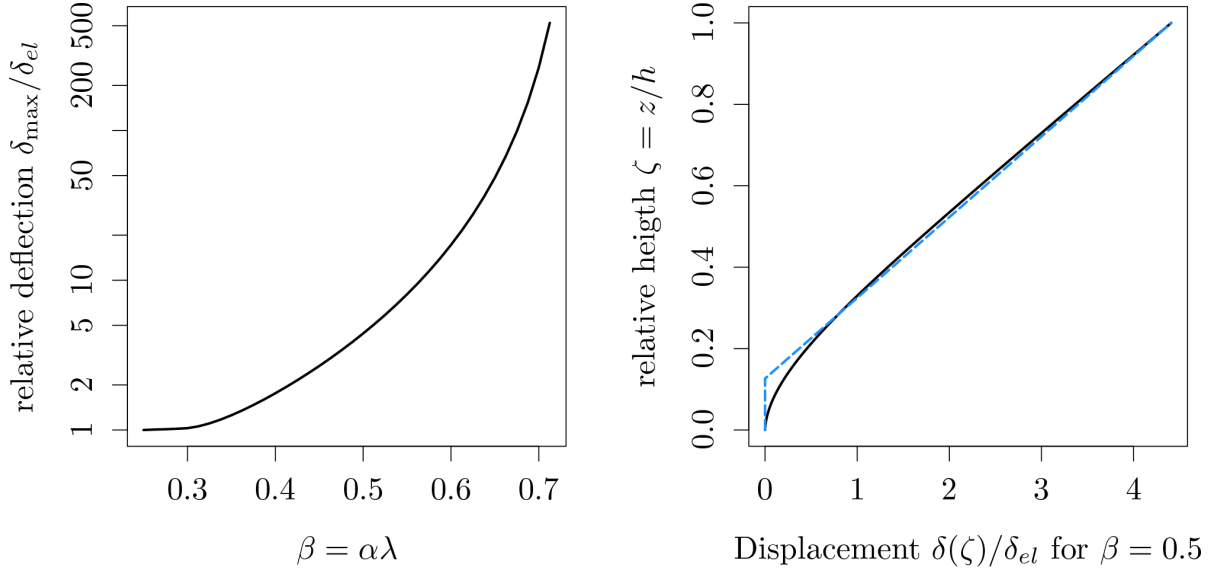


Figure 5.4: Deflections and deformed structure relative to the elastic deflection: a) Deflection in case of cracking, with $\beta \geq 0.25$ and b) deformed shape for $\beta = 0.5$ both plotted for $\lambda q/\sigma_c = h/(\sigma_c/\rho) = 0.01$ and $\sigma_t/\sigma_c = 0.1$ (black solid line). Closest possible layout of rigid block with a hinge (blue dashed line).

Masonry	ρ (kN/m ³)	σ_c (MPa)	E/σ_c	σ_c/ρ (m)
irregular stone	19	1.0-2.0	525-690	50-105
soft stone	13-16	1.4-3.2	500-640	100-200
square stone block	22	5.8-8.2	400-415	260-370
solid brick	18	2.6-4.3	420-435	140-240
semi-solid brick	15	5.0-8.0	700	330-530

Table 5.3: Values of the fundamental variables of several representative masonry materials from different Southern European countries. The range of σ_t/σ_c is considered 0.0-0.1. Italian values taken from [28].

Load-displacement curve or capacity curve

The deformed shape of the wall can be determined for any given loading conditions (defined by the shear factor α). Thus, its 'capacity curve', represented by the relationship between the base shear factor and the top displacement, can be plotted.

A reasonable dimensionless representation can be defined by using the following parameters as references: the product $\beta = \alpha\lambda$ representing the demand; and the ratio between the top displacement δ and the top displacement corresponding to the overturning limit as if it were a rigid block $\delta_{ov} - \delta/\delta_{ov}$, being $\delta_{ov} = t$ — representing the displacement.

Note that, considering these references, the maximum load corresponds to $\beta = 0.75$ and the maximum relative displacement to $\delta/\delta_{ov} = 1$.

Additionally, as the wall is 'rotating' around a region at its base, the lateral load effectively resisted is the sum of the horizontal action, represented by αmg plus the lateral effect of the moment derived from the shift in position of the weight of the element itself.

For that reason, in the chart of 'capacities' (Fig. 5.5) there are two curves represented. The first curve (dashed lines) does not take into account the effect of the overturning moment derived from the rotation of centre of masses of the wall. The second curve (solid lines), does account for the effect. In order to estimate this effect, the element was considered as if it were a rigid block. In other words, to the moment produced by the lateral force (Expr. 5.5) for $z = 0$, must be added the moment M_g derived from the rotation of the center of masses of the element itself

— M_v —,

$$M_g = mg \frac{\delta}{2} \quad (kNm) \quad (5.44)$$

This amounts must be subtracted from the lateral load bearing capacity of the wall. In terms of base shear factor the corresponding value V_g is

$$V_g = -V_{\max} \frac{\delta}{\delta_{ov}} = -V_{\max} \frac{\delta}{t} \quad (kN) \quad (5.45)$$

In the case of a displacement equal to the overturning displacement, the total capacity against horizontal load must be deducted, (on the scale of β it corresponds to the value 0.75), while for minor displacements δ , the subtraction will be linearly lower.

The ratio between actual deflection and overturning deflection would be (considering the Expressions 5.27 and 5.42):

$$\frac{\delta_\beta}{\delta_{ov}} = \mu \left(\beta, \frac{\lambda q}{\sigma_c}, \frac{\sigma_t}{\sigma_c} \right) \frac{\delta_{el}}{t} = \mu \left(\beta, \frac{\lambda q}{\sigma_c}, \frac{\sigma_t}{\sigma_c} \right) \frac{11}{5} \beta \lambda^3 \frac{q}{E} \quad (5.46)$$

Thus, the graph of capacities $\beta(\delta/\delta_{ov})$ can be plotted, as in Fig. 5.5, for predefined values in slenderness λ and in the relationships E/q , $\lambda q/\sigma_c$ and σ_t/σ_c .

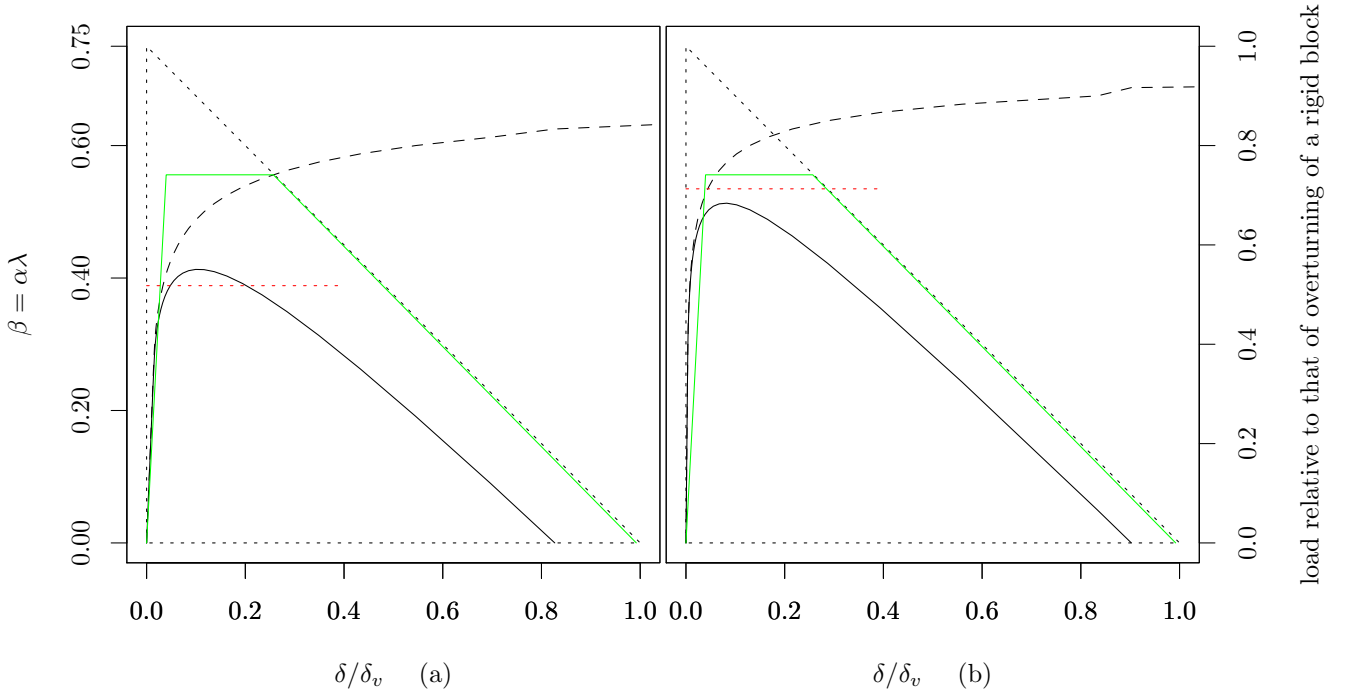


Figure 5.5: Actual capacity curve (solid lines) of a wall with these characteristics: $\lambda q/\sigma_c = 0.01$, $\sigma_t/\sigma_c = 0.1$ and (a): $\lambda = 6$, $E/q = 9000$, (b): $\lambda = 8$, $E/q = 90000$. Capacity curve of the same wall before discounting the effect of the rotation of the wall's center of masses (dashed line). Capacity curve of a rigid block with the same features (black dotted line). Trilinear curve according to [12]'s proposal (green solid lines). Maximum horizontal load according to [20, equations 14, 17]'s proposal (red dotted line). See section 5.3.2 for more details concerning the comparison with [12] and [20]'s proposal.

Simplification of the analytical formulation: trilinear version of the curve

Findings in previous sections have shown that the parameters that define the capacity curve according to the previous model are very few, dimensionless and relatively bounded:

- $\beta = \alpha \lambda$ product of the lateral load factor and the slenderness, with $0 < \beta < 0.75$;
- λ slenderness; considering the range $4 \leq \lambda \leq 12$;

- q/E ratio between weight per unit of wall surface area and elasticity modulus;
- $\lambda q/\sigma_c$ term linked to the stresses obtained in bending, given weight and slenderness;
- σ_t/σ_c quotient of the maximum tensile and compressive stresses. Regulations usually estimate it between 0 and 0.1;
- δ/δ_{ov} that spans between 0 and 1.

From these parameters, the q/E , σ_t/σ_c , λ , and $\lambda q/\sigma_c$, characterize the qualities of the masonry, from which thickness and slenderness are decisive; β characterizes the demand; and δ/δ_{ov} , the response.

In order to advance in the statistical characterisation of the trilinear approach, a table with data for the possible ranges of the parameters above is elaborated. Among them, q/E depends on the thickness of the masonry, which can be separated as an independent parameter

$$\frac{q}{E} = \frac{t\rho}{E} = \frac{t}{E/\rho} \quad (5.47)$$

where E/ρ is a characteristic length of the masonry. Its range of values depends on the values of E , between 2000 and 5000 MPa, and on ρ , between 15 and 25 kN/m³, although it is possible to correlate both variables: the greater the density, the greater the expectable modulus of stiffness. It is also worth remembering the meaning of the quotient contained in the variable $\lambda q/\sigma_c$ that was analysed in Expr. 5.43, expression in which the *scope*, $\mathcal{A} = \sigma_c/\rho$, is also a characteristic length of the masonry used in the order of a thousandth of the previous one. Finally, given the relationship σ_c/E , it is reasonable to use it or its inverse as a parameter for the regression.

Therefore, the expressions of regression proposed consider the following sequences of data to represent the parameters:

- $t \in [0.125, 0.25, 0.375]$ m.
- $E/\rho \in [50, 200]$ km, values every 12.5 km.
- $\lambda \in [4, 12]$ values every 0.5.
- $E/\sigma_c \in [500, 750, 1000, 1250]$.
- $\sigma_t/\sigma_c \in [0, 0.1]$, values every 0.02.
- $\beta \in [0, 0.75]$ values every 0.05.

deducing any additional analytical parameter, such as q/E and l/t , from above.

A crucial term in this approach, which deserves particular analysis is E/ρ , for which low values have been initially adopted. Although it would require a detailed study, since the usual approximations made by [39] ($E \approx 1000f_k$) or [6] ($E_m \approx 750f_m$, interpreting $f_m = f_k$) can lead to greater values than those listed in previous sequences in the case of ‘high-quality’ masonry.

To define the trilinear approximation to the analytical curve, the descending branch is assumed to be approximately parallel to the one corresponding to the behaviour of a rigid block, as experimental evidence demonstrates. Thus, the minimum and strictly necessary parameters to define the trilinear simplification are the following:

- the conventional elastic limit δ_y , which defines the initial elastic slope
- the limit load β_l , corresponding to the horizontal line, in the scale of β ,
- the point of collapse δ_c

These parameters along with the limit point δ_l , which defines the ultimate displacement for the limit load β_l , constitute the key points of the trilinear curve.

The trilinear representation that differs least from the complete analytical curve will be that which maintains the same area below it —energy— as well as minimises the sums of local differences between both curves. This could be done by minimising either the absolute values of the error or the squares of these. For consistency with other formulations and the intuition that indicates that errors of greater entity should have more influence in the adjustment than errors of lesser entity, this latter version is adopted.

Hence, the trilinear curve can be defined by its key points:

- the elastic initial line branch, between $(0, 0)$ and (δ_y, β_l)
- the horizontal line branch, between (δ_y, β_l) and (δ_l, β_l) ,
- the descending line branch, between (δ_l, β_l) and $(0, \delta_c)$.

being

$$\delta_l = \delta_c - \frac{\beta_l}{\beta_{\max}} = \delta_c - \frac{\beta_l}{0.75} \quad (5.48)$$

In the above expressions, all the displacements δ_i , $i \in (y, l, c)$ are implicitly related to the overturning displacement $\delta_{ov} = t$, that is, they abbreviate the expressions δ_i/δ_{ov} .

In the following, approximations to the key points required to construct the trilinear curve are determined. This constitutes a problem of minimisation of two variables (δ_y, β_l) since the other two can be deduced from these, using 5.48 and equating W in 5.49 to the area below the analytical curve.

The area below the trilinear curve, which must be equal to that of the analytical curve is:

$$W = \frac{1}{2}\delta_y\beta_l + (\delta_l - \delta_y)\beta_l + \frac{1}{2}(\delta_c - \delta_l)\beta_l \quad (J) \quad (5.49)$$

Additionally, the comparison is made between two graphs from which points can be obtained by defining linear intervals, with equally linear differences, although of arbitrary sizes. The integral of the square of the trapezoidal error for each interval is:

$$\int_1^2 \left(\varepsilon_1 + \frac{\varepsilon_2 - \varepsilon_1}{\Delta_{1,2}} x \right)^2 dx = \frac{1}{3}\Delta_{1,2} (\varepsilon_1^2 + \varepsilon_2^2 + \varepsilon_1\varepsilon_2) \quad (5.50)$$

and the aim is to determine δ_y , δ_l , δ_c , β_l to ensure

$$\min \sum_i \frac{1}{3}\Delta_i (\varepsilon_{i,1}^2 + \varepsilon_{i,2}^2 + \varepsilon_{i,1}\varepsilon_{i,2}) \quad (5.51)$$

where all the intervals i in which the curve has been divided are summed up, ensuring the fulfillment of conditions 5.48, and 5.49. In this latter expression W must be made equal to the integral for the analytical curve, taking into account the cases of change of sign in the differences —“starred” trapezoids—.

Therefore, the table of values for said approximations for all the explored cases described above is built. , with the help of R, remaining only to do the regression of said values based on the relevant variables of the description of the wall, established earlier in this section, and which will be analyzed later.

Two different examples of the adjustment are shown in Fig. 5.6. The parameters that define the characteristics of both masonry walls are indicated in Table 5.4. Furthermore, the calculation of the average period of oscillation according to Doherty’s proposal [14] has been included, using: δ_l as the effective displacement, $t = \delta_{ov}$, the mass m and a stiffness $k = V/\delta_l$ per unit length of the wall.

$$T = 2\pi\sqrt{\frac{m}{k}} = 2\pi\sqrt{\frac{m \frac{2}{3}\delta_l}{\alpha g m}} = 2\pi\sqrt{\frac{\lambda t \frac{2\delta_l}{3\delta_{ov}}}{\beta g}} \quad (s), \quad \text{with } \alpha = \frac{\beta}{\lambda}; \quad \text{also in the forms:}$$

$$T = 2\pi\sqrt{\frac{\zeta^* h \frac{\delta_l}{\delta_{ov}}}{\beta g}} = 2\pi\sqrt{\frac{\zeta^* \lambda \delta_l}{\beta g}} = 2\pi\sqrt{\frac{\zeta^* \delta_l}{\alpha g}}; \quad \zeta^* = \frac{2}{3}. \quad (5.52)$$

where ζ^* can be considered an equivalent relative height of the vibrating mass. It is worth mentioning that in the previous expressions, successively the thickness t , the height h or the displacement δ_l , with the acceleration of gravity g are the dimensional relevant terms. Later, in Section 5.2.2, a profound discussion on the characterisation of the fundamental period and the kinetic energy of the walls depending according to a number of models is included.

Regression expressions

A first consideration relative to the dimensionality of the possible expressions must be made in order to define the expressions of regression:

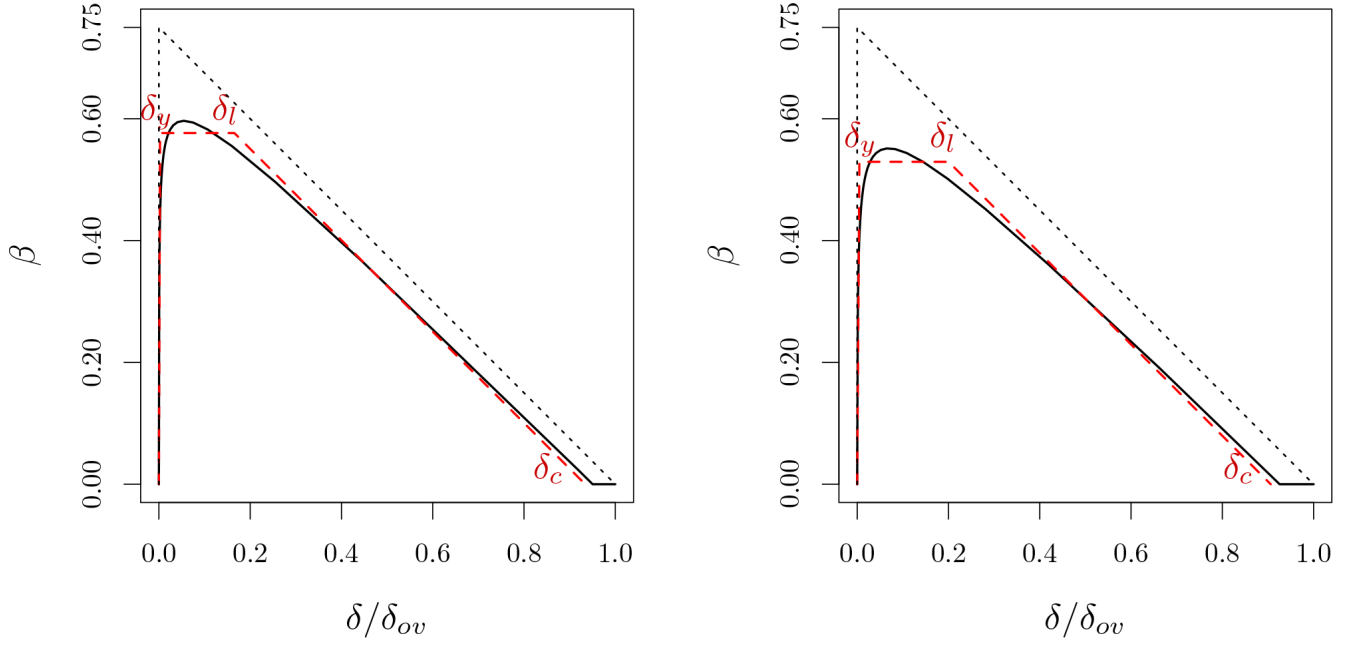


Figure 5.6: Examples of adjustments of the trilinear curves. Theory-based complete curve in black solid line, rigid block behaviour in black dotted line and trilinear curve in red dashed line. Key points outlined in red. Masonry characteristics detailed in Table 5.4

Case	E/σ_c	σ_c/ρ (m)	σ_t/σ_c	λ	t (m)	δ_y/δ_{ov}	δ_l/δ_{ov}	δ_c/δ_{ov}	β_l	T_{β_l} (s)
1	1000	120.0	0.1	8	0.250	0.003	0.165	0.934	0.576	1.521
2	750	133.3	0.0	12	0.125	0.005	0.200	0.906	0.529	2.139

Table 5.4: Predefined characteristics of the masonry considered in the cases included in Figure 5.6, and effective period according to Doherty's proposal

$$\begin{aligned}
\beta &= \beta \left(\frac{E}{\rho}, \frac{E}{\sigma_c}, \frac{\sigma_t}{\sigma_c}, t, \lambda \right) \equiv f_1 \left(\beta, \frac{E}{\rho}, \frac{E}{\sigma_c}, \frac{\sigma_t}{\sigma_c}, t, \lambda \right) = 0 \\
\frac{\delta_y}{\delta_{ov}} &= \frac{\delta_y}{\delta_{ov}} \left(\frac{E}{\rho}, \frac{E}{\sigma_c}, \frac{\sigma_t}{\sigma_c}, t, \lambda \right) \equiv f_2 \left(\frac{\delta_y}{\delta_{ov}}, \frac{E}{\rho}, \frac{E}{\sigma_c}, \frac{\sigma_t}{\sigma_c}, t, \lambda \right) = 0 \\
\frac{\delta_l}{\delta_{ov}} &= \frac{\delta_l}{\delta_{ov}} \left(\frac{E}{\rho}, \frac{E}{\sigma_c}, \frac{\sigma_t}{\sigma_c}, t, \lambda \right) \equiv f_3 \left(\frac{\delta_l}{\delta_{ov}}, \frac{E}{\rho}, \frac{E}{\sigma_c}, \frac{\sigma_t}{\sigma_c}, t, \lambda \right) = 0 \\
\frac{\delta_c}{\delta_{ov}} &= \frac{\delta_c}{\delta_{ov}} \left(\frac{E}{\rho}, \frac{E}{\sigma_c}, \frac{\sigma_t}{\sigma_c}, t, \lambda \right) \equiv f_4 \left(\frac{\delta_c}{\delta_{ov}}, \frac{E}{\rho}, \frac{E}{\sigma_c}, \frac{\sigma_t}{\sigma_c}, t, \lambda \right) = 0.
\end{aligned} \tag{5.53}$$

All of them being dimensionless variables, except for t and E/ρ , which are lengths. Thus, the range of the dimensional matrix that, for each expression, relates the six variables and their dimensions —one— is always one. Therefore, the required dimensionless parameters are five in the four cases, —the dimension of the null nucleus or nullity of the dimensional matrix—, according to Buckingham's theorem π of the theory of dimensional analysis [5]. Hence, the expressions will be in the following formats

$$\begin{aligned}
F_1 \left(\beta, \lambda, \frac{t}{\sigma_c/\rho}, \frac{E}{\sigma_c}, \frac{\sigma_t}{\sigma_c} \right) &= 0 \\
F_2 \left(\frac{\delta_y}{\delta_{ov}}, \lambda, \frac{t}{\sigma_c/\rho}, \frac{E}{\sigma_c}, \frac{\sigma_t}{\sigma_c} \right) &= 0 \\
F_3 \left(\frac{\delta_l}{\delta_{ov}}, \lambda, \frac{t}{\sigma_c/\rho}, \frac{E}{\sigma_c}, \frac{\sigma_t}{\sigma_c} \right) &= 0 \\
F_4 \left(\frac{\delta_c}{\delta_{ov}}, \lambda, \frac{t}{\sigma_c/\rho}, \frac{E}{\sigma_c}, \frac{\sigma_t}{\sigma_c} \right) &= 0
\end{aligned} \tag{5.54}$$

in which the thickness, that coincides with the displacement that characterizes the overturning condition: $t = \delta_{ov}$ has been divided by a “masonry length” to define the required dimensionless term.

To determine the parameters that define the capacity curve, various types of approaches have been evaluated, resulting in the expressions detailed in Fig. 5.8 are those which fit best. To elaborate this simplification, Buckingham’s theorem π of the theory of dimensional analysis ([5]) has been applied. As a result of its application, the following four dimensionless parameters have been selected in order to consider the particular characteristics of each wall studied: λ , $t/(\sigma_c/\rho)$, E/σ_c and σ_t/σ_c . Among them, the width t of the wall is divided by the “scope” $\sigma_c/\rho = \mathcal{A}$, that constitutes the “length” which represents best the characteristics of the masonry (see comments to (5.43)) in order to obtain a significant dimensionless magnitude. And the list includes the relationships E/σ_c and σ_t/σ_c that normally represent the mechanical parameters in reflections associated with stress–strain laws of masonry materials.

An example of the adjustment of the regression formulae is included in Fig. 5.7, demonstrating the excellent accuracy of the proposal. Nonetheless, further research should contemplate alternatives in which a loss of accuracy is compensated by a better agreement between expressions, or by a greater physical significance of the parameters involved in the formulae.

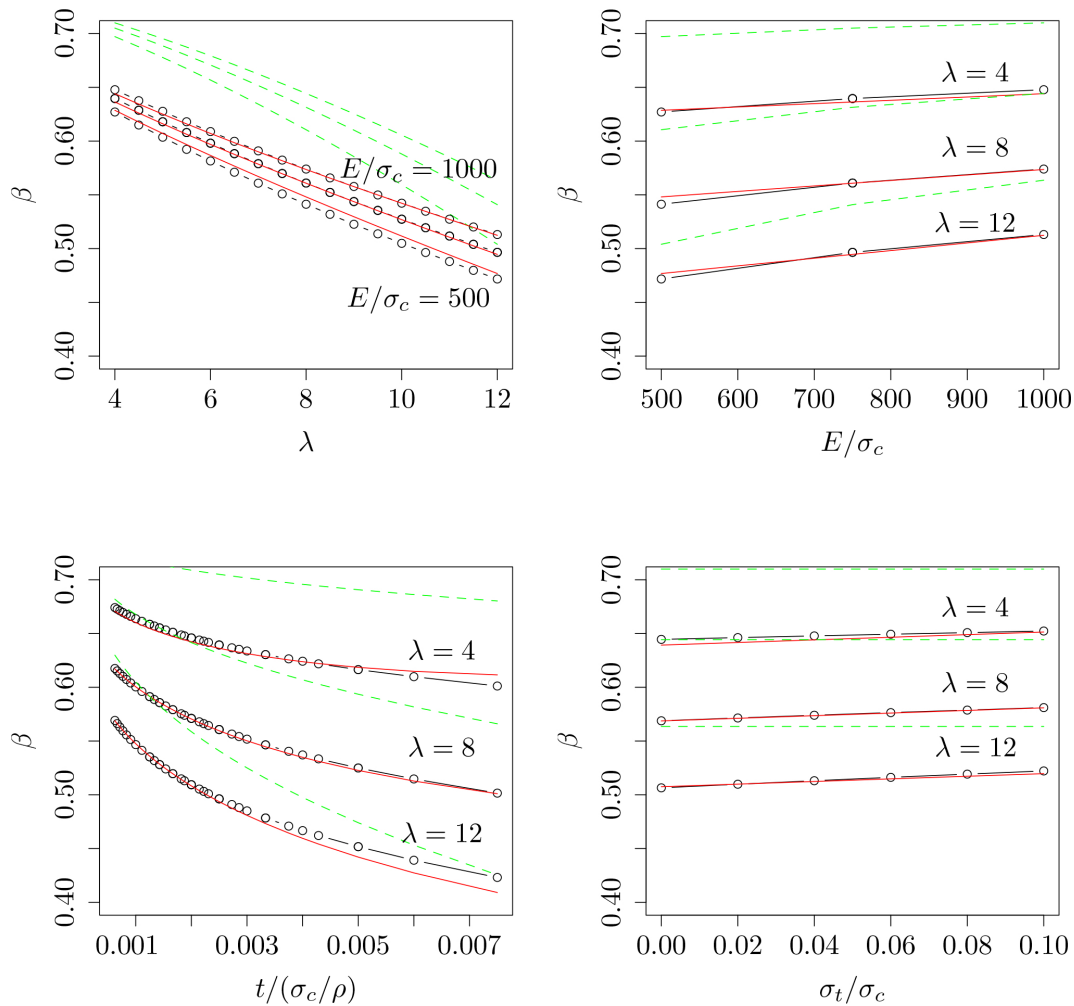


Figure 5.7: Values of $\beta(\lambda, t/(\sigma_c/\rho), E/\sigma_c, \sigma_t/\sigma_c)$ for default values of $\lambda = 8$, $(\sigma_c/\rho)/t = 533$, $E/\sigma_c = 750$, $\sigma_t/\sigma_c = 0.04$ (points) according to our analytical model. Our regression of adjustment (red solid lines). Values of the parameter β according to [20] approach (green dashed lines). See section 5.3.2 for more details concerning the comparison with [20]’s proposal.

$$\beta = 0.734 - 0.013\lambda + \frac{5.025}{10^6} \frac{E\lambda}{\sigma_c} + \frac{10.816}{10^6} \frac{E}{\sigma_c} + 0.122 \frac{\sigma_t}{\sigma_c} + 11.376 \frac{t}{\sigma_c/\rho} - 1.115 \sqrt{\frac{\lambda t}{\sigma_c/\rho}} \quad (5.55)$$

$$100 \frac{\delta_y}{\delta_{ov}} = -0.027\lambda + \frac{4.893}{10^3} \lambda^2 - \frac{0.057}{10^3} \frac{E\lambda}{\sigma_c} + \frac{0.193}{1000} \frac{E}{\sigma_c} - 0.388 \frac{\sigma_t}{\sigma_c} - 76.886 \frac{t}{\sigma_c/\rho} - 4.395 \frac{\lambda t}{\sigma_c/\rho} \quad (5.56)$$

$$10 \frac{\delta_l}{\delta_{ov}} = 0.257\lambda - \frac{1.052}{100} \lambda^2 + \frac{1.413}{10^3} \frac{E}{\lambda\sigma_c} - \frac{0.571}{10^3} \frac{E}{\sigma_c} - 0.943 \frac{\sigma_t}{\sigma_c} + 0.096 \cdot 10^3 \frac{t}{\sigma_c/\rho} + 9.752\lambda \left(\frac{t}{\sigma_c/\rho} \right)^{\frac{2}{3}} - 41.991 \frac{\lambda t}{\sigma_c/\rho} \quad (5.57)$$

$$\frac{\delta_c}{\delta_{ov}} = 1.02 - \frac{1.074}{100} \lambda + \frac{0.321}{10^3} \lambda^2 - \frac{0.186}{10^3} \frac{E}{\lambda\sigma_c} - \frac{0.056}{10^3} \frac{E}{\sigma_c} + 0.066 \frac{\sigma_t}{\sigma_c} + 0.746 \frac{t}{\sigma_c/\rho} - 0.708\lambda \left(\frac{t}{\sigma_c/\rho} \right)^{\frac{2}{3}} + 1.779 \frac{\lambda t}{\sigma_c/\rho} \quad (5.58)$$

Figure 5.8: Expressions for the values of the key points of the simplified trilinear curves.

5.2.2 Calculation of the fundamental periods and energies

As a first approximation to the calculation of the period of a cantilever, it is worth noting again the straightforward proposal of Doherty ([14]): to determine this period as a function of the relationship between δ_l/δ_{ov} and β (T_{δ_l} , see eq. 5.52). Based on this consideration, it can be stated that this parameter shows a better agreement than others for the different proposals of capacity curves illustrated in Figure 5.5. Therefore, it can be deduced that T_{δ_l} could constitute a suitable parameter for the comparison between theoretical and experimental results of various studies.

However, as mentioned above, the expression 5.52 has the character of approximation. Therefore, to interpret the experimental results correctly, this brief section is dedicated to analysing the alternatives in formulating the fundamental period of the wall.

Rigid rotation around an elastic hinge

Considering that the movement is represented by a rigid rotation around a hinge located at the base, the expression of the rotational dynamic equilibrium in the hinge could be expressed as

$$K_\theta \theta(t) + \int_0^h \frac{m}{h} \frac{\partial^2}{\partial t^2} (\theta(t)z) z dz = 0 \quad (5.59)$$

that is to say

$$K_\theta \theta + \ddot{\theta} \frac{mh^2}{3}; \quad \text{with } K_\theta = \frac{M}{\theta} = \frac{V \frac{2}{3} h}{\frac{\delta}{h}} = V \frac{2h^2}{3\delta} \quad (5.60)$$

so for this condition

$$T = 2\pi \sqrt{\frac{\frac{mh^2}{3}}{\alpha g m \frac{2h^2}{3\delta}}} = 2\pi \sqrt{\frac{m \frac{\delta}{2}}{\alpha g m}} = 2\pi \sqrt{\frac{\lambda t \frac{\delta}{2\delta_{ov}}}{\beta g}} \quad (s) \quad (5.61)$$

It is reasonable to assume that the hinge could be produced in (or assimilated to) a higher position in respect to the base, such as $z_r = h(1-\nu)$ where ν would be the fraction of the oscillating height. In this case, the expressions 5.59, 5.60 would refer to this fraction. Thus, the movements and forces in relation to the immobile base would be, for the maximum values:

$$\begin{aligned} \delta &= \delta_r \quad (m); \\ \tilde{\theta} &= \theta_r \nu \quad (rad); \\ V &= V_r \quad (kN); \\ M &= M_r + V_r(1-\nu)h \quad (kNm). \end{aligned} \quad (5.62)$$

Although now, only the movement of the upper part must be considered for the purposes of dynamic equilibrium. This fact implies that the expression for the period obtained in Expr. 5.61 only correspond to the oscillating fraction, of height νh and therefore of slenderness $\lambda_r = \nu \lambda$. The period obtained is

$$T = T_r = 2\pi \sqrt{\frac{\lambda_r t \frac{\delta}{2\delta_{ov}}}{\beta_r g}} = 2\pi \sqrt{\frac{\frac{1}{2} \delta}{\alpha_r g}} = 2\pi \sqrt{\frac{\nu m \frac{1}{2} \delta}{\alpha g m}} \quad (s) \quad (5.63)$$

Hence, using the horizontal force as a reference ($\alpha m g = \alpha_r m_r g$), the period of solely a fraction of oscillating wall

(Expr. 5.63) can be recognised as being lower than that of the complete wall oscillating (Expr. 5.61). This is done by referring the base shear factor α_r to the total mass m , instead of to the oscillating mass $m_r = \nu m$.

Elastic cantilever

In the case of complete elastic behaviour, first, already published solutions are compared. Clough and Penzien (2003) [9], example E8-3, Expression (c), provides the period $T_0 = 2\pi\sqrt{0.228m/\frac{\pi^4 EI}{32h^3}} = 1.7196\sqrt{\frac{mh^3}{EI}} = \eta_1\sqrt{\frac{mh^3}{EI}}$. Where 1.7196, the η_1 coefficient is the value of η_i for the first mode of vibration. Whereas, from the Expression (4) in Orhan (2007)[31] can be deduced a slightly higher value for the same coefficient, $\eta_1 = 1.7870$.

As authors' interest lies in the properties of deformed structures, a review of its analysis is presented. Considering, as usual, time and position as separable variables ($\delta(z, t) = \phi(z)h(t)$), and using the harmonic solution at time $h(t) = \sin(\omega_0 t)$; the following differential equation is obtained for the deformation when the oscillations are undamped:

$$-\frac{m}{h}\omega_0^2\phi(z) + EI\frac{\partial^4\phi(z)}{\partial z^4} = 0 \quad (5.64)$$

where, for the cantilever case, $\phi(0) = \phi'(z)|_{z=0} = \phi''(z)|_{z=h} = \phi'''(z)|_{z=h} = 0$.

If the dimensionless form $\varphi(\zeta) = \phi(h\zeta)/h$ is used, the equation takes the form of:

$$-\varphi + \gamma^4\frac{\partial^4\varphi}{\partial\zeta^4} = 0; \quad \gamma^4 = \frac{EI}{h^3m\omega_0^2}, \quad (5.65)$$

whose solution results in

$$\varphi = \frac{\gamma^2}{2} \left(\mu \left(\cosh \frac{\zeta}{\gamma} - \cos \frac{\zeta}{\gamma} \right) + \tau\gamma \left(\sinh \frac{\zeta}{\gamma} - \sin \frac{\zeta}{\gamma} \right) \right) \quad (5.66)$$

with

$$\mu = \varphi''(\zeta)|_{\zeta=0} = \frac{hM(0)}{EI} \quad (5.67)$$

$$\tau = \varphi'''(\zeta)|_{\zeta=0} = \frac{h^2V(0)}{EI} = \alpha mg \frac{h^2}{EI} \quad (5.68)$$

The basic parameter is

$$\gamma^4 = \frac{EI}{h^3m\omega_0^2} = \frac{1}{12\lambda^2h^2} \frac{E}{\rho} \frac{g}{\omega_0^2} \quad (5.69)$$

In order to determine the fundamental period $T_0 = 2\pi/\omega_0$, the possibility of deformation has to be established—and therefore the possibility of non-zero values for bending moments and internal shear forces—ensuring that

$$\int_0^h \phi^{IV}(z)dz = \frac{\tau}{h^2} = \phi'''(z)|_{z=0} = -\frac{1}{h^2} \int_0^1 \varphi^{IV}(\zeta)d\zeta \quad (5.70)$$

$$\int_0^h \phi^{IV}(z)zdz = \frac{\mu}{h} = \phi''(z)|_{z=0} = \frac{1}{h} \int_0^1 \varphi^{IV}(\zeta)\zeta d\zeta \quad (5.71)$$

Solving μ in the first,

$$\mu = -\tau\gamma \frac{\cosh \frac{1}{\gamma} - \cos \frac{1}{\gamma}}{\sinh \frac{1}{\gamma} - \sin \frac{1}{\gamma}} \quad (5.72)$$

is obtained an expression that when substituted in the second, and solving the resulting homogeneous equation for the condition $\tau \neq 0$, allows one to obtain an expression in γ whose roots correspond to the different oscillation modes.

Table 5.5 contains numerical solutions for the first four values of γ_i as well as the corresponding coefficients η_i for the expression of $T_{0,i}$ which is derived from the angular velocity obtained from Expr.5.69:

$$T_{0,i} = \eta_i\sqrt{\frac{h^3m}{EI}} = \eta_i\sqrt{\frac{12m\lambda^3}{E}} = 2\eta_i h\lambda\sqrt{\frac{3\rho}{Eg}} \text{ (s)} \quad (5.73)$$

Mode	1 st	2 nd	3 rd	4 th
γ_i	0.53330	0.21303	0.12731	0.09095
η_i	1.78702	0.28515	0.10184	0.05197

Table 5.5: Coefficients for the first free oscillation modes of the elastic cantilever ($\eta_i = 2\pi\gamma_i^2$). $T_{0,i} = \eta_1\sqrt{\frac{mh^3}{EI}}$.

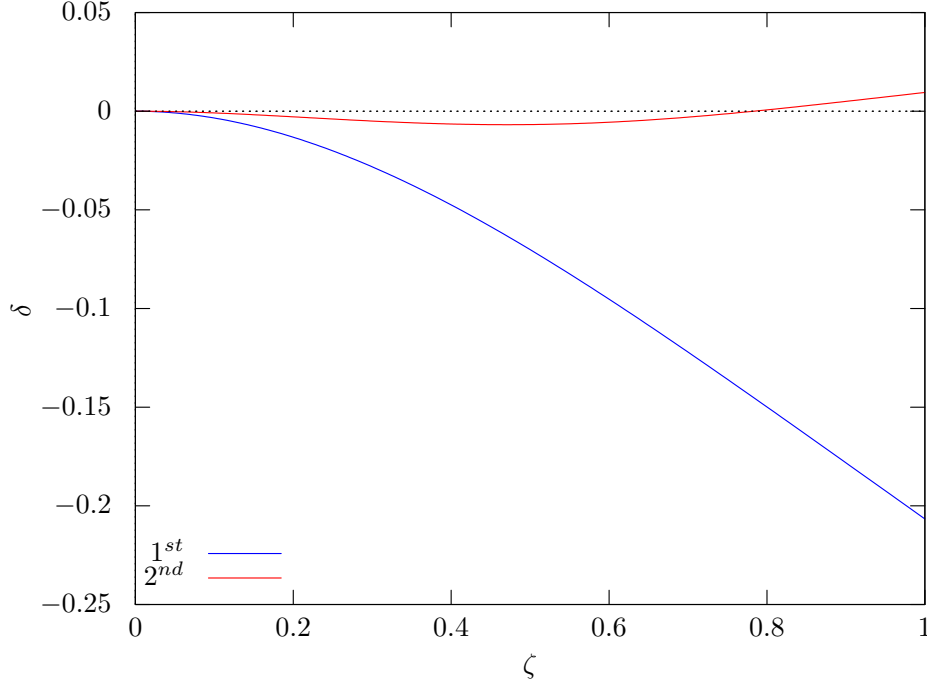


Figure 5.9: 1st and 2nd free vibration modes of a constant section elastic cantilever structure for an equal base shear demand: $\tau = h^2V(0)/EI = \alpha mg h^2/EI = 1$.

The first two vibration modes (in beam–cantilever format) for the same base shear value are represented in Fig. 5.9.

A number of the basic parameters can be determined for the deformation corresponding to the first mode, namely:

$$V(0) = m\delta_m\omega_0^2 \int_0^h \frac{1}{h}\varphi(\zeta)dz = \frac{1}{2,5543}m\omega_0^2\delta_m \quad (kN) \quad (5.74)$$

$$M(0) = m\delta_m\omega_0^2 \int_0^h \frac{1}{h}\varphi(\zeta)zdz = \frac{1}{3,5160}m\omega_0^2h\delta_m \quad (kNm) \quad (5.75)$$

$$z_F = \frac{M(0)}{V(0)} = 0,7265 h \quad (m) \quad (5.76)$$

$$W_{\text{kinet.}} = \frac{m}{2}\omega_0^2\delta_m^2 \int_0^h \frac{1}{h}\varphi(\zeta)^2dz = \frac{1}{4}\frac{m}{2}\omega_0^2\delta_m^2 \quad (J) \quad (5.77)$$

$$W_{\text{elast.}} = \int_0^h \frac{Mc}{2}dz = \frac{\delta_m^2 EI}{2h^3} \int_0^1 \varphi''(\zeta)^2d\zeta = 3.09059 \frac{\delta_m^2 EI}{2h^3} \quad (J). \quad (5.78)$$

where m/h is the mass density per unit height and δ_m the maximum displacement at the end of the cantilever, where z_F is the height of the horizontal resultant force, and where $W_{\text{kinet.}}$ and $W_{\text{elast.}}$ correspond to the maximum energy in each case for instants separated $T/4$ in time.

Rigid block

As a term of comparison, the classical expression for the oscillation of a rigid block, according to [24] is considered:

$$\theta(\tau) = \operatorname{atan} \frac{t}{h} \left(\theta_0 - \operatorname{atan} \frac{t}{h} \right) \cosh p\tau \quad (\text{rad}) \quad (5.79)$$

$$T = \frac{4}{p} \cosh^{-1} \left(\frac{1}{1 - \theta_0 / \operatorname{atan} \frac{t}{h}} \right) (s); \quad p^2 = \frac{mgR}{I_0} \quad (5.80)$$

where θ is the inclination and τ the time variable, being $R = \frac{1}{2}\sqrt{t^2 + h^2}$ the radius of rotation of the centre of gravity of the mass, $I_0 = 4mR^2/3$ the polar inertia of the mass with respect to the vertex around which the block pivots, and $\theta_0 = \delta/h$ the maximum inclination corresponding to the amplitude of the oscillation for which the period is evaluated, having thus

$$T = \frac{4}{p} \cosh^{-1} \left(\frac{1}{1 - \operatorname{atan} \frac{\delta}{h} / \operatorname{atan} \frac{t}{h}} \right) (s); \quad p^2 = \frac{3g}{2\sqrt{t^2 + h^2}} \quad (5.81)$$

Given that $\delta/h = \delta/(t\lambda)$, with $\delta/t \leq 1$, for usual values $\lambda > 4$, and considering that $\operatorname{atan}(x) \approx x - x^3/3 + x^5/5 + \dots$, in the regions of interest, with $0 < \delta/t < 0.9$, it is sufficient approximate to consider the next form, introducing the relationship between the rocking displacement and the instability displacement in the rigid model, that equals the width

$$T = 2\pi \sqrt{\frac{8h\sqrt{1+1/\lambda^2}}{3\pi^2 g}} \operatorname{arccosh} \left(\frac{1}{1 - \frac{\delta}{t}} \right) (s) \quad (5.82)$$

If the following relationship for the equilibrium of the rigid block is also used

$$\alpha\lambda = \frac{3}{4} \left(1 - \frac{\delta}{t} \right) \quad (-) \quad (5.83)$$

another more interesting form for the expression of the period is obtained:

$$T = 2\pi \sqrt{\frac{2t\sqrt{1+1/\lambda^2}}{\pi^2 g\alpha} \left(1 - \frac{\delta}{t} \right) \operatorname{arccosh}^2 \left(\frac{1}{1 - \frac{\delta}{t}} \right)} = 2\pi \sqrt{\frac{2t\sqrt{1+1/\lambda^2}}{\pi^2 g\alpha} \psi \left(\frac{\delta}{t} \right)} (s) \quad (5.84)$$

expression in which the bulk of the non-linearity of the problem is described by the function $\psi(x)$ on the relative displacement δ/t , and whose polynomial regression eases its interpretation

$$\psi(x) = (1-x) \operatorname{arccosh}^2 \left(\frac{1}{1-x} \right) \approx 1.895x - 1.159x^4 - 0.694x^{28} \quad (5.85)$$

Therefore, this constitutes an approximate expression (Fig. 5.10) with which the period of the block can be estimated for the Housner model with a form that can be compared with other models as shown in table 5.6.

$$T \approx 2\pi \sqrt{\frac{\zeta^* \delta}{\alpha g}} (s), \quad \zeta^* = \frac{3.79}{\pi^2} \sqrt{1 + \frac{1}{\lambda^2}} \left(1 - 0.6116 \left(\frac{\delta}{t} \right)^3 - 0.3663 \left(\frac{\delta}{t} \right)^{27} \right) \quad (5.86)$$

In this expression the numerical term ζ^* inside the root ranges, for mean values of λ and δ/t , between 0,34 and 0,40.

The maximum kinetic energy in the rotation —at the instant in which the support point changes— is

$$\begin{aligned} W_{k,\max} &= \frac{m}{6} t^2 (1 + \lambda^2) \dot{\theta}_{\max}^2 \quad (J); \\ \dot{\theta}_{\max} &= p \left(\theta_0 - \operatorname{atan} \frac{1}{\lambda} \right) \sinh p\tau; \quad \tau = \frac{T}{4}; \\ \dot{\theta}_{\max} &= p \sqrt{\theta_0 \left(2 \operatorname{atan} \frac{1}{\lambda} - \theta_0 \right)} \quad (\text{rad/s}). \end{aligned} \quad (5.87)$$

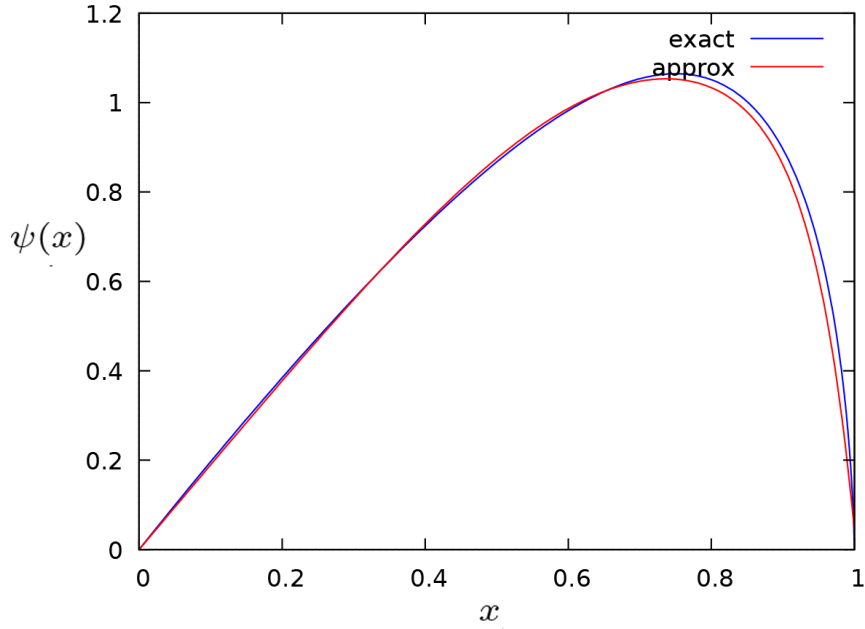


Figure 5.10: Function $\psi(x)$ for determining the period of the rigid block according to Housner (exact), and its approximation (approx), Eq. 5.85.

That expression can be related to a formulation such as $W_k = \mu m \omega_0^2 \delta^2 / 2$, and doing so a value dependent on λ and δ/t is obtained for the effective mass coefficient μ . The dependency $\mu(\lambda, \delta/t)$, can be separated into two independent components, as shown in Fig. 5.11: $\mu(\lambda, \delta/t) = \lambda^{-2} \varrho(\delta/t)$ where $\varrho(\delta/t)$ is perfectly defined and independent of λ . That suggests expressing the kinetic energy in a form as:

$$W_k = (\mu \lambda^2) \frac{1}{2} m \omega_0^2 \left(\frac{\delta}{\lambda} \right)^2 \quad (J) \quad (5.88)$$

Hence, the resultant expression reflects that the relevant kinetic energy depends on the vertical movements of the mass, as δ/λ is the maximum vertical displacement experienced by the block for the corresponding horizontal displacement δ .

All these findings referring to the values of the dynamic parameters are summarised in Table 5.6.

It is noteworthy the element that constitutes the fundamental difference between the models: the relevant movement. For Housner, the dynamic, relevant movement in terms of energy is the vertical. Whereas, in all other models, this relevancy corresponds to the horizontal movement. This constitutes an issue that deserves further research.

Parameter		Elastic cantilever	Rigid rotation around an elastic hinge	Doherty et al. [14]	Housner [24]**
$z_F = \zeta h$	ζ	0.7265	2/3	2/3	2/3
$T = 2\pi \sqrt{\frac{\zeta^* \delta}{\alpha g}}$	ζ^*	0.3915	1/2*	2/3	3/8
$W_{k,\max} = \frac{\mu}{2} m \omega_0^2 \delta_i^2$	μ	1/4	1/3	-	2/3 λ^2

Table 5.6: Dynamic parameters (z_F height of the resultant, T period and $W_{k,\max}$ kinetic energy) according to these hypotheses: 1: Elastic cantilever, 2: Rigid rotation around an elastic hinge (*: or $\nu/2$ being ν the fraction of the oscillating mass, if the hinge does not match with the base), 3: Doherty et al., 4: Housner (**: uses the rotational inertia around the pivot, which is 4/3 of that of the mass located in the centre of gravity, at 1/2 of h. The expression for μ is an approximation for medium values of δ/t , see Fig. 5.11).

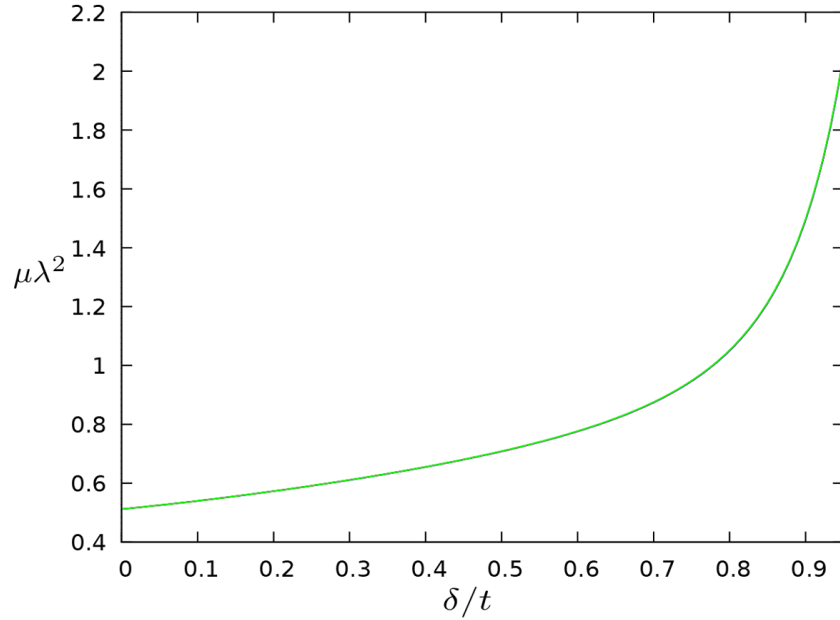


Figure 5.11: Equivalent mass coefficient $\mu\lambda^2$ for comparison with other models by applying the standard formulation of the kinetic energy to the rocking movement of a rigid body with equation 5.88.

5.3 Results and discussion

Our proposal has resulted in being an approach capable of determining analytically the parameters of the trilinear curve that characterise the resistance of the wall in a quick and straightforward manner, by means of the equations (5.55) to (5.58). Among them, the δ_l/δ_{ov} relationship eases the determination of the dynamic properties of cantilever walls, (Table 5.6, equation 5.52,...). Moreover, these properties solely depend on a small set of non-dimensional geometric and mechanical relationships.

In this section, we compare the results of our approach with those of a number of experimental tests reported in the literature in order to validate it. Moreover, our proposal is compared with other recent proposals and a seismic code, the NZSEE [29].

5.3.1 Comparison with different experimental studies reported in the literature

To assess the level of reliability of the analytical formulation presented, the results are compared to the findings of four specific walls that have been tested experimentally [26, 19, 18, 11]. The four cases have been chosen for several reasons: they are cantilever URM walls subjected to out-of-plane loading; the articles provide sufficient information to define the most influential properties of the walls for the elaboration of its analytical capacity curves; their capacity curves or periods of vibration against displacement are graphically documented, which allows the accurate evaluation of the proposal formulated herein; and the specimens are built with a variety of materials—stone and clay brick—and exhibit significant variations in their dimensions (similar to parapets and façades). It should be noted that there are very few experiments reported in the literature that comply with all these requirements and that façade walls can be assimilated into a cantilever wall when the mortar is not strong enough to provide sufficient bond to the wall assemblage, as usually occurs in traditional buildings made of poor quality material as *sacco* stone masonry [16].

The most significant experimental conditions and characteristics of the specimens selected are presented in Table 5.7. Those properties that are not mentioned in their corresponding paper have been established based on other research studies. Moreover, the most influential properties of these masonry specimens (t , σ_c/ρ , λ , E/σ_c and σ_t/σ_c) are summarized in Table 5.8.

Additionally, the following considerations were made to obtain the experimental relationships between periods and displacements. The analytical periods have been obtained applying the eq. included in the second row of Table

Sample	Description
1: [26] Lam	<ol style="list-style-type: none"> 1. A shaking-table test that served as support for Doherty's experimental-based formulation [14]. 2. The complete curve that relates the frequency and the amplitude. 3. 1.4Wx1Hx0.11T m, represents a standard parapet. Traditional extruded clay buildings bricks of 230x110x76 mm 4. $\sigma_c = 25.4$ MPa, estimated according to [2].
2: [19] Giaretton	<ol style="list-style-type: none"> 1. Testing clay brick walls in two phases. The former consisted of applying a harmonic motion of constant amplitude with an increasing table acceleration. The latter consisted of three tests carried out under stable free-rocking motion oscillation to measure the rocking periods of the same specimens already cracked. 2. The results in terms of periods versus displacements (phase 2). 3. 1.18Hx 1.2Wx 0.23T m [P2-A(1180) element], represents a parapet wall. Traditional extruded clay building bricks of 230x75x110 mm. 4. $E = 294f_m = 3763$ [2] and $\rho = 20000 \text{ kg/m}^3$, solid clay brick. $\sigma_t = 0$.
3: [11] Degli	<ol style="list-style-type: none"> 1. A series of static out-of-plane tests under controlled displacement conditions -releasing the panels after static pulling- and some vibration tests. The load is applied by pulling of a single cable anchored at two-thirds of the wall height. 2. The relationship between the horizontal load at the centre of gravity and the displacement at this point. 3. 1.1Hx0.9Wx0.22T m [Panel 1], represents a parapet. Traditional irregular stone wall of poor quality masonry. 4. The initial $E = 76$ MPa, for a $T_0 = 0.19$ (known data) is defined according to Eq. 5.73 and $\sigma_c = 3.16$ MPa, irregular class (IR++) [1].
4: [18] Ferreira	<ol style="list-style-type: none"> 1. Two complete displacement controlled cycles by means of an airbag. 2. The complete force displacement relationship. 3. 2.5H x 1.3W x 0.65T [non-load-bearing sample: Wall 1], represents a residential façade. Traditional regular stone masonry wall 4. $\sigma_c = 4.14$ MPa, partially regular class (PR) [1].

Table 5.7: Brief description of the samples and their corresponding experiments: 1. The experiment, 2. The results documented in terms of relationships between displacements and frequencies or forces, 3. Dimensions and materials, 4. Estimate of the undocumented properties.

5.6, considering a value of 0.44 for the factor ζ^* . This figure constitutes an intermediate value between 0.39 and 0.5, the values that would be applicable in the case of an elastic cantilever and a rigid rotation around an elastic hinge, respectively. In the same vein, the resultant forces in the cases of the Degli and the Ferreira experiments have been moved to a point located at 0.7 the height of the wall. Which, again, constitutes an intermediate between the $0.7265h$ and the $2/3h$ indicated in the first row of Table 5.6 in the same cases of the aforementioned ζ^* factor.

Finally, the frequencies estimated by the NZSEE regulations ([29]) proposals are also compared with the experimental and analytical results. The comparison between the analytical and the experimental results are presented in Fig. 5.12 in terms of relationships between periods and displacements, and in Table 5.9 in terms of elastic periods. Despite the variety in the experimental conditions, both results exhibit an enormous agreement between experimental and analytical results in the cases of Lam, Ferreira and Degli experiments.

In the case of the Giaretton specimen, the results are not so accurate at small displacements (< 15 mm). This inconsistency may be because the displacements documented by the researchers present a noticeable irregularity when these are smaller than 15-20 mm (as it can be seen in [19]). Furthermore, this element was cracked until the collapse in the phase prior to collecting the data, the first phase of the research. This fact may have influenced the results at small displacements, which are more sensitive than larger ones. Nevertheless, at medium and large displacements ($\delta > 30$), our proposal also shows a good agreement with the experimental results.

In addition, the NZSEE proposals ([29]) for the estimation of the main periods of a parapet have been included in Figure 5.12. It can be seen that both the NZSEE06 and the NZSEE17 results show lower accuracy than the analytical formulation herein proposed.

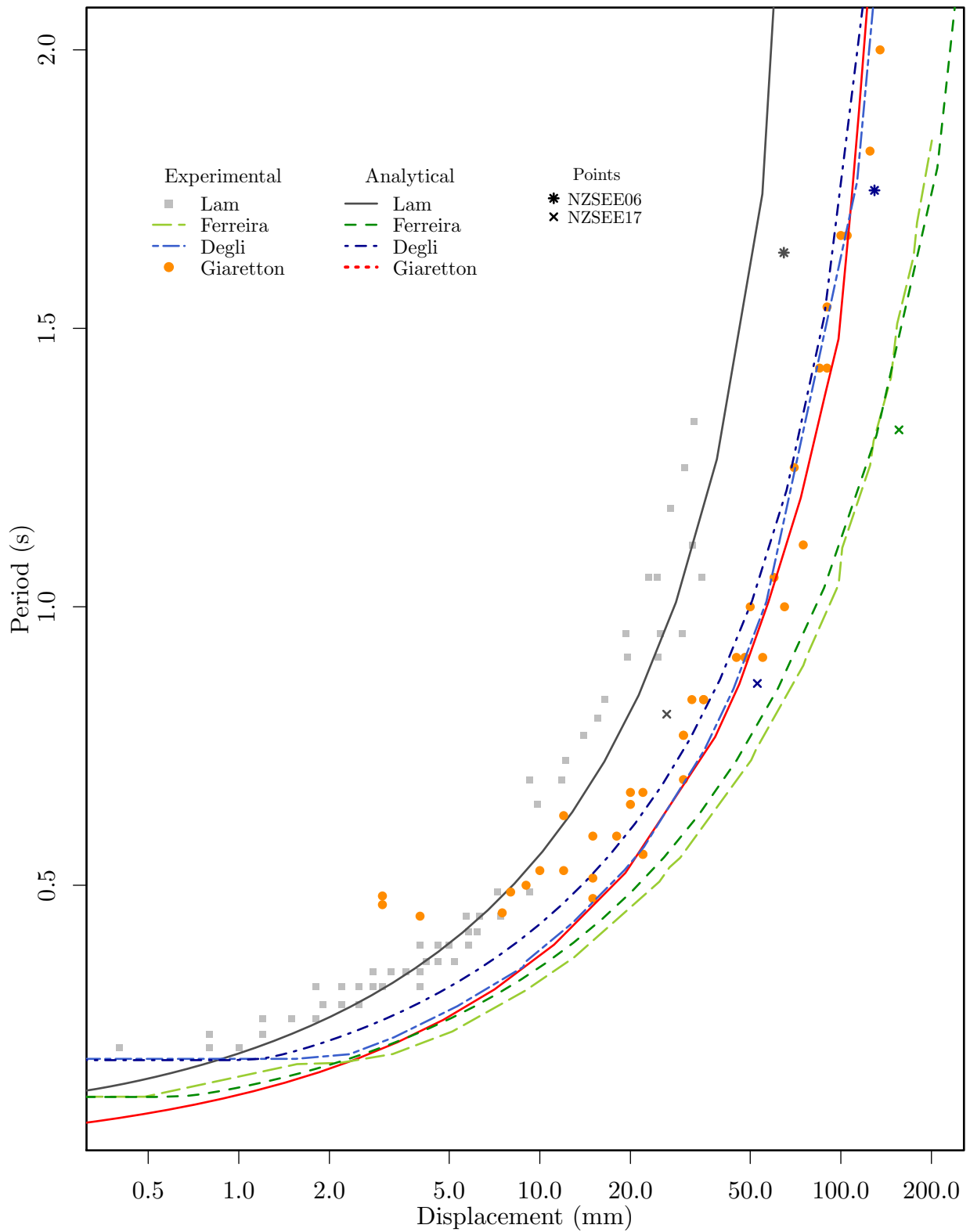


Figure 5.12: Comparison between the experimental results of four different samples with dissimilar materials and the analytical results of the methodology herein proposed in terms of periods

Sample	λ	t (m)	E/ ρ (m)	E/ σ_c	σ_t/σ_c
1	9.00	0.11	19826	16.14	0.008
2	5.10	0.23	188160	294.00	0.000
3	5.00	0.20	3453	3.16	0.400
4	3.85	0.65	25238	128.00	0.128

Table 5.8: Values of the fundamental variables of the published specimens selected for assessing the accuracy of our theory-based proposal.

Elastic frequency (Hz)	Experimental estimate	Theoretical estimate
1	5-10	7.95
3	5.40	5.37
4	8.39	8.38

Table 5.9: Comparison between the experimental estimate of the especimens selected and their value according to the theory-based proposal included in Table 5.6

5.3.2 Comparison with other proposals

Our proposal has also been compared with those of Derakhshan et al.,(2003) [12], Godio and Beyer (2017) [20] and the NZSEE regulation [29].

Firstly, the similarity of our proposal with the approach provided in [12] is evident, although therein the research is focused on a simply-supported overburdened wall with a crack at a height ζh , and where ψ is the ratio between the overburdening load and the weight.

Here, we rewrite the four equations that define the key parameters of Derakhshan's model in our format, since they are those which we have used for the comparisons shown in Figure 5.5. Namely: the lateral per unit length load (eq. 21), the lateral load for the beginning of the displacement of a rigid wall, (eqs. 27 and 31), the limit displacement that defines the instability as a rigid wall (eq. 28), and the reduction factor to obtain the maximum empirical lateral load (eqs. 30, 32).

$$h\hat{w} = \frac{\rho t^2}{\zeta(1-\zeta)} \left\{ 2(1-\zeta) \left(1 - \frac{\Delta}{t} - \left(\frac{1+c}{2} \right) \frac{a}{t} \right) + \psi \left((2-\zeta) - 2\frac{\Delta}{t} - (1+c(1-\zeta))\frac{a}{t} \right) \right\} \quad (5.89)$$

$$\hat{F}_0 = h\hat{w}_{\max} = \frac{\rho t t_n}{\zeta} \left(2 + \frac{2-\zeta}{1-\zeta} \right) \quad (5.90)$$

$$\frac{\hat{\Delta}}{t} = \frac{1 + \left(\frac{1-\zeta/2}{1-\zeta} \right)}{1 + \frac{\psi}{1-\zeta}} \quad (5.91)$$

$$P_{uMR} = \gamma \left(1 - \lambda \frac{t_n}{\sigma_c/\rho} \frac{t_n}{t} \left(+ \frac{(1-\zeta)(2\psi+2-\zeta)}{2(1-\zeta) + (2-\zeta)\psi} \right) \right) \quad (5.92)$$

having

$$\begin{aligned} \frac{a}{t} &= \lambda \frac{t_n}{\sigma_c/\rho} \frac{t_n}{t} (1-\zeta + \psi) = \frac{\lambda q}{\sigma_c} \frac{t_n}{t} (1-\zeta + \psi) \\ c &= \frac{1}{1-\zeta + \psi}; \quad \sigma_c = 0.85 f_c; \quad \gamma = 0.83. \end{aligned}$$

In these equations, we have also identified the nominal width t_n , used in the determination of the weight, and the effective resistant width t . Additionally, therein, the shear factor is $\alpha = \hat{F}_0/(\rho t_n^2 \lambda)$. Thus, the maximum ordinate of the curve β_* is $\beta_{*,0} = \alpha \lambda = \hat{F}_0/(\rho t_n^2)$, the maximum lateral force in the trilinear curve is $\beta_{*\max} = P_{uMR} \hat{F}_0/(\rho t_n^2)$ with $\rho t_n = q$, and the abscissas are $\delta_* = \Delta/\hat{\Delta}$; using the values proposed by them for the comparison with a

cantilever wall: $\zeta = 2/3$ and $\psi = 0$. Finally, it should be noted regarding this model that, except from the effect of the relationship between the load and the weight (ψ) and the equivalent position of the middle crack (ζ), the lateral load in the β scale only depends on the product $\lambda q/\sigma_c$.

On the other hand, the approach of Godio and Beyer [20] proposes an expression dependent on the quotient between the vertical load and the Euler's buckling load for the determination of the maximum thrust relative to the overturning.

$$Q_{\max} = \alpha \rho t h = \left(1 - \sqrt{\frac{P}{P_E}}\right) Q_0 = \left(1 - \sqrt{\frac{\rho t h}{\frac{\pi^2}{\lambda_m^2} E t}}\right) \alpha_0 \rho t h; \quad \alpha_0 = \frac{3}{4\lambda} \quad (5.93)$$

i.e.:

$$\beta = \frac{3}{4} \left(1 - \frac{\lambda}{\pi} \sqrt{48 \frac{\lambda q}{E}}\right). \quad (5.94)$$

although, for distributed loads said authors prefer to use the power 0.4 rather than the root (power 0.5). Therefore, this model makes β dependent only on the product $\lambda^2 \lambda q/E$.

As can be seen in Figure 5.5, the aforementioned expressions for β fit well with our model, although they do not include the effects of the relationships E/σ_c , σ_t/σ_c . In addition, regarding the same parameter β , Figure 5.7 reveals that, despite presenting different results in values, there is a noticeable similarity between the tendencies of our proposal and that of [20].

Finally, we have compared the periods obtained by applying our proposal (T_b) with those resulting from the application of the NZSEE regulation [29, equation C8.24] (T_a); in which a displacement of value $\delta_t = 0.24\delta_{ov}$ is fixed. To perform the comparison, T_b has been formatted as in equation (5.86) and in table 5.6, and an approximated value of 0.40 has been assumed for ζ^* . Moreover, for the approximated reduction of β to λ in T_b , we have considered a rough approximation for β that can be deduced from Figure 5.7: $\beta \approx 0.71(1 - 0.025\lambda)$.

$$T_a = \sqrt{0.65h \frac{9.8}{g} \left(1 + \frac{1}{\lambda^2}\right)} = \sqrt{\frac{h}{g} \frac{\delta_t}{\delta_{ov}} 26.54 \left(1 + \frac{1}{\lambda^2}\right)} \quad (5.95)$$

$$T_b = 2\pi \sqrt{\frac{\zeta^* \delta_l}{\alpha g}} = \sqrt{\frac{h}{g} \frac{\delta_l}{\delta_{ov}} 15.79 \frac{1}{\beta}} = \sqrt{\frac{h}{g} \frac{\delta_l}{\delta_{ov}} 22.24 \left(\frac{1}{1 - 0.025\lambda}\right)}, \quad (5.96)$$

The comparison (Figure 5.13), reveals differences lesser than 10% between both estimates.

5.4 Conclusions

This Chapter presents a theory-based approach for elaborating the complete capacity curve of a cantilever URM wall subjected to OOP seismic loading. This approach is based on well-known mathematical relationships between external forces, internal forces and displacements and includes the second order effects. Moreover, we provide a formulae to build a trilinear simplified, practical version of these capacity curves in a straightforward manner (Fig.5.8). This simplification has been carried out respecting the criteria of energy conservation below the curve and minimum quadratic error. This results in simplified trilinear capacity curves that take into account all the mechanical and geometrical properties considered significant to the wall studied. Additionally, our theory-based approach's capability to determine linear and non-linear period-displacement relationships has been demonstrated via comparison with several published experimental tests for different geometries and materials (Fig. 5.12).

The results of our work demonstrate that the critical factor which defines the behaviour of the elements studied is the relationship between two variables. The former being the independent variable, which represents the action of the lateral force, $\beta = \lambda\alpha$, characterised by the product of the slenderness and the base shear factor. The latter being the dependent variable, which represents the response and is characterised by the displacement relative to the overturning displacement, $\delta/\delta_{ov} = \delta/t$.

Additionally, the high stability obtained in the maximum values of the β shows that this is a very representative parameter. The range in which it oscillates is limited to $\beta = 0.45 - 0.68$ for cantilevers with very different

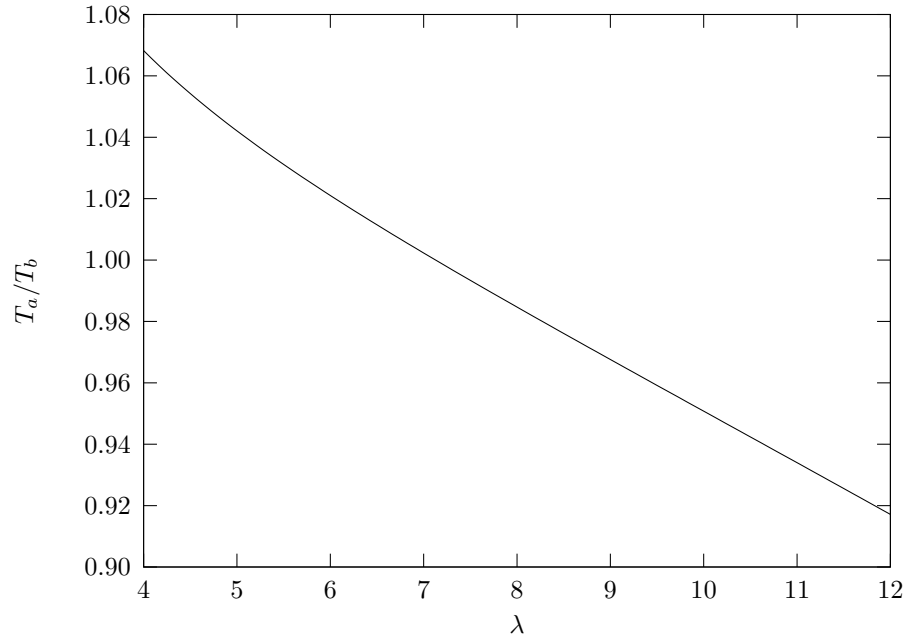


Figure 5.13: Quotient between the period estimated according to the NZSEE regulation [29] (T_a , eq. 5.95) and the analytical approach and formulae herein proposed (T_b , eq. 5.96).

geometrical and mechanical characteristics; which represents a range from 60% to 90% of the force that would overturn the parapet according to the rigid block model. This fact justifies the analysis of the actual behavior of flexible walls in relation to the highly simplified rigid block model.

Moreover, the parameters that influence the capacity curves of these elements have been determined: $\lambda, t, E/\rho, E/\sigma_c$ and σ_t/σ_c . Such parameters correspond to both, its geometric qualities, restricted to its slenderness λ , and the mechanical qualities of the masonry used. In particular, E/σ_c and σ_t/σ_c , and those that relate the geometric qualities of the masonry and the materials used, namely the relationship between the thickness, t , and the ‘scope’ \mathcal{A} of the masonry itself: $t/(\sigma_c/\rho) = t/\mathcal{A}$.

Additionally, an in-depth discussion about the different alternatives when determining the dynamic parameters of the wall—rotation of the wall around an elastic hinge located at different heights and the wall behaving as an elastic cantilever or as a rigid block—is included. This allows us to contribute a number of comparable expressions (Table 5.6) to characterise the kinetic energy of this type of element and its fundamental period, which depends on the equivalent relative height of the vibrating mass, ζ^* . Moreover, it permits the establishment of the most likely and adequate range of this parameter according to the experimental tests f: $\zeta^* = 0.4 - 0.44$.

Thus, this work contributes to extending and simplifying the applicability of the methodologies devoted to analysing the behaviour of cantilever masonry walls under seismic events as trilinear capacity curves constitute an operational and effective tool for assessing the vulnerability of these elements.

Future lines of research should expand the scope of the proposed approach to cantilever URM walls with a vertical pre-compressing force acting on top or to walls connected to other elements, such as floor structures or perpendicular walls.

References

- [1] Celeste Maria Nunes Vieira de Almeida. “Paredes de alvenaria do Porto: tipificação e caracterização experimental”. Phdthesis. Universidade do Porto, 2013. URL: <http://hdl.handle.net/10216/72621>.
- [2] Nasser Almesfer et al. “Material properties of existing unreinforced clay brick masonry buildings in New Zealand”. In: *Bulletin of the New Zealand Society for Earthquake Engineering* 47.2 (2014), pp. 75–96.

- [3] Filip Anić et al. “A review of experimental and analytical studies on the out-of-plane behaviour of masonry infilled frames”. In: *Bulletin of Earthquake Engineering* 18 (2020), pp. 2191–2246. DOI: [10.1007/s10518-019-00771-5](https://doi.org/10.1007/s10518-019-00771-5). URL: <https://doi.org/10.1007/s10518-019-00771-5>.
- [4] PG Asteris et al. “Numerical modelling of out-of-plane response of infilled frames: State of the art and future challenges for the equivalent strut macromodels”. In: *Engineering Structures* 132 (2017), pp. 110–122.
- [5] E. Buckingham. “On physically similar systems. Illustrations of the use of dimensional equations”. In: *Physical Review* 4 (1914), pp. 345–376. URL: <https://doi.org/10.1103/PhysRev.4.345>.
- [6] ICBO (International Conference of Building Officials). *Earthquake regulations for seismic isolated structures*. 1991.
- [7] Stavri Gjergji Burda. “Study of the seismic performance of traditional masonry buildings in the “Barceloneta” neighbourhood of Barcelona.” MA thesis. Universitat Politècnica de Catalunya, 2020.
- [8] Liborio Cavaleri, Maria Zizzo, and Panagiotis G Asteris. “Residual out-of-plane capacity of infills damaged by in-plane cyclic loads”. In: *Engineering Structures* 209 (2020), p. 109957.
- [9] Ray W. Clough and Joseph Penzien. *Dynamics of structures*. 3rd ed. Berkeley: “Computers & Structures Inc., 2003.
- [10] D D’Ayala and E Speranza. “Definition of collapse mechanisms and seismic vulnerability of historic masonry buildings”. In: *Earthquake Spectra* 19.3 (2003), pp. 479–509.
- [11] Stefania Degli Abbati and Sergio Lagomarsino. “Out-of-plane static and dynamic response of masonry panels”. In: *Engineering Structures* 150 (2017), pp. 803–820.
- [12] Hossein Derakhshan, Michael C. Griffith, and Jason M. Ingham. “Out-of-Plane Behavior of One-Way Spanning Unreinforced Masonry Walls”. In: *Journal of Engineering Mechanics* 139.4 (2013), pp. 409–417. DOI: [10.1061/\(ASCE\)EM.1943-7889.0000347](https://doi.org/10.1061/(ASCE)EM.1943-7889.0000347).
- [13] Hossein Derakhshan et al. “Seismic assessment of out-of-plane loaded unreinforced masonry walls in multi-storey buildings”. In: *Bulletin of the New Zealand Society for Earthquake Engineering* 47.2 (2014), pp. 119–138.
- [14] K.T. Doherty et al. “Displacement–based seismic analysis for out–of–plane bending of unreinforced masonry wall”. In: *Earthquake Engineering and Structural Dynamics* 31 (2002), pp. 833–850.
- [15] Dina F D’ayala. “Force and displacement based vulnerability assessment for traditional buildings”. In: *Bulletin of Earthquake Engineering* 3.3 (2005), pp. 235–265.
- [16] Gianmarco de Felice. “Out-of-plane seismic capacity of masonry depending on wall section morphology”. In: *International Journal of Architectural Heritage* 5.4-5 (2011), pp. 466–482.
- [17] Tiago Miguel Ferreira et al. “A simplified four-branch model for the analytical study of the out-of-plane performance of regular stone URM walls”. In: *Engineering Structures* 83 (2015), pp. 140–153.
- [18] Tiago Miguel Ferreira et al. “Experimental characterization of the out-of-plane performance of regular stone masonry walls, including test setups and axial load influence”. In: *Bulletin of Earthquake Engineering* 13.9 (2015), pp. 2667–2692.
- [19] Marta Giaretton, Dmytro Dizhur, and Jason M Ingham. “Dynamic testing of as-built clay brick unreinforced masonry parapets”. In: *Engineering Structures* 127 (2016), pp. 676–685.
- [20] Michele Godio and Katrin Beyer. “Analytical model for the out-of-plane response of vertically spanning unreinforced masonry walls”. In: *Earthquake Engineering & Structural Dynamics* 46.15 (2017), pp. 2757–2776. URL: <https://doi.org/10.1002/eqe.2929>.
- [21] Michele Godio and Katrin Beyer. “Trilinear model for the out-of-plane seismic assessment of vertically spanning unreinforced masonry walls”. In: *Journal of Structural Engineering* 145.12 (2019), p. 04019159.
- [22] Michael Craig Griffith et al. “Experimental investigation of unreinforced brick masonry walls in flexure”. In: *Journal of Structural Engineering* 130.3 (2004), pp. 423–432.
- [23] Lutz Hermanns et al. “Performance of buildings with masonry infill walls during the 2011 Lorca earthquake”. In: *Bulletin of Earthquake Engineering* 12.5 (2014), pp. 1977–1997.
- [24] George W. Housner. “The Behaviour of inverted pendulum structures during earthquakes”. In: *Bulletin of the Seismological Society of America* 53.2 (1963-02), pp. 403–417.
- [25] Sergio Lagomarsino. “Seismic assessment of rocking masonry structures”. In: *Bulletin of earthquake engineering* 13.1 (2015), pp. 97–128.

- [26] NTK Lam, JL Wilson, and GL Hutchinson. “The seismic resistance of unreinforced masonry cantilever walls in low seismicity areas”. In: *Bulletin of the New Zealand Society for Earthquake Engineering* 28.3 (1995), pp. 179–195.
- [27] T.T.K. Lam et al. “Time–history analysis of URM walls in out–of–plane flexure”. In: *Engineering Structures* 25 (2003), pp. 743–754. DOI: [10.1016/S0141-0296\(02\)00218-3](https://doi.org/10.1016/S0141-0296(02)00218-3).
- [28] NTC18. “Aggiornamento delle Norme tecniche per le costruzioni, 20 febbraio”. In: *Decreto Ministeriale del Ministero delle Infrastrutture e dei Trasporti* 42 (2018).
- [29] NZSEE. “Improvement of the Structural Performance of Buildings in Earthquakes. 2006-2012”. In: *New Zealand Society for Earthquake Engineering: New Zealand* (2012), p. 343.
- [30] Carlos Olmedo. “Structural efficiency variation with the problem size in some bending problems”. Phdthesis. Madrid: Universidad Politécnica de Madrid, 2015. URL: <http://oa.upm.es/39799/>.
- [31] Sadettin Orhan. “Analysis of free and forced vibration of a cracked cantilever beam”. In: *NDT&E International* 40 (2007), pp. 443–450.
- [32] Bharat Pradhan et al. “Prediction Equations for Out-of-Plane Capacity of Unreinforced Masonry Infill Walls Based on a Macroelement Model Parametric Analysis”. In: *Journal of Engineering Mechanics* 147.11 (2021), p. 04021096.
- [33] M Saba, J Lizarazo-Marriaga, and E Quiñones-Bolaños. “Overstress analysis of the Cartagena de Indias walls under different scenarios of masonry mechanical strength”. In: *Case Studies in Construction Materials* 13 (2020), e00410.
- [34] M Saba et al. “Petrographic of limestone cultural heritage as the basis of a methodology to rock replacement and masonry assessment: cartagena de Indias case of study”. In: *Case Studies in Construction Materials* 11 (2019), e00281.
- [35] Omar Al Shawa et al. “Out-of-plane seismic behaviour of rocking masonry walls”. In: *Earthquake Engineering & Structural Dynamics* 41.5 (2012), pp. 949–968.
- [36] Yanan Shi, Dina D’Ayala, and J Prateek. “Analysis of out-of-plane damage behaviour of unreinforced masonry walls”. In: *14th international brick and block masonry conference*. 2008, pp. 02–17.
- [37] Ana Simões et al. “Fragility curves for old masonry building types in Lisbon”. In: *Bulletin of Earthquake Engineering* 13.10 (2015), pp. 3083–3105.
- [38] Luigi Sorrentino et al. “Review of out-of-plane seismic assessment techniques applied to existing masonry buildings”. In: *International Journal of Architectural Heritage* 11.1 (2017), pp. 2–21.
- [39] British Standard. “Eurocode 6—Design of masonry structures—”. In: *British Standard Institution. London* (2005).
- [40] ABK-A Joint Venture. *Methodology for Mitigation of Seismic Hazards in Existing Unreinforced Masonry Buildings: Wall-testing, Out-of-plane*. The Corporation, 1981.

Chapter 6

Demand of non-structural elements of RC buildings. Filtering effects

This Chapter presents a study of the seismic wave transmission of four to six-storey RC Spanish residential buildings with a structure comprising reinforced concrete frames and interior and exterior unreinforced masonry infill walls and parapet walls by means of a case study. It is particularly focused on the building properties that influence non-structural elements (NSE) damage and collapse; due to that non-structural exterior unreinforced masonry infill walls and parapets are the cause of the majority of fatalities during some medium magnitude earthquakes. As mentioned before, in the 2011 Lorca earthquake, $M_w=5.2$ only one building collapsed; however, there were nine fatalities as a result of falling debris of these elements.

The seismic wave suffers a process of filtering from the seismic source to the point at which the element under analysis is located. This transformation depends on several factors, being these the main ones with respect to the NSE demand: (i) the soil between the epicenter and the building and (ii) the building on which the NSE is located. Figure 6.1 schematises the whole process.

Herein, the seismic wave transmission that provokes the building, factor (ii), is analytically studied ((2)→(3)) in Fig. 6.1). That is to say, from the base of the building to the NSE base.

To do that, two Lorca buildings and Lorca synthetic accelerograms at the location of both buildings will be used. With respect to the accelerograms, the actual seismic records are not available for the building emplacements as the nearest seismic station at the time of the incident was the LOR Seismic Station (LOR). For that reason, the transformation from the nearest point where records are available (LOR) to a point near to the building base and with the same soil characteristics [(1)→(2)] is taken from the publication by Alguacil et al. (2014) [4].

The performance-based design to which seismic engineering is tending highlights the importance of non-structural elements both in the seismic design of new buildings and in the assessment of existing ones. Although the performance-based concept is starting to become widely incorporated in building codes and standards, also with respect to NSEs ([26]), its application to the latter is not still so extended.

Non-structural components are commonly divided into three macros categories: architectural components, mechanical and electrical components, and building contents [23], in which damage to a large part is generally related to displacement and acceleration responses of the structure [40].

Several studies have focused on the seismic performance of non-structural components and on the influence of the seismic performance of the building in the NSE seismic demand [12]. Within the methods for characterizing the NSE demand, Floor Response Spectrum (FRS) approaches have been used, for instance, to assess the seismic performance of valuable non-structural components in RC buildings [5]. Moreover, the FRS approaches are been implemented on the latest regulations as a first attempt to incorporate the NSE safety on the building design, for example, the European code [19] and the Italian regulation [30], [26].

Within this context, some of the proposal of FRS approaches will be studied by means of a Spanish case study in order to investigate its possible implementation on the upcoming Spanish seismic regulation [13], which is currently

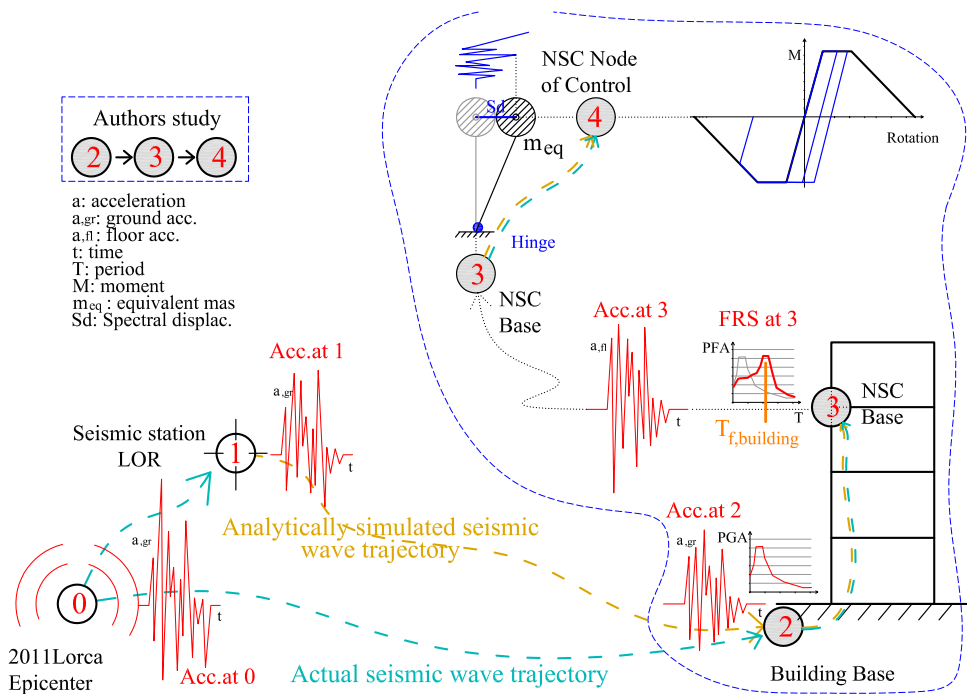


Figure 6.1: Schema of the seismic wave transformations from the earthquake origin to the NSC Node of Control.

- Actual transformations [0 → 2 → 3 → 4]: (0) Epicentre → (2) Building base → (3) NSC base → (4) NSC node of control.
- Analytically simulated transformations [1 → 2 → 3]: (1) LOR Station (actual registers) → (2) Building base [[4]] → (3) NSC base (input used for state of damage analysis)

in draft version. The case study is a prime example of the buildings whose NSE debris caused the nine fatalities during the 2011 Lorca earthquake. Moreover, Operational Modal Analysis have been carried out on the building in order to characterise its fundamental period as an infilled framed RC building. Both cases, bare structure and infilled frame structure are studied.

6.1 4 to 6-storey RC residential buildings: case studies

In Section 2.2.3, the main urban, structural and design features of the building type that caused the major number of fatalities due to falling debris of NSE during the Lorca earthquake was characterised. It was typified by 4 to 6-storey RC residential building located in an urban history block, with a RC framed structural system with one-way joist floor system and wide beams and one basement storey used as parking. Moreover, it would present solely one vertical communication core, a facing brick façade composed by two single-leaf layers separated by an air gap, single-leaf masonry interior infill walls, masonry parapets and several masonry chimneys. Additionally, the most hazardous NSEs of this building type were identified: unreinforced masonry parapets and façade walls, infill walls located on staircases, suspended ceilings and masonry chimneys.

Furthermore, Figure 6.2 provides a map in which the location of the nine fatalities incurred during the earthquake is illustrated. On it, the 4 to 6-storey RC31-pre and RC31-low typologies are highlighted to show the strong correlation between the causalities and the presence of said RC type of buildings.

6.1.1 Case studies

From all the 4 to 6-storey RC residential buildings included in the reports (section 2.2.3), two have been selected and modelled for a number of reasons: being representative of the aforementioned type and a great deal of information being available about their materials, dimensions, original and reparation plans, photographs and definition of the

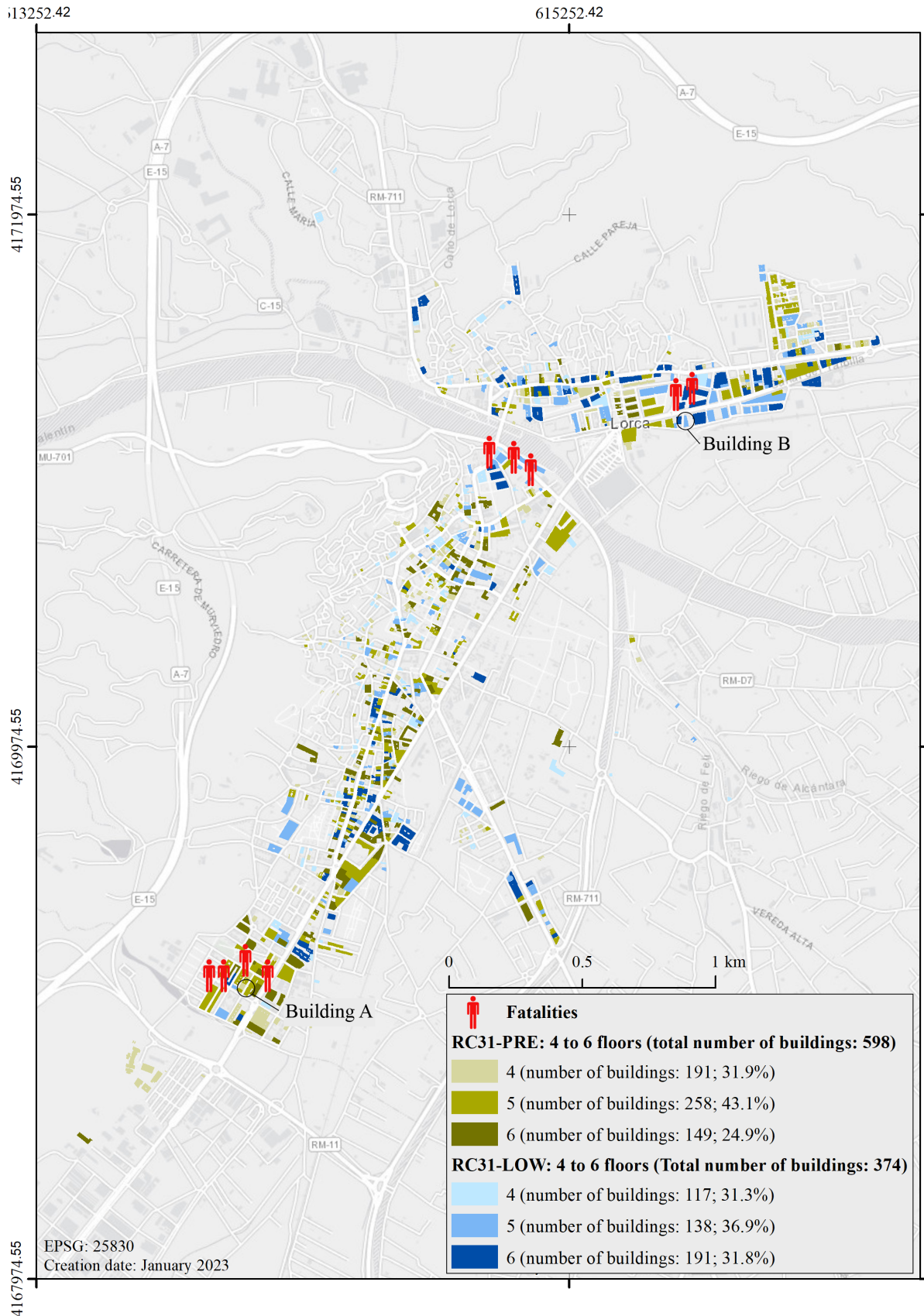


Figure 6.2: Map including all the typologies of RC buildings considered in this study: 4-6 storey RC31-pre and RC31-low buildings. Heights distinguished by colours. Moreover, the location of the fatalities incurred during the 2011 Lorca earthquake are marked. Buildings A and B used as case studies in this Chapter, see Appendix B

damages suffered during the earthquake. Both case studies share several features: both are five-storey buildings with a RC frame structure. Furthermore, both show less stiffness in their ground-floors, which is a common deficiency detected in multi-storey family housing with commercial units on their ground floors. The lack of interior and exterior infill walls implies less stiffness in such floors. However, they also present significant differences in their structural features, such as age, geometry, column dimensions and positions, which allow the authors to evaluate and compare results.

The case studies, Building A and building B, can be described as follows:

Building A

Building A (Figure 6.3) is an irregular construction in plan, representative of the 1970s residential type. It was designed according to outdated Spanish building regulations, [17] and [15] It is located in the corner of an urban expansion block with a central courtyard in the neighbourhood of La Viña (in the south of the city).

According to the European Macroseismic Scale criteria (EMS-98), the experts considered it as a type D vulnerability building with a moderate level of seismic design. A moderate (improved) level of earthquake-resistant design means that special measures of detailing (to improve ductility) are partially implemented. After the earthquake, it presented a Moderate level of damage according to the same scale (EMS-98): slight structural damage, moderate non-structural damage. Specifically, it showed slight generalized damage to ground floor and basement floor columns, and moderate damage to infill masonry walls on all floors, particularly noticeable in the interior elements. The compressive strength of the concrete of this building is 17.5 MPa (cylindrical specimens) and its steel reinforcement is comprised of reinforcing bars of the type B-400S steel.

The measurements of the building are approximately $37 \times 22 \text{ m}^2$ in plan, and the height of the stories are 4.45 m for the ground floor and 2.85 m for the floors above that. The columns dimensions are notably variable in thickness and width. For further information see Appendix B (photographs, details about their structure, NSEs and state of damage after the earthquake ...).

Building B

Building B (Figure 6.3) is located within an urban history block in the neighbourhood of San Diego, it was built in the 2000s and designed according to contemporary regulations [18] and [42]. It is located in the north of the city (see Fig. 6.2)

This building presented type 3 damages according to EMS-1998 [20]. Specifically, it showed moderate structural damage manifested as cracks to several ground floor columns, and severe non-structural damage, manifested as several exterior and interior IMWs collapsed on the ground floor as well as cracks and fissures caused by internal shear forces on the IMWs of the ground and the first floors. Additionally, the first-floor north-facing façade presented a severe risk of collapse caused by pounding with the adjacent building, severe damages to the roof chimneys that led to their enforced demolition and the localised collapse of an unreinforced masonry parapet. Moreover, it presented a distinct soft storey ground floor. The compressive strength of the concrete of this building is 25 MPa (cylindrical specimens) and its steel reinforcement is of the type B-400S.

The measurements of the building are approximately $40 \times 15 \text{ m}^2$ in plan, and the height of the stories are 3.90 m for the ground floor and 2.80 m for the floors above that. For further information see Appendix B (photographs, details about their structure, NSEs and state of damage after the earthquake).

Structural models of both buildings were recreated using the Software SAP2000 for both cases: the bare structure and the infilled structure model.

6.2 Bare structure models

The criteria used for the bare structure model represented in Fig. 6.3 is the following. This model is performed considering the non-linear range, for that reason, columns and beams were modelled as 1D unconfined RC frames with concentrated plasticity at their extremes (modelling parameters taken from [22]). Their dimensions were taken

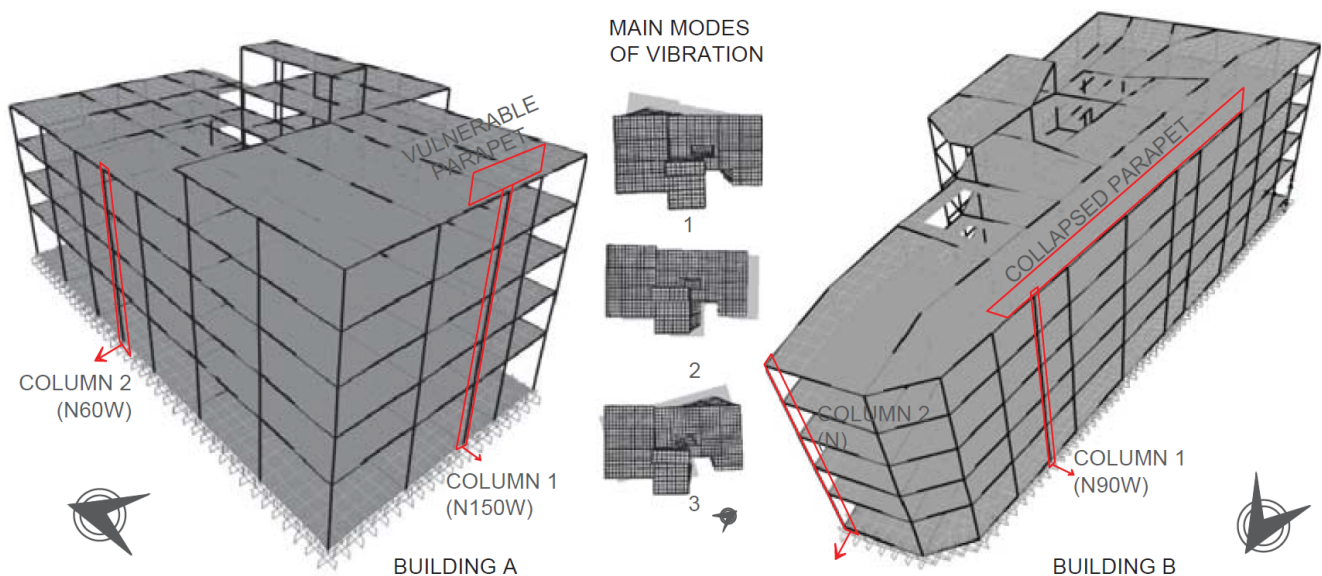


Figure 6.3: Bare structure models of Building A and Building B

from the layouts provided by the architects who conducted the reparation after the earthquake. Floor systems were modelled as 2D finite elements that behave as semi-rigid diaphragms. In addition, the authors have followed the criteria established by the contemporary regulations at the time of construction for the determination of their ultimate and service loads and steel reinforcement requirements of each RC element. Moreover, the connections between the structural frames and the foundations (rigid footings) and basement walls were modeled as fixed restraints.

Modal analysis of both models was carried out considering real inertia to be 125% of RC gross inertia ($1.25 EI$), in order to take into account a more than likely increase in the global stiffness of the buildings due to the presence of staircases and some masonry infill walls. It reveals that the main modes of vibration of both buildings are 0,9 s, 0,8 s and 0,7 s (T1, T2 and T3 respectively) when considering the secant stiffness.

Small differences in terms of fundamental natural periods have been found among these buildings. It is worth noting that the analysis of Building A shows that its most flexible modes of vibration are concentrated within these two ranges of periods: the fundamental one, between 1 and 0,8 s (from T1 to T3) and the second one, between 0,3 and 0,2s (from T4 to T8), which involve little mass, but that may be relevant as they are similar to the period of maximum acceleration during the Lorca event. The total weight in the seismic load combination was around 24300 kN for Building A and 32350 kN for Building B. Moreover, the modal results show that a global torsion is likely to occur due to the asymmetry of the buildings and to the eccentricity of their centres of mass in relation to their centres of rotation.

As mentioned before, the accelerograms applied as inputs at the base of the buildings are the synthetic accelerograms elaborated by [4] at different points in the city of Lorca. The accelerograms corresponding to the nearest point to the locations of the buildings have been applied for each building. In order to recreate the actual seismic event as realistically as possible, the inputs in the two orthogonal horizontal directions have been applied in the actual direction of the seism with respect to the buildings orientation.

6.2.1 Results in terms of Floor Response Spectra and discussion

The Floor Response Spectra (FRS) studied in this subsection include the comparison between linear and non-linear behaviour variations in terms of acceleration that represent the existence of a more flexible ground floor, and transformations floor to floor. 5% of damping of the NSEs has been accounted for the determination of the FRS. The predictions made by the simplified method of EN-1998 [19] were also analysed. These simplified European predictions describe the hazard by means of a single parameter, the value of the peak ground acceleration- a_{gr} - in the emplacement of reference. In these cases, the peak ground acceleration values have been taken from the new

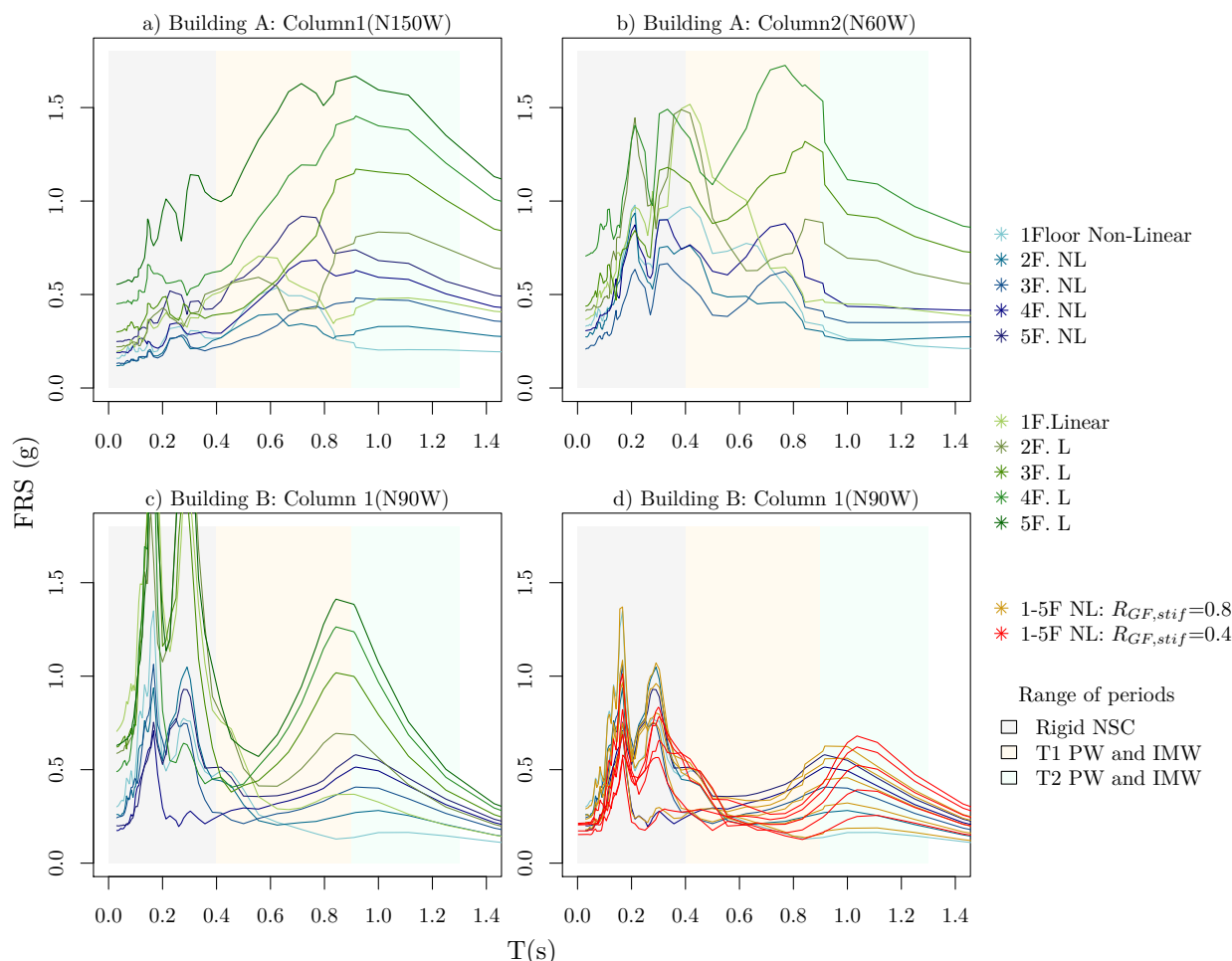


Figure 6.4: a) and b) Comparison between linear and non-Linear FRS in two points of Building A for two different directions of motion c) and d) Comparison of FRS of three different Ground Floor Stiffness Ratios ($R_{GF, stif}$): 1, 0.8 and 0.4.

Range of periods: Rigid NSC, elastic period for rigid NSE such as URM Spanish parapets according to OMA analysis (see also Fig. 5.12); T1 PW and IMW, values of T1 for Spanish parapets and infill walls according to [16]’s trilinear simplification; T2 PW and IMW, values of T1 for Spanish parapets and infill walls according to [16]’s trilinear simplification. See the said publication for greater detail.

proposal for the Spanish hazard map [25] which constitutes an improvement over the previous one included in the Spanish regulation in force, NCSE-02 [41].

In both buildings, the selection of the points where the FRS are studied was based on a number of parameters related to the vulnerability of their non-structural elements, which depends on its position, elevation, length, distance to the centre of torsion, etc. Figure 6.4 highlights the strong influence of the motion directionality in the seismic response of NSE by contrasting the FRS in orthogonal directions of Building A. The results show that during the Lorca earthquake, directionality is especially relevant for short-period elements, whereas for intermediate and long-period elements the peak floor spectral accelerations are similar: 1.7 g for Linear Analysis and 0.9 g for Non-Linear Analysis).

Additionally, in the same figure (Fig. 6.4), graph c) contrasts the Linear and Non-Linear FRS of Building B, showing again the same substantial differences in the range of intermediate and long-periods (linear peak floor spectral acceleration is more than twice the value of the homologous non-linear acceleration).

Moreover, due to the characteristics of this particular seismic event, (high short-period content), the FRS of both buildings exhibited a change in tendency (increased and decreased) in terms of acceleration in the short-period content of the FRS of some floors. This situation may be considered as a localised effect derived from the existence

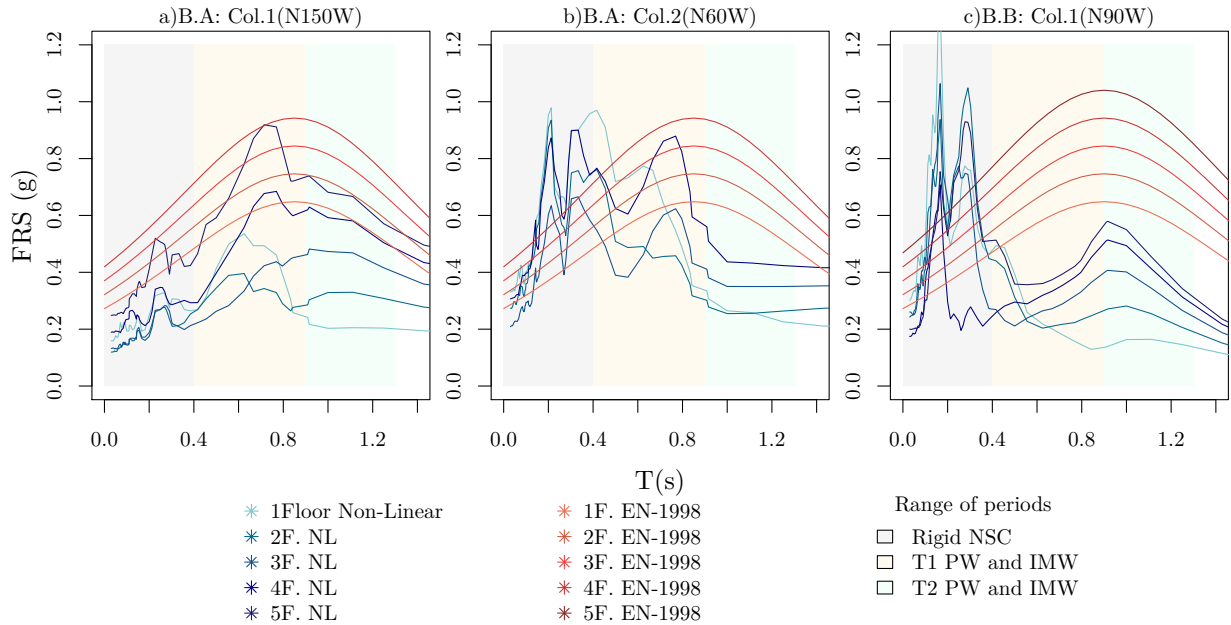


Figure 6.5: Comparison between non-linear and [19] FRS: a) and b) in two points of Building A for two different directions of motion; and c) in column 1 of building B. B.A.= Building A; B.B.= Building B; Col.= Column.

of modes of vibration in that range of periods, even when they involve little mass, thereby stressing the importance of considering such modes of vibration as a modifying factor of the FRS.

Finally, the possibility of a soft storey was computed. This phenomenon is defined by the stiffness of the lateral force-resisting system in any storey being less than 70% of the stiffness of an adjacent storey (above or below) or less than 80% of the average stiffness of the three storeys (above or below) [21]. The soft storey is quantified by means of the relative storey stiffness and can be compared by considering different elastic modulus, moments of inertia or column lengths [36]. In this study, the moment of inertia of the structural elements located in the ground floor has been considered to be the most appropriate parameter of control for this phenomenon in Building B ($R_{GF,stif}$).

In Figure 6.5 d), a comparison between the FRS of Building B considering different degrees of ground-floor stiffness in relation to the upper floors is made ($R_{GF,stif} = 1$, $R_{GF,stif} = 0.8$ and $R_{GF,stif} = 0.4$) allowing the authors to conclude that although this difference increases the acceleration slightly, it is not particularly relevant in global terms. However, it is commonly agreed that this phenomenon induces a crucial localised concentration of inter-storey drift and increases the possibility of fragile collapse.

The comparison between EN-1998 [19] predictions and the Non-Linear Time History Analysis (NLTHA) FRS predictions in the same three points previously analysed (Building A: Columns 1 and 2 and Building B: Column 1) shows that, for this type of buildings and seismic spectra, the predictions of this simplified method present certain lack of accuracy for some range of periods. For the intermediate and long-period elements, the simplified predictions can be considered to be significantly overestimated for Building B, whereas the predictions are extremely consistent for the highest floors of Building A.

The predictions also underestimate FRS acceleration for short periods, where this situation can represent a risk to safety for rigid NSEs such as unreinforced masonry chimneys. In these buildings in particular, chimneys suffered significant damages: in Building A some chimneys resulted in partial collapse causing falling debris, and, in Building B several chimneys had to be demolished. This underestimation could be due to the fact that this particular earthquake presented higher acceleration in short-periods, in contrast to the fundamental periods of the building; and EN-1998 [19] predictions amplify mainly the accelerations in periods similar to those of the building.

6.2.2 Conclusions for the bare structure model

The research findings of this study with bare structure models have provided some evidence that, for the analysed typology, it is crucial to consider the entrance of the structure in the non-linear range when characterising the FRS. Furthermore, the results from the Lorca case study illustrate that [19] FRS proposal underestimates the actual demand for some frequencies, even after considering the increment of the peak ground acceleration that introduces the new proposed maps for Spain [13]. Moreover, the FRS obtained highlights the relevance of the modes of vibration that involve less mass.

In the following, the infill masonry walls are incorporated in the modelisation of the buildings in order to study their influence on the FRS in the linear range of the whole building. To do that, Operational Modal Analysis are performed to characterise their main period considering the current NSEs. Then, the accuracy of the Eurocode formulae (EN-1998, [19]) for characterizing the FRS in this case, and the possibility of implementing the proposals already included in the Italian code (NTC-18) in the upcoming Spanish regulation (NCSR-22, [13]) is studied through the analysis of the response of the same case study, Building A.

6.3 Model updating considering non-structural elements

Several experimental campaigns has shown that frame-infill interaction can produce an important modification to the whole system stiffness ([37]). Furthermore, the force distribution in the frame elements can vary significantly if compared to the case of the bare frame ([14]).

For these reasons, this section addresses the characterization of the seismic demand of NSEs with an infilled frame model through the study of the response of a building in Lorca pertaining to the described structural type, by means of the FRS method. The infilled frame model is created in SAP2000 with masonry infills simulated by equivalent struts. Next, an updating process of the model has been performed, that is, the parameters of a finite element model have been adjusted in order to put in agreement its predictions — in terms of eigenvalues and eigenvectors — with the measurements obtained by modal testing. Said calibration is performed so as to fit with the main elastic period of the building, identified by means of ambient vibration tests conducted with a Tromino device.

The FRS results obtained with the numerical model by a Linear Time History Analysis (LTHA) simulating the Lorca earthquake, are compared with the results suggested by the Eurocode in force and by the Italian Building Code. Specifically, in the case of the Italian Building Code, both the simplified formulation for moment resisting frame buildings and the modal superposition spectrum-to-spectrum approaches are considered. Finally, the potential resonance of the dynamic behaviour between the obtained FRS and the natural periods of the masonry parapets located at the top of the building is discussed.

6.3.1 Dynamic properties and numerical model of the case study

In this section, the Operational Modal Analyses carried out on said case study in order to characterize the frequency of its fundamental modes and the numerical model built on the basis of said data are described.

The case study is Building A, which has been already described in section 6.1.1 and in further detail in Appendix B (see Figures 6.3 and 6.10).

Dynamic properties: Operational Modal Analysis

Measuring the resonance frequencies of structures and soils is relatively easy and in the last few decades it is commonly done under ambient excitation ([10], [28] and [3]). Furthermore, in recent times, the interest of the structural engineering community in the Experimental Modal Analysis (EMA) for modal identification (resonance frequencies, damping ratios, and mode shapes) is being replaced by the Operational Modal Analysis (OMA) ([39] and [27]). This change is due to the fact that the OMA has the capability to implement economical and quick tests that rely solely on the responses of the structure without affecting the operating conditions of the building [35].

For this case study, the ambient vibrations were recorded for ten minutes on different point located at different levels of the building (see Figures 6.10) using a Tromino (MoHo s.r.l.) portable 3D velocity sensor (Fig. 6.6).



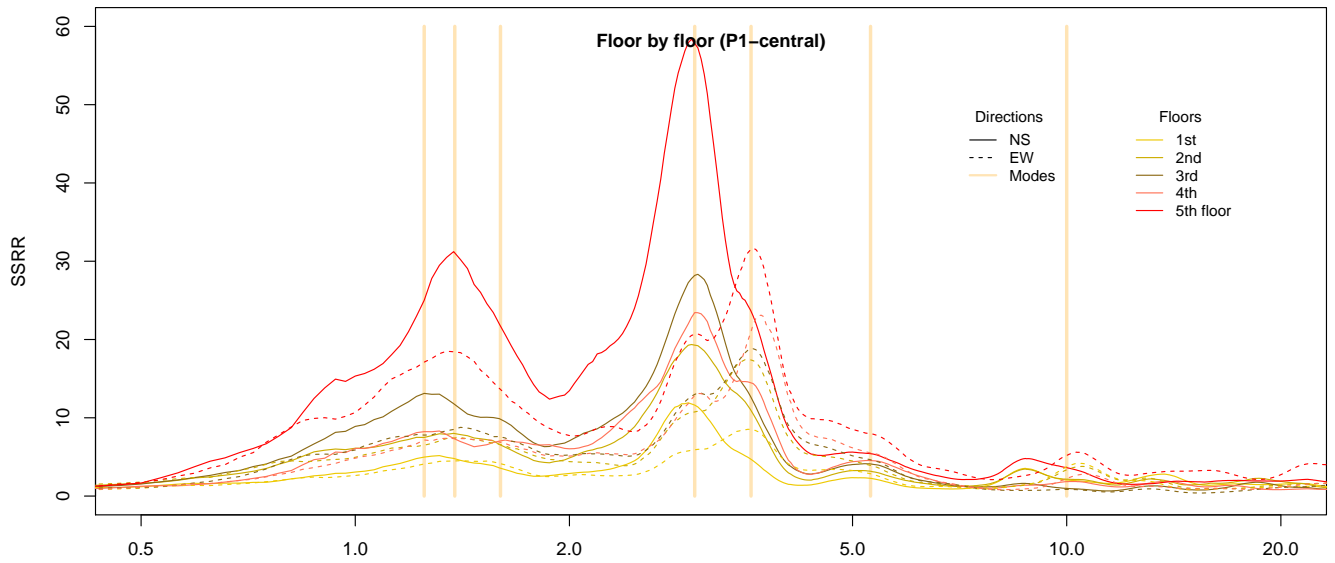
Figure 6.6: Photograph of the Tromino (MoHo s.r.l.) portable 3D velocity sensor during the measurements in Lorca

Main frequencies identification Three different methods have been applied to analyse the results of the ambient vibration tests:

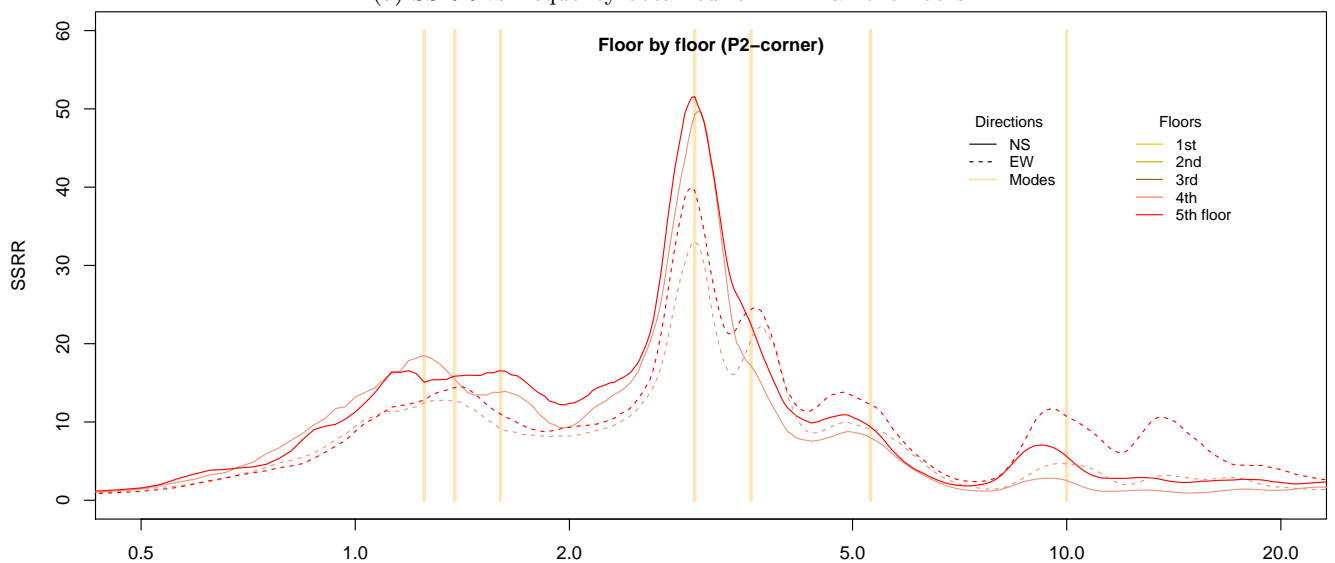
- SSR: Standard Spectral Ratio
- EFFD: Enhanced Frequency Domain Decomposition
- SSI: Stochastic Subspace Identification

The Standard Spectral Ratio (SSR) is one of the most easy, popular, widely accepted and used reference site method to evaluate site response [29]. The SSR is a technique where the site response is defined as the ratio of the Fourier amplitude spectrum of ground motions recorded at a soil-site to that of ground motions recorded at a rock-site record located nearby, from the same earthquake and component of motion ([6]). Nonetheless, nowadays, this method of analysis is also used by some authors to characterise frequencies of buildings from single station measurements (see [10] and [11]). This because some of the main features of the dynamic behavior of a structure can be assessed even with a single instrument [34] with some precautions. Nonetheless, simultaneous measurements are always preferable as they allow getting the phase information and greater accuracy. Therefore, the spectral ratio between the homologous recordings at the different levels and the reference recording at the underground floor (SSR, Standard Spectral Ratio) have been analysed obtaining the results in terms of frequencies indicated in Table 6.1. For the application of this technique, the software included in the Tromino (MoHo s.r.l.) used for the experimental tests has been used. In Figure 6.7, the results for the central point floor by floor, for the P2 located in a corner floor by floor, and for the points P1, P2, P3 and P4 of the forth floor are shown. See also Table 6.1 for the results in numerical values and Fig. 6.10 for the location of points P1, P2, P3 and P4.

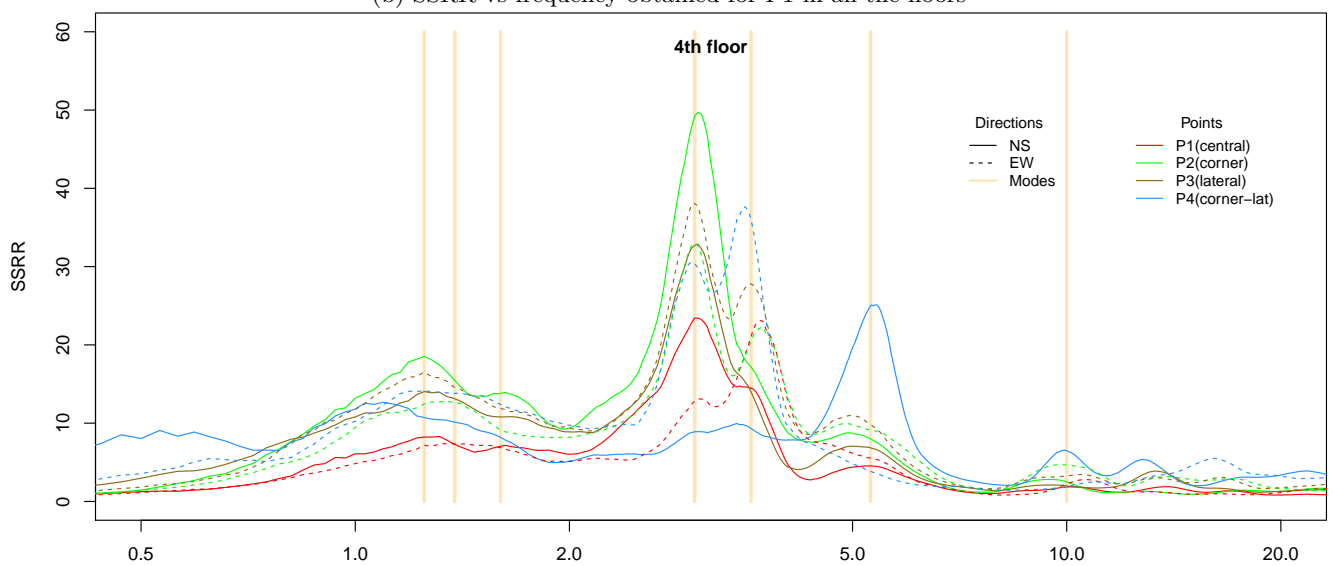
The Enhanced Frequency Domain Decomposition (EFDD) is one of the OMA methods that has received significant interest from the engineering community involved in the identification of the modal features of structures. The great attention towards this method is driven by its capability as a user-friendly and fast processing algorithm for computing natural frequencies and mode shapes through assuredly and reasonably accurate estimates ([1] and [35]). The EFDD represents an improvement of the Frequency Domain Decomposition (FDD), which was based on the fact that introducing a decomposition of the spectral density function matrix, the response spectra can be separated into a set of single degree of freedom systems, each corresponding to an individual mode. By using this decomposition technique close modes can be identified with high accuracy even in the case of strong noise contamination of the signals. Also, the technique clearly indicates harmonic components in the response signals



(a) SSRR vs frequency obtained for P1 in all the floors



(b) SSRR vs frequency obtained for P1 in all the floors



(c) SSRR vs frequency obtained for the 4th floor

Figure 6.7: Results in terms of SSRR vs frequencies according to the SSRR technique for Building A. See Fig. 6.10 for the location of points P1, P2, P3 and P4.

[8]. For the application of this technique, a Matlab code has been developed. See Fig. 6.9b and Table 6.1 for results.

The data driven Stochastic Subspace Identification (SSI) techniques is considered to be the most powerful class of the known identification techniques for natural input modal analysis in the time domain [9]. In the SSI techniques a parametric model is fitted directly to the raw times series data returned by the transducers. A parametric model is a mathematical model with some parameters that can be adjusted to change the way the model fits to the data. In general we are looking for a set of parameters that will minimize the deviation between the predicted system response (predicted transducer signal) of the model and measured system response (transducer signal). This process is often called model calibration (see Figure 6.8). Moreover, this technique permits the vibration-based structural health monitoring, which usually needs to extract vibration characteristics from operational vibration measurements [38]. For the application of this technique, another Matlab code has been developed. See Table 6.1 for results.

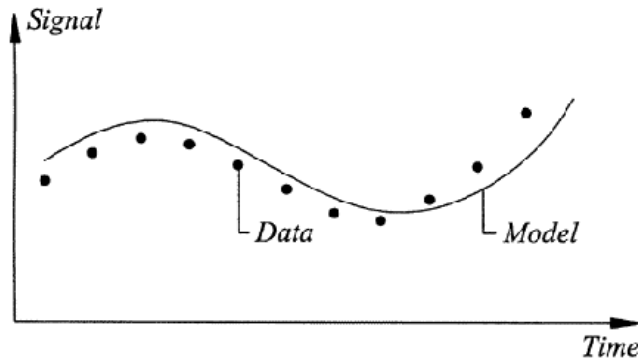


Figure 6.8: Conceptual schema of the SSI technique.

Table 6.1 summarises the results in terms of frequencies, Freq[Hz] (and periods, T[s]) for each of the methods.

Freq[Hz] (T[s])	Values in order					
SSR	1.25 (0.80)	1.38(0.72)	1.60(0.62)	3.00(0.33)	3.60(0.28)	5.30(0.19)
EFDD	-	-	-	2.96(0.34)	3.55(0.28)	4.91(0.20)
SSIL	-	-	-	2.95(0.34)	2.98(0.34)	-

Table 6.1: Main frequencies of vibration of Buildings A. Values ordered for an easy comprehension of similar results.

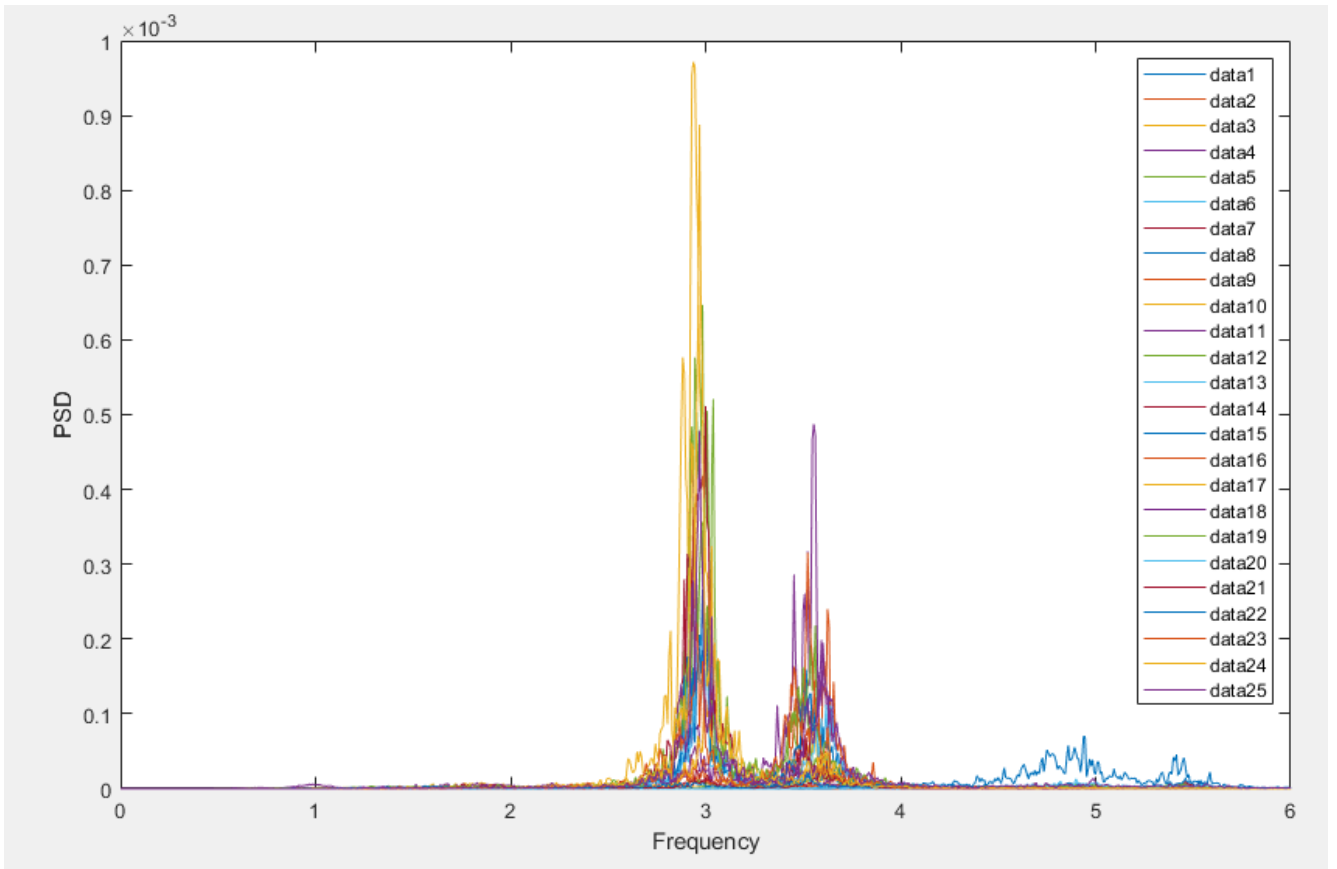
All the OMA carried out reveal that there is a dominant frequency at 2.95-3.00 Hz (corresponding to a period of 0.33-0.34 s). Therefore, the real fundamental period of this building is around T=0.34s by conjunction of results between methods. This value is extremely dissimilar to that obtained from the numerical model of the bare structure, around 1.0 Hz (bare structure model detailed in the previous section of this Chapter and in [32]).

This result is in line with the conclusions of several experimental campaigns: frame-infill interaction can produce an important modification to the whole system stiffness ([37]) and the force distribution in the frame elements can vary significantly if compared to the case of the bare structure ([14]). For said reasons, an enhanced numerical model including the infills was created .

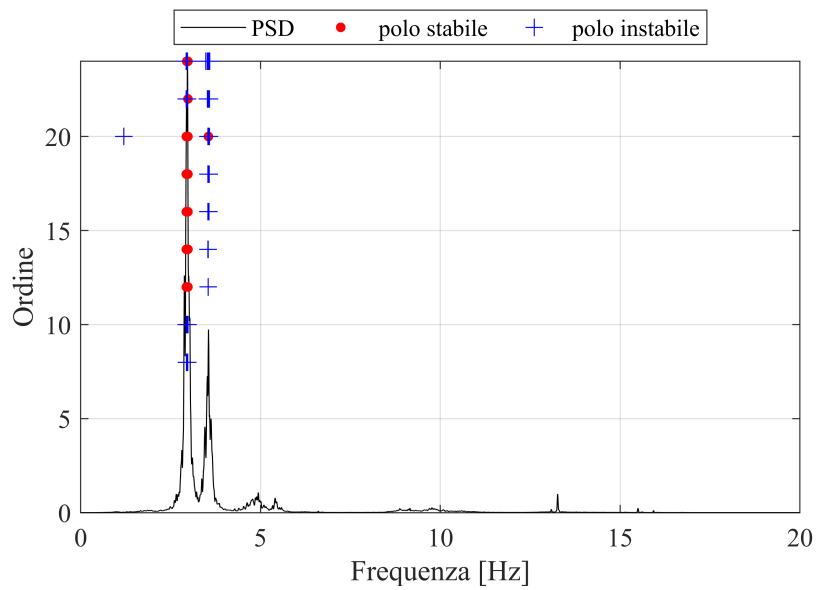
Numerical model

The structural model of the building (Fig.6.10) was recreated in a similar way to the bare structure model: columns and beams were modeled as 1D RC elements and floor systems as rigid diaphragms composed by 2D finite elements. Nonetheless, as the model was built so as to reproduce the linear behavior, plasticity of structural elements was not introduced. Additionally, the slab of the stairs and the RC walls constituting the elevator structure were modeled.

Moreover, in order to capture the global behaviour of the structure in the linear range, the infill panels, representing the NSE, were modelled by means of two equivalent diagonal struts. Previous research has shown that equivalent diagonal single-strut models provide reliable approximations of the global response of the structure, such



(a) Power Spectral Density of the registers of Building A



(b) Stable poles for the EFDD

Figure 6.9: Building A

as the natural frequencies of a building or the definition of the mode shapes (Asteris et al. 2013 [7]).

Only the infills that directly affect the global behaviour were modelled, i.e., those located within a RC frame or connected to the main structure. Conversely, the contribution of interior or exterior infills which were not directly connected to any frame element (beams or columns) were neglected. Nevertheless, the masses of all the infill masonry walls were included in the model. It is worth mentioning that the distribution of the infills is quite irregular in this typology of buildings and in constant change.

The diagonal struts were modelled only with axial stiffness and with the following characteristics: an elastic modulus E equal to that of the masonry itself, assumed as 2995 MPa ([7]), panel thickness t equal to the actual thickness of the infill divided by two as there are two struts, and an equivalent strut width w . Then, the cross-sectional area of the equivalent strut is wt . As reported in Bovo et al. (2020), [7], several studies to evaluate the strut width w can be found. In this case, the initial tentative model considered an optimal width equal to $0.24d$, according to Bovo et al. (2020), where d is the diagonal length of the equivalent axial strut. The exterior and interior infills were differentiated by their dissimilar thickness as follows.

With the aim to not introduce in the model double strut thickness, the value equal to one-half of the real thickness has been introduced in the model. Therefore, the wall thicknesses considered in the models are:

- For the perimeter walls: 8.5 cm (real thickness of the masonry: 10+7cms)
- For the interior partition walls: 4cm (real thickness: 7cms)

Next, a model updating process was performed, which, as mentioned before consists in adjusting one or various parameters of the finite element model in order to obtain the predictions of the model - in terms of eigenvalues - in agreement with the measurements obtained by modal testing. Specifically, parametric analyses on the value of the infills w/d ratio were performed in order to reach the natural period obtained in the experimental campaign. The frequency of the numerical model was equal to that of the experimental analyses for a w/d ratio of 0.30. With this value, the main period of the analytical model was the same as that identified in the modal operational analyses, $T=0.34$ s. This fundamental mode constitutes a torsional mode (Fig. 6.10), which is consistent with the irregular design of the building.

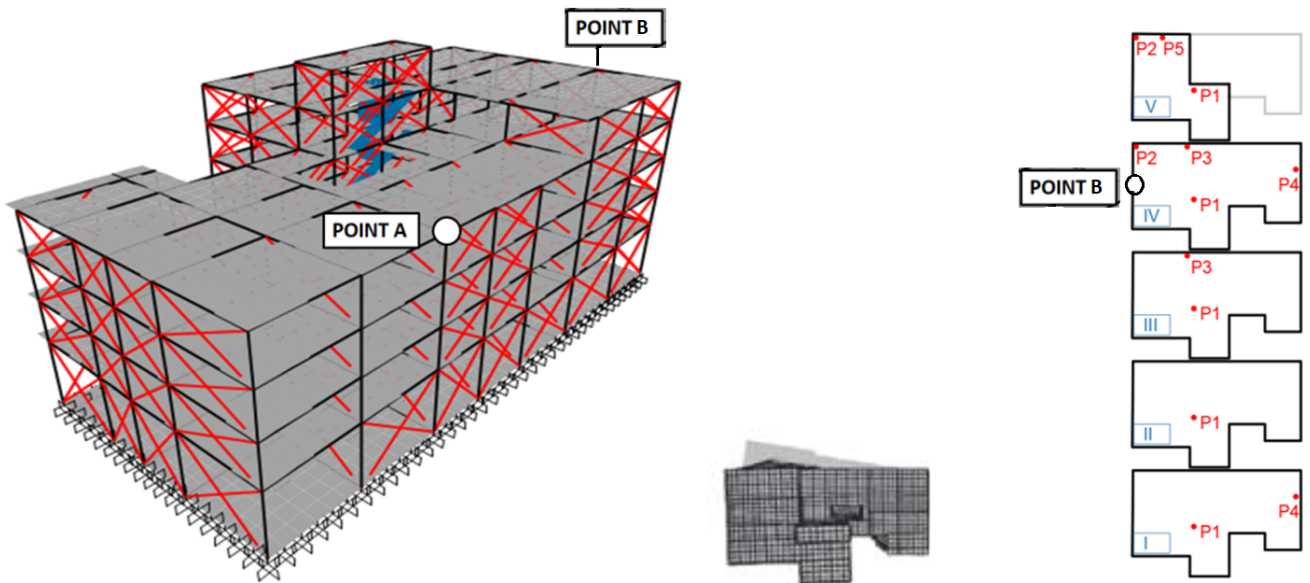


Figure 6.10: (Left) 3D model of the case study: a RC residential building of Lorca (diagonal struts in red; stairs and wall of the elevator in blue). (Centre) First mode of vibration. (Right) Location of the Tromino Device during the Ambient Vibration Tests carried out (Number of Floor in Roman Numbers).

Modal shapes results In the following, the different mode shapes obtained in the two proposed models for Building A are compared. As Fig. 6.11 illustrates, the mode shapes do not vary substantially when comparing the bare structure with the infilled frame model. In both models, the first mode shape corresponds to a rotation

around a centre of rotation located at a point close to the SE corner. The second mode shape corresponds to flexion in the EW direction. And the third mode shape corresponds to a rotation around a centre slightly displaced from the centre of the building itself in the west direction.

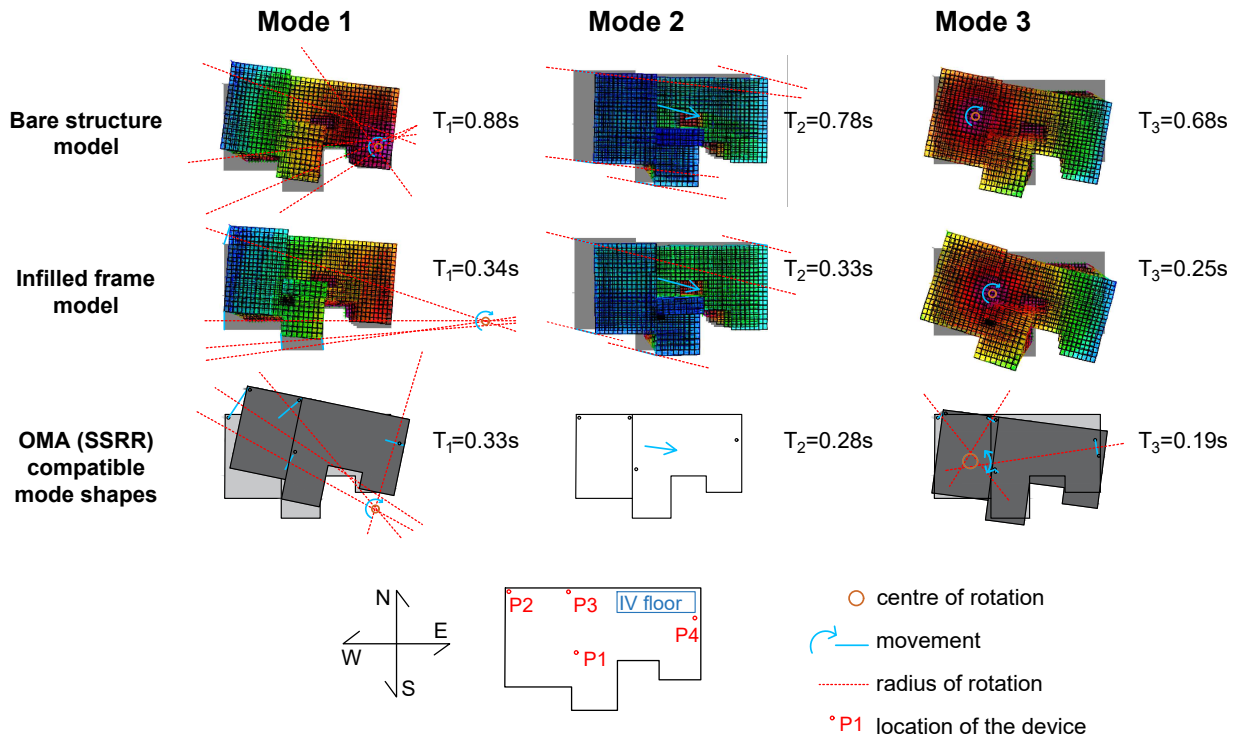


Figure 6.11: Comparison of the mode shapes of the firsts three modes of Building A. Obtaining from: top) modal analysis of the bare structure numerical model; centre) modal analysis of the bare structure numerical model; and bottom) comparison of the SSRR resulting from the operational modal analysis.

In addition, in order to check the compatibility of the results obtained in terms of mode shapes from the analysis of both numerical models with those obtained from the OMA carried out in situ, the outputs provided by Standard Spectral Ratio (SSR) method are employed. This methodology can provide certain useful information about the mode shapes from single station measurements (see [10] and [11]) when the ambient noise is not very dissimilar between the consecutive measurements and the modes are separated enough in terms of frequencies so as to not produce coupling between them. That is to say, when the maximum response of the vibration mode studied is not influenced by the coupling effect with the closest modes to it and therefore, the mode shapes of each mode can be considered independent. This coupling effect can be identified visually in the SSRR graphs. Nonetheless, in the best case, this method only provides information about the relationship between the movement maximum values of the different points studied in absolute figures homogenized at a certain scale.

The SSRR data used for the study of the compatibility between results in terms of mode shapes are those referring to the 4th floor, as this is the most relevant floor in terms of movements and that in which more measurements were taken (see Fig. 6.12). The results of the said study are also shown in Fig. 6.11. As can be seen in said Figure, the results acquired based on the SSRR outputs are in general terms compatible with those obtained in the modal analyses of both numerical models. Specifically, the possible movements corresponding to the first mode can also represent a rotation around a centre close to the SE corner; and the third mode a rotation around a centre slightly displaced from the building centre in the west direction. Whereas, concerning the second mode, the effect of coupling with the first one prevent us from recognizing with accuracy the points' movements, although the

graph does permit the clear identification of the mode as flexion in the EW direction, since the maximum responses are very superior to those in the NS direction for all the points measured.

Finally, the specific values of the modes are compared, obtaining that, the periods (in seconds) provided by the bare structure model are around twice those obtained in the OMA for the three main modes of vibration. Besides, when updating the infilled frame numerical model in order to fit the period of the first mode of vibration obtained in the OMA, a good correspondence is obtained for the three main modes of vibration in terms of periods as well as mode shapes, which validates the model proposed for the purpose of studying the FRS.

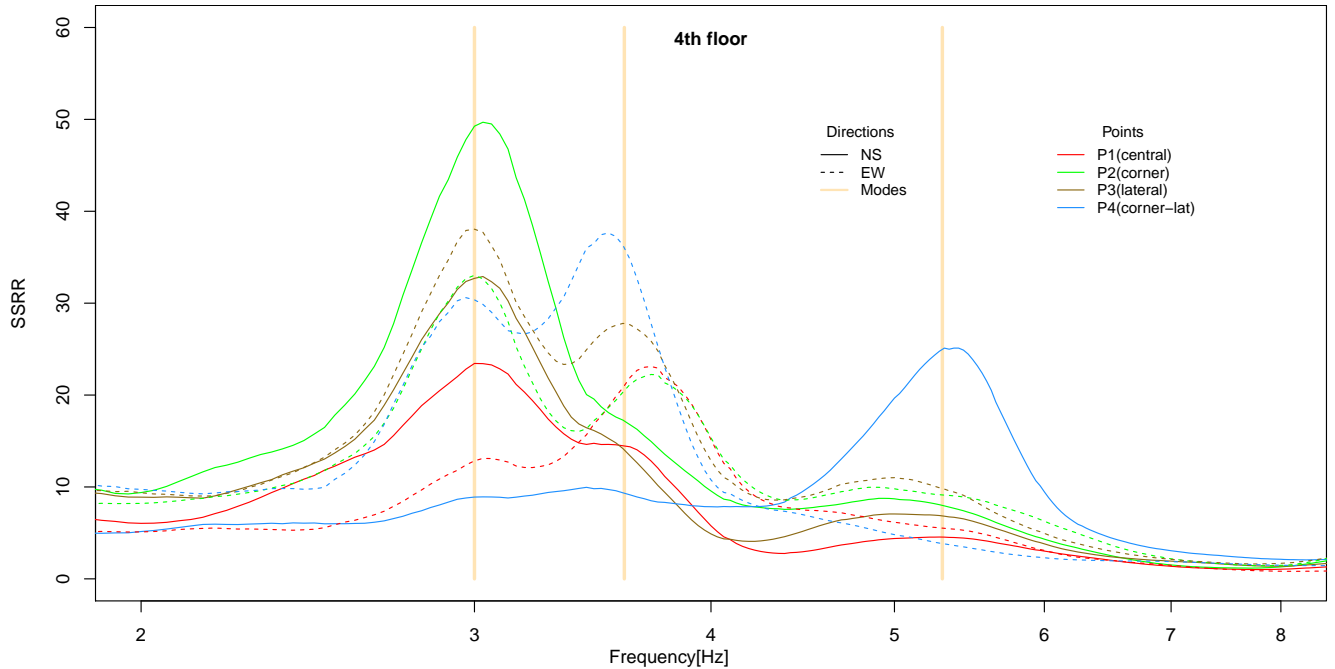


Figure 6.12: SSRR vs frequency obtained for the 4th floor according to the SSRR technique for Building A. See Fig. 6.10 for the location of points P1, P2, P3 and P4.

6.3.2 Floor Response Spectra

The FRS of the building were obtained through numerical simulations, by considering two different horizontal directions for the same point (point A), located on the roof of the building (Fig. 6.10), as an extremely vulnerable parapet was located there. These results are compared with those proposed by the Italian and the European regulations, paying special attention to the fact that the first mode of this building is torsional.

Numerical simulations

The Lorca 2011 earthquake was a very shallow seismic event (1 km deep), with magnitude equal to $5.2 M_w$; an acceleration of 0.37 g was recorded by the LOR accelerograph station in the centre-north part of the town. Synthetic accelerograms were developed by [4] for 11 different points of Lorca from the records collected at the LOR station during the earthquake. In the present work, a Linear Time History Analysis (LTHA) with the synthetic accelerograms developed for the nearest point to the building (among the 11 above mentioned) was carried out. The N-S and E-W accelerograms were applied with their actual direction with respect to the building orientation. A 5% damping for both the building and the NSE was considered.

In addition, a modal analysis was carried out on the numerical model for the application of the procedures to characterize the FRS according to the Italian code. In the numerical simulations, this means to consider the 85% of the total mass in both horizontal directions. The inclusion of this huge number of modes is justified by the fact that NSE are extremely rigid elements. Therefore, their fundamental period in the elastic range is very low, thus, the resonance will appear when the low period modes of the building are excited. Therefore, despite the fact that these modes are characterized by very low modal mass participation ratios, they should not be overlooked.

European and Italian regulations proposals

In the Spanish regulation in force (NCSE-02, [41]), there is no reference to a procedure for the calculation of the FRS; however, the European regulation could be applied to Spanish buildings. In the following, the methods provided by the Italian regulation are presented and applied, being these proposals more up-to-date according to the state-of-the-art.

The commentaries of the Italian regulation (MIT-19) provide from simple to complex formulae that include simplified and general methods. Herein, the general formulation (MIT19 General Formulation), the simplified formulation (MIT19 Simplified Formulation) and the simplified formulation for Moment Resisting Frame buildings (MIT19 Simp. Formulation for MRF) are briefly summarized and applied to the case study. For further information of these procedures see [19], MIT19 [26] and [33]. For the sake of brevity, not all the parameters involved in each formulation are described here.

EC8 proposal The European regulation, indicated herein as EC8 proposal, suggests the following formula (Eq. 6.1) to characterize the FRS of a building, being S_a the spectral acceleration. It only takes into account the PGA (Peak Ground Acceleration), the period of the NSE T_a , the main period of the building T_1 , the height z at which the NSE under study is located, the total height of the building h_b , and a factor that accounts for the NSE non-linear behaviour q_a . The PGA is 0.478g in Y direction and 0.307g in X direction, z is 13m and h_b is 15.85m.

$$S_a(T_a, z) = \frac{PGA}{q_a} \left(\frac{3 \left(1 + \frac{z}{h_b}\right)}{1 + \left(1 - \frac{T_a}{T_1}\right)^2} \right) - 0.5 \geq \frac{PGA}{q_a} \quad (6.1)$$

MIT19-Nmodes: General Formulation This formulation (Eqs. 6.26.3) is based on a modal superposition approach, in which the results of the general modes i, j are combined using the SRSS rule. It takes into account the particular spectral acceleration for each specific mode and the NSE damping factor ξ_a .

In order to apply this formulation to a building with torsional modes, the modal shapes (Φ) for the specific points under study and modal participation factors (Γ) in both horizontal directions (X and Y independently) were taken from the 3D numerical model. Φ_{ij} is the j -th component of the i -th modal shape. This procedure cannot be followed without the 3D model for a building whose main modes are torsional. A different spectrum for each of the two directions was obtained. Therefore, it was worthwhile to study the actual direction of the NSE in order to combine the spectra and the type of loading to be considered (in-plane or out-of-plane loading).

$$S_{a,ij}(T_a, \xi_a) = \Gamma_i \varphi_{ij} S_e(T_i) R(T_a/T_i; \xi_a) \quad (6.2)$$

$$R = \left[\left(2\xi_a \frac{T_a}{T_i} \right)^2 + \left(1 - \frac{T_a}{T_i} \right)^2 \right]^{-\beta}, \text{ with } \beta = 0.4 - 0.5 \quad (6.3)$$

The amplification factor R considers the coupling between the i -th vibration mode of the structure and the fundamental mode of the NSE through the coefficient β , herein considered 0.5. The values of all the values of Φ and Γ cannot be reported for space limitation.

MIT19-Simp-Nmodes: Simplified Formulation This constitutes a simplified multimodal formulation based on Degli Abbati et al. (2018) [2]. In this case, the results of the different modes are also combined by using the SRSS rule. The non-linearity of the structure could be included by varying the period and the viscous damping of the building ξ_i corresponding to the period. Eq. 6.4 shows its values for each mode considered, being $\eta(\xi_a)$ the damping correction factor for the NS element ($\eta(\xi_a) = [10/(5 + \xi_a)]0.5$).

$$S_{a,i}(T_a, \xi_a, z) = \begin{cases} \frac{11\xi_i^{-0.5}\eta(\xi_a)PFA_i(z)}{1 + [11\xi_i^{-0.5}\eta(\xi_a) - 1](1 - T_a/aT_i)^{1.6}} & \text{for } T_a < aT_i \\ 11\xi_i^{-0.5}\eta(\xi_a)PFA_i(z) & \text{for } aT_i \leq T_a < bT_i \\ \frac{11\xi_i^{-0.5}\eta(\xi_a)PFA_i(z)}{1 + [11\xi_i^{-0.5}\eta(\xi_a) - 1](T_a/bT_i - 1)^{1.2}} & \text{for } T_a \geq bT_i \end{cases} \quad (6.4)$$

where a and b are parameters defining the range of periods of maximum amplification of the spectrum ($a=0.8$ and $b=1.1$), and PFA, the Peak Floor Acceleration, which can be determined by means of Eq. 6.5.

$$PFA_i(z) = S_e(T_i, \xi_i) \left| \Gamma_i \varphi_i(z) \sqrt{1 + 0.0004\xi_i^2} \right| \quad (6.5)$$

MIT19-Simp-MRF: Simplified Formulation for MRF This formulae includes the parameters a , b and a_p , which have been calibrated to take into account the elongation of the fundamental period due to system non linearity and the contribution of the higher modes. The values of parameters are $a=0.8$, $b=1.4$ and $a_p=5.0$ for $T_1 < 0.5s$; $a=0.3$, $b=1.2$ and $a_p=4.0$ for $0.5s < T_1 < 1.0s$ –this case study–; and $a=0.3$, $b=1.0$ and $a_p=2.5$ for $T_1 > 1s$. In general terms, it considers the PGA as the input and provides conservative values. Eq. (6.6) shows its formulation:

$$S_a(T_a, z) = \frac{1}{q_a} \begin{cases} PGA \left(1 + \frac{z}{h_b}\right) \left[\frac{a_p}{1 + (a_p - 1)(1 - T_a/aT_i)^2} \right] & \text{for } T_a < aT_i \\ \geq PGA & \\ PG \left(1 + \frac{z}{h_b}\right) a_p & \text{for } aT_i \leq T_a < bT_i \\ PGA \left(1 + \frac{z}{h_b}\right) \left[\frac{a_p}{1 + (a_p - 1)(1 - T_a/bT_i)^2} \right] & \text{for } T_a \geq bT_i \\ \geq PGA & \end{cases} \quad (6.6)$$

6.3.3 Results in terms of Floor Response Spectra

The numerical simulations results in terms of FRS for the cases described are shown in Figures 6.13 and 6.14.

Firstly, in Figure 6.13, the effect on the FRS results of two Building A columns of the seismic directionality is studied by means of the application the seismic input in three different directions. Moreover, three different accelerograms corresponding to the earthquake of Lorca are applied in order to assess the influence of the frequential content variation of the seismic input even for the same seismic event. Specifically, in said Figure, the LTHA of these cases are represented:

- The results in terms of FRS floor by floor for two different columns of the building with out-of-plane acceleration in orthogonal directions are shown. See Figure 6.3 for the locations of Columns 1 and 2 on Building A and Figure 6.10 for the infilled framed model used for the analysis.
- The application of these three different inputs: the synthetic accelerogram elaborated for SP11 (the nearest point to Building A, [4]), the synthetic accelerogram elaborated for SP2 (the nearest point to Building B, [4]); and the actual accelerograms recorded at the LOR station (LOR).
- The application of these three different inputs in three different directions: in the same direction as the Lorca actual earthquake; with the North direction of the input (main one) applied in the longitudinal direction of the building; and with the North direction of the input (main one) is applied in the transversal direction of the building.

The results, illustrated in Figure 6.13 show that all the parameters involved in the study —directionality of the earthquake, specific frequency content and location of the NSE under study— influence the NSE seismic demand.

Secondly, the various predictions of the different code proposals for the case study are graphed in Figure 6.14, together with the results of the numerical simulations.

The numerical solution obtained by Linear THA and considering 30 modes is considered as the reference solution. It provided several peaks for the periods of the modes that characterize the structure, which were concentrated in a series of intervals: 0.34s (2 modes), 0.25s (1 mode), 0.12-0.07s (27 modes). The Floor Spectra Acceleration obtained with this method reached the extremely high value of almost 12 g in the X direction for NSE with a

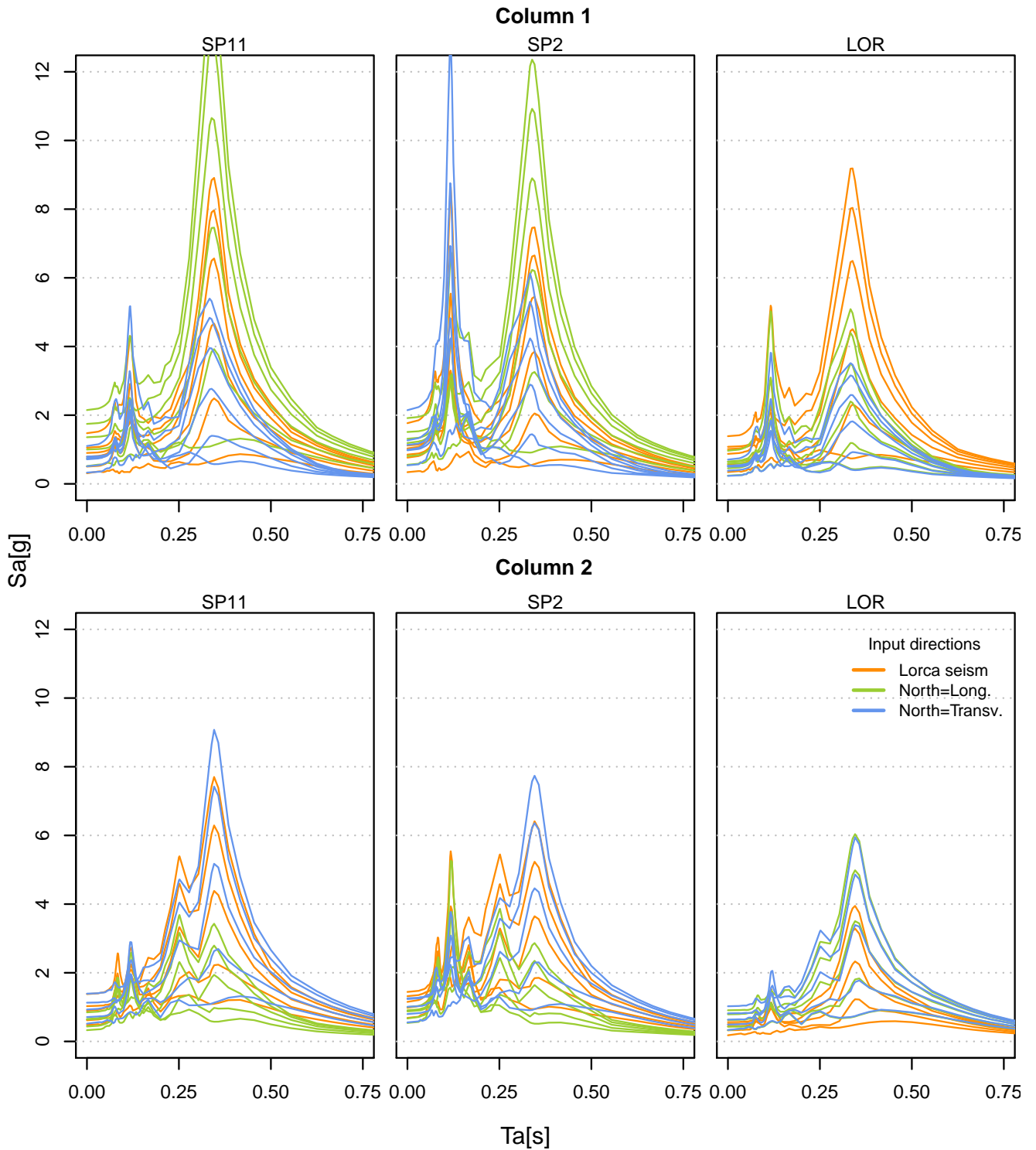


Figure 6.13: FRS floor by floor for two different columns of the building with out-of-plane acceleration in orthogonal directions (See Figure 6.3 for the locations of Columns 1 and 2 on Building A and Figure 6.10 for the infilled framed model used for the analysis). LTHA with synthetic the accelerograms elaborated for SP11 (the nearest point to Building A), SP2 (the nearest point to Building B) and LOR (the accelerograms recorded at the LOR station). The three colours represent three different orientations for the seismic inputs: Orange= in the same direction as the Lorca actual earthquake; Green= the North direction of the input (main one) is applied in the longitudinal direction of the building; and Blue= the North direction of the input (main one) is applied in the transversal direction of the building

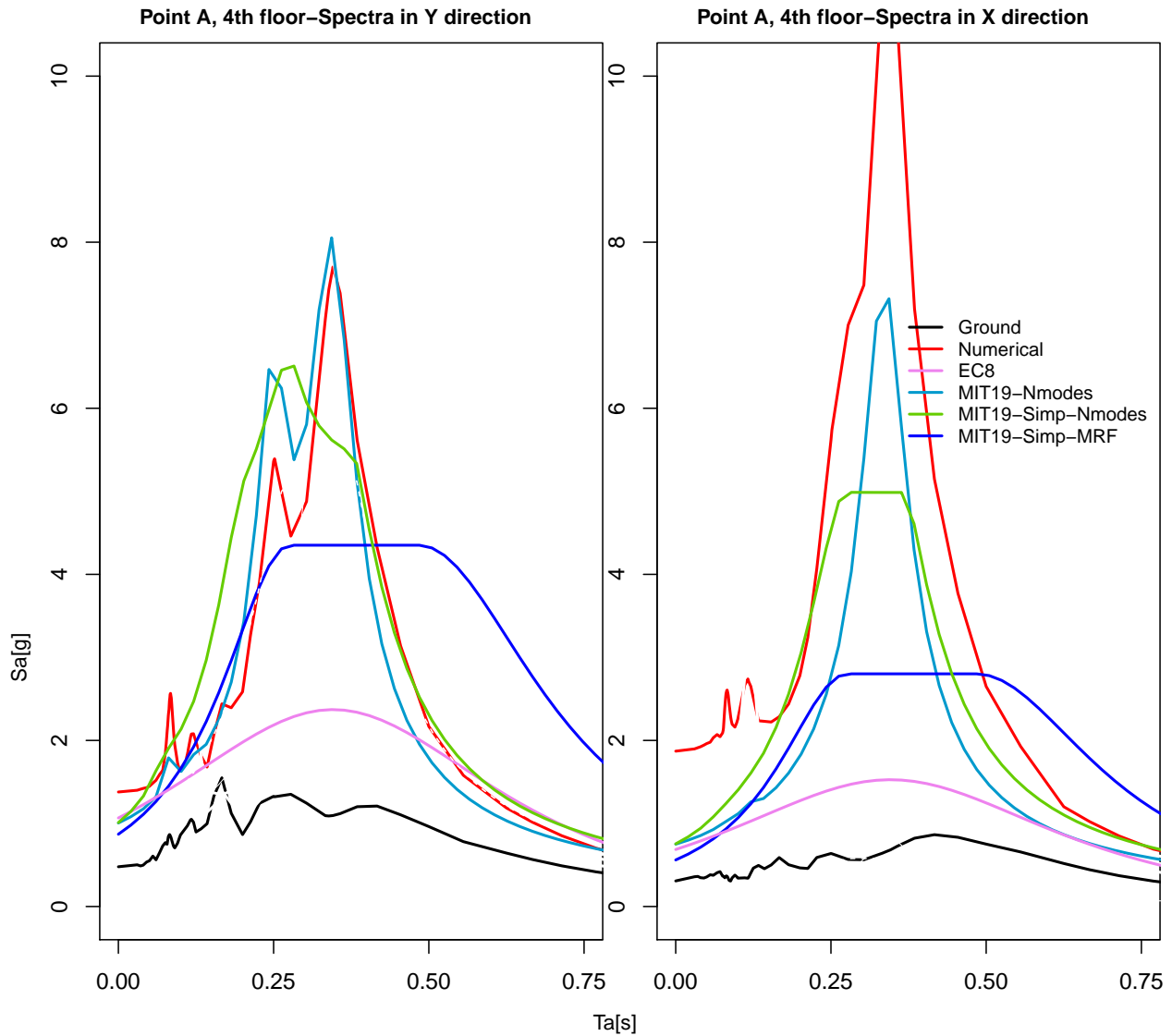


Figure 6.14: Spectra in X (longitudinal) and Y (transversal) direction for the point A of the case study building (4th floor).

period of around 0.35-0.4s (the main period of the building). Nonetheless, for rigid elements ($T < 0.25$ s) the accelerations are notably smaller.

When compared with the numerical spectra, the results predicted by the various codes indicates that the Italian regulation (the General Formulation - MIT19-Nmodes) provides a formulation that, although complex to use, can be much more reliable for 4 to 6-storey RC residential Spanish buildings. Nonetheless, none of the methods ensures to cover the maximum spectral values for all the periods that can characterize the NSE. In particular, the results of the EC8 proposal, which uses as seismic input the PGA and the period of the main mode of vibration instead of the S_a of each specific mode and a SRSS combination of them, are extremely unsafe.

In the case of Spanish parapets, OMA carried out on samples of two buildings have shown that their main frequency in the elastic range in the range of 15 and 20 Hz (around $T=0.05-0.07$ s). The results for the SSR technique are shown in Fig. 6.15 for a sample located in Building A. Said Figure reflects that NSE are elements with a very low period, always inferior to 0.06s in this particular case. Moreover, other parapets of different lengths pertaining to a building from a different city obtaining similar results. Nonetheless, Housner demonstrated ([24]) that rocking walls do not have a unique natural period, as the period is strongly influenced by their displacements.

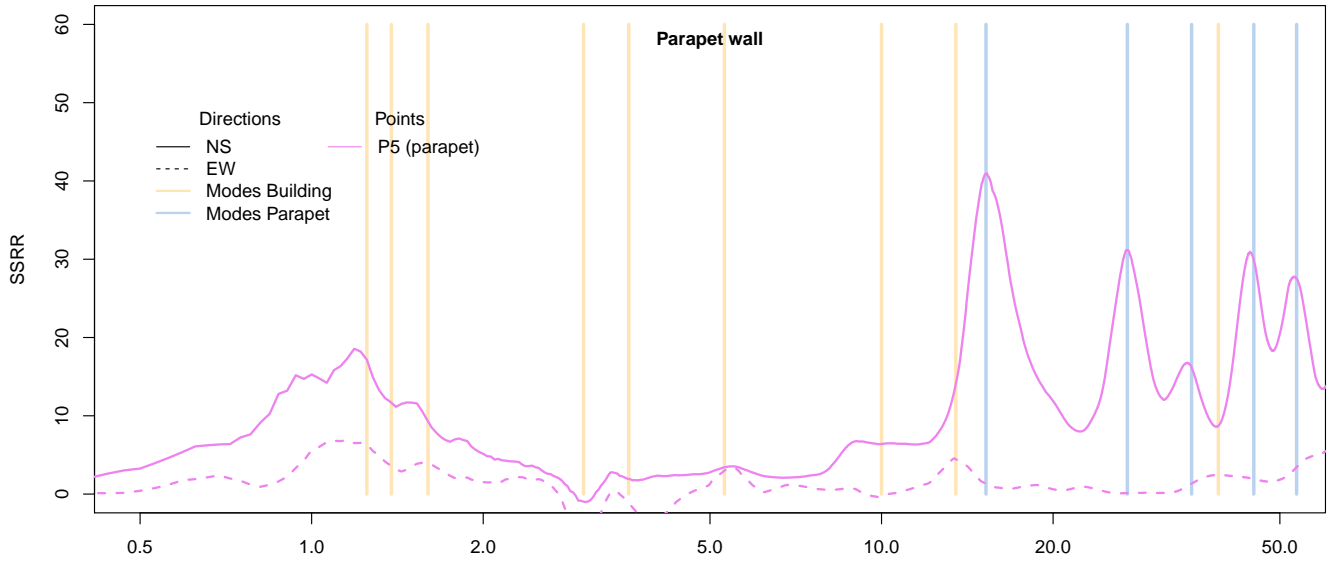


Figure 6.15: Results in terms of frequencies according to the SSRR technique for a parapet located in the fifth floor of Building A.

These NSEs can reach periods greater than 0.5 s in the non-linear range ([16] and [31]).

Finally, the results for three different models and analyses: (i) bare structure model and LTHA; (ii) bare structure model and NLTHA; and (iii) infilled frame model and LTHA were illustrated in Figure 6.16. Said Figure shows in red line the extreme case (iii) infilled frame model and LTHA and in blue and green the extreme cases (i) bare structure model and NLTHA and (ii) bare structure model and NLTHA. The interpretation of said results leads the researcher to the consideration of the importance of the intermediate damage states of the building, since they could result in greater FRS demand for NSE with intermediate main periods, $T = 0.4-0.8s$ (gray points indicates possible intermediate states that depends on the frequency content of the seismic wave).

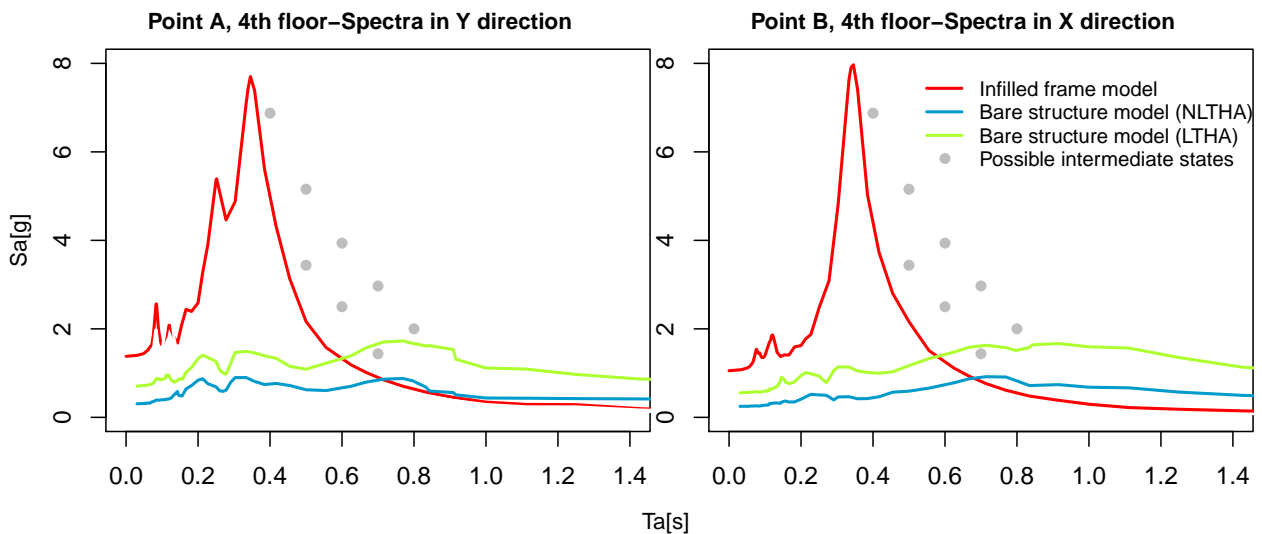


Figure 6.16: Spectra in X (longitudinal) and Y (transversal) direction for the 4th floor, points A and B of Building A considering three different models and analyses: (i) bare structure model and LTHA; (ii) bare structure model and NLTHA; and (iii) infilled frame model and LTHA. Gray points indicates possible intermediate states that depends on the frequency content of the seismic wave.

6.3.4 Conclusions and recommendations

An adequate characterization of the FRS is a key aspect when designing NSE in seismic prone areas. Nonetheless, the Spanish regulation in force does not include any method of characterization for this type of seismic demand. Furthermore, the European regulation provides an oversimplified formulation that gives rise to very unsafe results in some cases, such as the case study shown in this work.

For that reason, in light of the results, it would be sensible to implement the Italian regulation methods for the characterization of FRS in the upcoming Spanish regulation (NCSR-22, [13]). This implementation will permit not only the design of less dangerous NSEs, such as façades or parapets, but also a more adequate design of particular NSEs and crucial devices pertaining to buildings of special importance, e.g. hospitals or nuclear power stations, which have to remain within the elastic range during the seismic events. Nevertheless, it is worth mentioning that any of the methods provides completely safe results.

On the other hand, the torsional modes that characterize the building under study require the creation of a 3D model of the structure in order to obtain the FRS in both directions, necessary, as they present extremely different characteristics in terms of spectral magnitude-NSEs' period. The manner of combining loads derived from FRS of different directions for NSEs in order to produce safe results deserves further discussion.

Finally, future lines of research should also consider intermediate damage states of the building —those between the non-damaged infilled frame model and the bare structure model (where all the NSEs are implicitly considered in collapse state)— for the elaboration of the FRS.

Acknowledgements

The financial support of the Italian Department of Civil Protection (ReLUIS 2022-2024 Grant-WP4) and the KUK AHPÁN-RS project: Amenaza y Riesgo Sísmico en América Central y Sureste de España, Ministry of Science and Innovation of Spain (Grant RTI2018-094827-B-C22 funded by MCIN/AEI/ 10.13039/501100011033 and by “ERDF A way of making Europe”) are gratefully acknowledged. Thanks to AIA Architects (Lorca) for providing the data and reports of the case study. This study was conducted thanks to a scholarship granted by the Reale Collegio di Spagna in Bologna to Laura Navas-Sánchez to carry out her PhD at UNIBO.

References

- [1] M Danial A Hasan et al. “Enhanced frequency domain decomposition algorithm: a review of a recent development for unbiased damping ratio estimates”. In: *Journal of Vibroengineering* 20.5 (2018), pp. 1919–1936.
- [2] Stefania Degli Abbati, Serena Cattari, and Sergio Lagomarsino. “Theoretically-based and practice-oriented formulations for the floor spectra evaluation”. In: *Earthquakes and Structures* 15.5 (2018), pp. 565–581.
- [3] Hanan Al-Nimry, Musa Resheidat, and Marwa Al-Jamal. “Ambient vibration testing of low and medium rise infilled RC frame buildings in Jordan”. In: *Soil Dynamics and Earthquake Engineering* 59 (2014), pp. 21–29.
- [4] G Alguacil et al. “Characterization of earthquake shaking severity in the town of Lorca during the May 11, 2011 event”. In: *Bulletin of earthquake engineering* 12.5 (2014), pp. 1889–1908.
- [5] Luisa Berto et al. “Seismic safety of valuable non-structural elements in RC buildings: Floor Response Spectrum approaches”. In: *Engineering Structures* 205 (2020), p. 110081.
- [6] Roger D Borcherdt. “Effects of local geology on ground motion near San Francisco Bay”. In: *Bulletin of the Seismological Society of America* 60.1 (1970), pp. 29–61.
- [7] Marco Bovo, Michele Tondi, and Marco Savoia. “Infill modelling influence on dynamic identification and model updating of reinforced concrete framed buildings”. In: *Advances in Civil Engineering* 2020 (2020).
- [8] R. Brincker, L. Zhang, and P. Andersen. “Modal identification of output-only systems using frequency domain decomposition”. In: *Smart materials and structures* 10.3 (2001), p. 441.
- [9] Rune Brincker and Palle Andersen. “Understanding stochastic subspace identification”. In: *Conference Proceedings: IMAC-XXIV: A Conference and Exposition on Structural Dynamics*. Society for Experimental Mechanics. 2006.

- [10] Silvia Castellaro. “Soil and structure damping from single station measurements”. In: *Soil Dynamics and Earthquake Engineering* 90 (2016), pp. 480–493.
- [11] Silvia Castellaro et al. “Dynamic Characterization of the Eiffel Tower”. In: *Procedia engineering* 199 (2017), pp. 3332–3337.
- [12] Samit Ray Chaudhuri and Roberto Villaverde. “Effect of building nonlinearity on seismic response of non-structural components: a parametric study”. In: *Journal of structural engineering* 134.4 (2008), pp. 661–670.
- [13] NCSR-22. Norma de Construcción Sismorresistente (upcoming). “Consulta pública previa sobre el borrador de Real Decreto por el que se aprueba la Norma de Construcción Sismorresistente NCSR-2022. Last visit 10/05/2023”. In: (). URL: www.mitma.gob.es/el-ministerio/buscador-participacion-publica/audiencia-e-informacion-publica-sobre-el-proyecto-de-real-decreto-por-el-que-se-aprueba-la-norma-de-construccion-sismorresistente-ncsr-22.
- [14] Francisco J Crisafulli, Athol J Carr, and Robert Park. “Analytical modelling of infilled frame structures: A general review”. In: *Bulletin of the New Zealand society for earthquake engineering* 33.1 (2000), pp. 30–47.
- [15] P.D.S.-1. Ministerio de Planificación del Desarrollo. “Decreto 3209/1974, España. Norma Sismorresistente”. In: *RD 3209/1974, Spain* (1974). URL: www.boe.es/diario_boe/txt.php?id=BOE-A-1974-1869.
- [16] K.T. Doherty et al. “Displacement-based seismic analysis for out-of-plane bending of unreinforced masonry wall”. In: *Earthquake Engineering and Structural Dynamics* 31 (2002), pp. 833–850.
- [17] EH-73. “Comisión Permanente Instrucción para el proyecto y la ejecución de obras de hormigón en masa o armado”. In: *RD 3062/1973, Spain* (1973). URL: www.boe.es/eli/es/rd/2008/07/18/1247.
- [18] EHE-08. “EHE-08 Comisión Permanente del Hormigón Instrucción de Hormigón Estructural”. In: *RD 1247/2008, Spain* (2008). URL: www.boe.es/eli/es/rd/2008/07/18/1247.
- [19] EN-1998. “Eurocode 8: Design of structures for earthquake resistance - Part 1 : General rules, seismic actions and rules for buildings”. In: *European Committee for Standardization, Brussels*. (2003).
- [20] European Seismological Commission. “European Macroseismic Scale 1998”. In: *Cahiers du Centre Européen de Géodynamique et de Séismologie*. Ed. by G. Grünthal. Vol. 15. Luxembourg: Conseil de l’Europe, 1998. ISBN: 2-87977-008-4.
- [21] FEMA-310. “American Society of Civil Engineers for the Federal Emergency Management Agency, Washington, D.C. Handbook for the Seismic Evaluation of Buildings—A Prestandard.” In: (1998).
- [22] FEMA-356. “Prestandard and Commentary for the Seismic Rehabilitation of Buildings”. In: (2000), pp. 100–400.
- [23] Andre Filiatrault and Timothy Sullivan. “Performance-based seismic design of nonstructural building components: The next frontier of earthquake engineering”. In: *Earthquake Engineering and Engineering Vibration* 13.1 (2014), pp. 17–46.
- [24] George W Housner. “The behavior of inverted pendulum structures during earthquakes”. In: *Bulletin of the seismological society of America* 53.2 (1963), pp. 403–417.
- [25] IGN, 2015. Developed by IGN and UPM. Last visit 08/02/2022. URL: <https://www.ign.es/web/mapas-sismicidad>.
- [26] MIT-19. “Istruzioni per l’applicazione dell’«Aggiornamento delle “Norme tecniche per le costruzioni”», 21 gennaio”. In: *Decreto Ministeriale del Ministero delle Infrastrutture e dei Trasporti* 7 (2019).
- [27] Aleksey Mironov et al. “Condition monitoring of operating pipelines with operational modal analysis application”. In: *Transport and Telecommunication* 16.4 (2015), p. 305.
- [28] Masoud Mirtaheri and Fatemeh Salehi. “Ambient vibration testing of existing buildings: experimental, numerical and code provisions”. In: *Advances in Mechanical Engineering* 10.4 (2018), p. 1687814018772718.
- [29] Himanshu Mittal, Ashok Kumar, and Rebecca Ramhmachhuani. “Indian national strong motion instrumentation network and site characterization of its stations”. In: *Scientific Research Publishing* (2012).
- [30] NTC18. “Aggiornamento delle Norme tecniche per le costruzioni, 20 febbraio”. In: *Decreto Ministeriale del Ministero delle Infrastrutture e dei Trasporti* 42 (2018).
- [31] Laura Navas-Sánchez and Jaime Cervera Bravo. “A theory-based simplified trilinear model for characterisation of the out-of-plane behaviour of URM walls”. In: *Engineering Structures* 259 (2022), p. 114058. DOI: [10.1016/j.engstruct.2022.114058](https://doi.org/10.1016/j.engstruct.2022.114058).

- [32] L. Navas-Sánchez et al. “Damages in non-structural elements of RC. residential buildings caused by the 2011 Lorca earthquake”. In: ed. by 17WCEE 17th World Conference on Earthquake Engineering. Vol. 10a-0048. 2021.
- [33] Simone Peloso. “Progettazione sismica degli elementi non strutturali: seismic design of non structural elements: floor acceleration spectra”. In: *Hilti Seismic Academy. Available online (last visit 10/05/2023)* (2022). URL: www.hilti.it/content/dam/documents/pdf/e4/services/seismic-academy-2022/2_Peloso_Seismic_Academy_2022.pdf.
- [34] Davide Prati et al. “Passive single-station techniques applied for dynamic characterization of reinforced concrete buildings”. In: *TEMA 6.1* (2020), pp. 18–28.
- [35] Carlo Rainieri and Giovanni Fabbrocino. “Learning operational modal analysis in four steps”. In: *6th International Operational Modal Analysis Conference, IOMAC 2015*. International Operational Modal Analysis Conference (IOMAC). 2015.
- [36] Pathmanathan Rajeev and S Tesfamariam. “Seismic fragilities for reinforced concrete buildings with consideration of irregularities”. In: *Structural Safety* 39 (2012), pp. 1–13.
- [37] Mingming Song et al. “An application of finite element model updating for damage assessment of a two-story reinforced concrete building and comparison with lidar”. In: *Structural Health Monitoring* 17.5 (2018), pp. 1129–1150.
- [38] Dan-Jiang Yu and Wei-Xin Ren. “EMD-based stochastic subspace identification of structures from operational vibration measurements”. In: *Engineering Structures* 27.12 (2005), pp. 1741–1751.
- [39] Lingmi Zhang and Rune Brincker. “An overview of operational modal analysis: major development and issues”. In: *Proceedings of the 1st International Operational Modal Analysis Conference, April 26-27, 2005, Copenhagen, Denmark*. Aalborg Universitet. 2005, pp. 179–190.
- [40] Ying Zhou et al. “Seismic demands of structural and non-structural components in self-centering precast concrete wall buildings”. In: *Soil Dynamics and Earthquake Engineering* 152 (2022), p. 107056.
- [41] NCSE-02. Comisión permanente de normas sismorresistentes. “España. Norma de construcción sismorresistente: Parte general y edificación”. In: *RD 997/2002, Spain* (2002). URL: www.boe.es/eli/es/rd/2002/09/27/997.
- [42] NCSE-94. Comisión permanente de normas sismorresistentes. “Norma de construcción sismorresistente: Parte general y edificación”. In: *RD 2543/1994, Spain* (1994). URL: www.boe.es/eli/es/rd/1994/12/29/2543.

Chapter 7

Conclusions and future lines of research

The summary and conclusions drawn from this PhD dissertation are presented below, classified in specific sections concerning the different objectives developed in the study.

Regarding the state of the art of the vulnerability of buildings within the context of seismic risk studies

A state-of-the-art concerning different aspects of the vulnerability assessment of buildings and non-structural elements has been elaborated. Said work also includes the contributions to the vulnerability field of previous seismic risk studies within which the city of Lorca can be included. Moreover, some aspects of buildings and non-structural elements' vulnerability concerning this city and its typologies of buildings are introduced and possible lines of research revealed.

Regarding the map exposure of Lorca and the characteristics of each typology of buildings

One of the main objectives of this dissertation has been to analyse and summarise the information available about the vulnerability of the main typologies of Lorca buildings and to complete it through the analysis of a database of 300 building reports elaborated by architects and engineers.

In this sense, a series of exposure maps have been contributed in order to facilitate the comprehension of the typologies presented in Lorca and their statistical and graphical distribution. Moreover, each masonry and reinforced concrete typology has been thoroughly studied, described and statistical results obtained from the research into the reports' database. Concerning the masonry buildings' typologies, M11-pre, M31-pre and M34-pre (according to RISK-UE denomination), the features related to seismic vulnerability have been identified employing the CARTIS and the GNDT forms compilation. Concerning the reinforced concrete typologies, the main urban, structural and design features of the typology of buildings that caused a major number of fatalities during the Lorca earthquake have been characterised: a four to six-storey infilled frame reinforced concrete residential building located in an urban history block. The most hazardous non-structural elements of this building typology would be unreinforced masonry parapets and façade walls, infill walls located on staircases and suspended ceilings. The results in terms of seismic vulnerability characterization presented in Chapter 2 for the city of Lorca are also of great value to a considerable number of urban nuclei of Spain.

Regarding the development of a methodology for the assessment and selection of fragility curves for seismic risk studies

A methodology for assessing fragility curves for a particular typology of building in a specific seismic-prone area for seismic risk studies from a set of curves available in the literature has been developed. This consists of a multi-dimensional index based on several variables divided into key dimensions that facilitates the creation of a rational ranking of fragility curves in terms of adequacy. The three key dimensions are technical suitability, suitability for the local system, and building class similarity. The novelty of the proposal, therefore, lies in organising all the variables involved according to the literature in a practical way and giving them scores so that the application of the methodology proportionates the researcher with a classification of the assessed fragility curves according to their adequacy to the area under study. An outcome for which there was no methodology available up until now.

In this context, the fragility curves employed in the previous seismic risk projects developed for Costa Rica have been explored by applying the developed methodology in this interesting country from a seismic vulnerability standpoint. As a result, it is concluded that in the diverse vulnerability projects, fragility curves with very different probabilities of damage are being employed for buildings with the same attributes. Furthermore, the results in terms of ranking the different fragility curves studied have proven to be robust in the application case of the most extended typology in Costa Rica, reinforced confined masonry buildings of one and two storeys.

In addition, the proposed methodology has proven to permit the evaluation of the reliability level of the fragility curves employed depending on the class the curve was classified into based on their score. Therefore, it allows the establishment of not only the adequacy and uncertainty related to the selected fragility curves but also an easy identification of those aspects in which each of the evaluated fragility curves has obtained better and worse scores. As well as the determination of the typologies in which the fragility curves introduced as inputs are insufficient or their scores too low, revealing possible future lines of research in seismic vulnerability. In this respect, it has been revealed that the fragility curves employed in seismic risk studies in the region of Murcia can be improved. Furthermore, the classification along with a systematised representation of the fragility curves have proven to allow the researcher to compare results and draw conclusions easily.

Finally, the specific criteria considered to build this index are currently being validated with a survey of experts and the implementation of the fuzzy Analytic Hierarchy Process (AHP). Furthermore, an open database with an increasing number of fragility curves evaluated is being created in order to facilitate the selection for future seismic risk studies.

Regarding the elaboration of fragility curves for Lorca buildings

The elaboration of fragility curves that characterise accurately the vulnerability of the specific buildings located in an area is crucial for accomplishing better seismic risk studies. For this reason, with the objective of improving the fragility curves employed in the latest seismic risk study carried out in Murcia (the RISMURII project, 2014) for masonry residential buildings, new fragility curves based on a more advanced method which uses actual buildings as samples have been contributed.

Within this context, the simplified RE.SIS.TO method has been employed to estimate the seismic vulnerability of nineteen samples of buildings and the Monte Carlo method to account for its variability. The typologies for which fragility curves have been developed are those composed of load-bearing masonry walls made of rubble stone and/or fieldstone (M11-pre), load-bearing unreinforced masonry walls with wooden flooring systems (M31-pre) and load-bearing unreinforced masonry walls with reinforced concrete joists flooring systems (M34-pre). Typologies that are extensive within Murcia and that can be found all over Spain according to different authors. Furthermore, a method for taking into account that the direction of the seismic event is unpredictable when developing fragility curves on the basis of the simplified RESISTO method has been proposed. Said method ponders the building's capacities in its two main directions in order to construct a unique fragility curve.

Future lines of research should consider the calibration of the fragility curve proposed with the empirical results of the 2011 Lorca earthquake, though this is not a straightforward task.

Regarding the capacity and demand of non-structural elements

As the nine fatalities during the 2011 Lorca earthquake were due to falling debris from non-structural elements, reaching a better understanding of their vulnerability is considered crucial. In this sense, some contributions have been made in the fields of capacity and demand characterisation. Both of them are currently considered areas under development.

In relation to the characterisation of the non-structural elements' capacity, this work has contributed to extending and simplifying the applicability of the methodologies devoted to analysing and representing the behaviour of cantilever masonry walls under seismic events as trilinear capacity curves, which constitute an operational and effective tool for assessing the vulnerability of said elements.

Specifically, a theory-based approach for elaborating the complete capacity curve of a cantilever unreinforced masonry wall subjected to out-of-plane seismic loading is presented; as well as the formulae to build a trilinear

simplified, practical version of these capacity curves in a straightforward manner. The proposal is based on well-known mathematical relationships between external forces, internal forces and displacements, and includes the second-order effects. Besides, it is able to particularise for each wall the complete and the trilinear capacity curves according to the relationships between mechanical and geometrical properties determined as influential, namely, $\lambda, t, E/\rho, E/\sigma_c$ and σ_t/σ_c . The approach's capability to determine linear and non-linear period-displacement relationships has been demonstrated via comparison with several published experimental tests for different geometries and materials. Furthermore, the characterisation of the oscillating periods and the kinetic energies of the walls are thoroughly discussed by means of comparable expressions.

Future lines of research should expand the scope of the proposed approach to cantilever unreinforced masonry walls with a vertical pre-compressing force acting on top or to walls connected to other elements, such as floor structures or perpendicular walls.

In relation to the characterisation of the non-structural elements' demand, this work has contributed several findings and recommendations concerning the Floor Response Spectra definition from the results of a number of case studies. Said outcomes are valid for a widely extended type of buildings in Spain whose non-structural elements' falling debris caused all the fatalities during the 2011 Lorca earthquake: four to six-storey infilled frame reinforced concrete residential buildings.

The seismic wave transmission from the building base to the base of the non-structural element studied is highly influenced by the building properties, hence both the bare structure and the infilled frame structure models have been studied. On the one hand, the research findings of bare structure models have provided evidence that, for the analysed typology, it is crucial to consider the entrance of the structure into the non-linear range when characterising Floor Response Spectra. Moreover, the Floor Response Spectra obtained highlight the relevance of the modes of vibration that involve less mass and the importance of modelling the masonry infills. On the other hand, an updated infilled frame reinforced concrete structure model with diagonal struts has been performed according to the results of Operational Modal Analyses carried out in situ which have permitted the characterisation of these buildings' main frequency (around 3Hz). Among the results, it has been ascertained that the torsional modes that characterize the buildings under study require the creation of 3D models. Moreover, in terms of seismic demand, the outcomes illustrate the fact that the European regulation (EN-1998) provides an oversimplified formulation that gives rise to very unsafe results in some cases, such as this one, even after considering the increment of the Peak Ground Acceleration proposed by the most advanced Spanish hazard maps. In light of these and other results presented, and taking into account that the Spanish regulation in force does not include any method of characterization for this type of seismic demand, this recommendation is provided: to implement the Italian regulation (NTC18) methods for the characterization of Floor Response Spectra in the upcoming Spanish regulation (NCSR-22) currently under development, so as to facilitate the design of safer non-structural elements and crucial devices.

Future lines of research should consider the study of how to combine loads derived from floor Response Spectra of different directions and investigate the intermediate damage states of the building —between the non-damaged infilled frame model and the bare structure model — for the elaboration of the Floor Response Spectra.

General conclusions

An adequate characterisation of the vulnerability of the building and non-structural element stock of a region is crucial for the improvement of the seismic codes as well as for carrying out seismic risk studies that lead to an effective reduction of human and economic losses. Specifically, in the case of Lorca, the exposure study has shown the city presents highly vulnerable unreinforced masonry buildings and extremely dangerous non-structural elements pertaining to reinforced concrete buildings. These later elements were the cause of the nine fatalities incurred during the 2011 Lorca earthquake. For these reasons, a profound study of several aspects of the said Spanish buildings and non-structural elements has been carried out.

In the context of the seismic vulnerability of buildings, the state-of-the-art in the field and previous seismic risk studies have revealed the lack of a rational method to select the most appropriate fragility curve from those available in the literature. A fact that has led to an inconsistency between successive studies in a number of regions: the selection of very dissimilar fragility curves to characterise the vulnerability of the same typology. Consequently, a methodology based on a multidimensional index that allows the assessment and ranking of the fragility curves available in the literature into classes according to their adequacy for the specific typology under study has been

contributed. The methodology has been employed in several countries with good results and an application for practitioners is been developed thanks to a competitive aid awarded by a Spanish bank.

The application of the said methodology to the case of Lorca has identified the limited adequacy of the fragility curves employed in previous seismic studies for the Lorca unreinforced masonry buildings. Therefore, more appropriate fragility curves for these typologies have been contributed after assessing their vulnerability by means of the application of a well-known simplified methodology, RE.SIS.TO. This research has pointed out some features in these buildings that increase their vulnerability, such as an excessive distance between walls that should be retrofitted. Furthermore, new fragility curves have been elaborated on the base of real samples of Lorca buildings considering the uncertainty in the structural configuration of the buildings by means of a Monte Carlo simulation. Additionally, as the directionality of the seism has proven to be a crucial parameter in said buildings' capacity, a simplified methodology to account for this aspect has been provided and applied. These procedures have led to much more adequate fragility curves according to the methodology already presented.

Furthermore, within the context of the seismic vulnerability of non-structural elements, the capacity and the demand of the most vulnerable elements present in Lorca have been studied: unreinforced masonry parapets pertaining to four to six-storey infilled frame reinforced concrete residential buildings.

On the one hand, concerning the capacity, an analytical approach derived from theoretical considerations to characterise the complete out-of-plane seismic response curve of unreinforced masonry cantilever walls has been elaborated and validated with experimental tests from different studies. This theory-based proposal can also serve as a reference for more complex models such as load-bearing or simply supported walls. Moreover, the characterisation of the oscillating periods and kinetic energies of cantilever walls has been profoundly discussed. Furthermore, a straightforward way of elaborating a simplified trilinear version of the curves obtained with the theory-based formulae by means of a series of straightforward mathematical expressions for practitioners has been contributed.

On the other hand, the non-structural elements demand of the reinforced concrete Spanish residential buildings has been studied by means of a series of case studies. Firstly, a bare structure model has been elaborated and results studied. After that, the said model has been updated so as to fit its main frequencies with those obtained in the Operational Modal Analyses carried out in the actual building. Once the infilled frame building was calibrated, the formulae proposed in the Italian and European regulations were tested to find the one that best agrees with the Linear History Analysis. The results reveal the advanced methods provided by the Italian regulation are more accurate for this typology, so their implementation as guidelines in the upcoming Spanish regulation NCSR-22 is recommended.

Finally, based on the knowledge learnt throughout this PhD dissertation, a future line of research for seismic risk studies is proposed: the implementation of fragility curves that account for the interaction effects between the directionality of the seismic faults and the main directions of the buildings in Geographic Information Systems (GIS) or interactive maps. That is to say, another step towards a more advanced combination between the earthquake hazard—the closer seismic faults, their potential and directionality—and the exposure and vulnerability of the area—the building stock with their characteristics, location and resistance in the buildings' main directions—.

Hazards do not have to turn into disasters.

Appendices

Appendix A

RESISTO: example of application

Herein, the building graphed in Fig. A.1 is described and analysed in order to illustrate the RE.SIS.TO procedure.

A.0.1 Description

The case study building is located in a block of the old part of the city, protected by PEPRI, which is the Special Comprehensive Protection and Rehabilitation Plan in sector II of the historic-artistic complex of Lorca. It is located inside an urban history block and between party walls, whose access is through a pedestrian street, which communicates to a street of normal circulation.

The house is distributed over 2 floors and a chamber above ground level, has an approximate age of 81 years and a total constructed area of 180 m^2 in plant view as stated in the cadastral information. It presents an elongated floor plan due to the narrowness of its width of plot, and it develops longitudinally, with a circulation that crosses the different dependencies. Vertical communication is carried out through a core of staircases, giving access to the different levels of the house.

The structural and constructive main characteristics are these:

The building has a structure based on masonry load-bearing walls composed of rounded stone or quarry rock. This is a traditional construction in which rocks are used as basic construction material, according to regulations a poor quality mortar, giving rise to a heavy building with little resistance to lateral loads due to lack of connection between vertical and horizontal elements. The floors are made of wood and do not have horizontal rigidity. The cover has the same construction system as the slabs with a curved tile finish.

The summary of surface areas is these:

- Ground floor: 132 m^2
- First floor: 102 m^2
- Second floor: 55 m^2
- Tower floor: 10 m^2
- TOTAL: 300 m^2

The total surface area in which it was necessary to performed an intervention after the 2011 Lorca earthquake was 144 m^2 .

These are the description of the building and its state of damage element by element after the earthquake according to the experts from *AIA Architects*, Lorca (see Section 2.2.1).

“The staircase is built on the basis of self-supporting elements with a shape vault, combined with a wooden structure and forms an element of bracing of the vertical walls with the slabs. The wall coverings are plaster, the floors with ceramic tile and ceramic tiling on the vertical walls of the wet areas. The interior and exterior carpentry is made of wood.

According to the constructive characteristics of the building, the vulnerability of the building is Class A in the EMS-98 scale.

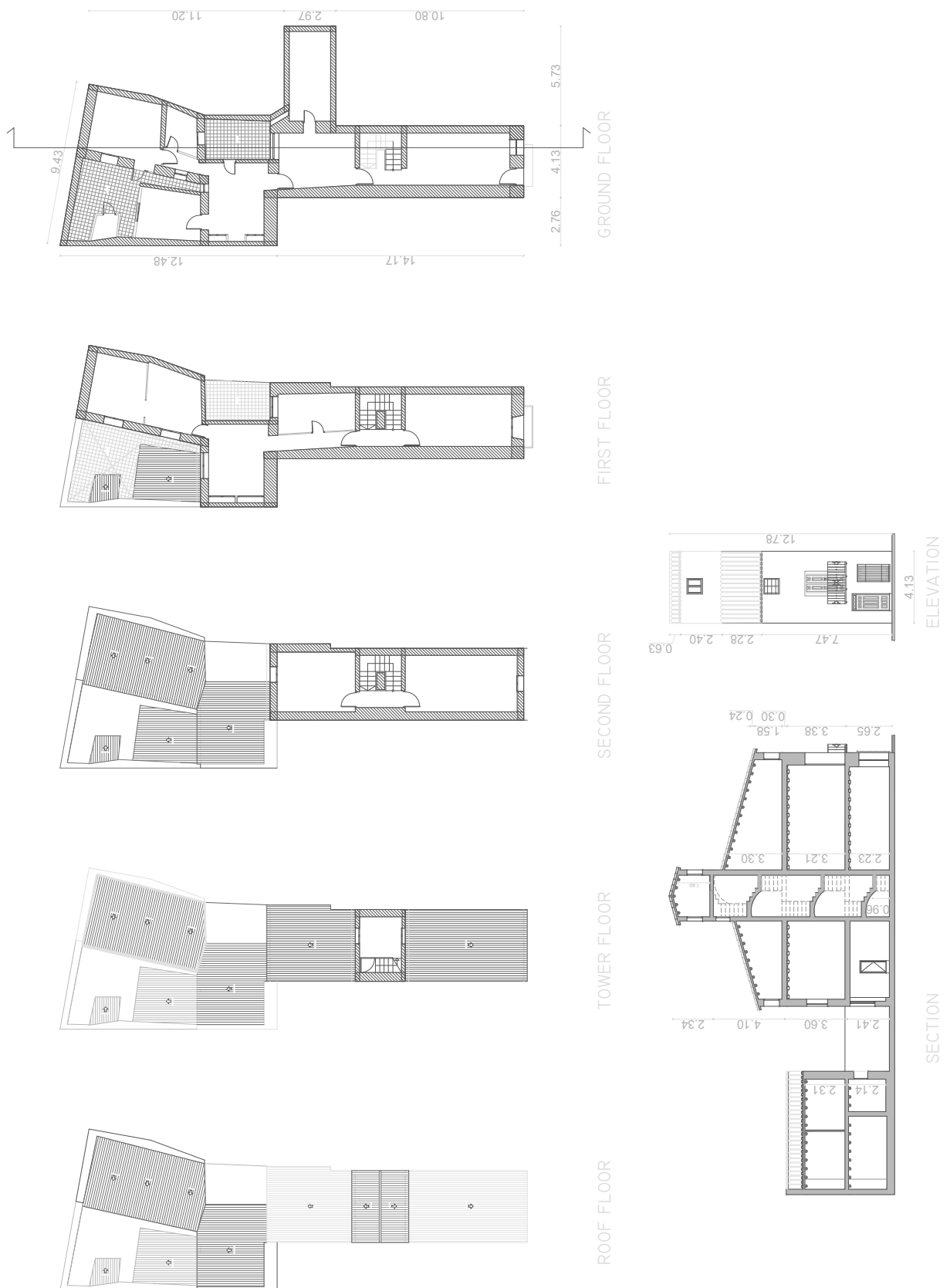


Figure A.1: Geometry of the building selected to illustrate the RESISTO method

The damage it presented after the earthquake is described by the experts after an visual inspection. EMS-98 damage grades are scaled from 1 (lowest) to 5 (highest), representing a linear increase in the strength of the vibration. The house presented severe damage (severe structural damage, very severe non-structural damage), which represents Grade 4 damages according to EMS-98.

Structural damages:

- Load-bearing walls with widespread cracks and fissures due to the two seismic movements that have shaken this building, have caused bracing elements such as slabs and roofs, lose solidarity, marked by vertical cracks.
- Forgings with serious deficiencies, with displacements and deflections in logs of wood that have an impact on cracks in supporting walls and large subsidence in flooring, fissures and cracks in coatings.
- Partially collapsed roof, broken hurdle board. Structure of deformed wood, ditto forged.
- Staircases disconnected from load-bearing walls, the earthquake caused the decoupling of the elements that brace it to the whole.

The damages produced to non-structural elements are described below.

- Collapse of chimneys, collapsed on the roof, breakage and tile detachment.
- Cracks and fissures in stairs on all floors. sections in landings in encounter with inclined section.
- Cracks in plaster coatings.
- Cracked detached ceilings, with risk of collapse.
- Misalignment of wood carpentry, doors and windows, preventing their correct functioning.
- Cracks and fissures in ceramic tiling in bathrooms and kitchens.
- Cracks and fissures in the cladding of the exterior enclosure in the patio.
- Damage to walls and roof of the storage room in the backyard.

Structural damage is widespread and irreversible, with the danger of imminent collapse of the building and danger to surrounding people and properties. The structure is unstable, almost all the load-bearing walls are severely cracked and disconnected. It is impossible to proceed with the adoption of security measures and rehabilitation without risk for workers. From the analysis of these circumstances, it is concluded that, after the earthquake of May 11 2011, the building is in a state of imminent collapse. Thus, proceeds as an emergency, the demolition of the property, which must be carried out under the supervision of a qualified project management and adopting the measures relevant in terms of occupational safety by the commissioned company”.

A.0.2 Application of the RE.SI.STO method

Assessment of the floor shear resistance and pseudo-acceleration

The areas of the resistant masonry walls in the x and y directions are shown in Fig. A.2 for the case study selected as an example. The total value was determined with the aid of the CAD.

$A_{x,i}$				$A_{y,i}$				$A_{t,i}$				h			
Gf	1st	2nd	3rd	Gf	1st	2nd	3rd	Gf	1st	2nd	3rd	Gf	1st	2nd	3rd
16.6	10.5	4.2	1.5	29	23.3	13.6	2.6	162	112	61	12	2.4	3.6	4.1	2.4

Table A.1: Areas in square meters [m^2] of load-bearing walls in the building under study and interstorey height [m]. $A_{x,i}$: walls area in x direction. $A_{y,i}$: walls area in y direction. $A_{t,i}$: total surface area of the floor. h: interstorey height. Gf: ground floor.

According to the considerations pointed out in the experts’ reports, since the design indications are absent in this case, the material is defined as that of the material of M11 type —“Bare rubble masonry (pebbles, irregular masonry stones)”— and is used for the calculation. The report aforementioned specifically indicates that the load-bearing masonry wall is composed of rounded stone or quarry rock; which constitutes a traditional construction in which rocks are used as basic construction material. Moreover, according to expert judgement, the binder is defined as a poor-quality mortar. Next, the mechanical parameters of the material as a whole are defined on the basis of the indications included in the Italian regulation NTC08, Chapter 8. Said properties are shown in Table A.2 for the M11, M31 and M34 material types. Further information on these materials is found in section 2

The values obtained for the different floors of the building taking as an example are shown in Table A.3.

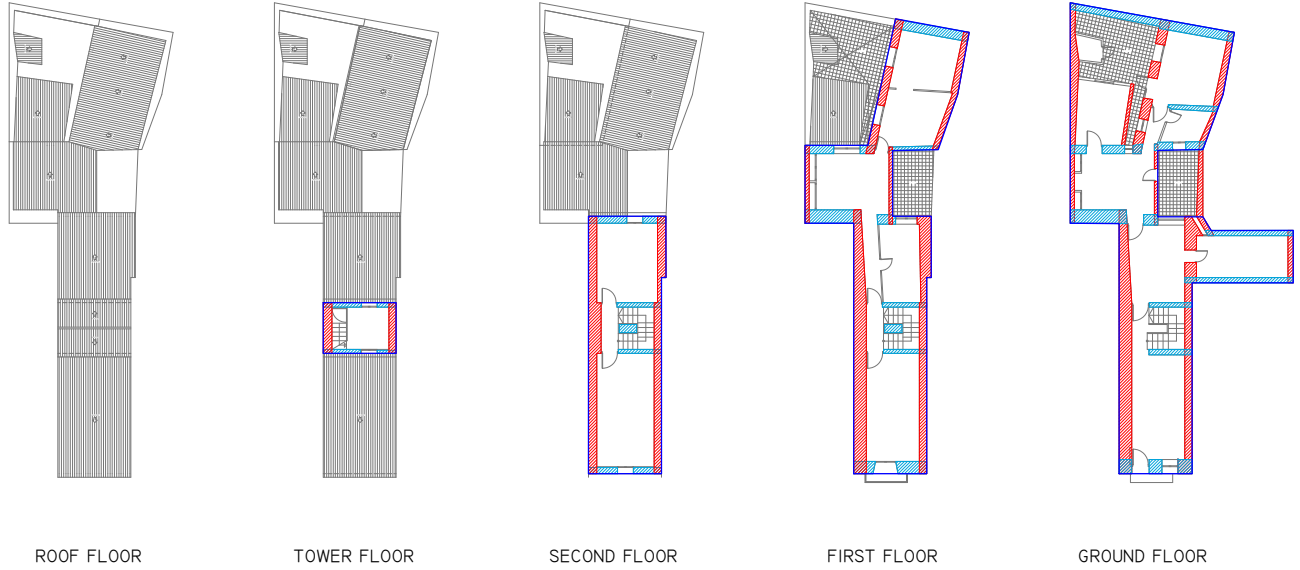


Figure A.2: Representation in plan view of the areas of load-bearing masonry walls of the building under study: x-direction in red and y-direction in turquoise

Mechanical property	Type of masonry	
	M11	(M31 and M34)
$f_m [N/mm^2]$	1.0-(1.5)-2.0	5.0-(6.5)-8.0
$\tau_0 [N/mm^2]$	0.018-(0.025)-0.032	0.08-(0.12)-0.17
$f_{v0} [N/mm^2]$	-	0.20-(0.28)-0.36
$E [N/mm^2]$	690-(870)-1050	3500-(4550)-5600
$G [N/mm^2]$	230-(290)-350	875-(1140)-1400
$w [kN/m^3]$	19	15

Table A.2: Values for the mechanical properties: minimum-(medium)-maximum according to the NTC08 regulation.

Loads				Self weight				FS Material			
Gf	1st	2nd	3rd	Gf	1st	2nd	3rd	Gf	1st	2nd	3rd
5.1	5.1	5.1	2.6	3.45	3.45	3.45	2.45	W+Cñ	W+Cñ	W+Cñ	W+Cñ

Table A.3: Values of loads per unit area of each floor [kN/m^2]. FS = flooring system. W= wood. Cñ =“Cañizo” (straw and canes joint with plaster).

The relationships between the resistant and demand cuts allow the identification of the weakest floor (the one with the minimum value of this ratio) and define the resistance of the building in terms of spectral acceleration (S_a). Table A.4 shows the values of resistant cuts, demand cuts and the relationships between them, for each floor

of the building.

Floor	$q[kN/m^2]$	W [kN]	$\sigma_0[kN/m^2]$	$V_r[kN]$	z [m]	$\sum zW/\sum zW_{total}$	F [kN]	V_s	S_a [g]
Gf	17.94	2906	171.86	849	2.40	1.00	1193	7837	0.108
1st	25.74	2883	145.90	501	6.00	0.85	2960	6644	0.075
2nd	27.83	1698	115.07	182	10.10	0.47	2934	3684	0.049
3rd	29.22	351	85.51	58	12.50	0.10	750	750	0.077

Table A.4: values of resistant cuts, stress cuts and the relationships between them, considering $\tau_0 = 15kN/m^2$ and $w = 19kN/m^3$

In the case in question, the weak plane results in being the First Floor. Consequently, the pseudo-acceleration is equal to $S_a = 0.049g$ before applying the C_{rid} . However, this acceleration value is highly conventional, since it does not consider the real complexity of the construction in question.

Calculation of the Reductive Coefficient (C_{Rid})

(No. of Class) of each parameter In the following, the Class Parameters are described.

(1) Type and organization of the resistant system In the particular case of the building considered as an example of application of the procedure, the Class is established as D, according to Fig. A.3 and the description made by the experts (AIA Architects):

”The building has a structure based on masonry load-bearing walls composed of rounded stone or quarry rock. This constitutes a traditional construction in which rocks are used as basic construction material, according to regulations it presents a poor quality mortar, giving rise to a heavy building with little resistance to lateral loads due to lack of connection between verticals and horizontal elements. The floors are made of wood and do not have horizontal rigidity. The cover has the same construction system as the slabs with a curved tile finish.”

(2) Quality of the resistant system In the particular case of the building considered as an example, the Class is established as D, according to Fig. A.4 and the description made by the experts (AIA Architects) already included in parameter 1 Type and organization of the resistant system.

(3) Resistance This parameter has already been evaluated in section A.0.2.

(4) Location of the building and foundations In the particular case of the building considered as an example of application of the procedure, the Class is established as A since the building is located in a soil type B according to the European regulation EN-1998 and do not present slopes.

(5) Horizontal structural elements In the particular case of the building considered as an example, the Class is established as D, according to Fig. A.5 and the description made by the experts (AIA Architects) already included in parameter 1 Type and organization of the resistant system. Moreover, the building does not present well-connected horizontal structural elements ($\alpha = 0\%$) that can influence this parameter.

(6) Plan configuration In the particular case of the building considered as an example, the Class is established as D.

(7) Elevation configuration In the particular case of the building considered as an example, the Class is established as C. Moreover, the building does not present irregularities due to porticos at ground floor that can influence this parameter.

(8) Maximum distance between walls In the particular case of the building considered as an example, the Class is established as A, being the maximum distance between walls equal to 6.7, their thickness 0.44m and the ratio 15.



(a)



(b)



(c)



(d)

Figure A.3: Photographs of the building under study

(9) Roof system In the particular case of the building considered as an example, the Class is established as D since it constitutes a thrusting roof. Moreover, the building does not present concrete roof with hollow blocks, with a weight $> 200\text{kg}/\text{cm}^2$ that can influence this parameter and the ratio Roof perimeter-Support length is 1.4.

(10) Non-structural elements In the particular case of the building considered as an example, the Class is established as D since it presents balconies without efficient connections and tiles that constitute a danger to the pedestrians (Fig. A.6).

(11) State of conservation In the particular case of the building considered as an example, the Class is established as C since the state of conservation is poor but the significant damages seem to be provoked by the



(a)



(b)



(c)



(d)

Figure A.4: Photographs of the building under study

earthquake.

Scores A summary of the parameters involved and the values of C is included in Table A.5

Number of the parameter	(1)	(2)	(3)	(4)	(5)	(6)	(7)	(8)	(9)	(10)	(11)
Class	D	D	-	A	D	D	C	A	D	D	C
C_{rid}	0.89	0.98	-	1.00	0.93	0.96	0.96	1.00	0.96	0.98	0.96

Table A.5: Values of the parameter (1) to (11) for the building under study



(a)



(b)



(c)



(d)

Figure A.5: Photographs of the building under study

Values of C_{rid}	
Inferior limit	0.60
Superior limit	1.00
Building under study	0.69

Table A.6: Values of the reductive coefficient C_{rid} for the building under study

Therefore, for the building used as example, the building collapse pseudo-acceleration is $S_{(a,c)} = C_{rid} \cdot S_a = 0.054 \cdot 0.69 = 0.037g$ for the most vulnerable floor and direction.



Figure A.6: Photographs of the building under study

Calculation of the Peak Ground Acceleration (PGA_C)

The collapse ground acceleration of the building in question is $PGA_c = 0.046g$ ($Sa_c * 1.25$).

A.0.3 Vulnerability and comparison Demand—Capacity

For the building taken as an example, the reference values obtained from the compilation of the form and from the statistical evaluation of the PGA are those included in Table A.7:

Parameter	
PGA_C	0.046g
PGA_D EN-1998 and new hazard maps (IGN and UPM)	0.228g ($T_R = 475$ "years")
$PGA_C/PGA_D(SLV)$	20%

Table A.7: Summary of parameters for the building taken as an example

Therefore, in this case, the resistant capacity corresponds to 20% of the expected acceleration, relative to the limit state of life protection.

A.0.4 RE.SIS.TO classification

For the building in question it results:

$$(PGA_c)/(PGA_d) = 19\%$$

Based on the results obtained, the building is in Class IV.

Appendix B

Buildings A and B

B.1 Building A

B.1.1 Report

The purpose of this report is to describe the deficiencies detected in the residential building on the occasion of the inspection turned to the same after the aforementioned earthquake that occurred in Lorca on May 11, 2011. The building makes up a consolidated block and is distributed over 5 floors of height above ground and a basement floor. The use of the ground floor is low commercial and the rest of the building is for residential use.

The building is approximately 33 years old and has an area total built of 3329 m² as stated in the cadastral information. The system of vertical circulation is formed by stairs and elevator, giving access to the houses, which in total add up to 21 houses.

The structure of the building is porticoed with reinforced concrete with plane slabs. The exterior enclosure is double-layered with an air chamber, being the termination in seen brick. Common areas: the interior divisions are made of hollow brick, the marble stone floors and stairs with railings in iron profiles and wooden handrails, the coverings of vertical walls in interiors of the ground floor is covered with marble in the entrances and hall, and the rest are lined with with plaster plaster and plaster false ceilings.

According to the constructive characteristics of the building (structure with medium level of seismic resistant design, DSR), the vulnerability of the structure is of Class D, according to the EMS-98 scale. EMS-98 damage grades are scaled from 1 (lowest) to 5 (highest), representing a linear increase in the strength of the vibration.

Description of deficiencies and damage observed

Appearing at the property object of said report, on June 10, 2011, accompanied by the representative of the community of Owners XXX, I have carried out an ocular inspection of the building. From the aforementioned inspection, as well as the analysis and study of the set of information obtained, the existence of a series of damages and deficiencies in Building A, housing and commercial premises, which will proceed to describe below, safe from hidden defects that could not have been detected at that time. Well then, the earthquake has produced in the building object of this report the damages detailed below. The building has Grade 2 damage, Moderate damage on the EMS-98 (light structural damage and moderate non-structural damage).

Structural pathologies

Detail of the structural pathologies:

- *Columns with head damage, in contact with beams, break and detachment in vertices, due to exhaustion by compression of the concrete. Some have main armor and buttress discovered.*
- *Two pillars with broken concrete section, one of them with sheared at 45° (due to element depletion under shear stress).*
- *Sectioned pillar on the 4th floor at the head.*
- *Cracks and fissures in the meeting beam of slabs at different levels.*

- Crack in basement wall.
- Cracks in beams with cracks at 45° where they meet the column, beam with cracks longitudinal and oblique.
- Collapsed stair slabs from the ground floor to the 1st floor.

Non-structural elements' pathologies .

The damages produced to the rest of non-structural of elements of the house are described below.

- Cracks, fissures in exterior walls and plant dividing walls. low, due to shear efforts, with landslides, in areas common and commercial low.
- Damage to the connections with the external coating.
- Cracks, fissures and detachments due to shear forces, in ceramic brick partitions, including plaster linings and paintings and cladding in the Common Areas (including basement).
- Cracks and fissures due to shear forces in brick partitions. ceramic, including plaster coatings and paints, in the Homes on the different floors of the building. partitions for which facilities run.
- Cracks and collapse of false plaster ceilings in common areas and dwellings.
- Cracks and fissures in the elevator shaft enclosures, damages and misalignment of elevator doors (deformation of the the cabin).
- Cracks in the coating of stairs in common areas, with detachment of steps, risers and skirting boards, detachment of the railing anchor point in flight of stairs.
- Detachment of the marble cladding with loss of verticality in hallway.
- Cracks, detachments and fissures in bathroom ceramic tiling and kitchens, by shear and bending, in the houses.
- Misalignment of interior wood carpentry in areas common and houses.
- Cracks in roof parapets (sills) and chimneys with breaks. of auctions
- Terrace flooring with breaks.

Previous actions

In attention to the deficiencies detected, indicated in the previous point of this report, and prior to proceeding with its repair, should take the following security measures:

1. Shoring of damaged structural elements.
 - 1.1. Prop up sectioned pillars, with oblique and 45° cracks.
 - 1.2. Prop up stairs from the ground floor to the 1st floor.
2. Demolition of enclosures with risk of collapse.
3. Demolition of cladding and false plaster ceilings

Conclusions and measures to be taken

Once the building has been analyzed, the following conclusions are reached.

1. The building has structural damage. According to the Royal Decree 997/2002, of September 27, which approves the Regulation of Earthquake-resistant construction, in particular point "1.3.3 of the Compliance with the Standard during the period of useful life", and having an earthquake of intensity VII occurred on the EMS-98 scale, IGN data; the analysis of the consequences of the earthquake on said construction, by a "competent professional" (technician specialized in pathologies and structural calculus). In addition, periodic inspections are recommended in order to carry out follow-up to rule out incidents. hidden.
2. Damaged non-structural elements must be submitted to their demolition and/or repair depending on the intensity of the damage. (Enclosures, divisions, coatings, paintings, facilities, etc...)
3. All facilities must be reviewed and repaired by companies authorized to guarantee their operation. (Electricity, plumbing, etc...)
4. All rehabilitation and structural repair actions of the building will be carried out through the facultative direction of a competent technician/s and under the guidelines of an execution project that includes the technical prescriptions necessary for said intervention.

Photographs and structural design



(a)



(b)



(c)



(d)

Figure B.1: Photographs of Building A: general

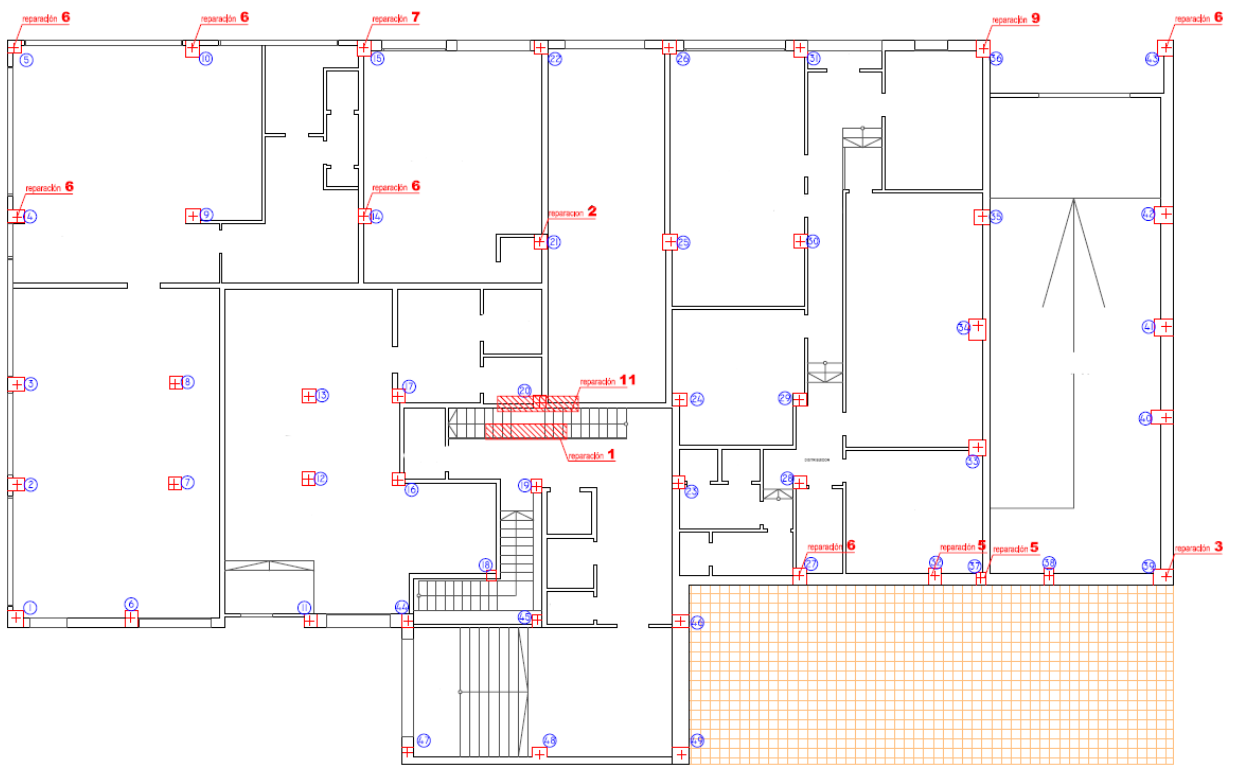


Figure B.2: Building A: structural design



(a)



(b)



(c)



(d)

Figure B.3: Photographs of Building B: structural elements damage



(a)



(b)



(c)



(d)

Figure B.4: Photographs of Building A: non-structural elements damage

B.2 Building B

B.2.1 Report

The purpose of this report is the description and assessment of the deficiencies detected in the residential and commercial building, on the occasion of the inspection made to it after the aforementioned earthquake that occurred in Lorca on May 11, 2011.

The building is located on the edge of a consolidated block, presenting an irregular shape, facing three streets. It is distributed over 5 floors above ground level and a basement floor below ground level. The use of the ground floor is for commercial use, the garage basement and the rest of the building is for residential use. The building is approximately 9 years old and has a total constructed area of 3594 m², as stated in the cadastral information. It has a vertical communication core made up of stairs and an elevator, giving access to four homes per floor, which total 20 homes.

The structure of the building is made of porticos by RC with flat forged one-way type. The building presents a cantilever over the ground floor in the perimeter of the façade. The exterior enclosure is double-layered with an air chamber, with the finish in exposed brick and single-layer plastering. The ground floor sectors with commercial premises have granite cladding. The access to the building has a fence of marble and granite.

In the common areas: the interior divisions are made of hollow brick, the marble floors and stairs with iron profile railings and wooden handrails, the vertical wall coverings in interiors are made of plaster with marble cladding on the access plinth and The false ceilings are made of plaster with molding. The interior of the house is made up of hollow ceramic brick partitions, with a plaster coating. The floors are made of glazed stoneware type ceramic and the coatings in wet areas are glazed ceramic. The interior carpentry is made of lacquered wood and the exterior is made of white lacquered aluminum with a shutter with an iron railing on the exterior on the balconies.

According to the construction characteristics of the building (structure with a medium level of earthquake resistant design, DSR), the vulnerability of the structure is Class D, according to the EMS-98 scale. The EMS-98's damage grades are scaled from 1 (lowest) to 5 (highest), representing a linear increase in the strength of the vibration.

Description of deficiencies and damage observed

Appearing in the property object of said report, on August 24, 2011, accompanied by the representative of the Community of Owners of Building B, I have carried out a visual inspection of the building. From the aforementioned inspection, as well as from the analysis and study of the information obtained, it has been verified the existence of a series of damages and deficiencies due to the earthquake, in said building, which will be described below, except of hidden vices that could not have been detected at that time. The building presents damage of type Grade 3, Severe Damage in EMS-98 (moderate structural damage and serious non-structural damage).

Structural pathologies

The structure visible on all its floors has been completely revised and 32 damaged pillars on the ground floor have been marked and numbered. A schematic floor plan of the building is attached, with the numbering of the pillars. The damage is described below:

- *P1: Horizontal cracks in the column head where the beam meets. Elevator shaft beam damage.*
- *P2: Reinforcements seen at the head of the pillar.*
- *P3: Large concrete spalls at the vertex of the head of the pillar.*
- *P4: Spalling of concrete at the vertex of the head of the pillar.*
- *P5: Spalling of concrete at the vertex of the column head.*
- *P6: Spalling of concrete at the vertex of the column head.*
- *P7: Coqueras at the vertex of the pillar (Phase of execution of work).*
- *P8: Spalling of concrete at the vertex of the head of the column.*
- *P9: Spalling of concrete at the vertex of the column head.*
- *P10: Oblique crack in the head of the pillar and collapsed element.*
- *P11: Spalling of concrete at the vertex of the column head.*
- *P12: Spalling of concrete at the vertex of the column head.*
- *P13: Spalling of concrete at the vertex of the column head.*

- P14: Spalling of concrete at the vertex and face of the column head.
- P15: Large spalling of concrete at the vertex of the head of the pillar.
- P16: Spalling of concrete at the vertex of the column head.
- P17: Significant damage to the vertex of the pillar head, vertical and oblique cracks.
- P18: Large spalling of concrete at the vertex of the head of the pillar.
- P19: Concrete spalling at the vertex of the column head.
- P20: Spalling of concrete at the vertex and face of the column head.
- P21: Spalling of concrete at the vertex of the head of the column.
- P22: Spalling of concrete at the vertex of the head of the column.
- P23: Spalling of concrete at the vertex of the head of the column.
- P24: Slight spalling of concrete at the vertex of the column.
- P25: Slight spalling of concrete at the vertex of the pillar.
- P26: Spalling of concrete at the vertex of the column head.
- P27: Spalling of concrete at the vertex and face of the column head.
- P28: Slight spalling of concrete at the vertex of the pillar.
- P29: Slight spalling of concrete at the vertex of the pillar.
- P30: Slight spalling of concrete at the vertex of the column.
- P31: Slight spalling of concrete at the vertex of the pillar.
- P32: Spalling of concrete at the vertex of the column head.
- Damage to the ramp slab for pedestrian access to the building.
- Cracks and fissures in the stair slabs at the meeting of the stringer with the landing and slabs from the ground floor to the 1st floor.

Non-structural elements' pathologies .

The damage observed in non-structural elements of the Residential Building is described below.

Basement

- Large cracks and fissures in garage access enclosures, with significant collapses. Risk of landslides (walls must be secured or rebuilt).
- Marked access ramp slab, with cracks.
- Access door deformed and completely disconnected (It should not be used until it is correctly repaired).

Ground floor

- Landslides, cracks and fissures in the external enclosures of the building's façade envelope (premises). Widespread disconnections of exterior enclosure.
- Cracks and cracks in the ceramic hollow brick partitioning of the common areas of the partition walls and room dividers. Enclosure of accesses and elevator shaft reconstructed. Damaged facility room enclosures.
- Facade cladding detached and fallen.
- Stair slab with cracks, damage to stair coverings bp to 1st with damage to footprints and detached risers.
- Cracks, fissures and collapse of the false plaster ceilings in the Common Areas.
- Deformed and disconnected access doors.
- Cracks and fissures in the exterior walls of the façade envelope, due to shear stress, marked inside in plaster and outside in exposed brick. Displacements, and collapses of exposed brick at the joint with the adjoining building, risk of landslides, on Av. X.
- Cracks and fissures in ceramic hollow brick partitions, separators, dividing walls and divisions of dependencies, of Dwellings and Common Areas, due to depletion under shear stress. Oblique cracks, 45° and in "X". Widespread disconnections, collapses and displacements. In housing type E, the dividing wall is to be demolished and reconstructed.
- Cracks and fissures in the enclosures of the outer envelope of patios, due to shear depletion.
- Cracks in the false plaster ceilings and moldings in the common areas and homes. • Fissures and detachments in the coating of stairs in common areas (especially the skirting board of stairs and corridors).
- Detachment and cracks in ceramic tiling in bathrooms and kitchens, due to shear and bending, in homes.
- Misalignment of the wooden carpentry inside the houses.

First floor

- Some cracks and fissures in ceramic hollow brick partitions, room dividers and unit divisions, Common Areas and Homes, due to depletion under shear stress.
- Some cracks and fissures in the enclosures of the outer envelope of patios, due to shear depletion.
- Fissures in false plaster ceilings in the houses.

- In type E housing, joists and vaults marked on the kitchen ceiling.
- Detachment and cracks in ceramic tiling in bathrooms and kitchens, due to shear and bending, in homes.

Third floor

- Some cracks in the exterior walls of the façade envelope, due to shear stress, between facing brick and single-layer cladding.
- Fissures and some cracks in ceramic hollow brick partitions, partitions and divisions of dependencies, Homes and Common Areas, due to shear stress exhaustion.
- Some cracks and fissures in the enclosures of the outer envelope of patios, due to shear depletion.
- Some cracks in the false plaster ceilings in the houses.
- Detachment and cracks in ceramic tiling in bathrooms and kitchens, due to shear and bending, in homes.

Fourth floor

- Some fissures and cracks in ceramic hollow brick partitions and divisions of dwellings in Dwellings and Common Areas, due to depletion under shear stress.
- In housing type B, gallery enclosure with displacement.

Roof floor

- Cracks and fissures in the enclosure of the room for telecommunications facilities.
- Façade sills with cracks, cracks, collapses, and partial collapses. They must be reconstructed (study earthquake resistant construction system). Note, patio sills in good repair.
- Cut throat chimneys, 4 units.

General

- Expansion joints with breaks and detachments of facing brick, recompose and execute sealing. Collapses of facing brick enclosures on the 1st and 2nd floor. It will have to be demolished and redone.
- Elevator walls with provisional repairs, must be demolished and rebuilt.

Previous actions

In response to the deficiencies detected, indicated in the previous point of this report, and prior to proceeding with their repair, the following security measures should be adopted:

1. Propping up pillars with severe damage.
2. Demolition and/or shoring of enclosures with risk of collapse. (Garage access sector, roof railings).
3. Demolition of cladding and false plaster ceilings with risk of falling.

Conclusions and measures to be taken

Once the building has been analyzed, the following conclusions are reached.

1. The building has moderate structural damage. According to Royal Decree 997/2002, of September 27, which approves the Seismic-resistant Construction Standard, in particular point "1.3.3 of Compliance with the Standard during the period of useful life", and having occurred an earthquake of intensity VII on the EMS-98 scale, IGN data; a rehabilitation project must be carried out by analyzing the consequences of the earthquake on said construction, by a "competent professional" (technician specialized in pathologies and structural calculation). In addition, periodic inspections are recommended in order to carry out follow-up to rule out hidden incidents.
2. Damaged non-structural elements must be demolished and/or repaired depending on the intensity of the damage. (Enclosures, divisions, coatings, paintings, installations, etc...)
3. All facilities must be reviewed and repaired by authorized companies that guarantee their operation. (Electricity, plumbing, etc...)
4. All the actions of rehabilitation and structural reinforcement of the building will be carried out by the optional direction of a competent technician/s and under the guidelines of an execution project that includes the technical prescriptions necessary for said intervention.

Photographs and structural design



(a)



(b)



(c)



(d)

Figure B.5: Photographs of Building B: general

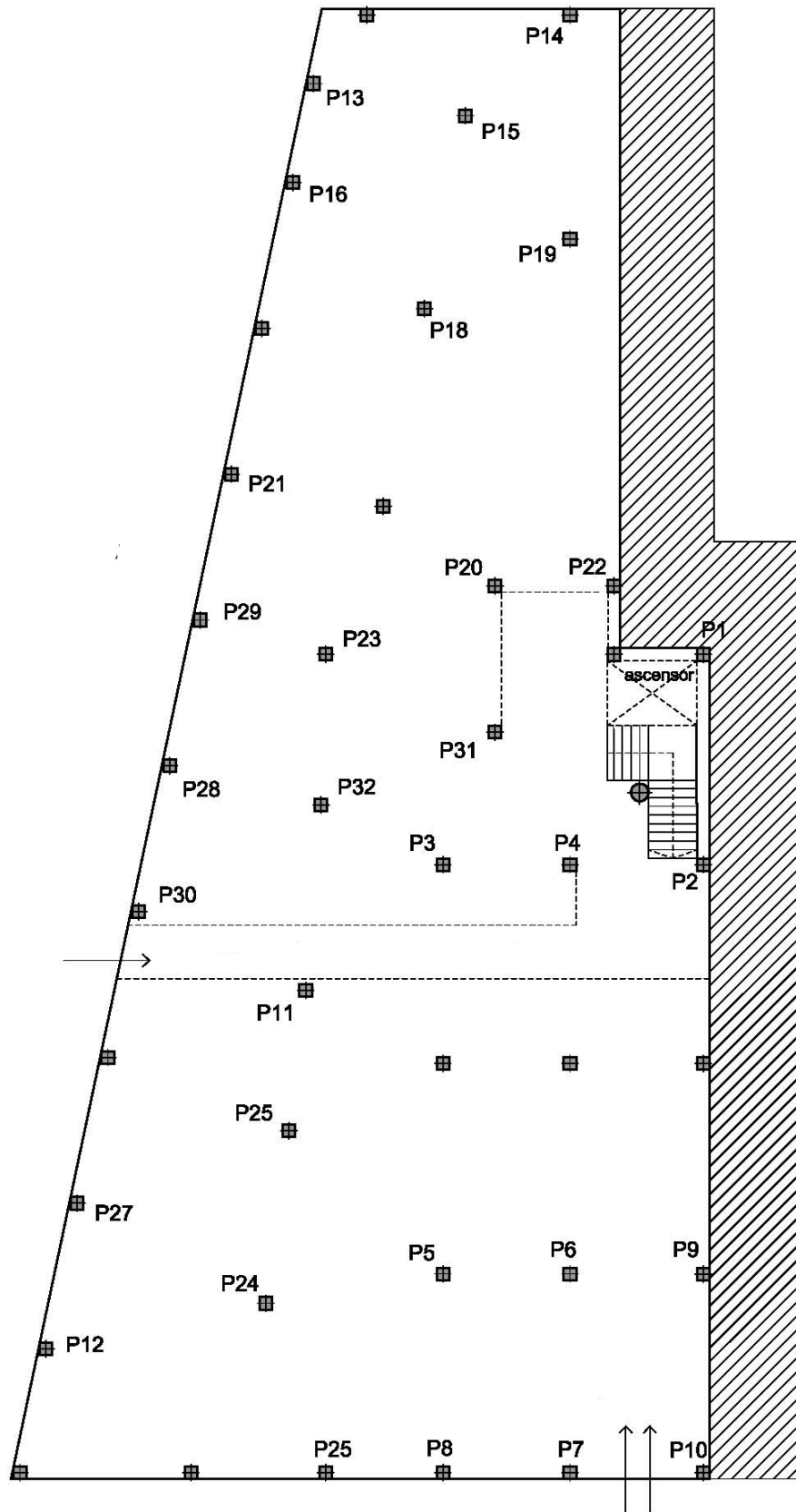


Figure B.6: Building B: structural design (damaged columns enumerated)



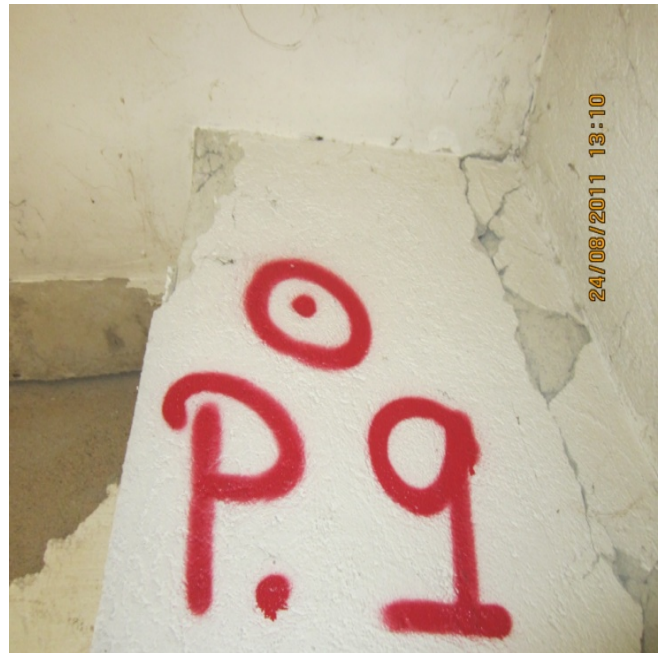
(a)



(b)



(c)



(d)

Figure B.7: Photographs of Building B: structural elements damage



(a)



(b)



(c)



(d)

Figure B.8: Photographs of Building B: non-structural elements damage